Aus dem Institut für Tieranatomie der

Ludwig-Maximilians-Universität München

Lehrstuhl für Tieranatomie II

insbesondere Allgemeine Anatomie, Histologie und Embryologie

Vorstand: Prof. Dr. Dr. Dr. habil. F. Sinowatz

Under Supervision of

Prof. Dr. Dr. Dr. habil. F. Sinowatz,

Head of Institute of Veterinary Anatomy II

Ludwig-Maximilians-Universität, München

Morphological, Glycohistochemical, and Immunohistochemical Studies on the Embryonic and Adult Bovine Testis

A thesis

submitted for the

Doctor Degree in Veterinary Medicine

Faculty of Veterinary Medicine

Ludwig-Maximilians-Universität, München

By

Abd-Elmaksoud Ahmed

From

Kafr El sheikh-Egypt

Munich 2005

Gedruckt mit Genehmigung der Tierärztlichen Fakultät der

Ludwig-Maximilians-Universität München

Dekan:	Univ.-Prof. Dr. A. Stolle
Referent:	Univ.-Prof. Dr. Dr. F. Sinowatz
1. Korreferent:	Univ.-Prof. Dr. H. Zerbe
2. Korreferent:	Univ.-Prof. Dr. W. Klee
3. Korreferent:	Univ.-Prof. Dr. R. Mansfeld
4. Korreferent:	Univ.-Prof. Dr. R. Wanke

Tag der Promotion: 15. Juli 2005

Contents

To

My Wife and My Son

1. INTRODUCTION

The testis is strongly related to the sexual characteristics of the male individual and to its reproductive power. This correlation was observed more than two thousands years ago. Aristotle made one of the earliest descriptions of this relationship in men and in animals, three centuries before Christ. He described how castration of immature male birds prevented the development of sexual characteristics, such as coloring of the crest and attraction to females. He linked these changes in the bird to those observed in castrated boys who experienced the persistence of a high-pitched voice of childhood into adulthood and the lack of sexual hair development. The first convincing evidence of the role of the testis in the maintenance of male sexual characteristics was given in the middle of the nineteenth century by Berthold (1849) who showed that atrophy of the cock's comb observed after castration was prevented by implantation of the testis into the abdominal cavity.

Now, it is well established that testis comprises unique functions in the male body (Schlatt et al., 1997): (i) it contains proliferating totipotent stem cells (ii) it is the only male organ where the meiosis occurs and (iii) it determines the phenotype of the individual by its endocrine activity. All these specific features are regulated by defined endocrine and local mechanisms to ensure the coordinated expression pattern of the required genes.

In the present approach, I have studied the embryonic development and morphological organization of the bovine testis using advanced morphological and molecular biological techniques.

2. REVIEW OF LITERATURE

2.1. Prenatal development of the testis

Although sex is genetically determined at the process of fertilization, the sexual differentiation between male and female takes place when their gonads are morphologically identified. Previously, several investigations have emphasized that the Sry (Sex determining region of the Y-chromosome) is the main trigger in this process (Gubbay et al., 1990; Sinclair et al., 1990; Koopman et al, 1991; Eicher et al., 1995; Tilmann and Capel, 1999). However, more recent studies using various gene knock-out mice have additionally denoted that other players such as homeobox genes, growth factors, transcription factors and other molecules as sonic hedgehog could participate in the urogenital system development (Marker et al., 2003). These and other yet unknown genes may affect development of the urogenital tract beginning at early stages of organogenesis as well as at later fetal and postnatal periods.

In the following sections, I will review the mechanism of gonadal development and the important factors affecting this process.

2.1.1. Sexual determination and gonadal emergence

The process of mammalian sex determination involves complex interacting networks of cellular and hormonal signals, which lead finally to the development of male or female phenotype. It is now well established that three main sequential steps are involved in this process (Habert et al., 2001). The first step begins with the establishment of chromosomal sex at the time of fertilization in which the genetic sex of the embryo is decided when an X-or a Y-bearing sperm fertilizes the oocyte. In the second step, sex determination occurs when the fate of the indifferent gonad is determined by the expression of the Y-linked genetic switch in the XY embryos (gonadal sex). The third step culminates in the differentiation of male or female internal and external genitalia (phenotypic sex) that depends mostly on the hormonal secretion of the developing testis. Importantly, each step in this process is dependent on the preceding one and under normal circumstances, chromosomal sex agrees with phenotypic sex (George and Wilson, 1994; Habert et al., 2001). The male phenotype is controlled by two testicular hormones, the anti-Müllerian hormone (AMH) [also known as Müllerian inhibiting substance (MIS)] secreted by fetal Sertoli cells which induces regression of the Müllerian ducts, and testosterone produced by Leydig cells which induces differentiation of the Wolffian ducts into male reproductive organs, although conversion of testosterone into dihydrotestosterone is required for masculinization of the external genitalia. In the absence of

testis and therefore in the absence of both AMH and testosterone, the Wolffian ducts regress, creating a permissive environment for the differentiation of the Müllerian ducts and thereby female reproductive organs (Jost et al., 1973). In order to a normal testis or ovary to be formed, several sequential developmental phases need to be completed (Tohonen et al., 2003). First, the indifferent gonad is established. Second, the migration of the primordial germ cells from extragonadal sites to the newly formed indifferent gonads (gonadal ridge). Third, the critical step of the sex determination takes place during a transient period. Finally, differentiation of the various testicular or ovarian cell lineages enables the development of normal testis or ovary structure and function.

2.1.1.1. Indifferent gonad: common origin

During the initial phase of sexual development, the gonads develop in a non-sex-specific manner, being morphologically identical in XX and XY embryos and are therefore named indifferent gonads (Habert et al., 2001). Early in the life of any mammal, the first sign of the gonads is the development of the urogenital ridge on either side of the dorsal mesentery of the hindgut. They are particularly prominent in the midtruncal region (Noden and Lahunta, 1985). This structure derives from the intermediate mesoderm and represents the common anlage of kidneys and gonads. On the ventromedial surface of the urogenital ridge, the coelomic epithelium begins to thicken and rapidly becomes several layers thick. Proliferation and mitotic divisions soon cause this region to bulge into the coelomic cavity as genital ridge. This thickened genital ridge extends longitudinally and thus parallel to the mesonephric ridge but medial to it (Rüsse, 1991; George and Wilson, 1994). Gonadal ridge can be histologically recognized at 9.5 days post conception (dpc) in the mouse (Kaufman, 1992), at 21-22 and 28 dpc in pig and sheep embryos respectively (Rüsse, 1991). It can be also identified at 12 mm CRL in horse and 7 mm CRL in dog (Rüsse, 1991). However, in bovine embryos of days 27 to 31, the gonadal ridge starts to appear (Wrobel and Süß, 1998). The gonadal ridge consists of coelomic surface epithelium and the underlying mesenchyme. These elements constitute the so-called somatic component of the gonads (Gier and Marion, 1970). Along its length, the bovine gonadal ridge is covered by a columnar, mostly two-layered coelomic epithelium with elongated or round nuclei (Schrag, 1983; Wrobel and Süß, 1998). Between the high coelomic epithelium and the underlying mesenchyme, a relatively thick basal lamina-like demarcation is established. When the bovine gonadal ridge develops at 27 days, and as species-specific character, it contains a certain number of the primordial germ cells (PGCs, the founders of the future germ cells lineage). PGCs exist in this site before the formation of gonadal ridge itself

whereas they are already observed intraembryonically in the area of the future gonad at day 23. Within the gonadal ridge (days 27-31) and later in the still sexually indifferent gonadal fold (the period betweens days 32 and 39 covers the life span of the bovine gonadal fold or indifferent gonad), the PGCs are unevenly distributed (Wrobel and Süß, 1998). PGCs of the indifferent bovine gonad (32-39 days) are generally found in the outer periphery of the organ. A smaller number are located in the cranial peduncle, but the most are concentrated at the caudal end and the side facing away from the attachment of the mesogonad (Wrobel and Süß, 1998). The original gonadal ridge increases rapidly in diameter but little in length, resulting in a globular gonad by 32 days in canine and 38 days in bovine embryos (Gier and Marion, 1970). The origin of gonadal blastema cells from coelomic mesothelium, mesenchymal cells, elements of the mesonephros and coelomic mesothelium or from both mesonephros and mesenchyme have been proposed for different mammalian species (Zamboni and Upadhyay, 1982; Wartenberg, 1985; Satoh, 1991; Tilmann and Capel, 1999; McLaren, 2000). On the other hand, the reinvestigation of the intermediate mesoderm in 30-to 40-day-old bovine embryos revealed that vestigial nephrostomial tubules, and not the coelomic mesothelium of lateral plate origin are the parent tissue and immediate precursors of the blastemas for the Müllerian infundibulum, adrenal cortex, gonadal rete and gonad proper (Wrobel and Süß, 1999, 2000). The vestigial nephrostomial tubules seen in the bovine embryo are pronephric and not mesonephric in nature. Consequently, the indifferent mammalian gonad is defined as a modified homologue of the pronephros situated in the zone of pro-/mesonephric overlapping (Wrobel and Süß, 1999, 2000). In order to reinforce this new origin of gonadal primordia, Wrobel and his colleagues (2002) have used the genus Acipenser as a model system for vertebrate urogenital development because most higher vertebrates, including man belong to this category. This species is a suitable model to explain the origin of the gonads in vertebrates with a less-developed or regressed pronephros. This study suggested the opistho/mesonephric nephrostomial tubules as a gonadal origin. However, irrespective of a pronephric/mesonephric (Wrobel and Süß, 1999, 2000) or opistho/mesonephric (Wrobel et al., 2002) nature of the nephrostomial tubules that provide the cells for the gonadal primordium, in both cases they have concluded that coelomic mesothelial surface cells of the lateral plate origin apparently are not involved in vertebrate gonadogenesis. These results may be strengthened by another study from mouse in which the mesonephric tubules are not essential for gonadal development whereas the gonads and adrenals still form in Pax 2-deficient mouse even though they lack mesonephric tubules and urogenital ducts (Capel, 2000). A number of genes have been identified that are essential for the formation of the

indifferent gonad. Some of these are important in the differentiation of the intermediate mesoderm and the urogenital system as a whole. The most important genes in this process are the steroidogenic factor-1 (SF-1) and the Wilms tumor gene product (WT-1). Other genes that have been also implicated to have a function during the formation of the indifferent gonad are Emx2, Lim1, and M33. Absence or mutations of one of these genes result in several anomalies ranging from slight aberration to complete absence of the kidneys or gonads (Capel, 2000; Tohonen et al., 2003).

2.1.1.2. Primordial germ cell migration: fact or myth

The indifferent gonad consists of four major cell types: the supporting, steroidogenic, connective, and germ cell lineages (Tohonen et al., 2003). Although the first three types may originate either from mesonephros or from pronephros/mesonephros overlapping as reviewed above, PGCs may however develop extragonadally and migrate from their origin to combine with the somatic component of the gonad. PGCs have been identified in extragonadal sites in many mammalian species including rat, mouse, human and rabbit (Byskov and Hoyer, 1994). In mouse, the ancestors of the PGCs are apparently derived from the proximal epiblast cells adjacent to the extraembryonic ectoderm and not from yolk sac endoderm as was formerly believed. However, the proximal epiblast cells were in no way predetermined for a PGC fate, so even cells from the distal tip of the epiblast could give rise PGCs if transplanted at the appropriate time to the proximal location. In the same time, cells of the proximal epiblast failed to develop to the PGC when they transplanted in the distal epiblast. Therefore, the cellular environment (proximal epiblast) and not the cells themselves are responsible for the development of these ancestors to PGCs. The latter can be identified in mouse embryos at 7-7.5 dpc (McLaren, 2003). Toward the end of gastrulation, about 24 h after the establishment of the germ lineage, the posterior visceral endoderm moves in to form the hindgut, carrying the germ cells from the cluster and distributing them along the length of the hindgut. The germ cells move from the ventral to the dorsal side of the gut, up the dorsal mesentery and into the newly forming genital ridge. PGCs proliferate while they migrate via the gut mesenteries and enter the gonads between 10.5 and 12 dpc in the mouse. PGCs migration, proliferation, and survival rely on the c-kit receptor and stem cell factor (SCF) signaling pathway. Therefore, mutations in either Steel (Sl) that encodes the c-kit ligand (SCF) or White Spotting (W) gene which encodes c-kit receptor tyrosine kinase (the receptor of SCF) interfere with germ cell proliferation and migration. Moreover, TGFβ is thought to be involved in PGCs migration, as it has been shown to inhibit PGCs proliferation and to exert a

chemotropic effect on germ cell cultures (McLaren, 2003; Tohonen et al., 2003). Although the mechanisms of PGCs migration are poorly understood, four models have been postulated (Zuckermann and Baker, 1977): *active*, by amoeboid movement, *passive*, by differential growth of the surrounding tissues, *passive*, via the blood stream, and *chemotactic* under the influence of inductors diffusing from the presumptive gonadal area. During their migration, PGCs must interact with a constantly changing environment. Therefore, they must be able to alter their adhesive properties as they encounter diverse cell populations and extracellular matrix (ECM) molecules. The major ECM molecules that may be involved in PGCs migration are fibronectin and laminin, which line their migratory pathways (Fujimoto et al., 1985; Garcia-Castro et al., 1997). In the bovine embryo, the situation may be completely different when compared with that of the mouse model described above. By using of alkaline phosphatase and glycohistochemistry, Wrobel and Süß (1998) have tried to answer the question of how bovine PGCs colonize the gonadal ridge. In this study, the first potential PGCs were identified in an 18-day-old trilaminar embryo in the caudal wall of the proximal yolk sac at a distance of less than 100 μm from the germ disc. When the trilaminar embryonic disc converted by morphogenic folding (from 18 through 23 days) into a cylindrical embryonic body, the PGCs were incorporated into the embryo at the area that derived from the proximal yolk sac (hind-and mid-gut). Consequently, in 23- to 25-day-old embryos putative PGCs (alkaline phosphatase and lectin positive) are situated predominantly in the axial body region at the level of the mesonephros. So, when the gonadal ridge develops in this region (about day 27), it contains a certain number of PGCs present from the very beginning. Wrobel and Süß (1998) have therefore deduced that the assumption of chemoattraction of PGCs by gonadal ridge, of active immigration from extraembryonic site, or of passive transportation via the blood stream are not necessary to explain the initial settlement of bovine PGCs in the gonadal ridge. The study of Wrobel and Süß (1998) has recently been reinforced by Freeman (2003) who described the active migration of germ cells in mice and man as a myth. He stated, moreover, that the displacement of PGCs could only be explained by the global growth movements of the embryo. Generally, germ cells are not needed for the testis development and differentiation (McLaren, 1988), but they are required for the initial organization of the ovary into characteristic follicles and for the maintenance of these follicles thereafter. In the case of the germ cell loss, the follicular structure of the ovary either never forms or rapidly degenerates (McLaren, 1995).

2.1.1.3. Sex determination

In mammals, the genetic sex of the embryo is established at fertilization with the inheritance of an X or Y chromosome from the male. However, the sex-determining process is set in motion only during the period of organogenesis when the gonads develop (Swain and Lovell-Badge, 1999). In the 1990s, it was discovered that sex is genetically determined in mammals by the presence or absence of a single gene on the Y chromosome, SRY (Gubbay et al., 1990; Sinclair et al., 1990). Expression of this gene is sufficient to initiate the testis pathway in XX gonads (Koopman et al, 1991; Eicher et al., 1995), thereby overriding any bias of the XX gonads for the ovarian pathway. The gene SRY (human) or its homologous Sry (mouse) acts as a developmental switch, initiating a pathway of gene activity that leads to the differentiation of testis rather than ovary from the indifferent gonad (genital ridge) in mammalian embryos. In mouse, several sex reversal from female to male occurred after a small genomic fragment carrying the mouse Sry gene was introduced as a transgene into XX embryo (Koopman et al., 1991). The Sry gene encodes a member of the high mobility group (HMG) family of transcription factors that has been shown to activate transcription by binding and bending DNA (Kamachi et al., 2000). The early events following Sry expression include rapid changes in the topographical organization of cells in the XY gonad and increase in the cell proliferation (Brennan et al., 1998; Schmahl et al., 2000). Moreover, a number of cellular pathways initiated by Sry are required for the development of the testis. These male-specific cellular pathways are: 1) the organization of the somatic supporting cell lineage, the pre-Sertoli cells, to surround germ cells in testis cord structures; 2) a dramatic increase in the size of XY versus XX gonad; and 3) the formation of a male-specific vasculature (Capel, 2000; Tilmann and Capel, 2002). Therefore, it is though that the action of Sry triggers the differentiation of the Sertoli cell lineage in the testis and that the Sertoli cells in turn direct the differentiation of the rest of the cell types, thereby, without the action of Sry the Sertoli cells would become follicle cells (Swain and Lovell-Badge, 1999). In the mouse, Sry is expressed in the genital ridge as a wave from anterior to posterior that lasts about a day and a half so that each cell sees it a few hours only. This transient nature of Sry expression in the gonad suggests that it acts as a switch toward Sertoli cell fate but is not involved in the maintenance of cell identity or cell function. Therefore, Sry must in some ways activate other genes that are involved in defining and maintaining Sertoli cell identity (Swain and Lovell-Badge, 1999). A candidate for this type of downstream gene is Sox9. Its protein product is related to Sry as it contains a similar HMG box domain and is thought therefore to be involved in determining the fate of Sertoli cells. In conclusion, the main actors in mammalian sex

determination can be divided at least into three groups : (1) General transcription factors, which are involved at several stages from early genital ridge developmental through to differentiation of cell types in the gonads and this include Lim1, Sf1, Wt1 and GATA4. (2) Specific promoters of testis development such as Sry and Sox9. (3) Promoters of ovarian development such as Dax-1 and Wnt1 (reviewed by Swain and Lovell-Badge, 1999). In bovine embryos, the SRY gene was detected as early as the 4- to 8-cell stage and through to the blastocyst stage. The expression of SRY at these early stages and the previous observation that in vitro-produced male bovine embryos develop faster in culture than female embryos suggest that sex differences are evident prior to gonadal differentiation and that preimplantation bovine embryos may have sexually dimorphic gene expression at least with respect to SRY transcripts (Gutierrez-Adan et al., 1997).

2.1.1.4. Gonads differentiation: the point of no return

Although the genetic sex is determined at conception, sexual differences between fetuses can be first recognized at the time when the gonads become sex differentiated (Byskov and Hoyer, 1994). There are three different cells lineage in the gonad as well as the germ cells (Fig. 1). The supporting cell linage will give rise to Sertoli cells in the testis and follicle cells in the ovary. These cells surround the germ cells and provide an appropriate growth environment. The steroidogenic cell lineage produces the sexual hormones that will contribute to the development of the secondary sexual characteristics of the embryo. These cells will differentiate to the Leydig cells in the testis and to theca cells in the ovary. The connective cells lineage, comprising peritubular myoid and stroma cells, will participate in the formation of the organ as a whole (Capel, 2000). An increase in proliferation and differentiation of cells believed to be Sertoli cell precursors has been reported as the first signs of diverging male development in alligators where this change precedes cord formation by 1-4 days. The increase in the size of the male gonad is common to many species and led to the theory that an increase in the growth rate of XY embryo results in testis determination. Early testis development is characterized by the formation of testicular cords that contain Sertoli and germ cells, with the Leydig cells excluded to the interstitium. The connective cell lineage is a major contributor to cord formation as the peritubular myoid cells surround the Sertoli cells and together they lay down basal lamina. The testis is also characterized by rapid and prominent vascularization. Organization of the ovary takes place later than that of the testis and less structured, with the connective tissue lineage giving rise to stromal cells and with no myoid cell equivalent (Swain and Lovell-Badge, 1999; Capel, 2000).
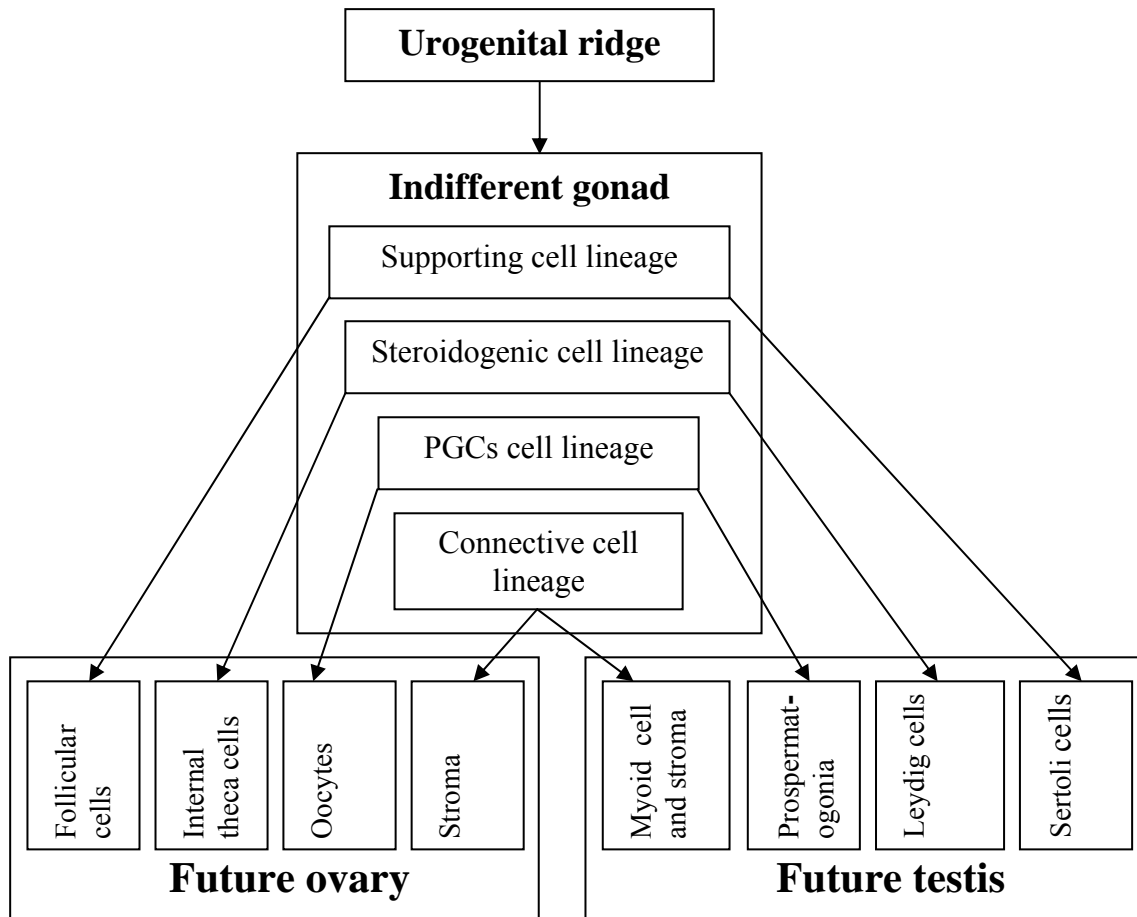
Fig 1: Differentiation of indifferent gonad into the ovary and the testis (modified from Vaiman and Pailhoux, 2000)

2.2. Testicular growth during fetal and postnatal periods

The testis has some features that characterize its mode of growth (Orth, 1993). First, it enlarges relatively rapidly during both the fetal and neonatal period even though puberty occurs considerably later in postnatal life. Second, each population of cells within the testis expands during a particular period of development and, at least in the case of Sertoli and spermatogenic cells; these periods are distinct from each other and inversely correlated. Third, the factors that regulate growth of testicular cells as far as they have been identified and studied, are apparently specific to each cell population and originate both intra- and extra-testicularly.

2.2.1. Developmental changes in the fetal testis

2.2.1.1. Differentiation of testicular cords and stroma

The process of testicular differentiation takes place at 31 dpc/17 mm CRL (sheep), 27 dpc/24 mm CRL (pig), 30 dpc/16-17 mm CRL (horse), 29 dpc/19-20 mm CRL in dog (Rüsse, 1991) and 39-40 dpc/20 mm CRL in bovine embryos (Schrag, 1983; Sinowatz et al., 1987; Rüsse, 1991; Wrobel, 2000a). The first visible event leading to testicular differentiation begins with the development of tunica albuginea and formation of testicular or primitive sex cords (Schrag, 1983). Development and proliferation of testicular stroma is an important morphogenic factor in the embryonic period because it is a necessary prerequisite for correct seminiferous tubules formation. The proliferating stroma forms the passage-ways for the septal blood vessels that originate in the outer layer of the tunica albuginea and run in a centripetal direction towards the central mediastinum (Wrobel, 2000a). The early event in the differentiation of testicular stroma is the appearance of a few isolated mesenchymal cells at the extreme periphery of the gonad, below the coelomic epithelium and amongst the somatic and the germinal cells in this area. These cells increase rapidly in number in subsequent stages and thereafter differentiate into mature connective tissue cells that become organized into a discrete continuous stromal layer, the tunica albuginea (Zamboni and Upadhyay, 1982). In bovine (2 cm CRL), the newly formed tunica albuginea (TA) appears as a thin layer composed of spindle shaped fibroblasts, collagen fibers and blood vessels. With increasing in size and age, the TA of bovine fetal testis increases in thickness and number of layers to differentiate finally into two layers: outer fibrous (tunica fibrosa) and inner cellular with large blood vessels (tunica vasculosa). The connective tissue septa (septula testis) originate from the inner layer of TA divide the testicular parenchyma into several pyramidal compartments (Schrag, 1983). During the bovine testicular development, stromal proliferation dominates in two regions: (1) in the inner layer of the tunica albuginea and (2) in the central mediastinum testis. The proliferating stroma cells of the tunica albuginea subdivide the thick, plate-like testicular cords in the testicular periphery and cleave a way for the blood vessels that immigrate from the large albugineal vessels in a central direction (Wrobel, 2000a). Contrary to the situation described in bovine (stroma of the developing septula testis originates from the inner cellular layer of the TA), the stroma of the developing mouse testis is thought however to be derived from the mesonephric migrating stromal precursor cells (Martineau et al., 1997; Capel et al., 1999; Tilman and Capel, 1999). In general, the main feature that distinguishes a fetal testis from an ovary is the presence of testicular cords. These contain the

seminiferous epithelium that is separated from the surrounding peritubular tissue by a basal lamina. The trigger mechanism for gathering of somatic and germ cells to form testicular cords remains to be determined. As described in rat fetuses, the first recognizable event in an indifferent gonad destined to become a testis is the emergence of large cells that aggregate together and eventually enclose the germ cells within solid cords. These cells are identified as pre-Sertoli cells by their capacity to produce AMH. The forming seminiferous cord is rapidly surrounded by a distinct basal lamina. A similar sequence of events is reported to occur in human fetuses, except that segregation of plate-like structures containing somatic cells apparently precedes their development into cords (Orth, 1993). In bovine, the first cellular aggregation to form testicular cords appears in embryo with 20 mm CRL as circular zone under the simultaneously developed tunica albuginea. These newly differentiated cords consist of two types of cell populations, fetal Sertoli cells (pre-Sertoli cells) and primordial germ cells (Schrag, 1983). During the early stage of testicular development, two areas could thus be distinguished: a peripheral region consisting of newly developed seminiferous cords, connective tissue, and blood vessels; and a nearly central cord-free mediastinum region (Wrobel, 2000a). The peripheral area may be divided into two zones. A narrow outer zone contains plate-like cords with a thick diameter, and a large inner (central) zone is filled with a network of thinner cords. Only the thick outer cords transform into the permanent seminiferous tubules, whereas the thinner cords in the central zone are transitory structures that disappear between 45 and 110 dpc. The majority of the initial bovine seminiferous tubules lies in a plane perpendicular to the long axis of the testis and arrange in a rosette-like fashion around the central rete testis (Wrobel, 2000a). It is thought that the initiation of testicular organogenesis is either spontaneous or regulated by local factors produced within the genital ridge. Of these factors, transforming growth factor-β, insulin-like growth factors, fibroblast growth factor-9, hepatocyte growth factor, and neurotrophic factors could be possible candidates regulating testis morphogenesis (reviewed by Abd-Elmaksoud and Sinowatz, 2005/in press). The interaction between Sertoli cells and the surrounding extracellular matrix seems to be critical for seminiferous cord formation in the fetal testis as well (Orth, 1993).

2.2.1.2. Basal lamina, peritubular cells and extracellular matrix

The ultrastructural studies indicate that the formation of an intact basal lamina surrounding the cords is an early and essential event because the process of the enclosure of testicular cords must occur as fast as possible. In rats, it takes less than 24 hr (Byskov and Hoyer, 1994)

while in sheep the lamina propria shows clear signs of morphological specialization three weeks after the gonadal differentiation (Bustos-Obregon and Courot, 1974). The bovine tubular basal lamina makes its first appearance in the period between 39 and 58 dpc. The thickness of this structure increases steady due to addition of new dense lamellae and translucent interspaces to reach 1.2 µm at day 215 pc. At this age, 7 to 10 dark lamellae can be observed (Schrag, 1983). Presumptive Sertoli cells (pre-Sertoli) appear to cooperate with a subpopulation of mesenchymal cells, presumably the future peritubular cells, to produce the extracellular material surrounding both cell types in young fetuses (Sinowatz and Amselgruber, 1986; Orth, 1993). This is suggested by the observation that the basal lamina underlying the seminiferous epithelium in the postnatal testis is a shared product of Sertoli and peritubular myoid cells (Skinner et al., 1985). Moreover, co-cultures of rat Sertoli cells and peritubular myoid cells indicate that the formation of the basal lamina requires a cooperation between the two cell types (Byskov and Hoyer, 1994). In the fetal testis, the nature and localization of the extracellular matrix may be critical in promoting aggregation of Sertoli cells into cords. This idea is supported by the finding that cords fail to form in the presence of cAMP (Taketo et al., 1984), an effect that may be related to inhibition of matrix synthesis by the nucleotide. Indeed, when older fetal testis already containing cords are incubated with cAMP, the basal lamina eventually disintegrates and disappearance of the cords themselves occurs shortly thereafter (Orth, 1993). Furthermore, the immunohistochemical observations on the normal sequence of events in developing testes have also provided support for the idea that the extracellular matrix is critical for cord formation. For example, before the appearance of the cords some of the basal lamina constituents (fibronectin and laminin) are distributed uniformly between the somatic cells of the fetal rat testis. However, as cells aggregate to form cords by about 13.5 dpc, these two matrix factors become restricted to the newly formed basal lamina of the tubular lamina propria. The latter also contains collagen type IV and V and heparan sulfate proteoglycan. At least some of these components are essential for aggregation of Sertoli cells into seminiferous cords in vitro (Orth, 1993). In rat testis, it was suggested that laminin probably mediates connection between the Sertoli cells and the seminiferous tubule basal lamina and this attachment is important for the morphology of Sertoli cells and for the differentiation of cords composed of Sertoli cells in vitro (Tung and Fritz, 1993). In bovine testis, all testicular cords were surrounded by continuous heparan sulfate and laminin positive basal laminae shortly after the testicular differentiation (Wrobel, 2000a). Although, evidence from organ culture experiments suggested that peritubular myoid cells might arise from a population of cells that

migrate into the genital ridge from the mesonephros (Martineau et al., 1997), the peritubular cells in the prenatal period of bovine testis are described as fibroblasts (Schrag, 1983) or undifferentiated mesenchyme-like cells which have the potential to differentiate into contractile cells, Leydig cells and fibrocytes (Wrobel et al., 1988). While peritubular cells are important in maintaining the structural integrity of the seminiferous tubule, they also appear to produce paracrine factors that may be important in regulatory interactions in the tubule. Initial observation with co-culture of peritubular and Sertoli cells indicated that the presence of peritubular cells could alter Sertoli cell morphology and enhance Sertoli cell function, including the production of transferrin and androgen binding protein (Skinner et al., 1985). Moreover, the Leydig cells in culture are significantly affected by altering the composition of the extracellular substrate. So, the attachment, shape, proliferation of the cells and the expression of gene products are all markedly influenced by the extracellular matrix components (Dym, 1994). Thus, the production of extracellular matrix of a specific composition is likely to have important implications not only for seminiferous cord formation in vitro and perhaps in vivo as well but also for Sertoli, myoid, and Leydig cells interactions and functions.

2.2.1.3. Fetal Sertoli cells: differentiation and proliferation

The differentiation of Sertoli cells in vivo and their subsequent proliferation during fetal and neonatal life are complex events involving presently unknown signals for the initiation of differentiation from within the testis as well as humeral factors from extratesticular sites. In normal animal, this sequence of events resulting in the complement of mature Sertoli cells required to support spermatogenesis and fertility. Although there are, at present, several clearly identifiable factors modulating this progression, it appears that, once initiates, the process continues in an orderly fashion and is completed prior to puberty (Bardin et al., 1994). In mammals, the appearance of presumptive Sertoli cell is one of the first identifiable events in testicular differentiation. Early histological studies of the differentiating fetal rat testis indicated that these cells appear on day 13 pc and then aggregate and form testicular cords the following day (Magre and Jost, 1980). The signal responsible for eliciting the appearance of the presumptive Sertoli cells has not been identified but presumably is related to gene product, encoded on the Y chromosome, that signal the indifferent fetal gonad to develop into a testis (Bardin et al., 1994). The precise origin of the Sertoli cells is still uncertain. While several studies indicated that cells derived from the mesonephros or coelomic epithelium, or both can contribute to the Sertoli cells populations (Martineau et al., 1997; Karl and Capel,

1998; Tilmann and Capel, 1999), Wrobel and Süß (1999, 2000), suggested that the mobilized cells from the pronephros/mesonephros area may differentiate to most if not all of the somatic testicular cells. Following the initial appearance of distinct Sertoli cells and the early stages of organogenesis, there is a period of rapid proliferation. In many species including bovine, this critical proliferation phase begins in fetal life (Schrag, 1983; Orth, 1993; Bardin et al., 1994), continues during postnatal life, and ceases by the formation of functional blood-testis barrier prior to puberty (Sinowatz and Amselgruber, 1986; Orth, 1993; Bardin et al., 1994). Thereafter, all Sertoli cells apparently become terminally differentiated and mitotically quiescent, entering an extended G1 phase of the cell cycle (sometimes termed G0) (Orth, 1993). The role of FSH in development of the fetal Sertoli cells has been highlighted by the demonstration of maximum FSH binding to fetal testicular cells at precisely the time of maximum proliferation of Sertoli cells. Furthermore, addition of FSH to cultures of Sertoli cells derived from postnatal testes resulted in increased mitotic activity while the removal of fetal pituitary or treatment with an antiserum to FSH produced a dramatic reduction in Sertoli cell mitosis. In addition to the demonstrated role of FSH, other factors (e.g. testosterone) may be of importance in influencing the expansion of the Sertoli cell population (de Kretser and Kerr, 1994). Since Sertoli cell population in the adult animal is determined during this period, any disruption of the proliferative process will have a profound effect by reducing the ultimate Sertoli cell population, which will, in turn influence the testicular size of the adult animal (Bardin et al., 1994). Moreover, administration of the antimitotic agent cytosine arabinoside to neonatal rats partly arrests Sertoli cell proliferation, and the reduced number of Sertoli cells is accompanied by a significant decline in the production of spermatids by the developing testis (de Kretser and Kerr, 1994). Before birth, pre-Sertoli cells are predominantly arranged adjacent to the boundary tissue of the seminiferous cords, although some are displaced more centrally by the close packing of cells within the cords. The pre-Sertoli cells exhibit a conical or polygonal shape, with their cytoplasm often oriented radially within the seminiferous cord. Their nuclei are variable in shape and sometimes show deep indentations. A nucleolus is often present and is together with peripheral clumps of heterochromatin associated with the nuclear membrane. The cytoplasm of the fetal Sertoli cells is unremarkable, but tubular membranes of the endoplasmic reticulum are well represented, often bearing variable amounts of ribosomes. For this reason, these organelles are referred to as a transitional form between conventional smooth and rough endoplasmic reticulum (de Kretser and Kerr, 1994). In bovine, the pre-Sertoli cells develop a columnar shape toward the end of the fetal differentiation. A few short rough endoplasmic cisternae

develop into densely packed concentric or spiral accumulated piles, whose content increase continuously. This increase in rough endoplasmic reticulum is, however, more likely to be correlated with secretion of a special protein, i.e., the AMH (Schrag, 1983). Of the known fetal Sertoli cell functions, phagocytosis of the degenerative germ cells and secretion of AMH responsible for regression of the Müllerian ducts in the male fetuses (Bardin et al., 1994; de Kretser and Kerr, 1994).

2.2.1.4. Differentiation of germ cell lineage (prespermatogenesis)

The germ cell line is distinguished from all other cell lineages by virtue of its production of the reproductive (germ) cells. A germ cell is a cell whose descendants become gametes. The ontogeny of the germ cell line can be divided into two parts (McCarrey, 1993): (1) the developmental phase and (2) the differentiation phase. The developmental phase includes the period from the initial embryonic development, through the time when PGCs are first recognized in the early embryo, to the time they subsequently migrate and colonize the developing gonads in the fetus, and undergo sexual differentiation (this phase described above under PGCs migration). The differentiation phase in the male is the period of spermatogenesis that occurs within the testis and includes the differentiation of the prospermatogonia into spermatogonia, spermatocytes, spermatids, and finally spermatozoa. The early differentiation of germ cells prior to the onset of the spermatogenesis has been referred to as prespermatogenesis (Hilscher and Hilscher, 1976). Prespermatogenic differentiation includes an initial fetal phase of proliferation, a quiescent period during which germ cell mitosis ceases, and a second postnatally mitotic stage just before the onset of spermatogenesis. The germ cells that participate in these events are described by various terminologies as gonocytes, fetal spermatogonia, prespermatogonia or prepubertal spermatogonia (Hilscher and Hilscher, 1976; Byskov, 1986; Ertl and Wrobel, 1992). However, the terms gonocyte and fetal spermatogonium used in other species could not be corroborated by studies of bovine (Schrag, 1983), therefore, the term prespermatogonia is widely used by authors who have studied this period in the bovine (Schrag, 1983; Wrobel, 2000b). A distinguishing feature of germ cell differentiation in the male is that cells continue to undergo mitotic replication and do not enter meiosis during fetal stages when the female germ cells do. Thus, a primary influence of the fetal testicular environment on male germ cells is to inhibit their entry into meiosis (McCarrey, 1993). As mentioned above, prespermatogonia enter waves of mitotic divisions during the early testicular development and simultaneously they undergo morphological differentiation. In rat, cessation of mitosis occurs between day 18 and day 19 in the fetus, and division does not resume until one week later, 4 days after birth, while in

rabbit, mitosis arrested shortly after birth and does not begin again until 7 weeks of age (Gondos, 1977). Based on the kinetic studies, those cells undergoing mitosis in the fetal rat (and also in golden hamster) are referred to as M-prospermatogonia while the cells that resume division on days 4 and 5 postnatally just prior to the onset of spermatogenesis are called T2-prospermatogonia and are believed to be the germ cells that eventually transform into type A spermatogonia. Between these two phases of proliferating cells, another generation of non-dividing cells (T1-prospermatogonia) are present (Hilscher and Hilscher, 1976; Miething, 1998). The proliferation pattern of bovine germ cell was studied with monoclonal antibodies against Ki-67 and proliferating cell nuclear antigen (PCNA). As in rat and hamster, the bovine male germ cell population also shows periods of different proliferative activity in the time span between testicular cord formation in the embryo and the onset of spermatogenesis in the pubertal animal (Wrobel, 2000b). Germ cells with a high proliferation rate are observed from day 50 pc to day 80 pc. These cells are in transition from PGCs to prespermatogonia. After this period, the prespermatogonia proliferation decreases continuously to arrest at day 200 pc. Thereafter, these cells enter a phase of relative mitotically quiescence that lasts until the fourth postnatal week (Wrobel, 2000b). The PGCs are polygonal and equipped with slender cytoplasmic processes. Their size may vary slightly according to embryonic age and localization and the nucleus is mostly spherical. All PGCs show a positive alkaline phosphatase reaction and display a characteristic lectin pattern (Wrobel and Süß, 1998). At the end of the first multiplication period (about day 80 pc), the PGCs become alkaline phosphatase negative and change their lectin pattern (Süß, 1998) and hence were referred to as prespermatogonia (Wrobel, 2000b). The relatively large prespermatogonia, found mostly as single cells in the centre of the testicular tubules, contain spherical nuclei, each with up to four nucleoli that are not in contact with the nuclear membrane. Their cytoplasm has spherical mitochondria, sparse rER, small Golgi apparatus, free ribosomes, polyribosomes and various amounts of glycogen. The nuage, an aggregation of finely granular material is a characteristic component of male germ cells, is found in the nucleus and cytoplasm. Intercellular bridges between fetal germ cells are occasionally observed (Schrag, 1983; Wrobel, 2000b)

2.2.1.5. Fetal Leydig cells: origin, differentiation, and function

One of the most important events in testicular development is the differentiation of the steroid-secreting cells, the Leydig cells, in the interstitial compartment. In virtually all species examined, recognizable Leydig cells appear in the interstitium of the fetal testis shortly after development of the testicular cords. In rats and pigs, 1-2 days separate these events while in

humans and bovine the appearance of Leydig cells follow that of the cords by about 1 week (Sinowatz et al., 1987; Rüsse, 1991; Orth, 1993). The fetal Leydig cells of bovine are firstly recognized in the fetus of 3 cm CRL/46 dpc (Schrag, 1983; Sinowatz et al., 1987; Rüsse, 1991). Although the origin of fetal Leydig cells is a matter of debate, several studies have suggested a subpopulation of mesenchymal-like cells in the testis interstitium to be the source of these cells, with evidence obtained from many mammalian species including the rat, mouse, pig, ferret and human (Habert et al., 2001; Mendis-Handagama and Ariyarante, 2001). This concept is supported by the observation of a decrease in the number of mesenchymal cells in gonads of fetal pigs that corresponds temporally with the appearance of Leydig cells and is inversely related to the increasing in numbers of these cells (Orth, 1993). In bovine, these intertubular mesenchymal cells have been suggested to be not only the precursors of the Leydig cells (Schrag, 1983; Sinowatz et al., 1987; Wrobel et al., 1988) but also of the peritubular cells and fibrocytes (Wrobel et al., 1988). Because few mitotic figures are only seen among morphologically recognizable Leydig cells in the early stages of development and become rare thereafter, it has been suggested that most, if not all, fetal Leydig cells originate by differentiation from mesenchyme-like precursors and, once differentiated, no longer divide under normal conditions (Byskov, 1986; Orth, 1993). While some of the mesenchymal cells in the testis interstitium differentiate into fetal Leydig cells and many other interstitial cells types, others retain their undifferentiated characteristics and serve as reservoir of precursors for the adult Leydig cells in the postnatal testis (Habert et al., 2001; Mendis-Handagama and Ariyarante, 2001). Despite the exact signals that trigger the initial differentiation of Leydig cells are unknown, the testicular cords formation, particular extracellular matrix component (collagen type IV and laminin), and extragonadal factors (pituitary gonadotropins and thyroid hormones) have been suggested as trigger mechanisms (Orth, 1993; Mendis-Handagama and Ariyarante, 2001). Moreover, Sertoli cell-secreted factors could be also involved (Habert et al., 2001). In mammals, ontogenesis of the Leydig cell function involves at least two generations of cells. The first generation develops during fetal life. These fetal Leydig cells are responsible for the virilization of the male urogenital system. They regress thereafter, although some of them may persist in the adult life of rat. The second Leydig cell population appears during puberty and produces testosterone required for the onset of spermatogenesis and maintenance of male reproductive functions (Habert et al., 2001). Although a biphasic pattern of the Leydig cell development is well established for most if not all of mammalian species, a triphasic pattern (fetal, neonatal and adult Leydig cell population) has been suggested for pig and human (van Vorstenbosch et al., 1984; Prince, 2001). During testicular

differentiation, Leydig cells gain the characteristics of typical steroid-producing cells. Cytodifferentiation of Leydig cells begins with an increase in the cytoplasmic volume, development of smooth endoplasmic reticulum, an increase in the number and the size of the mitochondria, enlargement of the nucleus, and accumulation of lipid droplets. Gap junctions as well as small aggregates of particles have been described on the plasma membrane of the differentiated fetal Leydig cells (Schrag, 1983; Byskov, 1986; Sinowatz et al., 1987; Habert et al., 2001). In addition, fetal bovine Leydig cells occur primarily in clusters (Schrag, 1983). The morphological differentiation of the fetal Leydig cells is closely correlated with steroidogenic activity, which has been evaluated by measuring steroids in fetal blood, and by determining steroids produced by the testis (Byskov, 1986). Fetal Leydig cells remain in a fully differentiated state for a given period, and then undergo regressive changes, which begin shortly before birth in mouse, rat, hamster, and rabbit (Gondos, 1977). In human testis, such changes are seen beginning after their peak at 14-18 week of gestation and are associated with a decline in testosterone synthesis (Prince, 2001). Fetal bovine Leydig cells reach their maximum number at approximately 11-12 cm CRL (about 88 dpc) but dedifferentiate again to small spindle form mesenchymal cells during the final phase of pregnancy. Degenerated Leydig cells are however rarely seen (Schrag, 1983; Sinowatz et al., 1987; Setijanto, 1992). Leydig cells of bovine fetus are mainly localized between the seminiferous tubules and are never seen within the mediastinum testis (Wrobel, 2000a). The main function of Leydig cells is secretion of androgens. Testosterone is by far the most important androgen. Testicular androgens are responsible for the development and maintenance of the male internal and external genitalia, appearance of secondary sexual characteristics, the development of the musculoskeletal system, feedback inhibition of the hypothalamo-pituitary axis, and stimulation of spermatogenesis (Hall, 1994).

2.2.1.6. Testicular vasculature and intratesticular excurrent pathways

The early specification of vascular development suggests that construction of specific vasculature plays an important role in the developmental pattering as well as the physiological function of the organ (Brennan et al., 2002). In testis, blood vessels may be critical for testicular cords formation (Tilmann and Capel, 1999). Therefore, recruitment of vascular cells from the adjacent mesonephros has been characterized as an early step in the testicular development (Martineau et al., 1997). As mentioned above, downstream events of the Sry expression include an increasing in the size of the XY gonad, organization of testicular cords and appearance of a prominent blood vessel visible just beneath the coelomic epithelium. In contrast, the XX gonad has no similar morphological or vascular features (Capel, 2000;

Tilmann and Capel, 2002). The early differences in vascular development in XY gonads may be important for the differentiation and specification of the venous or lymphatic system to facilitate testosterone export that prevents the development of ambiguous sexual phenotypes. Furthermore, a high level of blood flow through the early testis may be important for the metabolic activities where increased oxygen and metabolite delivery are critical for growth, signaling, and initiation of the steroid synthesis. The efficient collection of testosterone for export may be driven by a high level of blood flow (Brennan et al., 2002). At least three cell types migrate into the XY gonad from the mesonephros. These cells were identified as peritubular myoid cells, perivascular, and endothelial cells (Martineau et al., 1997). The developing testis becomes well vascularized simultaneously with the testicular cord formation whereas capillaries grow between the arches of the testicular cords. In particular, the blood vessels in the developing tunica albuginea become clearly visible soon after sex differentiation (Byskov, 1986). In fetal pig testis, it was proposed that the ingrowing capillaries could stimulate the differentiation of testicular cords; therefore, the testicular cords were firstly differentiated in the simultaneously vascularized periphery of the gonads (Byskov and Hoyer, 1994). Testicular macrocirculation consists of a series of distributing and collecting vessels that conduct blood to and from the testis. The distribution of blood to the testis is achieved by the systematic divisions of feed arteries that arise from spermatic artery. The blood is returned from testis by an extensive network of collecting venules that converge near the inguinal canal to form the spermatic vein. The venous drainage differs within and between the species (Desjardins, 1993). The internal spermatic artery arises from the aorta and run directly to the testis. The degree of vascular (arteries and veins) convolutions continues to increase as the testis descends and it reaches almost adult proportion by the time the testis reaches the inguinal canal. In lamb, the general form of the pampiniform plexus become well developed at the time of the descent of testes (Setchell, 1970). The bovine testicular excurrent duct system is represented by straight tubules and rete testis while is not provided with an extratesticular rete as in many other mammals (Hees et al., 1987). Recently, it was shown in bovine embryos of about 30 to 35 dpc that mobilized cells of vestigial pro/mesonephric nephrostomial tubules give rise to the initial blastema of the adrenal cortex, rete testis, and gonad proper (Wrobel and Süß 1999, 2000). The three blastemas follow each other in cranio-caudal succession and are situated in the area between the mesonephros and coelomic cavity. With the separation of the blastema (the rete and gonadal blastema on one side and the adrenocortical blastema on the other side), the rete blastema remains in contact with the regressing mesonephros (Wrobel and Süß, 1999). At the beginning of its

morphogenesis, the rete anlage is completely an extragonadal structure situated within the cranial peduncle of the gonadal fold. One day before testicular differentiation (about 38 dpc), a small caudal portion of rete blastema is observed in the confines of the gonad proper (testis). On the other hand, the cranial portion maintains a broad contact area with the pro/mesonephric giant glomerulus. Shortly after the testicular differentiation (about 41 dpc), the cells in the area of the rete blastema begin to arrange in strands (Wrobel, 2000a). With increasing of age, the intensely growing rete testis reaches the caudal half of the testis and expands centrifugally in a peripheral direction. The organization of the rete tissue in strands becomes clearly visible because the latter are separated by connective tissue and a continuous basal lamina. After 85 dpc, the rete expands further peripherally and in a caudal direction and develops the first short straight testicular tubules to form the first connection with the seminiferous tubules. This process takes place by the continuous invasion of the latter by the immigrating rete cells with the simultaneous disappearance of the pre-Sertoli and prespermatogonia in the invaded area of the seminiferous tubules. From approximately 100 dpc on, a lumen can be identified in some strands of the rete testis while the straight testicular tubules remain solid until shortly before birth. The epithelium of the straight tubules is ultrastructurally identical to that of the rete testis since the former are extensions of the latter. In the second half of pregnancy, macrophages are found within the epithelium of rete and straight tubules (Wrobel, 2000a). The above-mentioned timeline of developmental changes in the bovine prenatal testis are summarized in table 1.

Table 1: Timeline of prenatal development of bovine testis

Age/dpc	Most clearly observed events
18 dpc	Appearance of PGCs in the caudal wall of proximal yolk sac
23-25 dpc	Localization of PGCs in the axial body region at the level of mesonephros
27-30 dpc	Emergence of the gonadal ridge
30-38 dpc	Stage of the indifferent gonads
39-40 dpc	Testicular differentiation (sex cord, basal lamina and tunica albuginea formation as well as initial appearance of pre-Sertoli cells)
40-50 dpc	Appearance of the 1st generation of Leydig cells Proliferation of Sertoli cells Rete cells begin to arrange in strands
50-80 dpc	Germ cells have a first maximum of proliferation rate and transform from PGCs to prespermatogonia.
80-100 dpc	Leydig cells reach their first maximum Proliferation of germ cells decreases Rete testis develops the first short straight tubule and a lumen can be identified in some strands of rete testis.
100-200	Prespermatogonial proliferation decreases steady Leydig cells regress or dedifferentiate to mesenchymal cells.
200-until birth	Prespermatogonia cease their multiplication

The data of this table are collected from Schrag, 1983; Sinowatz et al., 1987; Rüsse, 1991; Wrobel and Süß, 1998; Wrobel, 2000a,b

2.2.2. Developmental changes in the postnatal testis

At birth, the mammalian testis appears as an immature organ, which gains its full function only at puberty. Acquisition of testicular maturity is evidenced by a number of morphological changes at histological, cytological, and ultrastructural levels (Wrobel et al., 1988). The postnatal testicular development in the bovine was divided into four phases: infantile, proliferation, prepubertal, and pubertal phase (Abdel-Raouf, 1960; Sinowatz et al., 1983). During these phases, the testicular cells undergo gradual developmental changes to attain the pubertal form at about 40 week of age.

Infantile phase (from birth to 8th week)

During this phase, seminiferous tubules are small and solid (Sinowatz et al., 1983; Sinowatz and Amselgruber, 1986; Wrobel et al; 1986; Wrobel, 2000b). At 4 weeks post natum, the basal lamina is approximately 2 μm thick and the peritubular cell sheath consists of 1-2 layers of undifferentiated mesenchyme-like (Wrobel et al., 1988) or fibroblast-like (Sinowatz and Amselgruber, 1986) cells. However, the tubular epithelium consists of pre-Sertoli cells and a few, usually more centrally located prespermatogonia (Sinowatz and Amselgruber, 1986; Wrobel, 2000b). The germ cells in this stage resemble those of the preceding prenatal period in shape and size but start slowly to resume their mitotic activity with the beginning of 5th week (Wrobel, 2000b). In 4-and 8-week–old bovine testis interstitium, mesenchyme–like cells are the dominating elements. However, morphologically differentiated Leydig cells are encountered throughout the entire period of postnatal development. In 4-week-old testes, degenerating fetal and newly formed postnatal Leydig cells are seen in juxtaposition to each other. The transformation of mesenchyme-like cells into Leydig cells is initiated by rounding of cellular and nuclear contours and increase in cell mass. Although postnatal bovine Leydig cells do not survive from fetal periods but differentiate from mesenchymal precursors during postnatal development, a very small portion may also be derived from mitosis of already differentiating Leydig cells (Wrobel et al., 1988). The vascularization of the developing testis is subject to local and age-related differences. In the 4th and 8th week, the percentage of vessels is generally very high due to the existence of large, thin-walled structures, which did not allow an unequivocal classification into blood or lymph vessels (Wrobel et al., 1988). The connection between testicular straight and seminiferous tubules is rather simple during this phase whereas the straight tubules have a narrow lumen and possesses stratified epithelium rich in intercellular canaliculi and extensive cellular junctions (Wrobel et al., 1986).

Proliferation phase (8th -20th week)

In this period, numerous mitoses of the pre-Sertoli and prespermatogonia can be observed and many of the latter have been displaced to the basal aspect of the tubuli to contact the basal lamina (Sinowatz and Amselgruber, 1986; Wrobel, 2000b). At the end of the prespermatogenesis (at about 15th week), the tubular diameter increases to 80 μm and four to five cells are encountered per tubular cross-section. The second peak of germ cell proliferation begins in this phase (by week 18) and lasts until the mid of the next prepubertal phase (27 week). The germ cells in the second maximum phase of proliferation represent the expansion of the spermatogonia stem cell line, kinetically interpolated between prespermatogonia and the first differentiating (cycling) A-spermatogonia (Wrobel, 2000b). Above the spermatogonia (i.e. in the direction of the future lumen), opposing cell membrane of adjacent pre-Sertoli cells start the development of extended junctional complexes (Sinowatz and Amselgruber, 1986). The thickness of the multilayered basal lamina has increased to approximately 2.2 μm and mostly three layers of flattened peritubularly situated cells surround the basal lamina. These cells begin the first step of the transformation into contractile cells by appearance of small bundles of intracytoplasmic filaments connected to electron dense attachment plaques in the cellular process and in the subplasmalemmal area. With 16 weeks, the tubular basal lamina has further increased in thickness, measuring nearly 3 μm and the peritubular cells have proceeded in their transformation to myofibroblast cells. They can be now clearly separated by light microscope from other derivates of the mesenchymal-like cell line. In the interstitium, a considerable increase and differentiation of Leydig cells occurs and from the 8th week onward, only postnatal Leydig cells (second generation of Leydig cells) are present (Sinowatz et al., 1987). Furthermore, from week 16 on, capillaries, blood and lymph vessels could be identified by light microscope. Toward the end of this phase, the first signs of the terminal segments of seminiferous tubules can be observed and the stratified tubulus rectus epithelium adjacent to the seminiferous tubules reduces its layer by rearrangement of the individual cells (Wrobel et al., 1986).

Prepubertal phase (20th -32nd week)

Early in this phase (20-25 weeks), the seminiferous tubules begin to acquire a lumen and develop a terminal segment (Sinowatz and Amselgruber, 1986; Wrobel et al., 1986). The germ cells in the second maximum phase of proliferation represent the expansion of the spermatogonia stem cell line, interspersed between prespermatogonia and the first differentiating (cycling) A-spermatogonia (Wrobel, 2000b). Early stages of meiosis are

observed at the beginning of this phase and thereafter, many primary spermatocytes in different stages of meiosis can be seen. Furthermore, differentiation of pre-Sertoli cells to Sertoli cells also occurs (Sinowatz et al., 1983; Sinowatz and Amselgruber, 1986). The prevalence of junction specialization between adjacent Sertoli cells is much greater and divides the tubular epithelium into basal compartment containing spermatogonia and an adluminal compartment characterized by the later stage of spermatogenesis. At this age (24 weeks) therefore, a functional blood-testis barrier can be expected. The Sertoli cell maturation process includes distinct changes in the cell shape, nucleus, and cellular organelles as well as an increase in surface specialization and subsequent interaction with other Sertoli and germ cells (Sinowatz and Amselgruber, 1986). At the beginning of this stage, the thickness of the basal lamina is reduced to 2.5 μm with knob-like projections invading the bases of Sertoli cells and spermatogonia. Thereafter (at 25 weeks), the peritubular cells transform into contractile myofibroblasts and the general structure of the tubular lamina propria resembles the adult one (will be discussed latter). The degenerative phase of Leydig cells that started in the proliferation phase gradually decreases at 25 weeks and completely ceases at 30 weeks. Leydig cells that survive this degenerative process constitute the long-lasting adult population (Wrobel et al., 1988). From week 25 on, bovine Leydig cells acquire the adult ultrastructure, conformation, location, and topographic relationship to other intertubular constituents. Moreover, the undifferentiated mesenchyme-like cells become rare in the bovine testis from 30 week and onward. Also differentiation of the border region between seminiferous and straight tubules falls in this phase of postnatal development and is accompanied by decisive changes in the seminiferous tubule proper, marking the onset of puberty. These changes represented by formation of a lumen within the testicular cord, appearance of spermatocytes and spermatids, morphological shift from pre-Sertoli to Sertoli cells and elaboration of the structural equivalent of the blood testis barrier. Furthermore, terminal segment with two different regions could be first seen and the tubulus rectus epithelium close to this region becomes simple cuboidal (Wrobel et al., 1986).

Pubertal phase (32nd-40th week)

With 40 weeks, active spermatogenesis can be observed. The seminiferous tubules are hollow and the tubular epithelium demonstrates all stages of spermatogenesis up to that of elongated spermatids (Sinowatz et al., 1983; Sinowatz and Amselgruber, 1986; Wrobel, 2000b). The spermatogonia stem and precursor cell line resemble those of the adult bovine testis can be divided into basal spermatogonia stem cell line (BSC), aggregated spermatogonia precursor

cells (ASPC) and committed spermatogonia precursor cells (CSPC). Furthermore, within the basal tubular compartment, three types of cycling spermatogonia (A-, I-, B-Sg) and preleptotene primary spermatocytes can be identified in this phase by using of PGP 9.5 immunohistochemistry (Wrobel et al., 1995a, b; Wrobel, 2000b). Most of Sertoli cells have completed their morphological differentiation and now attain the adult structure. Degeneration of many germ cells in all stages of the development is observed (Sinowatz et al., 1983; Sinowatz and Amselgruber, 1986). In addition, the adult situation of the terminal segment and straight tubules is nearly achieved (Wrobel et al., 1986).

2.3. Morphological overview of the adult testis

2.3.1. Anatomical structure

The testes of bull are large, elongated oval with vertical long axis, posterior attached border and somewhat flattened medial surface. A testicle of an adult bull weights about 250- 300 grams and measures on the average about 10 to 12 cm in length. The width is about 6 to 8 cm and the anterior posterior diameter about the same (Dyce et. al., 1987; Nickel et. al, 1999). The greater part of the surface of the testicle is covered by a serous membrane, *tunica vaginalis propria*, which is the visceral layer of the serous envelope of the cord and testicle; this is reflected from the attached border of the testis, leaving an uncovered area at which the vessels and nerves in the spermatic cord reach the testis. The tunica vaginalis enables the testis, which is sensitive to pressure, to glide freely in its envelopes. Beneath this serous covering is the *tunica albuginea*, a thick white fibrous capsule of dense irregular connective tissue. It consists predominantly of collagen fibers and a few elastic fibers. In stallion, boar, and ram occasional smooth muscle cells are present (Bloom and Fawcett, 1986; Dyce et. al., 1987; Wrobel, 1998).

2.3.2. Histological organization

The testis has a thick fibrous capsule, *the tunica albuginea*. The later is continuous with connective tissue trabeculae, so-called *septula testis,* which converge toward the mediastinum testis. These septa are rather complete in dogs and boars, whereas in other domestic animals, they are inconspicuous connective tissue trabeculae surrounding large intratesticular vessels. The testicular septa extend radially from the mediastinum to the tunica albuginea, dividing the organ into pyramidal compartments, *lobuli testis.* Each lobule is composed of one to four highly convoluted seminiferous tubules (Bloom and Fawcett, 1986; Wrobel, 1998). Eighty percent of the adult testis are made up of seminiferous tubules; the remaining 20% are

composed of supportive connective tissue, through which the Leydig cells are scattered. The tubules are usually highly convoluted loops, but they may also branch or end blindly. At the apex of each lobule, its seminiferous tubules pass abruptly into the *tubuli recti*, a segment of the excurrent duct system. They in turn are confluent with the *rete testis*, a plexiform system of epithelium-lined spaces in the connective tissue of mediastinum (Bloom and Fawcett, 1986). The intertubular spaces contain loose connective tissue, blood and lymph vessels, fibrocytes, free mononuclear cells, and interstitial endocrine (Leydig) cells (Wrobel, 1998). This general histological organization of the testis is illustrated in fig. 2 and is explained in details in the following sections.

2.3.2.1. Tubuli seminiferi contorti

The convoluted seminiferous tubules (tubuli seminiferi contorti) in most mammals are tortuous two-ended loops with a diameter between 150 and 300 μm and 30 to 70 cm long. They are lined by stratified germinal epithelium, surround by a lamina propria, and connected at both ends to straight testicular tubules by a specialized *terminal segment*. The length of all seminiferous tubules in the testis of adult bovine amounts to approximately 5000 m. Histologically, the seminiferous tubules consists of three components: lamina propria, sustentacular cells (Sertoli cells), and spermatogenic cells (Lesson and Lesson, 1970; Wrobel, 1998).
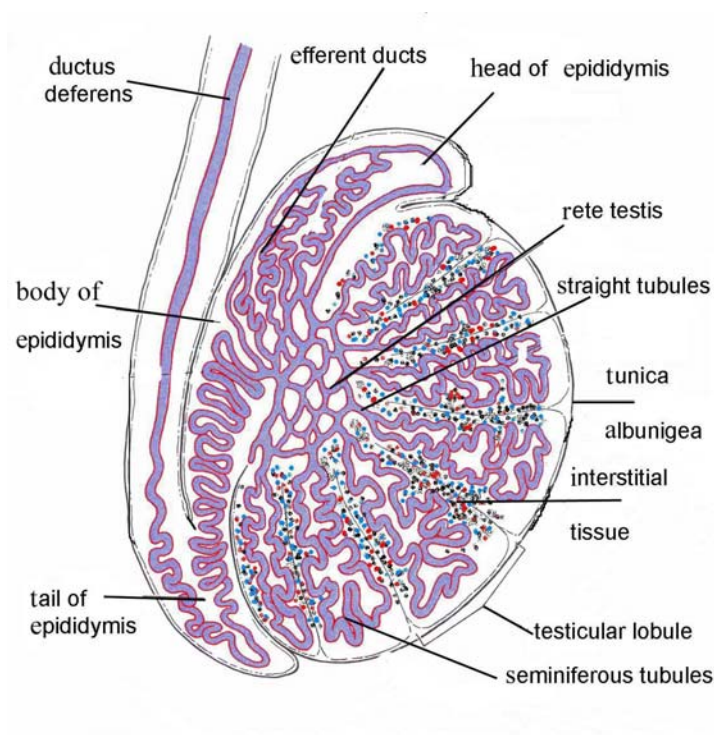
Fig 2: General overview of the histological organization of testis and epididymis

2.3.2.1.1. Lamina propria

The lamina propria of the seminiferous tubules is strategically located between the systemic circulation and the cell membranes of the Sertoli cells and spermatogonia. It consists of clearly defined cellular and acellular zones. Immediately adjacent to the seminiferous epithelium is a thin zone of extracellular matrix referred to as the basement membrane that has been shown by electron microscope (EM) to consist of two layers, basal and reticular lamina. Outside the basal lamina is a clear zone containing type I collagen fibrils in varying orientation. Peripheral to this collagen zone is a layer of flattened cells, the peritubular myoid or myofibroblasts cells, followed by a layer of lymphatic endothelial and fibroblast cells. Collectively, the structures surrounding the seminiferous tubules are referred to as the lamina propria (Christl, 1990; Dym, 1994). Although the lamina propria of the seminiferous tubules in adult reptiles, birds, and mammals follows this general scheme of organization (cellular and acellular zones), there is, on the other hand, considerable variation in thickness, homogeneity or lamellisation of the basal lamina, varying distribution or arrangement of collagen fibers, and in number and pronouncement of the layers of myofibroblasts of this lamina in the species so far studied. Therefore, three types have been recognized (Burgos et al., 1970; Christl, 1990). In the first type, the lamina propria is 1-3 μm thick and contains a single layer of myoid cells. It consists of an internal and external non-cellular lamella enclosing a single lamella of myoid cells and covered superficially by a layer of connective tissue cells. The internal non-cellular lamella is in turn made up of three layers: inner and outer homogenous layers and a middle one containing collagen. This type is found in rat, mouse, and hamster (Burgos et al. 1970; Bustos-Obregon, 1976; Christl, 1990; Maekawa et al., 1996). In a second type, the components of the internal lamella are fused together and the myoid cells are in form of one, or possibly two layers with homogenous material and collagenous fibers in between and on the external surface. The lamina propria in this type is 2-3.5 μm thick and present in the guinea pig (Burgos et al. 1970; Bustos-Obregon, 1976; Christl, 1990). A third type with several layers of myofibroblast cells separated by varying amounts of extracellular glycosaminoglycans, proteoglycans, and collagen fibers has been described in other animals and man. The lamina propria in this type is 2.5-4.5 μm thick (Burgos et al. 1970; Bustos-Obregon, 1976; Wrobel et al., 1979; Moniem et al., 1980; Christl, 1990; Holstein et al., 1996; Maekawa et al., 1996). The inner lamella (basal lamina) of this type of lamina propria may be a classical one with knob-like structure as in man, monkey, horse, dog, and cat (Bustos-Obregon, 1976) or be split into two layers as in rabbit and boar

(Bustos-Obregon, 1976) or into three layers as in camel (Moniem et al., 1980) or even give a multilayered appearance as in adult goat, ram, and bull (Bustos-Obregon, 1976; Wrobel et al., 1979). The basal lamina of the bull seminiferous tubules is multilayered and generally possesses smooth contours but occasionally exhibits knob-like projections which invaginate into the basal portions of spermatogonia and Sertoli cells. The thickness of the basal lamina measures between 0.4 and 0.8 µm and amounts up to 1.2 µm at the knob-like projections. In the even or slightly undulated portions of the basal lamina, 6-9 approximately parallel electron-dense layers are recognized which separated by less electron-dense or transparent interspaces. In knob-like projection up to 15 electron-dense layers can be identified (Wrobel et al., 1979). According to ultrastructural features as well as to alkaline phosphatase histochemistry, Böck et al. (1972) distinguished between two types of peritubular cells, i.e., (i) myoid cells and (ii) myofibroblasts. Differentiated myoid cells possess a continuous basal lamina and tightly packed parallel-oriented cytoplasmic filaments. They also exhibit a positive reaction for alkaline phosphatase. Myofibroblasts are surrounded by a discontinuous basal lamina, possess bundles of crossing cytoplasmic filaments, and lack alkaline phosphatase. The elongated peritubular cells of the bovine seminiferous tubules are arranged in 3-5 concentric layers around the tubules and considered as myofibroblasts with a somewhat higher degree of differentiation than the postpuberal human peritubular cells. In boars, these cells acquire all features of typical smooth muscle cells (Wrobel et al., 1979; Wrobel, 1998). Elastic tissue is situated mainly subjacent to the tubular basal lamina of bull testis and to a lesser degree between the peritubular cells. A peritubular space lined by endothelium-like cells may also surround the seminiferous tubules in bull (Wrobel et al., 1979). The outermost layer of the tubular lamina propria consists of fibrocytes, collagen fibrils, and fibroblast-like cells that may participate in the renewing of the contractile cells. Lymphocytes and monocytes invade the lamina propria but never the intact tubular epithelium (Bustos-Obregon, 1976; Moniem et al., 1980; Christl, 1990; Wrobel, 1998). Immunocytochemical studies on tissue section have demonstrated that the basement membrane immediately adjacent to the seminiferous epithelium is composed of laminin, type IV collagen, heparan sulfate proteoglycans, fibronectin, and nidogen/entactin (Dym, 1994).

Biological functions of the lamina propria

Generally, the myoid or myofibroblast cells have been shown to be contractile elements, involved in the transport of the spermatozoa and testicular fluid in the seminiferous tubule. Therefore, the lamina propria and its cells form the morphological basis for the peristaltic

movement of the seminiferous tubules firstly discovered by Roosen-Runge in 1951. Several substances (prostaglandins, oxytocin, TGF-β, NO/cGMP) have been suggested to affect the contraction of the peritubular myoid cell, since no nerves have been observed in or near this layer, but the exact mechanisms of contraction are still unknown (Holstein et al., 1996; Maekawa et al., 1996). Furthermore, the lamina propria constitutes a permeability barrier for substances penetrating the seminiferous tubules from the interstitium into the germinal epithelium (Dym and Fawcett, 1970). Recent studies have demonstrated that the peritubular myoid cells contribute to the contractile activity of testicular tubules and maintain mesenchymal-epithelial interactions with Sertoli cells both by cooperation in the secretion and deposition of extracellular matrix components (fibronectin, type I and IV collagens, proteoglycans) and by secretion of paracrine agonists or growth factors (PModS, TGF beta, IGF-I, activin-A). Some of these substances such as a peritubular factor that modulates Sertoli cell function (PModS) are known to affect the Sertoli cell function. Furthermore, it has been reported that myoid cells contain androgen receptors and are involved in retinol processing. All these studies indicate that the peritubular myoid cells not only provide structural integrity to the tubules but also take part in the regulation of spermatogenesis (Skinner et al., 1985; Dym, 1994; Maekawa et al., 1996; Verhoeven et al., 2000). Although the basal lamina was believed to serve as a selective barrier and scaffold to which cells adhere, it has become evident that the individual component of the lamina propria (laminin, type IV collagen, heparan sulfate proteoglycans, fibronectin, and nidogen/entactin) are regulators of biological activities such as cell growth, differentiation, and migration, and that they influence tissue development and repair (Dym, 1994; Erickson and Couchman, 2000).

2.3.2.1.2. Sertoli cells (sustentacular or supportive cells)

Sertoli cells are the only somatic (non-germinal) elements within the seminiferous tubules. They were first described by Sertoli in 1865 as columnar cells with cytoplasmic processes extending from the basal lamina to the lumen of the seminiferous tubule and enveloping the neighboring germ cells to provide them with physical support and "nurse" function (Maddocks and Setchell, 1988). There is a high correlation between the absolute number of Sertoli cells per paired testes and both testicular size and daily sperm production. Furthermore, the absolute number of Sertoli cells may be an important factor in establishing the maximal rate of sperm production by any given bull (Berndtson et al., 1987).

Morphological characteristics of Sertoli cells

Detailed accounts of the fine structure of mature Sertoli cells are now available for rodents (Chung, 1974; Fawcett, 1975), goat (Jurado et al., 1994), pig (Osman and Ploen, 1978a), horse (Johnson and Nguyen, 1986), buffalo (Pawar and Wrobel, 1991), bovine (Ekstedt et al., 1986; Sinowatz and Amselgruber, 1986, 1988; Wrobel and Schimmel, 1989), monkey (Dym, 1973), and human (Schulze, 1984). Presumptive bovine Sertoli cells undergo morphological differentiation to mature cells during the first 28 weeks of proliferative development. The maturation process includes distinct changes in cell shape, nucleus, mitotic activity and cellular organelles, as well as an increase in and differentiation of Sertoli cell surface specialization (Sinowatz and Amselgruber, 1986). The three-dimensional configuration of the adult Sertoli cell is extraordinary complex, but it can be thought of as basically tall columnar, resting upon the basal lamina, and extending upward through the full thickness of the epithelium to its free surface (Bloom and Fawcett, 1986; Ekstedt et al., 1986; Sinowatz and Amselgruber, 1988). As in other species, the bovine Sertoli cell is divided into several portions: the basal foot region, trunk region, lateral cell processes, and apical cell surface. The basal foot region rests upon the basal lamina and the trunk region extends toward the tubular lumen. From the trunk region of Sertoli cells, an elaborate system of thin processes radiate laterally to surround or separate spermatocytes and round spermatids and occupy all of the interstices among them. The apical Sertoli cell surface is indented by shallow or deep recesses partly lined by ectoplasmic specializations and houses elongated spermatids and spermatids residual bodies (Wrobel and Schimmel, 1989). Sertoli cells must continually alter their shape to accommodate the structural transformation and mobilization of germ cells from the base to the free surface of the seminiferous epithelium (de Kretser and Kerr, 1994). Sertoli cells have generally large oval or pear-shaped nucleus located in the broad basal portion of the cells. This nucleus is often deeply infolded and contains a large nucleolus (de Kretser and Kerr, 1994; Wrobel, 1998). On the electron micrographs, the outlines of the bovine nuclear cross-sections are irregular with numerous deep indentations causing their lobulated appearance. The karyoplasm appears homogenous and contains little heterochromatin. The nuclear envelope contains numerous pores and a small electron dense layer (lamina fibrosa) occurs on the inner nuclear membrane (Ekstedt et al., 1986; Sinowatz and Amselgruber, 1988). The complex nucleolus is a particular characteristic structure in the Sertoli cell nuclei. In man (Schulze, 1984) and rodents (Fawcett, 1975), the usual configuration of nucleolus resembles a tripartite structure composed of two amorphic lateral bodies and central part formed by a compact nucleolonema. In bovine the nucleolus is, however, a more complex structure

29

consisting of membrane-limited tubules within the strands of the nucleolonema and numerous vesicles of various sizes. The membrane bound structures have small ribosomes-like particles associated with their outer surface. Satellite heterochromatin bodies, common in many other species, are not found (Zibrin, 1972; Ekstedt et al., 1986; Sinowatz and Amselgruber, 1988). In general, the cytoplasmic components of Sertoli cells show a polarized distribution. The basal and lower trunk regions of the cytoplasm contain an abundance of organelles and inclusions, whereas the apical extensions usually exhibit only few of such structures (Sinowatz and Amselgruber, 1988; de Kretser and Kerr, 1994). The basal portion and the central trunk region of the sustentacular cell contain mitochondria, an inconspicuous Golgi complex, abundant sER, little rER, free ribosomes, microtubules, actin and vimentin filaments, lysosomes, and lipid inclusions (Sinowatz and Amselgruber, 1988; Wrobel, 1998). Sertoli cell mitochondria exhibit a great diversity in shape according to the species. They may be round, oval, spherical, or even S shape. In species so far examined, the mitochondria have many transversely oriented cristae, but the tubular form is often encountered, particularly in its spherical variety (de Kretser and Kerr, 1994). Sertoli cell Golgi apparatus consists of several dictiosomes, which are frequently located near the nucleus, but some are also found in the apical cytoplasm (Sinowatz and Amselgruber, 1988). Sertoli cells contain limited amount of rough or granular endoplasmic reticulum, which occurs as several short parallel cisternae or alternatively takes the form of small individual tubules principally in the base or trunk of the Sertoli cell cytoplasm (Sinowatz and Amselgruber, 1988; de Kretser and Kerr, 1994). Contrary to rER, Sertoli cell contains a well-developed system of sER (Sinowatz and Amselgruber, 1988). However, there is no general morphological pattern that can be applied to a description of Sertoli cell endoplasmic reticulum, since it has been referred as vesicular, tubular, cisternal, fenestrated, or lamellar. Species differences may account for such variations in fine structures (de Kretser and Kerr, 1994). In bovine, the sER often appears as sharply circumscribed, crescent-shaped, or conical masses of membranes in the Sertoli cell cytoplasm around developing acrosome. Furthermore, whorls of endoplasmic reticulum are often encountered in the basal part of the cells, lateral to the nucleus (Ekstedt et al., 1986; Sinowatz and Amselgruber, 1988). Sertoli cell cytoplasm also contains free ribosomes, polyribosomes, lipid droplets, and glycogen particles. In addition, Sertoli cells contain variable amounts of dense bodies usually referred to as collections of lysosomes, multivesicular bodies, and heterophagic vacuoles (Ekstedt et al., 1986; Sinowatz and Amselgruber, 1988; de Kretser and Kerr, 1994). Sertoli cells are endowed with an elaborate cytoskeleton together with contractile elements occupying most parts of the cytoplasmic matrix. A network of intermediate

filaments occurs in the cytoplasm and may also surround the Sertoli cell nucleus in an area devoid of other cell organelles. Microtubules are abundant but show no preferential orientation (Ekstedt et al., 1986; Sinowatz and Amselgruber, 1988). Generally, Sertoli cell shape, surface area, and volume percentages of organelles (sER, nucleus, lysosomes, and lipid inclusions) change in accordance with spermatogenetic cycle (Wrobel and Schimmel, 1989; de Kretser and Kerr, 1994). The Sertoli cells have specialized cell contacts with other Sertoli cells, germ cells and basal lamina. Inter-Sertoli cell junctions are functionally very important. By means of these junctions, the Sertoli cells form a continuous layer, dividing the seminiferous epithelium into basal and adluminal compartments. This continuous layer comprises the ultimate and tightest part of the blood testis barrier. The inter-Sertoli cell junctions are extensive occluding junctions. In the cytoplasm subjacent to the occluding junctions, there are bundles of microfilaments and subsurface cisternae of endoplasmic reticulum. Gap junctions are also found between neighboring Sertoli cells (Ekstedt et al., 1986). Different types of junctional specializations exist between Sertoli and germ cells, including desmosome-like junctions, Sertoli ectoplasmic specializations, and tubulobulbar complex (Ekstedt et al., 1986; Sinowatz and Amselgruber, 1988). Circumscribed contact areas in the form of desmosome-like junctions are found between Sertoli cells and spermatogonia, spermatocytes and round spermatids. They are characterized by complementary densities on the subsurface aspects of Sertoli and germ cells membranes, which consist of numerous densely packed filaments. As opposed to true desmosomes, no line of dense material in the extracellular space parallel to the cell membranes can be seen. Sertoli ectoplasmic specializations are asymmetric junctional specializations, which occur only on the Sertoli cell side. They consist (1) of filaments apposed to the Sertoli cell membrane over quite a distance, and (2) of a more deeply placed cisterna of sER, which occurs frequently but irregularly. Ectoplasmic specializations are first observed at the level of spermatocytes and occurred then between Sertoli cells and subsequent developmental stages. They are especially well developed in that part of Sertoli cells facing elongation-and maturation-phase spermatids and eventually disappear at the end of the maturation phase of spermatid development. Additionally, tubulobulbar complexes are formed between late spermatids and Sertoli cells. These consist of deep protrusions of spermatids which project in invaginations of adjacent Sertoli cells (Sinowatz and Amselgruber, 1988).

Sertoli cell functions:

Sertoli cells have nutritive, protective, and supportive functions for spermatogenic cells. In addition, they phagocytize degenerating spermatogenic cells and detached residual bodies of

spermatids as well as they release the spermatozoa into the lumen of the seminiferous tubules (spermiation). Sertoli cells mediate the action of FSH and testosterone on the germ cells, participate in the synchronization of spermatogenic events, produce an androgen-binding protein, and secrete constituents of the intratubular fluid, such as transferrin, androgen-binding protein, and inhibin (Wrobel, 1998). Experimentations over the last decades have revealed that Sertoli cells make and secrete a number of proteins that form the molecular basis for Sertoli-germ cell interactions. Glycoproteins secreted by the Sertoli cells can be placed in several categories based on their biochemical properties (Griswold, 1998). The first category includes the transport or bioprotective proteins that are secreted in relative high abundance and include metal ion transport proteins such as transferrin and ceruloplasmin. The second category of secreted proteins includes proteases and protease inhibitors, which allegedly are important in tissue remodeling processes that occur during spermiation and movement of preleptotene spermatocytes into the adluminal compartment. The third category of Sertoli cell secretions includes the glycoproteins that form the basal lamina between the Sertoli cells and the peritubular cells. Finally, the Sertoli cells secrete a class of regulatory glycoproteins that can be made in very low abundance and still carry out their biochemical roles. These glycoproteins function as growth factors or paracrine factors and include molecules such as AMH, c kit ligand, FGF, IGF, TGF, EGF, and inhibin (Griswold, 1998). All of these glycoproteins are implicated in the regulation of spermatogenesis and some of them have recently been reviewed by Abd-Elmaksoud and Sinowatz (2005/in press).

Blood-testis barrier

A well-recognized property of the testis is the maintenance, within the seminiferous tubules, of a highly specialized microenvironment created by the Sertoli cells that partition young and more mature germ cells into two compartments within the seminiferous epithelium. Many substances are found to diffuse readily from testicular blood vessels into the interstitial lymphatics but do not appear in the fluid collected from rete testis. Thus, a blood-testis permeability barrier seemed to be anatomically located either surrounding or actually within the wall of the seminiferous tubules (de Kretser and Kerr, 1994). The strategic and unusual location of Sertoli cell tight junctions in relation to the germ cells have given rise to the concept of an anatomic and functional subdivision of the seminiferous epithelium into (a) a basal compartment containing spermatogonia, preleptotene, and leptotene primary spermatocytes and (b) an adluminal component beyond the level of tight junctions that sequesters the more differentiated germ cells (advanced spermatocytes and spermatids) into a

unique physiological environment (Maddocks and Setchell, 1988; Sinowatz and Amselgruber, 1988; de Kretser and Kerr, 1994). The development of specialized junctions between Sertoli cells seems to be under hormonal control since the blood-testis barrier does not appear until the onset of spermatogenesis at puberty (Kormano, 1967). The unique cell-cell junctions between Sertoli cells are an effective intraepithelial component of the blood-testis barrier. However, the Sertoli cell interactions with other cell types in the peritubular contractile layer of the seminiferous tubules are now thought to provide an adventitial, albeit incomplete, component to the blood-testis barrier. This is particular so in rodents, but Fawcett (1975) suggests that in primates, including man, the extensive gaps in the multiple layers of tubular lamina propria mean that the blood-testis barrier depends exclusively on the Sertoli cell junctions. The division of the Sertoli cell by the junctional complexes is of major consequence for partitioning of all substances; those reaching the base of the seminiferous epithelium from the blood have more or less direct access to cells in the basal compartment. However, the presence of occluding junctions means that substances must pass through the Sertoli cell cytoplasm to reach germ cells in the adluminal compartment. Likewise, the fluid of the tubular lumen must be derived from material passed selectively through, or synthesized by the Sertoli cell (Setchell, 1970). While the physiological role of peritubular cells, collagen fibrils and other ECM components in the boundary wall in limiting the passage of cells and macromolecules and preventing the penetration of blood vessels is recognized (Dym and Fawcett, 1970), they may also play an important role in shielding the immunologically foreign haploid germ cells from immature surveillance. The blood-testis barrier is probably involved in the control of endocrine activity in the testis. As emphasized by Sharpe (1983), the various barriers in the testis (vascular endothelium, myoid cells, and tight junctions of the Sertoli cells) will not only selectively prevent certain substances from entering the testis, but may also act to prevent others from leaving the testis. These various barriers allow the creation of unique microenvironments within the tubules, and possibly in the interstitial space, and are probably essential for local interaction between the various cell types and compartment within the testis. The development of a tubular barrier formed by Sertoli cell junctions is retarded by the absence of pituitary hormones, but not entirely prevented (Vitale et al., 1973), and once established does not subject to hormonal modification. The only circumstance in which the barrier breaks down is following efferent duct ligation (Setchell, 1986) but this is probably a result of the increased intratubular pressure and not a response to the hormonal changes, which also occur (Main and Waites, 1978). In addition to the major blood-testis barrier in the seminiferous tubules, Kormano (1967) has demonstrated that at

puberty, the penetration of certain dyes into the interstitial fluid is reduced, and some may no longer penetrate at all. This implies some barrier at the level of the vascular endothelium.

2.3.2.1.3. Spermatogenic cells

Various spermatogenic cells, representing different phases in the development and differentiation of spermatozoon, are located between and above Sertoli cells. In addition to the cell population involved in spermatogenesis (cycling population), the bovine seminiferous epithelium contains a separate stem cell and spermatogonia precursor cell line. This population can adapt to changing demands and thus guarantees uninterrupted spermatogenesis (Wrobel et al., 1995a, b).

Spermatogonia precursor cell line (non-cycling population)

Spermatogonia precursor cells in the bovine seminiferous tubules are classified as basal stem cells (BSC), aggregated spermatogonia precursor cells (ASPC), and committed spermatogonia precursor cells (CSPC). Stem cells and spermatogonia precursor cells are morphologically similar to spermatogonia but differ in size, shape, and immunoreactivity. These cells are also located in the basal tubular compartment and in adult seminiferous epithelium quantitatively represent a minority in comparison to cycling spermatogonia. The self-renewing BSC give rise to ASPC that in turn develop to CSPC. The latter transform into new type A spermatogonia (A_1-Sg). The exact demarcation between CSPC and A_1-Sg would be the moment when CSPC enter S-phase in preparation for the first A-Sg mitosis (Wrobel et al., 1995a, b).

Spermatogenesis

The sequence of events in the development of spermatozoa from spermatogonia is referred to as *spermatogenesis* and is subdivided into three phases: (a) spermatocytogenesis, the process during which spermatogonia develop into spermatocytes; (b) meiosis, the maturation division of spermatocytes that results in spermatids with reduced (haploid) number of chromosomes; and (c) spermiogenesis, the process of transformation of spermatids into spermatozoa. The duration of spermatogenesis is 74 days in men and approximately 50 days in bulls, rams, and stallions (Wrobel, 1998).

Spermatocytogenesis

During spermatocytogenesis, spermatogonia multiply mitotically, resulting in A-, I- (intermediate), and B-spermatogonia and finally in preleptotene primary spermatocytes.

Primary spermatocytes no longer divide mitotically but undergo two meiotic divisions, which result in a fourfold increase in the number of germ cells. Therefore, the number of spermatozoa that originate from one A-spermatogonium is decisively influenced by spermatogonial proliferation during spermatocytogenesis. In most mammals, a variable number of generations of A-spermatogonia are followed by one generation of I-(intermediate) and B-spermatogonia, respectively. In a given tubular segment, the few A-spermatogonia are irregularly distributed. Daughter cells of A- and I-mitoses drift apart to achieve an even distribution (Wrobel, 1998). *A-spermatogonia* (A-Sg) are the largest spermatogonia and share an extensive contact area with the tubular basal lamina. They possess a spherical nucleus with prominent nucleoli. The karyoplasm is cloudy with little heterochromatin. Golgi apparatus is inconspicuous and endoplasmic reticulum, most of which is agranular, is scarce. Free ribosomes occur throughout the cytoplasm whereas the mitochondria are rare in the apical part of the cell or below the nucleus (Ekstedt et al., 1986, Wrobel et al., 1995a). *Spermatogonia intermediate type* (I-Sg) resembles type A but are somewhat smaller and have smaller nuclei. In addition, their karyoplasm exhibits a coarsely granulated texture. The contact area with the basal lamina is not as wide as in type A (Ekstedt et al., 1986, Wrobel et al., 1995). *B-spermatogonia* have spherical nuclei containing numerous chromatin particles and less prominent nucleoli. The cytoplasm resembles that of other spermatogonia but the contact area with the basal lamina is narrow (Ekstedt et al., 1986; de Kretser and Kerr, 1994; Wrobel, 1998). All B-spermatogonia of a given tubular segment form a cellular network, because they are interconnected by cytoplasmic processes. The mitotic division of B-spermatogonia results in the formation of the preleptotene primary spermatocytes (Wrobel et al., 1995a). These cells and their descendents are interconnected by true cytoplasmic bridges until shortly before spermiation. *Preleptotene primary spermatocytes* gradually lose contact with the basal lamina and move into the adluminal tubular compartment across the intercellular junctions between the Sertoli cells. Preleptotene primary spermatocytes are actively engaged in DNA synthesis whereas all chromosomes consists of two sister chromatids (de Kretser and Kerr, 1994; Wrobel, 1998).

Meiosis

During meiosis, two successive nuclear divisions occur, resulting in the formation of four haploid spermatids from one primary spermatocyte. *Primary spermatocytes* are the largest spermatogenic cells in the tubular epithelium and are located in the intermediate position between spermatogonia and spermatids. The prophase of the first maturation division is

characteristically of long duration and cells in the phases of this process demonstrate nuclear features based on the appearance and morphology of their chromosomes (de Kretser and Kerr, 1994; Wrobel, 1998). The prophase of the first maturation division is subdivided into the leptotene, zygotene, pachytene, diplotene, and diakinesis stages according to characteristic changes in nuclear chromatin (Ekstedt et al., 1986; Wrobel, 1998). During the *leptotene stage*, the nucleus appears light with an irregular envelope and chromosomes become arranged in thread-like strands. The Golgi apparatus is small and endoplasmic reticulum is scarce. More free ribosomes/polyribosomes are present than in spermatogonia. In *zygotene spermatocyte*, both the nucleus and the cytoplasm increase in size. The homologous chromosomes begin to pair and tetrads of four chromatids emerge. Visible evidence of pairing is the synaptonemal complexes seen with the electron microscope. The mitochondria become elongated and their cristae start to dilate. Late in this stage, groups of mitochondria approach each other and dense intermitochondrial substance appears. Completion of pairing initiates *the pachytene phase*, during which crossing over occurs between nonsister chromatids of paired chromosomes. In microscopic preparations, primary spermatocytes are best identified when they are in this phase of meiosis. The cytoplasm of cells in this stage contains numerous well developed organelles including Golgi apparatus, agranular endoplasmic reticulum, and mitochondria but the number of free ribosomes/polyribosomes appears lower than in the previous stages. During the *diplotene phase*, the paired chromosomes pull away from each other, but sister chromatids remain attached. Diplotene spermatocytes differ from pachytene spermatocytes in few respects only (Ekstedt et al., 1986; de Kretser and Kerr, 1994; Wrobel, 1998). During the prophase of the first meiotic division, the cells grow considerably. For instance, between preleptotene and diplotene, ovine primary spermatocytes increase in volume 4.8 times and their nuclei increase in volume 3.3 times. During *diakinesis*, chromosomes shorten and broaden and the four separate chromatids in each chromosome are clearly evident. Diakinesis is rapidly followed by the dissolution of the nuclear membrane, appearance of the spindle, and attachment of the bivalents to equator of the spindle during metaphase. Anaphase subsequently results in the movement of the members of each bivalent to opposite poles of the spindle, resulting in the daughter cell termed secondary spermatocytes that contain the haploid numbers of chromosomes, each composed of two chromatids (de Kretser and Kerr, 1994; Wrobel, 1998). *Secondary spermatocytes* are short-lived, intermediate in size between diplotene primary spermatocytes and spherical spermatids, and occur exclusively in phase 4 of the seminiferous epithelial cycle. After a short period of interphase, during which no duplication of genetic material occurs, secondary spermatocytes

undergo the second maturation division, with a short prophase followed by metaphase, anaphase, and telophase, which are essentially similar to those of mitotic divisions. During this division, centromeres divide and the sister chromatids of secondary spermatocytes separate and are distributed to each of the spermatids resulting from that division (Wrobel, 1998).

Spermiogenesis

Spermiogenesis is the process by which round spermatids formed from the second maturation division of meiosis undergo a complex series of cellular transformations to form mature elongated spermatids. No cell division is involved, but the process is in essence a metamorphosis in which a round cell is converted into a highly organized motile cell (de Kretser and Kerr, 1994; Wrobel, 1998). Ultrastructurally, the spermiogenesis has been divided into 15 distinctive steps represented by Arabic numerals (1-15). However, the process has also been grossly divided into four phases, namely, Golgi phase (step1 to step3), cap phase (step 4 to step 7), acrosomal phase (step 8 to step 12), and maturation phase (step 13 to 15) (Sinowatz and Wrobel, 1981). In routine histologic sections, Golgi and cap phases are characterized by spherical nuclei, whereas the acrosomal and maturation phases reveal elongated nuclei (Wrobel, 1998). The most important morphologic changes during spermiogenesis are formation of the acrosome, condensation of nuclear chromatin, outgrowth of a motile tail, and loss of excess spermatid materials (cytoplasm, water, organelles) not necessary for the later spermatozoon (Sinowatz and Wrobel, 1981; Bloom and Fawcett, 1986; Ekstedt et al., 1986; de Kretser and Kerr, 1994; Wrobel, 1998).

Spermatozoon

Spermatozoa vary in length between approximately 60 µm (boars, stallions) to 75 µm (ruminants). By light microscope, the spermatozoon seems to consist essentially of two portions: the head and the tail (Wrobel, 1998). The shape of the nucleus determines the shape of the head of spermatozoon, which is species-dependent and subject to great variations. The anterior two thirds of the nucleus are covered by acrosomal cap, with an outer and inner acrosomal membrane that fuses at the caudal end. The acrosomal cap contains several hydrolytic and proteolytic enzymes (e.g., acrosin), which are set free during the acrosome reaction of the capacitated spermatozoa in the uterine tube. In addition, it is known to contain several enzymes of lysosomal nature. Among those identified to date are hyaluronidase, neuraminidase, acid phosphatase, β-N-acetylglucosamidase, and aryl sulfatase. Acrosomal

enzymes are needed for the penetration of the zone pellucida during fertilization (Bloom and Fawcett, 1986; de Kretser and Kerr, 1994; Wrobel, 1998). The sperm tail presents four segments along its length recognizable with the light microscope by slight differences in thickness and in the nature of their sheaths. From proximal to distal, these regions are the neck, the middle piece, the principle piece, and the end piece. There are significant differences in the internal structure of these segments. These cannot be clearly resolved in fresh preparations but require special cytological techniques, or electron microscopy, for their demonstration (Bloom and Fawcett, 1986; Ekstedt et al., 1986; de Kretser and Kerr, 1994; Wrobel, 1998).

Seminiferous epithelium cycles (Spermatogenic cycles)

The cycle of the seminiferous epithelium is defined as a sequence of changes occurring in a given area of the seminiferous epithelium between two successive appearances of the same cellular association (Leblond and Clermont, 1952). The duration of the spermatogenic cycle is the interval between appearance of the stem spermatogonium and the release of spermatozoa, which are produced from it. It thus represents the length of time necessary for the formation of the spermatogenic series (Rüsse and Sinowatz, 1991). The duration of the seminiferous epithelial cycle is 13.5, 10.5, and 8.5 day in bovine, sheep, and boar respectively (Rüsse and Sinowatz, 1991). The cellular associations, which may be recognized during a cycle of the seminiferous epithelium, permit distinguishing various spermatogenic stages. Generally, two principal methods of classification may be used. One is based on the development of the acrosomic system (Leblond and Clermont, 1952) and the other on meiotic divisions, shape of spermatid nucleus, and release of spermatozoa into the lumen of the seminiferous tubule (Ortavant, 1958). According to the second classification, 8 stages may be defined in the seminiferous epithelial cycle of ram, bull, and boar (Rüsse and Sinowatz, 1991; Wrobel, 1998). In stage 1, spherical spermatids lie nearest to the lumen, followed basally by two generations of primary spermatocytes, i.e., late pachytenes and young preleptotenes/leptotenes. With the beginning of stage 2, the spermatids and their dark-stained nuclei are elongated. The two generation of primary spermatocytes are late pachytenes and young leptotenes/zygotenes. In stage 3, elongated spermatids are arranged in bundles and lie in deep apical recesses of the sustentacular cells. The pachytene spermatocytes of stage 2 have reached diplotene. A second generation of primary spermatocytes in zygotene is present in the basal region. By initiation of stage 4, the first and second maturation divisions take place. In addition to bundles of maturing spermatids and zygotene primary spermatocytes, either

diplotene or secondary spermatocytes, or spherical spermatids are seen. In stage 5, two generations of spermatids are present: older elongated spermatids and newly formed spherical spermatids. The zygotene spermatocytes of stage 4 enter the pachytene stage and are displaced in the direction of the tubular lumen. By stage 6, the bundles of the older spermatids have moved away from the vicinity of the sustentacular cell nuclei. In addition to spherical spermatids, pachytene spermatocytes and numerous spermatogonia are present. In stage 7, the maturation-phase spermatids achieve a position close to the tubular lumen and all other cells as in stage 6. At the end of the cycle (stage 8), spermatozoa leave the tubular epithelium (spermiation) after separation from their residual bodies. Remaining within the epithelium are spherical spermatids and two generations of primary spermatocytes (older pachytenes and young preleptotenes) (Wrobel, 1998). These stages are illustrated in fig. 3.
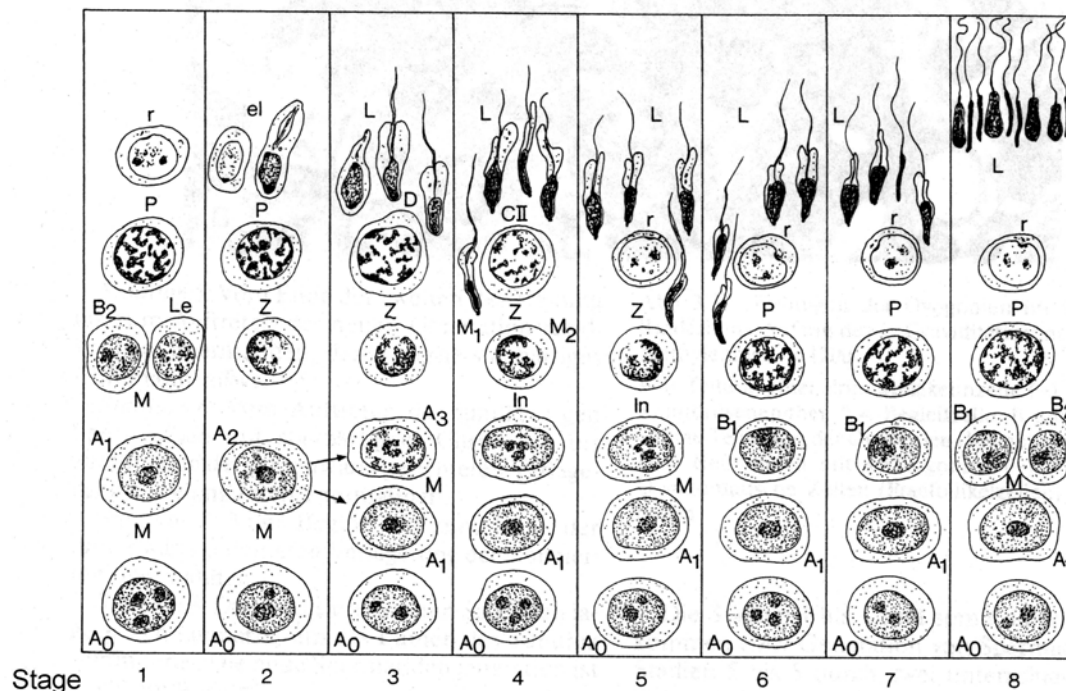
Fig 3: Cellular composition of the eight phases of the bovine seminiferous epithelial cycle. A_0 and A_1: stem cells; A_2 and A_3: type A spermatogonia; In: intermediate spermatogonia; B_1 and B_2: type B spermatogonia; M: mitosis; Le, Z, P, and D: primary spermatocytes in leptotene, zygotene, pachytene and diplotene stages. CII: secondary spermatocytes; M_1 and M_2: first and second maturation divisions; r, el, L: round, elongating, and elongated spermatids (from Rüsse and Sinowatz, 1991)

Spermatogenic waves

The succession of cellular associations takes place not only in a cross section, but also along the length of the seminiferous tubule (Perey et al., 1961). Therefore, a portion of tubule displaying one type of cellular association is followed by a portion of tubule displaying the

stage immediately preceding or following in the seminiferous epithelial cycle. There is a continuity of the segmental order (Perey et al., 1961). Each complete spatial series of cellular associations is called spermatogenic wave. If the stages 1 through 8 succeed each other along the length of the seminiferous tubule, the sequence is referred to as a regular spermatogenic wave, which is approximately 10 mm long in bulls. Variations, such as repetition of wave fragments (1-2-3-4-1-2-3-4) or inversions (1-2- 3-4-5-4-3-2), seem to occur more frequently, however, exactly what determines the spermatogenic cycles, segments, and waves is not known at this time (Wrobel, 1998).

2.3.2.2. Testicular interstitial tissue (intertubular tissue)

Interstitial tissue fills up the spaces between the seminiferous tubules and contains all blood and lymph vessels as well as nerves of the testicular parenchyma (Fawcett et al., 1973; Setchell et al., 1994). While Leydig cell is widely recognized as a major cell type of the interstitial compartment of the mature testis, a number of other cells have also been reported in this region. These cells include fibroblasts, light intercalated cells, macrophages, lymphocytes, plasma cells, occasional mast cells, and undifferentiated cells of mesenchymal origin (Fawcett et al., 1973; Wrobel et al., 1981; Bloom and Fawcett, 1986; Maddocks and Setchell, 1988; de Kretser and Kerr, 1994; Wrobel, 1998). Species-specific differences in the intertubular tissue organization are reported by Fawcett et al. (1973), who described three patterns of arrangements. In the first group (guinea pig, chinchilla, rat and mouse), Leydig cells comprise a small fraction of the testicular volume, and occur in clusters closely applied to blood vessels. The greater part of the interstitium is however occupied by extensive lymphatic sinusoids of irregular outline. The majority of large mammals (second group), including bull, ram, elephant, monkey and man, have a very different interstitial organization. In these species, Leydig cells do not have such an obvious association with blood vessels but present in clusters of varying size scattered in an edematous loose connective tissue, which is drained by conspicuous lymph vessels located centrally or eccentrically in each intertubular area. In the third group that includes the domestic boar, warthog, zebra, and naked mole rat, closely packed Leydig cells occupy large intertubular spaces and comprise 20-60% of the testicular volume. There is very little interstitial connective tissue in these species, and small lymphatic vessels are infrequently encountered.

Leydig cells

The mammalian Leydig cells are relatively large, polymorphous cells with spherical eccentrically located nuclei. They constitute approximately 1% of the entire testicular volume

in adult rams, approximately 5% in bulls, and 20 to 30% in boars. In seasonally breeding males (e.g., camel), interstitial cell volume and number may change during the year (Wrobel, 1998). Interstitial endocrine cells occur in cords or clusters. Not every cell is therefore in close contact with a capillary. The large spherical nucleus contains a small amount of peripherally disposed heterochromatin and one or two prominent nucleoli. Adjacent to the nucleus is a large clear area that is found in electron micrographs to be occupied by a well-developed Golgi apparatus. Although the Golgi complex is prominent and responds to gonadotropic stimulation by enlargement, the role of this organelle in the biosynthetic and secretory processes of this cell type is not known, whereas, there is no visual evidence of accumulation of a product in secretory granules in the Golgi region (Wrobel et al., 1981; Bloom and Fawcett, 1986; Maddocks and Setchell, 1988; de Kretser and Kerr, 1994; Wrobel, 1998). The cytoplasm is acidophilic in routine preparations and may contain a number of empty vacuoles where lipid droplets have been extracted. In common with other steroid-secreting endocrine cells, the most striking ultrastructural feature of Leydig cell is extensive smooth endoplasmic reticulum (Bloom and Fawcett, 1986; de Kretser and Kerr, 1994). Cisternal profiles of the granular reticulum are also present, but the bulk of the cytoplasm is filled with a branching and anastomosing system of smooth-surfaced tubules. These membranes contain the enzymes necessary for several of the steps in the biosynthesis of androgenic steroids (Bloom and Fawcett, 1986; de Kretser and Kerr, 1994; Wrobel, 1998). The mitochondria possess tubular cristae and are involved in the first step of steroid hormone production, e.g., transformation of cholesterol to pregnenolone. Lipid inclusions are found in all species but are particularly abundant in cats (Wrobel, 1998). Bovine Leydig cells are further characterized by an abundance of ribosome-associated endoplasmic reticulum, by mitochondria often containing crystalloid structures and displaying both tubular and lamelliform cristae, as well as by a relative paucity of lipid droplets and lysosomes. In addition, between adjacent Leydig cells intercellular canaliculi and gap junctions are frequently encountered (Wrobel et al., 1981; Wrobel, 1998).

Functions of Leydig cells

Leydig cells are the most important source of androgen. More than 90% of all androgens in the organism are produced by the testis. Among the main functions of testosterone (to be effective, in some tissues, testosterone must be converted into dihydrotestosterone by the enzyme 5α-reductase) are (a) the prenatal maintenance of the Wolffian duct and its differentiation into deferent duct and epididymis; (b) triggering of the growth and

maintenance of the function of the penis, male accessory glands, and secondary sex characteristics; (c) promotion of normal sexual behavior (libido); (d) control of spermatogenesis (together with follicle stimulating hormone (FSH)); (e) negative feedback action on the hypophysis and hypothalamus; and (f) general anabolic effects (Wrobel, 1998).

Light intercalated cells (LIC)

LIC comprise a regular constituent of the bovine intertubular compartment. They are a population of electron-lucid, irregularly shaped cells with slender, pleomorphic processes. Ultrastructurally, these cells have few mitochondria and lysosomes, poor developed endoplasmic reticulum and conspicuous microtubules. In addition, no special junctions are established between LIC and any other adjoining cell type. These cells are believed to be involved in testicular androgen storage and distribution (Wrobel et al., 1981).

Interstitial testicular macrophages and other mononucleated cells

Although the presence of macrophages, fibroblasts, lymphocytes, plasma cells and more rarely mast cells have been recognized for many years, very little is known of their functions in the testis (de Kretser and Kerr, 1994). In rat, specialized contacts are noted between Leydig cells and macrophages (Hutson, 1992). In addition, there is an approximate ratio of four to one between these cells in the normal rat testis (Bergh, 1985). The close association of these macrophages with Leydig cells suggests some functional association and the macrophages can be seen to engulf portions of Leydig cell cytoplasm (Miller et al., 1983). Furthermore, macrophages may play a role in Leydig cell steroidogenesis whereas their depletion from the testis leads to a reduction in testosterone secretion (Setchell et al., 1994). Most of the other mononucleated cells may also be functionally linked to Leydig cells, since steroidogenesis by hamster Leydig cells is enhanced in the presence of mast cells (Mayerhofer et al., 1989).

2.3.2.3. Intratesticular excurrent duct system

Bovine intratesticular excurrent duct system composed of terminal segment of the convoluted seminiferous tubules, tubuli recti, and rete testis. Spermatozoa are no longer produced within terminal segment and this portion is consequently considered as a part of the intratesticular excurrent duct system (Wrobel et al., 1982). The terminal segment of the seminiferous tubules is a short transitional distal zone that is lined by cells designated as modified Sertoli cells and connects between seminiferous tubules and tubuli recti. Ultrastructure of modified Sertoli cells of terminal segment is now available for several mammalian species including rat (Osman, 1978a), rabbit (Osman, 1979), ram, and goat (Osman and Ploen, 1979), boar

42

(Osman, 1978b), bovine (Osman and Ploen, 1979; Wrobel et al., 1982), monkey (Dym, 1974), and man (Lindner, 1982). These studies have shown that the epithelial lining of terminal segments consists of modified supporting cells which posses many features in common with the typical Sertoli cell in the spermatogenic portion of the seminiferous tubules. In bovine, each terminal segment is surrounded by a vascular plexus and subdivided into a transitional region, middle portion, and terminal plug. Modified supporting cells of the middle portion and terminal plug no longer display the typical Sertoli-Sertoli cell junctions seen in the transitional region and seminiferous tubule proper (Wrobel et al., 1982). The functions ascribed to modified Sertoli cells of the terminal segment include fluid transport and secretory activity as well as phagocytosis and intracytoplasmic degradation of spermatozoa (Dym, 1974; Osman, 1978b; Osman and Ploen, 1979; Wrobel et al., 1982). The terminal segment is joined to the rete by a tubulus rectus, which is really a narrow extension of the rete proper and is lined with similar cells (Setchell et al., 1994). The ultrastructure of the tubuli recti has been studied in the testis of rat, ram, rabbit, goat, bull, and man (Osman and Ploen, 1978b; Roosen-Runge and Holstein, 1978; Hees et al., 1987). In human, up to six seminiferous tubules can join a single tubulus rectus (Roosen-Runge and Holstein, 1978). The tubuli recti are lined with a simple epithelium that varies in height, from squamous to tall columnar according to species and regions. The cells are characterized by extensive lateral and tortuous basal plasma membranes and a luminal border with microvilli (Osman and Ploen, 1978b). A distal segment of the tubuli recti is found in bovine only and is characterized by a high epithelium, which is thrown into folds giving the lumen a festooned appearance (Osman and Ploen, 1978b). It is suggested that the epithelial cells of the tubuli recti are involved in fluid exchange and phagocytosis of spermatozoa (Osman and Ploen, 1978b; Sinowatz et al., 1979). The rete testis is a complicated network of intercommunicating channels that lies in the mediastinum of the testis parallel to the axis of the epididymis (de Kretser and Kerr, 1994). According to the location, rete testis may be either superficial/marginal as in rat, mice, hamster and man (Dym, 1976; Roosen-Runge and Holstein, 1978) or axial/central as found in the monkey, cat, dog, guinea pig, ram, rabbit, and bull (Dym, 1976; Hees et al., 1987). Further on, Roosen-Runge and Holstein (1978) have divided the rete testis into septal, mediastinal and extratesticular rete. The septal rete testis consists of the zone of the tubuli recti, which drain the seminiferous tubules. The region of the mediastinal rete is characterized by an irregular network of cylindrical strands, the chordae retis, which are considered as a common feature of bovine and human testis (Roosen-Runge and Holstein, 1978; Hees et al., 1989). An extratesticular rete is observed in the rat, mouse, hamster, monkey, ram, guinea pig, and man (Dym, 1976; Roosen-

Runge and Holstein, 1978), but not in bovine (Dym, 1976; Hees et al., 1989). The ultrastructure of cells lining the rete testis is well documented and seems to be rather similar in man (Roosen-Runge and Holstein, 1978), higher mammals (Dym, 1976; Hees et al., 1989), marsupials (Rodger, 1982) and even in birds (Barker and Kendall, 1984). The rete testis of buffalo has a stratified epithelium (Goyal and Dhingra, 1973), but in most other species, the cells are a mixture of columnar, cuboidal, and squamous, with a few intraepithelial lymphocytes and macrophages (Dym, 1976; Hees et al., 1989). The bovine testis has a central mediastinum consisting of longitudinally oriented rete channels and spacious lymph vessels embedded in stroma of the mediastinum. The latter represents a contractile-elastic unit and is composed of myofibroblasts, collagen bundles, and accumulations of elastin connecting the myofibroblasts (Hees et al., 1989). As described for tubuli recti, rete testis epithelial is capable of phagocytosing spermatozoa (Dym, 1976; Roosen-Runge and Holstein; 1978; Sinowatz et al., 1979)

2.3.2.4. Blood vessels, nerves, and lymphatics of the testis

The testicular artery has a straight abdominal portion and becomes highly coiled after reaching the spermatic cord. As the artery reaches the testis, it courses parallel to the epididymis and is embedded in the tunica albuginea. The testicular artery divides at the caudal testicular pole to form the arterial contributions to vascular layer of the tunica albuginea (Wrobel, 1998). Within the septula testis, centripetal arteries course to the mediastinum testis, where they form heavily convoluted coils. From these convolutes, smaller centrifugal arteries return to supply the testicular parenchyma. Most of the testicular veins empty into superficial veins situated in the tunica albuginea. These converge at the base of the spermatic cord to form the pampiniform plexus, which completely surrounds the windings of the testicular artery. This remarkable vascular topography in the mammalian spermatic cord is believed to allow venous-arterial steroid hormone transfer and to cool the arterial blood entering the testis. Thus, testicular androgen levels are increased and testicular temperature is lowered; these are two important requirements for spermatogenesis (Wrobel, 1998). The testis is supplied by nerves, which reach the gonad via three different routes: with the blood vessels of the spermatic cord (funicular nervous contribution), by the mesorchium (mesorchial nervous contribution), and by the ligamentous bridge between epididymal tail and testis (caudal nervous contribution) (Wrobel and Abu-Ghali, 1997). Nerves of the bovine testis are concentrated in the stromal compartments of the gonads, i.e. tunica albuginea, mediastinum and perivascular connective tissue (the so-called septula testis). The testicular lobules

containing the seminiferous tubules, Leydig cells, and the parenchymal microcirculation are completely devoid of any innervation in adult bull (Wrobel and Abu-Ghali, 1997). The lymphatics show considerable variation in pattern from species to species. In the common laboratory rodents, they form very extensive peritubular sinusoids. The aggregations of Leydig cells in these species are centrally located and closely associated with the walls of the blood vessels. They are surrounded by sinusoidal lymphatics. The steroid-secreting cells are thus interposed between the blood vascular elements on the one side and the lymphatic sinusoids on the other, and release their hormone into both. In larger species such as ram, bull, and man, the lymphatics are not sinusoidal but form thin-walled vessels more or less centrally located in the intertubular areas. The Leydig cells are not intimately related to either the blood vessels or the lymphatics, but evidently, they release androgen into the abundant extracellular fluid of the interstitial tissue, whence it diffuses to the tubules for its local effect on spermatogenesis, and to the vessels for its effect on distant target organs (Bloom and Fawcett, 1986).

2.4. Lectin histochemistry

Several approaches emphasize that the cell surface glycoconjugates have fundamental roles in a variety of cell functions, including development, growth regulation, and cellular locomotion (Hakomori, 1981; Gabius, 1987). Lectins have a specific binding affinity for the sugar residues of glycoconjugates; therefore, they are used as histochemical reagents to investigate the distribution of glycoconjugates in various tissues.

2.4.1. Definition

Originally, the term lectin (Latin legere: to choose) was coined by Boyed and Shapleigh (1954) to refer to a group of plant seed agglutinins, some of which are human blood group specific. With the discovery of carbohydrate-binding proteins in diverse biological sources (e.g., bacteria, sponges, sera of fish, snails, hemolymph of lobsters), the term lectin has been expanded to include sugar-binding proteins from any source (Ashwell and Morell, 1977). The most accepted definition of the lectin is given by Goldstein et al. (1980) as a carbohydrate-binding protein or glycoprotein of non-immune origin, which agglutinates cells and/or precipitates glycoconjugates. The lectins have also been defined as "proteins of non immunogloblin nature capable of specific recognition and reversible binding to carbohydrate moieties of complex carbohydrate without altering the covalent structure of any of the recognized glycosyl ligand" (Kocourek and Horejsi, 1983). These proteins of plant,

vertebrate, and invertebrate origin have specific affinities for particular terminal sugar residues or specific sugar sequences (Goldstein and Hayes, 1978). For this unique property, lectins have been introduced as histochemical reagents to study the distribution of glycoconjugates in various normal and malignant cells and tissues (Faraggiana et al., 1982; Spicer et al., 1983; Arya and Vanha-Perttula, 1984, 1985, 1986; Ertl and Wrobel, 1992, Verini-Supplizi et al., 2000; Pinart et al., 2001, 2002).

2.4.2. Physicochemical characters of the lectin

The binding of lectins to sugar moieties is comparatively weak. It does not result in the formation of covalent bonds but is reversible, like the reaction of an enzyme with a substrate. Indeed the precipitation reaction between a lectin and suitable polysaccharides or glycoprotein is analogous in many aspects to an antigen-antibody reaction, in which the lectin plays the role of antibody and the polysaccharide or glycoprotein the role of the antigen (Sharon, 1977). The composition, molecular weight, structure and number of the subunits as well as the number of carbohydrate-binding sites per molecule have distinguished several types of lectin from each other. For examples, the molecular weights are between 19.000 (*Phytolacca americana agglutinin*, Pa5) and 340.000-500.000 (*Limulus polyphemus agglutinin*) and the number of the subunits varies between two and four. In special cases up to 18 subunits may also be found (Goldstein and Hayes, 1978). Characteristically, all lectin molecules bear at least two carbohydrate-binding sites, a property essential to their ability to agglutinate cells or glycoconjugates. This character is of special importance to differentiate between lectins and other types of sugar-binding proteins. The latter include sugar specific enzymes (glycosidases, glycotransferases, etc.), transport proteins, hormones (thyroid-stimulating hormones, follicle-stimulating hormones, etc.), and toxins. In spite of similarities of these lectin-like molecules to the true lectins, most of them bear only one carbohydrate-binding site and have no ability to agglutinate cells or precipitate glycoconjugates (Goldstein et al., 1980). Most of lectins are metalloproteins, as they bind to Ca^{2+} and Mn^{2+}. Removal of bound Ca^{2+} and Mn^{2+} from native lectin results in a loss of carbohydrate-binding activity, suggesting an association between the metal-binding and saccharide-binding sites. In general, lectins tolerate very little variation at C-3 and C-4 of the sugar they bind, but, many lectins tolerate some variation at C-2 of the sugar, which they bind (Goldstein and Hayes, 1978).

2.4.3. Carbohydrate-binding specificity of lectins

It is of vital importance to establish the carbohydrate-binding specificity of a lectin in order that it may be a useful tool in biochemical and immunochemical studies. The carbohydrate-binding specificity of lectins was originally determined by measuring the ability of free monosaccharides or their alkyl glycosides to inhibit lectin-induced agglutination of cells or glycoconjugates. In general, lectins recognize D-pyranose sugars and in most instances, they express rather stringent, configurational, and structural requirements in the interacting constituents (Gallagher, 1984). It is extremely interesting and significant that most plant and animal lectins have been classified into a rather limited number of carbohydrate-binding groups (Goldstein and Poretz, 1986). These include the mannose/glucose-binding lectins, the galactose-binding lectins, N-acetylgalactosamine-binding lectins, the N-acetylglucosamine-binding lectins, the L-fucose-binding lectins, sialic acid-binding lectins, and lectins with complex carbohydrate-binding sites (table 2). This classification scheme proposed a system of nomenclature that first states the origin of the lectin and then, in parenthesis, cites the sugar-binding specificity and, if relevant, denotes the anomeric specificity or preference. However, this scheme does not take into account the influence on lectin reactivity of either the position of the complementary sugar in carbohydrate sequence (reducing terminal or internal) or of the synergistic effects of certain neighboring sugars (Gallagher, 1984).

Table 2: Lectin classified on the basis of their carbohydrate-binding specificity (Goldstein and Poretz, 1986).

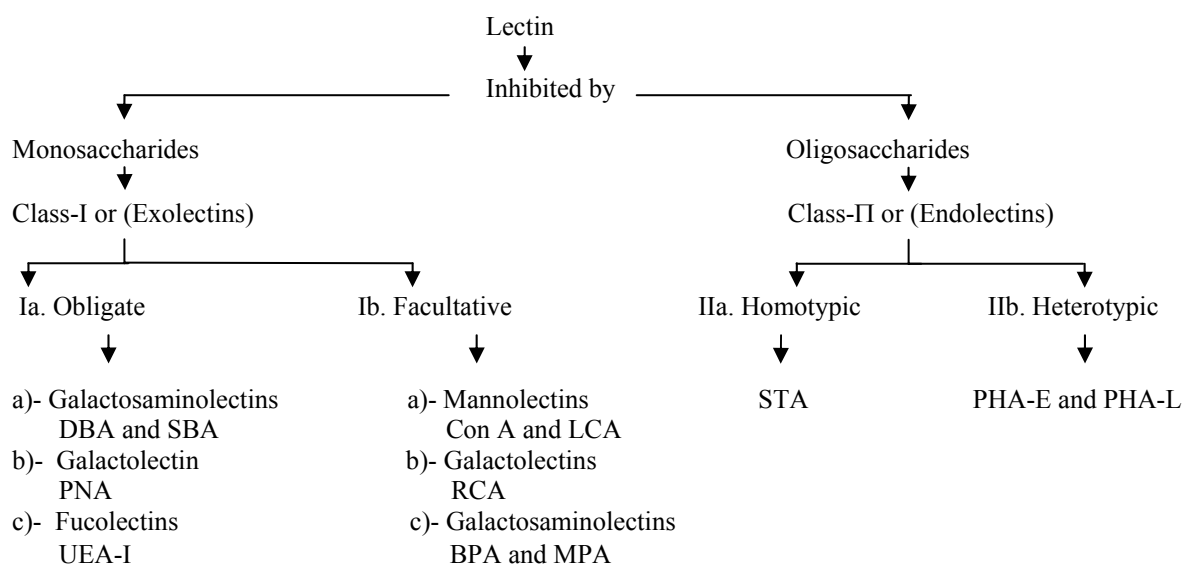| Sugar specificity	Latin name	Acronym
I. D-Mannose/D-Glucose-binding lectins	*Canavalia ensiformis*	Con A
	Lens culinaris	LCA
	Pisum Sativum	PSA
II. D-Galactose-binding lectins	*Arachis hypogaea*	PNA
	Griffonia simplicifolia I	GSA-I
	Ricinus communis	RCA-I and RCA-II
	Erythrina cristagalli	ECA
III. N-acetyl-D-galactosamine (GalNAc)-binding lectins	*Phaseolus limensis*	LBA
	Glycine max	SBA
	Helix pomatia	HPA
	Bauhinia purpurea	BPA
	Maclura pomifera	MPA
	Visea villosa	VVA
	Dolichos biflorus	DBA
IV. N-acetyl-D-glucosamine (GlcNAc)-binding lectins	*Triticum vulgare*	WGA
	Ulex europaeus II	UEA-II
	Griffonia simplicifolia II	GSA-II
	Laburnum alpinum	LAA
	Solanum tuberosum	STA
V. L- Fucose-binding lectins	*Ulex europaeus I*	UEA-I
	Lotus tetragonolobus	LTA
VI. Sialic acid-binding lectins	*Limulus polyphemus*	LPA
	Limax flavus	LFA
VII. Lectin with complex carbohydrate-binding sites	*Phaseolus vulgaris*	PHA-E and PHA-L

Lectins are also classified into two classes (Fig. 4) based upon their sensitivity to different carbohydrate inhibitors (Gallagher, 1984).

1. Class-Ι lectins (simpler binding mode):

In this case, lectin reactivity is directed principally towards a particular monosaccharide constituent in the ligand. These are the lectins, which are strongly inhibited by low concentrations of the appropriate free sugars or their methyl glycosides. Since all the class-I lectins will bind to appropriate external, non-reducing sugars in the complex saccharides, they may be described as *exolectins*. Two sub-classes may also be recognized: those, which have a stringent requirement for end-chain sugars, *obligate exolectins*, and those, which recognize both, end-chain and internal sugars, *facultative exolectins*.

2. Class-Π lectins (complex binding mode):

In the more complex binding mode, lectins react only with specific carbohydrate sequences and none of the individual sugars in the sequences plays a predominant role in the binding process. Potent inhibition of the agglutinating properties of these lectins usually requires oligosaccharide "haptens" of similar or identical structure to binding domains on the agglutinated materials. These lectins may thus be described as *endolectins*. They can be divided into the *homotypic endolectins*, which bind most strongly to homotypic sugar sequences, and *heterotypic endolectins*, which show the highest affinity for heterotypic sequences. This classification provides a simplified method, suitable for written and verbal communication, for describing the carbohydrate-binding properties of lectins (Gallagher, 1984).

Lectin
↓
Inhibited by

Monosaccharides — Oligosaccharides

Class-I or (Exolectins) — Class-Π or (Endolectins)

Ia. Obligate	Ib. Facultative	IIa. Homotypic	IIb. Heterotypic

a)- Galactosaminolectins   a)- Mannolectins   STA   PHA-E and PHA-L
   DBA and SBA   Con A and LCA
b)- Galactolectin   b)- Galactolectins
   PNA   RCA
c)- Fucolectins   c)- Galactosaminolectins
   UEA-I   BPA and MPA

Fig 4: Classification of lectin based upon their sensitivity to different carbohydrate inhibitors (Gallagher, 1984).

2.4.4. Biological roles of the lectins:

There is considerable support for the hypothesis that lectins function primarily as recognition molecules. This function may be expressed differently in various organisms and also in different organs or tissues of the same organism. These biological roles can be summarized in the following table (Lis and Sharon, 1986).

Table 3: Roles of lectins in nature

Plants	1-Attachment of nitrogen-fixing bacteria to legumes 2-Protection against phytopathogens (fungal, bacterial, and viral pathogen)
Animals	1-Endocytosis and intracellular translocation of glycoproteins 2-Regulation of cellular migration and adhesion 3-Recognition determinants in non-immune phagocytosis 4-Binding of bacteria to epithelial cell
Microorganisms	1-Attachment of bacteria and parasites (amoeba and plasmodium) to the host cells. 2-Recognition determinants in non-immune phagocytosis 3-Recognition determinants in cells adhesion of slime molds

2.4.5. Applications of the lectins:

The earliest applications of lectins, still in wide use, were for blood typing and for mitogenic stimulation of lymphocytes (Lis and Sharon, 1986). Now, the established uses of lectins are widely distributed in different branches of sciences. These are briefly reviewed in the following.

2.4.5.1. Application of lectins in histology

Lectins have been employed histologically in several areas (reviewed by Walker, 1988):

a) Reagent for mucin histochemistry

Lectins, in combination with oxidation-reduction sequences and enzyme digestion, have been used to refine the broad classification obtained by standard mucin histochemistry, and as such have been used to identify different subclasses of secretory and cell surface glycoconjugates.

b) Mapping of binding sites in animal and human tissue

At the level of tissue, lectins have been used as specific probes for various cell types as well as cells at various stages of differentiation or maturation. At the level of organ histology, lectins have been used to as probes for delineation of functional and anatomic segments or microenvironments. For example in a complex tissue such as kidney, lectin can be of value in the identification of the different structures, and can reveal heterogeneity in the distribution of glycoconjugates.

c) Characterization of glycoprotein alterations in diseased states

This can only be undertaken if the corresponding normal tissues have been examined under the same condition. For example, lectin histochemistry can provide a reliable specific diagnostic pattern for some glycoprotein storage diseases.

d) Identification of glycoconjugates alterations with malignancy

Lectins have been employed to differentiate between normal and malignant cells.

2.4.5.2. Application of lectin in cell biology:

In cell biology, lectins have been most successfully used as probes for cellular structures rich in glycoconjugates such as cell surface membrane or organelles involved in synthesis, storage, or turnover of complex carbohydrate. Lectins are most useful for biochemical isolation of cell surface macromolecules such as thyroid cell glycoproteins, thyroid receptors, or insulin receptors (Damjanov, 1987). Lectins have also been employed to separate germ cells from somatic cells (Lis and Sharon, 1986). Other major lectins applications are summarized in the table 4.

Table 4: Major applications of lectins (Liener et.al., 1986)

1)- Isolation, purification, and structural studies of carbohydrate-containing polymers
2)- Investigation of complex carbohydrate structures on surfaces of animal cells, bacteria, and viruses and of subcellular particles
3)- Investigation of the architecture of cell surfaces and its change upon malignant trans-formation
4)- Blood typing, structural studies of the blood group substances; identification of new blood types; diagnosis of secretors
5)- Isolation of lymphocyte subpopulations and of a stem cell-enriched fraction of bone marrow suitable for transplantation
6)- Studies of the genetics, biosynthesis, and function of cell-surface glycoconjugates
7)- Mitogenic stimulation of lymphocyte; studies of events occurring upon initiation of cell division; studies on lymphokines; studies of chromosomal constitution of cells and detection of chromosomal abnormalities
8)- Studies of specific carbohydrate binding sites on proteins

2.4.6. Factors affecting lectin-binding affinity

Lectins are specifically bound to sugars and sugars sequences in glycoconjugates. This binding is affected by many factors such as the neighboring sugars and even the sugars located in the core of the carbohydrate chain. Therefore, the lectins with the same terminal sugar specificities are not necessarily bound to the same glycoconjugates (Dulaney, 1979). Practical evidence has shown that the result obtained by lectin histochemistry are influenced

by the mode of fixation used for the tissue and that the differences with lectin staining after different fixation methods can be marked (Malmi and Söderstrom, 1988). An excellent result was obtained after fixation in Bouin׳s fluid or formaldehyde with acetic acid while poor result was obtained after the fixation in formaldehyde and paraffin embedding. The effects of fixation and tissue processing on lectin staining are probably mediated via two mechanisms. The fixative employed may alter the sugars responsible for the specific lectin binding or the glycoproteins in tissues may be dissolved and lost during the fixation or other tissue processing. In addition to the aforementioned factors, the lectin concentration, temperature, incubation period and pH value play an important role as factors greatly affect the result of lectins staining (Dulaney, 1979; Roth, 1983; Allison, 1987; Malmi and Söderstrom, 1988).

2.4.7. Lectin binding sites of the testis

Lectin histochemical analysis of the testes has allowed the staining patterns of spermatogenic cells to be visualized, thus allowing determination of the sequential glycosylation processes of acrosome development in rats (Arya and Vanha-perttula, 1984; Söderstrom et al., 1984; Malmi et al., 1990; Jones et al., 1993; Martinez-Menargues et al., 1999), mice (Lee and Damjanov, 1984; Arya and Vanha-perttula, 1986), hamsters (Ballesta et al., 1991), cat (Prem, 1992), dog (Montkowski, 1992), and humans (Malmi et al., 1987; Wollina et al., 1989; Arenas et al., 1998). Limited information is available on the farm animals such as bulls (Arya and Vanha-perttula, 1985; Ertl and Wrobel, 1992), goats (Kurohmaru, 1991), horse (Verini-supplizi et al., 2000) and boar (Cavola et al., 2000; Pinart et al., 2001, 2002). In this text, we consider some of these studies; however, full report about the distribution of lectin in different animal species is available in table 5.

In humans, a positive reaction to ConA was found in Sertoli, germ, and Leydig cells. Reaction to WGA was moderately intense in spermatogonia, spermatocytes, peritubular cells, and Leydig cell whereas was stronger in Sertoli cells, spermatids, and the matrix of the lamina propria. A slight reaction to PNA lectin was observed in the Sertoli cells, spermatogonia, and Leydig cells. Labeling was more intense in spermatocytes, spermatids, and peritubular cells. SBA lectin showed an intense reaction in the spermatids and a slight reaction in the lamina propria while no reaction to LTA was observed. UEA-I lectin labeled the lamina propria intensely whereas the seminiferous epithelium and Leydig cells were only slightly labeled (Arenas et al., 1998). In rat, some lectins such as UEA-I, SBA, and DBA gave rather specific staining of the mature acrosome, while others as PNA and RCA-I showed affinity for the early stages of acrosome formation or had a wide affinity for germinal and non-germinal cells

51

as ConA and WGA (Arya and Vanha-Perttula, 1984). In mouse, HAA, HPA, GSA-I, and UEA-II reacted only with spermatozoa. PNA, GSA-II, SBA, VVA, BPA, RCA-I, and RCA-II binding sites were recognized in spermatocytes and spermatozoa. WGA, PEA, LCA, and MPA were detected in spermatogonia, spermatocytes, and spermatozoa in increasing order of intensity. ConA, Suc.ConA, LAA STA, LTA, LPA, PHA-E, PHA-L, UEA-I, and LBA reacted with all spermatogenic cells with equal intensity (Lee and Damjanov, 1984). In cat, Con A, reacted with the entire seminiferous epithelium while GSA-I, GSA-II, MPA, PNA, and SBA expressed exclusively in the sperm (Prem, 1992). In dog, some lectins bind to the germinal epithelium (PNA, SBA) only others bind to the germinal epithelium as well as to the interstitial tissue (GSA-I, Con A, WGA, BPA, MPA). On the other hand, UEA-I, DBA, and GSA-II do not show any binding affinity to the canine testicular cells (Montkowski, 1992). In boars, the apical cytoplasm of Sertoli cells exhibited abundant glucosyl (ConA), galactosyl (HPA, DBA, SBA, and PNA), and fucosyl (AAA) residues. Spermatogonia and spermatocytes contained abundant glucosyl (ConA) and fucosyl (AAA) residues. In spermatids, galactosyl (SBA, and PNA) and glucosyl (ConA) residues increased progressively throughout spermatogenesis, and fucosyl (AAA) residues decreased (Pinart et al., 2001, 2002). In adult horse, the lectins showed a variable affinity for spermatids and Sertoli cell apical extensions. SBA, PNA, RCA-I, and WGA bound to the acrosomal structures of spermatids, whereas GSA-II labeled these structures only during Golgi and cap phases (Verini-Supplizi et al., 2000). The lectin-binding pattern of Sertoli cells was very similar to that of acrosome of spermatids during the maturation phase. In sexually immature horses, only the degenerated germinal cells and the Leydig cells showed reactivity towards lectins. The first cells reacted with SBA and DBA while the latter cells reacted with SBA, PNA, WGA, GSA-II, ConA, LCA, and DBA (Verini-Supplizi et al., 2000). In goat, DBA and GS-I were negative in the seminiferous epithelium, but SBA, GS-II, and PNA were positive in the acrosomal vesicle of the Golgi-phase spermatids and in the acrosome of the cap-, acrosome-, and maturation-phase spermatids. In addition, PNA was also positive in the plasma membrane and cytoplasm of the spermatogenic cells from the late pachytene spermatocytes to the maturation- phase spermatids. No reaction was observed with Sertoli or Leydig cells (Kurohmaru, 1991).

Table 5: Lectin-binding sites in the testis of different mammalian species

Lectin	acronym	Species	Reactive cells	References
I. D-Mannose/D-Glucose-binding lectins	Con A	Human	Sc, Spg, Spc, Spd, Lc, Lp	Malmi et al., 1987; Wollina et al., 1989; Arenas et al., 1998
		Rat	Sc, Spg, Spc, Spd, Lc, Lp, Mc	Arya and Vanha-Perttula, 1984
		Mouse	Sc, Spg, Spc, Spd, Lc	Lee and Damjanov, 1984; Arya and Vanha-Perttula, 1986
		Cat	Sc, Spg, Spc, Spd, Lc, Lp	Prem, 1992
		Dog	Sc, Spg, Spc, Spd, Lc	Montkowski, 1992
		Boars	Sc, Spg, Spc, Spd	Pinart et al., 2001, 2002
		Horse	Lc*	Verini-Supplizi et al., 2000
	LCA	Human	Spg, Spc, Spd, Lc, Lp	Malmi et al., 1987
		Mouse	Sc, Spg, Spc, Spz, Lc	Lee and Damjanov, 1984
		Horse	Lc*	Verini-Supplizi et al., 2000
	PSA /PEA	Mouse	Sc, Spg, Spc, Spz, Lc	Lee and Damjanov, 1984
II. D-Galactose-binding lectins	PNA	Human	Sc, Spg, Spc, Spd, Lc, Lp, Mc	Arenas et al., 1998
		Rat	Sc, Spd, Lc, Lp	Arya and Vanha-Perttula, 1984
		Mouse	Sc, Spc, Spd, Spz, Lc, Lp	Lee and Damjanov, 1984; ; Arya and Vanha-Perttula, 1986
		Cat	Spd	Prem, 1992
		Dog	Spd, Spz	Montkowski, 1992
		Boars	Sc, Spd	Pinart et al., 2001, 2002
		Horse	Sc, Spd, Spz, Lc*	Verini-Supplizi et al., 2000
		Goat	Spc, Spd	Kurohmaru et al., 1991
	GSA-I	Human	Spz	Lee and Damjanov, 1985
		Mouse	Spz	Lee and Damjanov, 1984
		Goat	-ve	Kurohmaru et al., 1991
	RCA-I	Human	Spc, Spd, Spz, Lc, Lp	Lee and Damjanov, 1985; Malmi et al., 1987
		Rat	Sc, Spg, Spc, Spd, Lc, Lp, Mc	Arya and Vanha-Perttula, 1984
		Mouse	Sc, Spc, Spd, Spz, Lc, Lp	Lee and Damjanov, 1984; Arya and Vanha-Perttula, 1986
		Horse	Sc, Spd, Spz	Verini-Supplizi et al., 2000
	RCA-II	Human	Spg, Spc, Spd, Spz, Lc, Lp	Lee and Damjanov, 1985; Wollina et al., 1989
		Mouse	Spc, Spz	Lee and Damjanov, 1984
III. N-acetyl-D-galactosamine (GalNAc)-binding lectins	DBA	Human	-ve	Arenas et al., 1998
		Rat	Spd	Arya and Vanha-Perttula, 1984
		Mouse	Spd, Lc, Lp	Arya and Vanha-Perttula, 1986
		Boar	Sc	Pinart et al., 2001, 2002
		Horse	dgc	Verini-Supplizi et al., 2000
		Goat	-ve	Kurohmaru et al., 1991
	SBA	Human	Spd, Spz, Lc, Lp	Lee and Damjanov, 1985; Malmi et al., 1987; Arenas et al., 1998
		Rat	Spd	Arya and Vanha-Perttula, 1984
		Mouse	Spd, Spz, Lc, Lp	Lee and Damjanov, 1984; Arya and Vanha-Perttula, 1986
		Boar	Sc, Spd	Pinart et al., 2001, 2002
		Horse	Sc, Spd, Spz	Verini-Supplizi et al., 2000
		Goat	Spd	Kurohmaru et al., 1991
	HPA	Human	SC, Spg, Spc, Spd, Spz, Lc, Lp	Lee and Damjanov, 1985; Malmi et al., 1987, Wollina et al., 1989; Arenas et al., 1998
		Mouse	Spz	Lee and Damjanov, 1984
		Boar	Sc	Pinart et al., 2001, 2002
	VVA	Human	Spd, Spz	Lee and Damjanov, 1985
		Mouse	Spc, Spz	Lee and Damjanov, 1984
	BPA	Human	Spd, Spz	Lee and Damjanov, 1985
		Mouse	Spc, Spz	Lee and Damjanov, 1984
	LBA	Human	-ve	Lee and Damjanov, 1985
		Mouse	Sc, Spg, Spc, spd, Spz	Lee and Damjanov, 1984
	MPA	Human	Sc, Spg, Spc, spd, Spz	Lee and Damjanov, 1985
		Mouse	Sc, Spg, Spc, Spz, Lc	Lee and Damjanov, 1984

Table 5: Continued

IV. N-acetyl-D-glucosamine (GlcNAc)- binding lectins	WGA	Human	Sc, Spg, Spc, Spd, Lc, Lp, Mc	Lee and Damjanov, 1985; Malmi et al., 1987; Arenas et al., 1998
		Rat	Spg, Spc, Spd, Sc, Lc, LP, Mc	Arya and Vanha-Perttula, 1984
		Mouse	Sc, Spg, Spc, Spz, Lc, Lp	Lee and Damjanov, 1984; Arya and Vanha-Perttula, 1986
		Cat	Sc, Spg, Spc, Spz, Lc, Lp	Prem, 1992
		Dog	Spg, Spc, Spz, Lc, Lp	Montkowski, 1992
		Boars	Sc, Spg, Spc, Spd	Pinart et al., 2001, 2002
		Horse	Sc, Spd, Lc*	Verini-Supplizi et al., 2000
	UEA-II	Human	Spz	Lee and Damjanov, 1985
		Mouse	Spz	Lee and Damjanov, 1984
	GSA-II	Human	Spz	Lee and Damjanov, 1985
		Mouse	Spc, Spz	Lee and Damjanov, 1984
		Cat	Spd, Lc, Spz	Prem, 1992
		Dog	-ve	Montkowski, 1992
		Horse	Spd, Lc*	Verini-Supplizi et al., 2000
		Goat	Spd	Kurohmaru et al., 1991
	LAA	Mouse	Spg, Spc, Spd, Spz	Lee and Damjanov, 1984
	STA	Human	Spg, Spc, Spd, Spz	Lee and Damjanov, 1985
		Mouse	Spg, Spc, Spd, Spz	Lee and Damjanov, 1984
V. L- Fucose-binding lectins	UEA-I	Human	Sc, Spg, Spc, Spd, Spz, Lc, Lp, Mc	Malmi et al., 1987; Arenas et al., 1998
		Rat	Spd	Arya and Vanha-Perttula, 1984
		Mouse	Spg, Spc ,Spd, Spz, Lc, Lp	Lee and Damjanov, 1984; Arya and Vanha-Perttula, 1986
		Cat	-ve	Prem, 1992
		Dog	-ve	Montkowski, 1992
	LTA	Human	-ve	Arenas et al., 1998
		Mouse	Spg, Spc ,Spd, Spz	Lee and Damjanov, 1984
	AAA	Human	Sc, Spg, Spc, Spd, Lc	Arenas et al., 1998
		Boar	Sc, Spg, Spc, Spd	Pinart et al., 2001, 2002
VI. Sialic acid-binding lectins	LPA	Human	Spg, Spc, Spd, Spz, Lc, Lp	Lee and Damjanov, 1985
		Mouse	Spg, Spc ,Spd, Spz	Lee and Damjanov, 1984
VII. Lectin with complex carbohydrate- binding sites	PHA-E	Human	Spg, Spc, Spd, Spz	Lee and Damjanov, 1985
		Mouse	Spg, Spc, Spd, Spz	Lee and Damjanov, 1984
	PHA-L	Human	Spg, Spc, Spd, Spz	Lee and Damjanov, 1985
		Mouse	Spg, Spc, Spd, Spz	Lee and Damjanov, 1984

Sc: Sertoli cell; Spg: Spermatogonia; Spc: Spermatocytes; Spd: Spermatids; Spz: Spermatozoa; Lc: Leydig cells; Lp: Lamina propria; Mc: Myoid cells; -ve: negative; Lc*: Leydig cells of the prepubertal horse; dgc: degenerated germ cells

Lectin binding sites of bull testis

In contrast to Arya and Vanha-Perttula (1985), who did not succeed to demonstrate lectin staining in male postnatal prepubertal bovine germ cells and discussed a cyclic affinity of the Sertoli cells for some of the lectins, Ertl and Wrobel (1992) stated that the lectin affinity in the developing testicular tubules of bull testis was restricted to the germ cell line, while the Sertoli cells and their precursors remained completely unstained. DBA served as a selective marker for prespermatogonia. After the gradual onset of spermatogenesis, the lectins revealed staining of Golgi complexes of most germ cell stages. Inner and outer membranes of the acrosomal complex of spermatids, especially during Golgi and cap phase of spermiogenesis,

were intensely stained with PNA, RCA-I, and SBA. In the intertubular tissue, BS-I, RCA-I, and UEA-I bound to vascular endothelia. Compartments of the intertubular extracellular matrix were stained with ConA, RCA-I, UEA-I, and WGA but no reaction was recorded with the Leydig cells. According to the first authors, the Sertoli cells displayed a staining pattern that varied with the stages of the spermatogenic cycle. A moderate staining of the Sertoli cell processes around the spermatogenic cells was found with PNA, RCA-I, ConA, and WGA. After the release of the mature spermatozoa, the apical cytoplasmic extensions of the Sertoli cells were strongly stained with the same lectins. At a later stage of the cycle, staining was located in the body of these cells and eventually in the basal portion of the Sertoli cells. The lectin-binding site of bull testis is summarized in table 6.

Table 6: Lectin binding sites of bull testis

Lectin	Acronym	Arya and Vanha-Perttula (1985)	Ertl and Wrobel (1992)
I. D-Mannose/D-Glucose-binding lectins	Con A	Basement membrane of seminiferous tubules, proacrosomal granule, and Sertoli cells	Intertubular extracellular matrix
II. D-Galactose-binding lectins	PNA	Basement membrane of seminiferous tubules, Sertoli cells, proacrosomal granule, acrosomal cap and early acrosome	Golgi phase of spermiogenesis, cap phase of spermiogenesis, and maturation phase of spermiogenesis
	RCA-I	Basement membrane of seminiferous tubules, proacrosomal granule, Sertoli cells, and acrosomal cap	Golgi complex of prespermatogonia, Golgi phase of spermiogenesis, cap phase of spermiogenesis, and vascular endothelium
III. N-acetyl-D-galactosamine (GalNAc)-binding lectins	DBA	Basement membrane of seminiferous tubules and early and late acrosome	Golgi complex of prespermatogonia, Golgi complex of spermatogonium, maturation phase of spermiogenesis, cytoplasmic droplet, and acrosome phase of spermiogenesis
	SBA	Basement membrane of seminiferous tubules, spermatogenic cells, and early and late acrosome	Golgi phase of spermiogenesis, cap phase of spermiogenesis, and maturation phase of spermiogenesis
IV. N-acetyl-D-glucosamine (GlcNAc)-binding lectins	WGA	Basement membrane of seminiferous tubules, acrosomal cap, early acrosome, proacrosomal granule, and Sertoli cells	Golgi complex of prespermatogonia, Golgi complex of spermatogonium, Golgi phase of spermiogenesis, cap phase of spermiogenesis, and acrosome phase of spermiogenesis
V. L- Fucose-binding lectins	UEA-I	Basement membrane of seminiferous tubules, proacrosomal granule, Sertoli cells, and acrosomal cap	Intertubular extracellular matrix and vascular endothelium

3. MATERIALS AND METHODS

3.1. Tissue collection

The present study was performed on the testes of 32 bovine embryos and of 15 sexually mature bulls (Deutsches Fleckvieh). All samples were collected within 30 min after slaughtering from Munich local abattoir. The age of embryos (table 7) was calculated from the measured crown-rump length (CRL) and by means of length-age tables in the literature (Rüsse, 1991). For convenience, the gestation period was divided into 3 stages: early, mid, and late gestation. The first stage extend up to 14 cm CRL/80 day post coitus (dpc), the mid gestation represent the period between the end of the early stage and up to 57 cm CRL/187 dpc while the late stage constitutes the remaining period of pregnancy (table 7). However, it is important to remind that embryos of the same age may differ considerably in length (CRL).

Table 7: CRL and suspected related age of bovine embryos

Stage of gestation	Early-stage					Mid-stage							Late-stage		
CRL/cm	2.5	3.5	6	10	14	18	20	23	30	36	40	57	63	80	90
Age/Days	43	50	60	75	80	100	108	110	130	141	159	187	210	245	285
No of embryos	4	2	2	3	2	2	2	3	2	2	1	2	2	2	1

Collected samples were analyzed by several methods that include

* Morphological examination of fetal (LM) and adult (LM and EM) testis.

* Identification of carbohydrates distribution (lectin histochemistry).

* Gene expression (Real time PCR and in situ hybridization) and protein localization (immunohistochemistry).

3.2. Morphological analysis

3.2.1. Tissue preparation

The collected materials were routinely fixed for light, fluorescent, and electron microscope.

3.2.1.1. Tissue fixation and processing for light microscope (LM)

For light microscopic examination, 3 different fixatives were used. These include Bouin's, methanol-glacial acetic acids (2:1), and 3.7 % formalin solutions. Embryos of small size (2.5-6 cm/CRL) and small samples of the embryonic (10-90 cm/CRL) and adult testicular tissue (0.5-1 cm) were fixed in Bouin's fluid and methanol-glacial acetic acid solutions for 12-24 h

according to the age. Thereafter, fixed samples were extensively washed in 70% ethanol (3 x 24 hr) to get rid of the fixative before the subsequent step of tissue processing. Exceptionally, formalin-fixed material was washed for 2 hr under the running tape water before ethanol immersion. Small embryos were transversely cut directly behind the level of the forelimb. Using automatic tissue processor (Shandon Duplex Processor, Shandon, Frankfurt, Germany), the tissue samples were dehydrated in graded series of ethanol (80%, 95% and absolute), cleared in xylene and impregnated with Paraplast® (Monoject Scientific Inc., Kildare, Irland). Subsequently, samples were embedded in paraplast blocks using Histostat Tissue Embedding Centre (Reichert-Jung, Wien). Sections (5μm) were cut on Leitz rotatory microtome (type 1521) and mounted on both 3-aminopropyltriethoxysilane-coated and uncoated glass slides. Paraffin sections were kept in incubator at 40°C until used for conventional staining, glyco (lectin)-and immuno-histochemical analysis.

3.2.1.2. Conventional histological staining.

As a general scheme for the ordinary stains, sections of paraffin-embedded testicular tissue were dewaxed (2 x 30 min), rehydrated in descending series of ethanol (100%, 95%, 70%) and distilled water. The subsequent stained sections were dehydrated again in ascending grades of ethanol (70%, 95%, 100%), cleared in xylene (2 x 10 min) and mounted with Eukitt® (Riedel de Haen AG, Seelze).

In this study, several conventional stains were carried out to investigate the general histological structure of fetal and adult testis in bovine. All of the staining techniques employed were performed according to Romeis (1989). These could be briefly described as following:

Haematoxylin and Eosin (H&E)

A selection of slides was routinely stained with H&E to differentiate the gonadal sex of the small-sized bovine embryos (2.5-6 cm/CRL) and for general histological studies. Generally, the cellular nuclei stained with H&E appear blue while the remaining elements of the testicular tissue show rosy red color.

Trichrome stain after Masson and Goldner

This stain is mainly used to differentiate between the different constituent of the tissues. Indeed, cellular nuclei are constantly dark blue (stained by Weigert᾽s Haematoxylin), collagen fibers exhibit green stain whereas the other cellular and tissue components (cytoplasm, muscle fibers,..) appear red.

Alcian blue 8 GX (pH 1.0 and pH 2.5)

Alcian blue stains the acidic mucosubstances (acidic mucopolysaccharides) with light blue color while the nuclei and background appear red and light pink respectively. At different pH values, Alcian blue is able to distinguish between sulfated and non-sulfated acidic mucosubstances. It is frequently clear that the acidic sulfated mucosubstances are easily demonstrable at highly acid pH (1.0) while the acidic non-sulfated ones, containing carboxyl groups, are detectable at comparatively lower pH value (2.5).

Periodic acid-Schiff reaction after McManus (PAS-Reaction) with and without Amylase digestion

PAS is essentially used to identify the aldehyde groups, which are formed through the oxidation of glycol with periodic acid. Therefore, PAS detect the carbohydrates or carbohydrate-rich macromolecules such as glycoproteins and glycogen. Basal lamina, reticular and collagen fibrils are known to contain glycoprotein and react positively with PAS. The PAS positive structures stain mainly with rose to purple red color while the background appears light pink. Importantly, since Amylase has the ability to digest glycogen, Amylase digestion was done to discriminate between glycoproteins and glycogen.

Elastic stain after Weigert (Resorcin-fuchsin)

With Weigert's elastic stain, the reactive elastic fibers appear predominantly blue black.

Toluidine blue stain

This stain is employed for identification of mast cells metachromasia. The metachromatic granules have constantly blue-violet appearance.

3.2.1.3. Light microscopic examination of the stained sections

Stained sections were evaluated by Leitz Dialux 20 Microscope and photos were taken by a Cannon digital camera (Cannon Powershot A95).

3.2.1.4. Morphometric studies

Measurements were taken with an eyepiece micrometer scale, which was calibrated with a stage micrometer at x 40. The diameter of tunica albuginea was measured from the basal lamina of the surface epithelium to the end of the inner vascular layer. The measurements of the diameter of the seminiferous cords represent in every case the average measurements of 20 seminiferous cords, 10 taken from the region near the tunica albuginea and 10 from the

rete testis region. The diameter of the seminiferous cords was measured from the basal lamina to the basal lamina and only tubules of a perfectly clear transversal section were measured. The Sertoli and germ cells found in these transversal sections were counted as well. Leydig cell count was performed using image tool program (UTHSCSA, v 3.00). First, 10 photos/age/embryo were taken by Cannon digital camera (Cannon Powershot A95). Importantly, all photos were taken at the same zoom and with the same objective (x 40). Then, the surface area of the photo was measured in photoshop program (Adobe® Photoshop® 7.0) and adjusted to 0.03 mm² of the testicular area. Finally the Leydig cells per photo was counted using image tool program and the average number for the 10 photos/age/embryo was calculated.

3.2.2. Tissue fixation and processing for electron microscope (EM)

Ultrastructure of the adult bovine testis was studied using transmission electron microscope. To accomplish this aim, small samples (about 1 mm) from different areas of the testes of 3 sexually mature bulls were directly collected within 30 min after slaughtering and fixed by immersion method. These samples were immediately fixed in formaldehyde-glutaraldehyde mixture (Karnovsky, 1965) at 4°C overnight. Subsequently, the specimens were washed (4 x 15 min) in 0.1 M cacodylate buffer (pH 7.2). All samples were then contrasted in 1.5% potassium ferrocyanide and 1% osmium tetroxide at 4°C for 2 hr in the dark. Later, they were again washed (3 x 20 min) in 0.1 M cacodylate buffer (pH 7.2). After dehydration in a graded series of ethanol (50%, 70%, 90%, 100%) and propylene oxide (Merck, Darmstadt, Germany) the specimens were gradually embedded in Epon (Polysciences, Eppelheim, Germany). Briefly, samples were firstly dipped (2 x 15 min) in propylene oxide (Merck, Darmstadt, Germany) then in propylene-Epon mixture (2:1) for 1 hr, in propylene-Epon mixture (1:1) overnight and finally in pure Epon for 30 min. Thereafter, testicular specimens were embedded in gelatin capsules (Plannet, Wetzlar) containing Epon and polymerized at 60°C for 24 hr. For general morphology, semithin sections (1μm) were cut using an ultramicrotome Ultracut E (Reichert-Jung, Wien) and stained with methylene blue (Sigma-Aldrich Chemicals GmbH, Deisenhofen, Germany) to be examined by light microscope. Ultra thin sections (60 nm) were cut from selected blocks, mounted on uncoated copper grids (SSI, Science Services, Munich, Germany) and routinely contrasted with uranyl-acetate and lead citrate (Reynolds, 1963) prior to examination with a Zeiss EM 902 (Carl Zeiss, Oberkochen) electron microscope. Photos of selected structures were taken on Maco ort 25c-films (Maco Photo Products, Hamburg, Germany).

3.3. Glycohistochemistry (Lectin histochemistry)

Distribution of sugar moieties (glycoconjugates) in the fetal and adult bovine testis was investigated using thirteen (Table 8) different fluorescein isothiocyanate (FITC) conjugated lectins (Sigma-Aldrich Chemicals GmbH, Deisenhofen, Germany). These lectins represent five groups (mannose-, galactose-, N-acetylgalactosamine (GalNAc)-, N-acetylglucosamine (GlcNAc)-, and fucose-binding lectins) of the known seven lectin binding groups described in my review (table 2). To shed light on the effect of fixation on glycoproteins, lectin-binding sites in adult bovine testicular tissue were studied in both Bouin᾽s-fixed paraffin-embedded and acetone-fixed frozen sections. The latter were cut with cryostat microtome (Reichert-Jung 2800 Figucut N), mounted on 3-aminopropyltriethoxysilane-coated slides, postfixed in cold acetone for 10 min, and stored at – 20°C until used. Staining of paraffin-embedded and frozen testicular tissue with lectins was done according to the following protocol:

1. Sections (5μm) of paraffin-embedded testicular tissue were dewaxed (2 x 30 min) in xylene, rehydrated in descending grades of ethanol and washed under tape water for 10 min.

2. Dewaxed (fetal and adult) and frozen (adult) sections were washed (3 x 5) in 0.05 M Tris-buffer (pH 6.8).

3. All sections were then incubated with FITC conjugated lectin (33 μg lectin-FITC/ml Tris-buffer) in humidified chamber at 4°C overnight.

4. Sections were again washed under tape water for 5 min and subsequently rinsed (3 x 5 min) in Tris buffer (pH 6.8).

5. Importantly, the hydrated sections were directly taken from Tris-buffer to be mounted with a mixture of polyvinyl alcohol 25/140 and ethylenglycol in Tris-buffer, pH 6.8 (Serva, Heidelberg, Germany). Covered slides were stored at – 20°C until examined by fluorescent microscope.

Controls

 Controls were performed by (1) substitution of the lectins with buffer, and (2) preincubation of the lectins with the corresponding hapten sugar inhibitor (e.g., fucose for UEA-I and LTA; GlcNAc for WGA; GalNAc for HPA, SBA and DBA; galactose for PNA, GSA-I and ECA; mannose for Con A, PSA, LCA) (Sigma-Aldrich Chemicals GmbH, Deisenhofen, Germany). Lectin-stained testicular tissues and their controls were evaluated using a Dialux 20 fluorescent microscope (Leitz GmbH, Wetzlar). The photos were taken by using Kodak film elite 400.

Table 8: FITC-labeled lectins used for investigation of sugar moieties in the bovine testis

Lectin group	Lectin source (Latin name)	Common name	Acronym	Sugar specificity	Binding inhibitor
I. D-Mannose (D-Glucose)-binding lectins	*Canavalia ensiformis Agglutinin*	Jack bean	Con A	α-D-Man > α-D-Glc	Man
	Lens culinaris Agglutinin	Lentil	LCA	α-D-Man	Man
	Pisum Sativum Agglutinin	Garden pea	PSA	α-D-Man	Man
II. D-Galactose-binding lectins	*Arachis hypogaea Agglutinin*	Peanut	PNA	β-D-Gal-(1-3)-D-GalNAc	Gal
	Griffonia simplicifolia I Agglutinin	Griffonia or Bandeiraea	GSA-I	Terminal α-Gal	Gal
	Erythrina cristagalli Agglutinin	Coral tree	ECA	α-D-Gal-(1-4)-GlcNAc	Gal
III. N-acetyl-D-galactosamine (GalNAc)-binding lectins	*Dolichos biflorus Agglutinin*	Horse gram	DBA	α-D-GalNAc(1-3) GalNAc	GalNAc
	Glycine max Agglutinin	Soybean	SBA	D-GalNAc	GalNAc
	Helix pomatia Agglutinin	Roman or edible snail	HPA	D-GalNAc	GalNAc
	Visea villosa Agglutinin	Hairy vetch	VVA	D-GalNAc	GalNAc
IV. N-acetyl-D-glucosamine (GlcNAc)-binding lectins	*Triticum vulgare Agglutinin*	Wheat germ	WGA	GlcNAc(β1-4GlcNAc) $_{1-2,}$ NeuNAc	GlcNAc
V. L- Fucose-binding lectins	*Ulex europaeus -I Agglutinin*	Gorse seed	UEA-I	α-L-Fuc	α-L-Fuc
	Lotus tetragonolobus Agglutinin	Asparagus pea	LTA	α-L-Fuc	α-L-Fuc

Man, mannose; Glc, glucose; Gal, galactose; GalNAc, N-acetylgalactosamine; GlcNAc, N-acetylglucosamine; NeuNAc, N-acetylneuraminic acid (sialic acid); α-L-Fuc, α-L-Fucose.

3.4. Gene expression and protein localization

The expression of two genes (FGF-1 and FGF-2) was investigated in the adult bovine testis.

3.4.1. RNA extraction

Within 20 min after slaughtering, approximately 500 mg of each adult testis were submerged in 5 ml of RNAlater (Qiagen, Munich, Germany) for RNA isolation. Total RNA was extracted using Tri-reagent (Sigma-Aldrich Chemicals GmbH, Deisenhofen, Germany) according to the following scheme:

1- Tissue samples were homogenized in Tri-reagent (1 ml per 50-100 mg of tissue) by using an Ultra-Turrax, T 25 homogenizer (Janke and Kunkel, iKA-Labortechnik, Stauffen, Germany).

2- After homogenization and dissociation, the samples were allowed to stand for 5 min at room temperature to ensure complete dissociation of nucleoprotein complexes.

3- Then 200 µl of chloroform per ml of Tri-reagent was added. The samples were shaken vigorously for 15 sec and allowed to stand again for 5 min at room temperature.

4- Samples were centrifuged at 14500 rpm for 20 min at 4°C. Centrifugation separates the mixture into 3 phases: a red organic phase (containing protein), an interphase (containing DNA), and colorless top aqueous phase (containing RNA).

5- The top phase was transferred to a new tube and mixed with 500 µl of isopropyl alcohol per ml of Tri-reagent. The mixed samples were allowed to stand 5 min at room temperature before centrifugation at 14500 rpm for 10 min at 4°C. The RNA precipitate will form a pellet on the side and bottom of the tube.

6- The precipitated RNA pellet was washed by centrifugation with ice-cold 75% ethanol (at least 1ml of ethanol per ml of Tri-reagent) at 7.500 rpm for 5 min at 4°C.

7- After centrifugation, the RNA pellet was dried and resuspended in RNase-free water.

3.4.2. RNA purification

In order to purify and cleanup the isolated RNA from genomic DNA, the dissolved RNA pellet was treated with DNase I according to the RNA cleanup protocol (Qiagen, Munich, Germany). Briefly, this was achieved as following:

1- The suspended RNA sample was adjusted to a volume of 100 µl with RNAse-free water.

2- Subsequently, 350 µl of RLT buffer (Qiagen, Munich, Germany) was added and the solution was thoroughly mixed.

3- Later, 250 µl of ethanol (100%) was added to the previously diluted RNA and thoroughly mixed by pipetting.

4- The total volume (700 µl) was applied to an RNeasy mini column and placed in a 2 ml collection tube to be centrifuged for 15 sec at 10.000 rpm.

5- The collection tube and flow-through was discarded whereas the RNeasy column was transferred into a new 2 ml collection tube.

6- Thereafter, 350 µl RW1 buffer (Qiagen, Munich, Germany) was pipetted onto the RNeasy column membrane and centrifuged for 15 sec at 10.000 rpm. Consequently, the flow-through was discarded.

7- To enable genomic DNA digestion, 80 µl of DNase I incubation mix was pipetted on the mini column silica-gel membrane and allowed to stand 15 min at room temperature. DNase I

mix was prepared by addition of 10 µl DNase I stock solution to 70 µl RDD buffer (Qiagen, Munich, Germany).

8- Afterwards 350 µl RW1 buffer was again added on the mini column silica-gel membrane and left to stand 5 min at room temperature. Then the column was centrifuged for 15 sec at 10.000 rpm and the flow-through was discarded.

9- Purified RNA was washed by 500 µl RPE buffer (Qiagen, Munich, Germany) and centrifuged for 15 sec at 10.000 rpm. Again, another 500 µl RPE buffer was added to the column and centrifuged for 2 min at 10.000 rpm to dry the RNeasy silica-gel membrane. Finally, the RNeasy silica-gel membrane column was placed in a new 2 ml collection tube and centrifuged at full speed for 1 min to eliminate any chance of possible buffer RPE carryover.

10- To elute, RNeasy column was transferred to a new 1.5 ml collection tubule and 50 µl RNase-free water was directly pipetted onto the the RNeasy silica-gel membrane. The tube was gently closed and centrifuged for 1 min at 10.000 rpm.

RNA concentration and purity were determined by ultraviolet spectrophotometry. All RNA samples used for assay were of high quality and purity (260/280 nm absorption ratio > 1.8).

3.4.3. Reverse transcription

Reverse transcription was performed using 1.5 µg of total RNA with 2 µl 10 x buffer, 2 µl dNTPs (0.5 mM), 2 µl oligo-dt (10 pM), 2 µl random decamer (100 pM), 0.5 µl RNase inhibitor (Ambion 40U/µl) and 1µl Ominiscript RT enzyme (4U/20 µl) (Qiagen, Munich, Germany) in a final volume of 20 µl. RNA was reverse transcribed at 37 °C for 60 min, followed by a 5 min enzyme inactivation phase at 93 °C. The reaction mixture was then chilled to 4 °C and the resulting cDNA was stored at –20 °C until assayed by real-time PCR. To detect residual DNA-contamination (genomic DNA) in the subsequent PCR reaction, a negative RT control was done through replacing Ominiscript RT enzyme (Qiagen, Munich, Germany) by water.

3.4.4 Primer design

Specific primers for the FGF-1 and FGF-2 genes were designed using Primer 3 software program (http://www.genome.wi.mit.edu/cgi-bin/primer/primer3_www.cgi). The sequence of primers encoding for both genes in bovine are shown in table 9.

Table 9: Primer, sense, and antisense sequences of FGF-1 and FGF-2

Target	Sequence of nucleotides		Fragment size (bp)
FGF-1	Forward	5′-GCC TTG AAA CAG CCA CAA CC-3′	189
	Reverse	5′-TGT CCT TCG TCC CAT CCA C-3′	
	Sense	5′-GGA GAG CAG AAT GAA GGC AC-3′	
	Antisense	5′-GTG CCT TCA TTC TGC TCT CC-3′	
FGF-2	Forward	5′-CGA GAA GAG CGA CCC ACA C-3′	236
	Reverse	5′-GCC CAG TTC GTT TCA GTG C-3′	
	Sense	5′-GTG CTG TTG CCG AAT ACT CA-3′	
	Antisense	5′-TGA GTA TTC GGC AAC AGC AC-3′	

Primer specificity was tested by running a regular PCR and the resulting PCR amplicons were evaluated by ethidium bromide agarose gel electrophoresis. The latter ensures the presence of a unique specific PCR product revealed by existence of a single band of predicted size for each pair of primers.

In real time PCR, primer specificity was further assessed by analysis of melting curve. This step is of great importance because SYBR Green I is not specific for the PCR product but can also bind to double-strand unspecific amplification side products (Yin et al., 2001).

3.4.5. PCR Standard

Absolute quantification of mRNA transcription allows the precise determination of transcript copies per cell, total RNA concentration, or unit mass of tissue. It requires the construction of a standard curve for each individual amplicon to ensure accurate reverse transcription and PCR amplification profiles (Bustin, 2000). RNA and DNA standards can be employed for standard curve quantification. In this thesis, I have used DNA standards to quantify the mRNA of FGF-1 and FGF-2 using an iCycler and SYBR Green I (BioRad, Munich, Germany). PCR standards for each growth factor were constructed from PCR products (PCR fragments) of the same gene with known numbers of molecules. These fragments were highly purified by QiAquick Gel Extraction Kit (Qiagen, Munich, Germany) according to the following scheme:

1. Five volumes of buffer PB (Qiagen, Munich, Germany) were added to one volume of the PCR samples and thoroughly mixed.
2. The samples were applied to QiAquick column previously placed in 2 ml collection tube and centrifuged for 30-60s.
3. To wash, flow-through was discarded and 0.75 ml buffer PE (Qiagen, Munich, Germany) was added to QiAquick column and centrifuged again for 30-60s. The QiAquick column was

then centrifuged for an additional 1 min at maximum speed and finally placed in a clean 1.5 ml microcentrifuge tube.

4. To elute DNA, 50 µl buffer EB (10 mM tris-Cl, pH 8.5) (Qiagen, Munich, Germany) was added to the centre of the QiAquick membrane and centrifuged for 1 min.

 Purification ensures the elimination of primers, nucleotides, polymerases, and salts. Concentration of the purified PCR amplicon DNA was determined by spectrophotometer (SmartSpec^{TM} 300, BioRad, Munich, Germany). Copy numbers/ µl of standard were calculated according to the following formula:

$$Y \text{ molecules/µl} = \frac{(Xg/\text{µl DNA}) \times [6.022 \times 10^{23}]}{(\text{Amplicon length in base pairs} \times 660)}$$

The PCR standards were made to dilution of 10^{11} (10 copies/ µl) and stored at -20 °C until used. By knowing copy numbers and concentration of the DNA fragment, the precise number of molecules added to subsequent real time runs can be calculated. In order to generate a standard curve, 5 different concentrations of a 10 fold dilution series standard have been measured.

3.4.6. Real Time PCR

Real time PCR was carried out using an iCycler (BioRad, Munich, Germany) and SYBR Green I as dsDNA binding stain. The reaction was performed in a 96-well optical plate included five, 10-fold dilutions in duplicate of the amplicon DNA standards (i.e. starting at 10^4 to 10^8 for FGF-1 and 10^6 to 10^{10} for FGF-2). Our unknown targets (FGF-1 and FGF-2) were assayed in triplicate along with single negative controls for the RT and PCR steps (i.e., no template controls). Each well contained 15 µl of reaction components (master mix, diluted cDNA and primers). The reaction master mix (iQ^{TM} SYBR$^{®}$ Green Supermix, BioRad, Munich, Germany) contains iTaq DNA polymerase, dNTP mix (dATP, dCTP, dGTP, and dTTP), KCL, Tris-HCL, MgCL$_2$, SYBR Green I, Fluorescein, and stabilizers. The real time PCR reaction was performed by addition of 7.5 µl 2 x SYBR Green supermix to 3.5 µl of cDNA (RT product diluted 1: 10) and 4 µl primer mix (forward+ reverse, 1.2 µM) in a total volume of 15 µl. The PCR thermal cycling program was accomplished by a 2 step temperature protocol, consisting of 95 °C denaturation for 3 min, followed by 40 cycles of 15 sec at 95 °C and 60 sec at 60 °C (annealing and data collection step). Melt curve analysis carried out immediately after the amplification protocol, was initiated by one cycle at 95°C for 1 min, followed by 150 cycles (10 sec each) starting from 95°C with a regular decrease of

0.2 °C (melting curve data collection was enabled at this step). In the so-called absolute real time PCR-technique, it is not necessary to include a house keeping gene for normalization, but careful quantification of the unknown targets requires a control gene to determine if pipetting errors are significant or not (Ginzinger, 2002). In this investigation, 18S was used as a control gene. Real time PCR products were further verified by routine ethidium bromide gel electrophoresis in 2% agarose gel. Commercial Sequencing of PCR products was additionally carried out to validate its specificity (GATC, Biotech, Konstanz, Germany).

3.4.7. Real time PCR data analysis

Optical data obtained by real time PCR was analyzed by using the default and variable parameters available in the software provided with iCycler (iCycler$^{®}$ Optical System Interface V 3.0 a, BioRad, Munich, Germany). A standard curve was generated by plotting the log of copy numbers versus threshold cycle (C_T). The C_T was defined as the cycle number when intensity of SYBR Green fluorescence exceeded 10x the standard deviation of baseline fluorescence. The slope of linear regression between copy numbers and threshold cycles was used to resolve PCR efficiency. From standard curve interpolation, the iCycler software automatically computed the correlation coefficient, PCR efficiency, and copy numbers of the 2 genes under investigation. To confirm amplification specificity, the PCR product was identified by melt curve analysis. As melting temperature was attained, the double stranded DNA denaturated and released SYBR Green I, causing a sharp decrease in fluorescence. This decline in fluorescence was plotted as fluorescence (F) versus temperature (T) (Yono et al., 2002). The negative first derivative of fluorescence with respect to temperature was thereafter plotted versus temperature change (-dF/dT vs. T) to generate a melting peak at a certain melting temperature for each amplified growth factor cDNA.

3.4.8. In situ hybridization

Formalin-fixed (3.7%), paraffin-embedded samples were used to localize the mRNA transcripts of FGF-1 and FGF-2 within the adult bovine testis. All solutions for in situ hybridization were prepared using DEPC-treated water and glassware sterilized at 200 °C. In addition, all steps prior to and during hybridization were conducted under RNase-free conditions. Sections were deparaffinised with xylene (3 x 10 min), immersed in absolute ethanol (2 x 5 min), and then allowed to air dry. Dried sections were dipped in 2 x saline sodium citrate (SSC) prewarmed in water bath (80 °C) for 10 min followed by cooling off for 20 min at room temperature. Slides were then washed in distilled water (2 x 5 min), Tris

buffer (2 x 5 min) and permeabilised for 20 min with 0, 05% proteinase E (VWR, Ismaning, Germany) in Tris buffer at room temperature. Sections were immersed again in Tris buffer (2 x 5 min), rewashed in distilled water (2 x 5 min), and post-fixed for 10 min in 4% paraformaldehyde/PBS (pH 7.4). After washing in PBS (2 x 5 min) and distilled water, slides were dehydrated in an ascending graded series of ethanol and air dried. Hybridization was carried out by overlaying the dried sections with 40 µl of biotinylated oligo-probe (100 pM/ml) diluted 1:20 in in-situ-hybridization solution (DAKO, Munich, Germany) and incubating them in a humidified chamber (using cover slips to prevent drying-out) at 38 °C overnight (sequences of probes are shown in table 9). RNase-free hybridization solution (DAKO, Munich, Germany) contains 60% formamide, 5 x SSC, hybridization accelerator, RNAse inhibitor, and blocking reagents. Afterwards slides were washed in 2 x SSC (2 x 15 min) prewarmed to 38 °C, distilled water (2 x 5 min) and Tris Buffer (2 x 5 min). Detection of transcripts was performed with ABC kit reagents and DAB (DAKO, Munich, Germany) according to the manufacturer's instructions. Bovine liver tissue sections were used as positive control while negative controls were carried out by: 1) omitting the biotinylated antisense oligo-probe, 2) using the biotinylated sense oligo-probe (sequences are shown in table 9)

3.4.9. Immunohistochemistry

In this study, 12 different proteins (table 10) were investigated. Antigen localization was achieved using either polyclonal or monoclonal antibodies combined with the avidin-biotin complex (ABC) technique (Hsu et al., 1981) according the following protocol:

1- Sections (5µm) of paraffin-embedded testicular tissue were dewaxed, rehydrated, and rinsed in PBS pH 7.4 (3 x 5 min).

2- For antigen retrieval, the slides were either heated (2 x10 min) in microwave (750 Watt) by using of citrate buffer pH 6 followed by cooling of for 20 min or treated with protease for 5 min at room temperature. Importantly, not all the antibodies used need this step (showed in table 10).

3- Endogenous peroxidase was blocked by soaking the sections in 7.5% v/v hydrogen peroxide/ distilled water for 10 min at room temperature followed by washing them under running tap water for additional 10 min.

4- They were thereafter rinsed in PBS pH 7.4 (2 x 5 min).

5- Non-specific protein binding was minimized by covering the slides with a serum-free protein blocking reagent (DAKO, Hamburg, Germany) for 10 min at room temperature.

6- Sections were then incubated with the primary antibodies either for ½ -1 hr at room temperature or overnight at 4°C. The sources, dilutions, and time of incubation of these antibodies are shown in table 10.

7- The slides were subsequently rinsed in PBS pH 7.4 (2 x 5 min) followed by incubation with biotinylated IgG (types, source, and dilutions are shown in table 10) for 30 min at room temperature.

8- Visualization of the bound antibodies was carried out with ABC kit reagents (DAKO, Hamburg, Germany) for 30 min followed by treatment with diaminobenzidine/ H_2O_2 (chromogenic substrate) for 10 min at room temperature. All incubations were performed in a humidified chamber. Sections were left unstained or counterstained in Mayer's haematoxylin, dehydrated, and mounted with Eukitt® (Riedel de Haen AG, Seelze).

Positive and negative controls

Negative controls were performed by omission of the primary antibodies while several bovine organs were used as positive controls according to the investigated antigen. For instance, nervous tissue (S100), corpus luteum (FGF-1 and FGF-2), ovary (Cx43), embryonic tissue (laminin), uterine tube (αSMA), and lymph nodes (CD4, CD8, and CD68) were used as positive controls.

Positive testicular sections were evaluated by Leitz Dialux 20 Microscope and photos were photographed by Cannon digital camera (Cannon Powershot A95).

Table 10: Identity, sources, and working dilutions of antibodies used in this study

Primary antibodies						Secondary antibodies		
Against	Source	Origin	Dilution	Incubation time	Antigen retrieval	Type	Dilution	source
S100	Dako, Hamburg	Rabbit	1:400	½ hr at room temperature	Not required	Biotinylated pig anti-rabbit IgG	1:300	Dako, Hamburg
FGF-1	Prof.Dr Schams	Rabbit	1:1000	Overnight at 4°C	Heating in microwave	Biotinylated pig anti-rabbit IgG	1:300	Dako, Hamburg
FGF-2	Prof.Dr Schams	rabbit	1:1000	Overnight at 4°C	Not required	Biotinylated pig anti-rabbit IgG	1:300	Dako, Hamburg
Cx 43	BD Bioscience, Heidelberg	Mouse	1:200	Overnight at 4°C	Heating in microwave	Biotinylated rabbit anti-mouse IgG	1:300	Dako, Hamburg
Laminin	Serotec, Düsseldorf	Rabbit	1:500	Overnight at 4°C	5 min treatment with protease at room temperature	Biotinylated pig anti-rabbit IgG	1:300	Dako, Hamburg
GalTase	Institute of veterinary anatomy II, LMU-Munich	Chicken	1:500	Overnight at 4°C	Not required	Biotinylated rabbit anti-chicken IgG	1:400	Rockland, USA
VEGF	Dako, Hamburg	Rabbit	1:800	Overnight at 4°C	Not required	Biotinylated pig anti-rabbit IgG	1:300	Dako, Hamburg
ACE	Institute of veterinary anatomy II, LMU-Munich	Chicken	1:500	Overnight at 4°C	Not required	Biotinylated rabbit anti-chicken IgG	1:400	Rockland, USA
αSMA	Dako, Hamburg	Mouse	1:200	1 hr at room temperature	Not required	Biotinylated rabbit anti-mouse IgG	1:300	Dako, Hamburg
CD4 (CC30)	Serotec, Düsseldorf	Mouse	1:100	Overnight at 4°C	Not required	Biotinylated rabbit anti-mouse IgG	1:300	Dako, Hamburg
CD8 (CC58)	Serotec, Düsseldorf	Mouse	1:50	Overnight at 4°C	Not required	Biotinylated rabbit anti-mouse IgG	1:300	Dako, Hamburg
CD68 (EBM 11)	Dako, Hamburg	Mouse	1:50	Overnight at 4°C	5 min treatment with protease at room temperature	Biotinylated rabbit anti-mouse IgG	1:300	Dako, Hamburg
CD68 (KP1)	Dako, Hamburg	Mouse	1:50	Overnight at 4°C	5 min treatment with protease at room temperature	Biotinylated rabbit anti-mouse IgG	1:300	Dako, Hamburg

FGF-1: acidic fibroblast growth factor; FGF-2: basic fibroblast growth factor; Cx43: connexin43;

GalTase: galactosyltransferase; VEGF: vascular endothelial growth factor;

ACE: angiotensin converting enzyme; αSMA: alpha smooth muscle actin.

4. RESULTS

4.1. Microscopic structure of the bovine testis

In this study, the testicular morphogenesis of fetal testis and the microscopical organization of adult testis were investigated by light microscope using different conventional stains including H&E, PAS, Masson-Goldner՚s trichrome, Weigert՚s elastic stain, Alcian blue, and toluidine blue. The ultrastructure of the different testicular compartments of adult testis was considered as well.

4.1.1. Fetal testis: emergence and morphogenesis

For convenience, the bovine gestation period was divided into 3 stages: early, mid, and late gestation. Developmental changes in the testicular morphogenesis were therefore analyzed in details during these phases.

4.1.1.1. Early stage of gestation (2.5-14 cm CRL/43-80 dpc)

All critical events that characterize testicular development are seen in this period. These are indicated by the appearance of the tunica albuginea, organization of the testicular cords, multiplication of germ cells, differentiation of Leydig cells, and establishment of connection between solid testicular cords and rete testis strands.

With the beginning of this stage (2.5 cm CRL/43 dpc), the gonadal anlages protruded into the coelomic cavity as paired bean-shaped structures on either side of the dorsal mesentery of the hindgut medial to the mesonephros (Fig. 5).
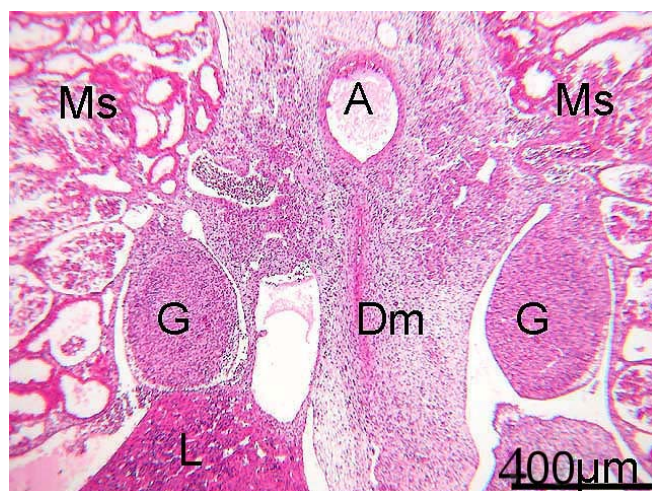
Fig 5: Overview of the bovine embryonic gonads position. The gonadal anlages (G) are located on either side of the dorsal mesentery (Dm) medial to the mesonephros (Ms). Dorsally the aorta (A) is identified while ventrally the liver (L) is recognized. Bovine embryo with 2.5 cm CRL, H.E.

The incipient gonads are covered by a thin layer of simple cuboidal to columnar cells (coelomic epithelium). These cells are oriented in various directions and contain large round

to elongated nuclei occupying most of the cellular cytoplasm. The basal lamina of these cells is not evident with conventional stains (e.g., PAS) at this age. Directly beneath the coelomic epithelium, a relatively thick layer (50-60 μm) of mesenchymal cells is present. This layer outlines the first step of the testicular tunica albuginea (TA) formation. The development of TA at the gonadal extreme periphery is timely coincident with the aggregation of both somatic (pre-Sertoli) and germ (primordial germ) cells to form the testicular cords, the precursors of the seminiferous tubules. The first cords are 30 μm in diameter and are clearly recognizable at the gonadal periphery whereas the gonadal interior consists of a network of polygonal mesenchymal cells and thin walled-blood spaces, some of them filled with blood. One week later (3.5 cm CRL/50 dpc), the testicular shape, size, and architectures are progressively differentiated. The testes are ovoid in shape (Fig. 6) and start to prepare for separation from their site of origin. The increase in testicular size at this age is mainly due to proliferation of stroma, immigration of testicular blood vessels from the inner layer of TA, differentiation of Leydig cells and partial expansion of the rete testis strands into the gonadal inside.
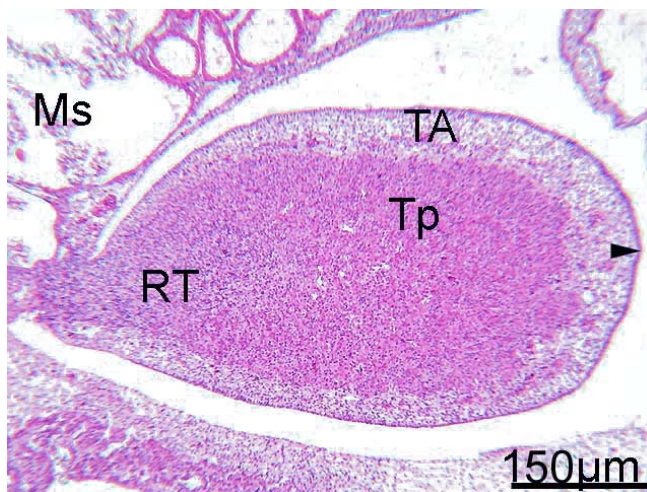
Fig 6: Embryonic testis of 3.5 cm CRL bovine embryo. Superficially, the testis is covered by tunica albuginea (TA) and thin layer of coelomic epithelium (arrowhead). The testicular parenchyma (Tp) comprises large area of the gonadal tissue while the rete testis (RT) is mainly restricted to the attached border with the mesonephros (Ms), H.E.

The surface epithelium (coelomic epithelium) becomes resting upon clearly defined basal lamina. TA increases in thickness to about 100-110 μm and begins to differentiate into two layers: an outer fibrous layer (tunica fibrosa) with numerous spindle cells (fibroblast-like cells) containing elongated nuclei and locate parallel to the long axis of the gonad and inner cellular layer with several blood vessels (tunica vasculosa) (Fig. 7).

In addition to TA, two other testicular areas are clearly recognized at this age: a peripheral region consisting of newly developed seminiferous cords, connective tissue, and blood vessels (Fig. 7), and a nearly cord-free central mediastinum region. Connective tissue trabeculae that originate from the inner cellular layer of the TA and penetrate deeply to join the developing

mediastinum testis are also identified. These trabeculae subdivide the testicular cords in the testicular periphery and cleave a way for the blood vessels that immigrate from large albugineal vessels in a central direction.
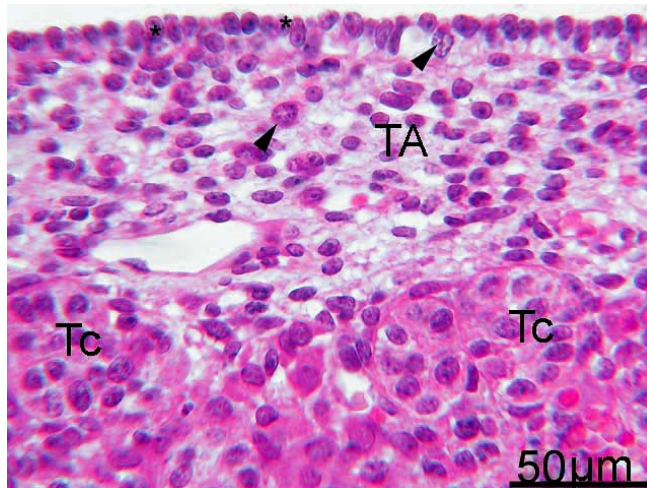
Fig 7: The testicular surface epithelium (asterisks) is a simple cuboidal epithelium and rests upon distinct basal lamina. Both surface epithelium and tunica albuginea (TA) are shown to contain some sporadic primordial germ cells (arrowheads). The inner layer of TA contains blood vessels while initial testicular cords (Tc) are peripherally seen. Bovine fetus with 3.5 cm CRL, H.E.

The forming testicular cords are rapidly surrounded by a marked basal lamina and a layer of peritubular cells. These cords have the same diameter as in the previous age (Fig. 8). Differentiated testicular cords are lined by two types of cell populations: a large number of dark polygonal cells with irregular nuclei, pre-Sertoli cells, and a small number of large, light, round cells with relatively round nuclei, the PGC (Fig. 8).
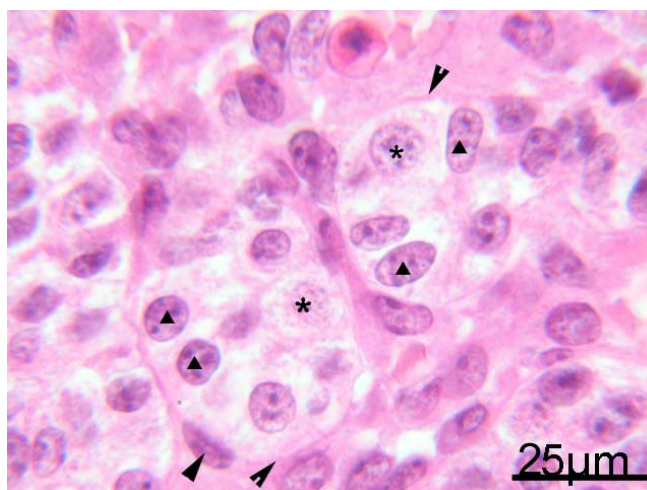
Fig 8: Newly differentiated testicular cords are surrounded by distinct basal lamina (notched arrowheads) and one layer of peritubular cells (arrowhead) while are lined by pre-Sertoli (triangles) and primordial germ cells (asterisks). Bovine fetus with 3.5 cm CRL, H.E.

The bovine pre-Sertoli cells are mainly arranged on the basal lamina of these cords, despite some are displaced more centrally by the close packing of cells within the cords particularly at the end of the early gestation period whereas the number of pre-Sertoli cells was relatively increased (table 11). The pre-Sertoli cells display a polygonal shape with their cytoplasm often oriented radially within the cords. Their nuclei are variable in shape and rarely show

deep indentations. A nucleolus is often present, and is together with peripheral clumps of heterochromatin associated with the nuclear membrane (Fig. 8). PGCs are polygonal with light cytoplasm and spherical nuclei (Fig. 8). They are located either at the periphery of cords or slightly central. PGCs rarely come in direct contact with the basal lamina of testicular cords. Both in the surface epithelium and in the TA, some sporadic PGCs are identified (Fig. 7).

The most important finding at this age is the identification of fetal Leydig cells within the interstitium. These cells are polygonal with large round nuclei that appear somewhat darker than that of pre-Sertoli and germ cells (Fig. 9). These nuclei contain at least 2 nucleoli. The cytoplasm of the fetal Leydig cells is mostly acidophilic and contains some lipid droplets especially at the end of this stage. Fetal Leydig cells are mainly situated between the testicular cords but never seen within the mediastinum.
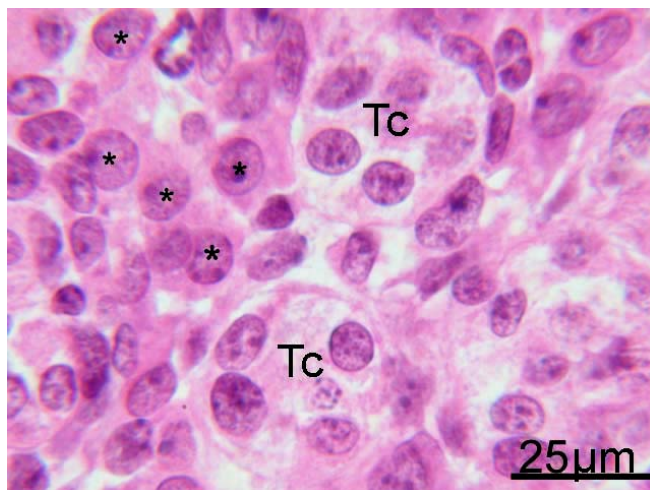
Fig 9: In addition to the testicular cords (Tc), the fetal Leydig cells (asterisks) are easily recognized in the testicular interstitium of bovine fetus with 3.5 cm CRL, H.E.

At this age (3.5 cm CRL/50 dpc), rete testis arranges in solid strands and occupies the attached border of the testis with the mesonephros (mesorchial side). This area appears generally darker than the remaining testicular parenchyma (Fig. 6) however, due to absence of a distinct basal lamina between these strands; it is difficult to separate them from the surrounding stromal cells at the level of the light microscope.

Toward the end of this stage of gestation (10-14 cm CRL/75-80 dpc), the testis has significantly increased in size. The surface epithelium is composed of simple cuboidal cells, which are progressively flattened during their development. The large round nuclei of these cells with their prominent nucleoli fill a large part of the cytoplasm and sometimes bulge partially out into the coelomic cavity. The TA showed drastic differentiation at this age and has considerably increased in thickness (125-200 μm). The deeper zone of TA contains numerous well-developed blood vessels (Fig. 10).
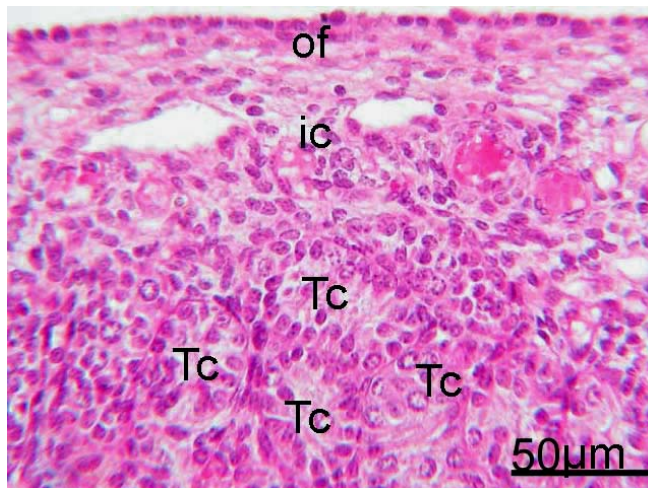
Fig 10: The testicular albuginea is differentiated into two layers: an outer fibrous (of) and inner cellular (ic) including numerous blood vessels. The angular form appears to be the predominant shape for the peripherally situated testicular cords (Tc). Bovine fetus with 10 cm CRL, H.E.

The peripheral area of the testicular parenchyma is divided into two zones. A narrow outer zone contains plate-like cords with thick diameter (50-57 µm) and a large inner zone is filled with a network of thinner cords (35-40 µm). In the outer region (Fig. 10), the cords are mostly convoluted and anastomose with each other (i.e., few cross section are seen whereas the angular form in the predominant) while in the central area they are mainly straight as indicated by the several cross sections seen in this area (Fig. 11).
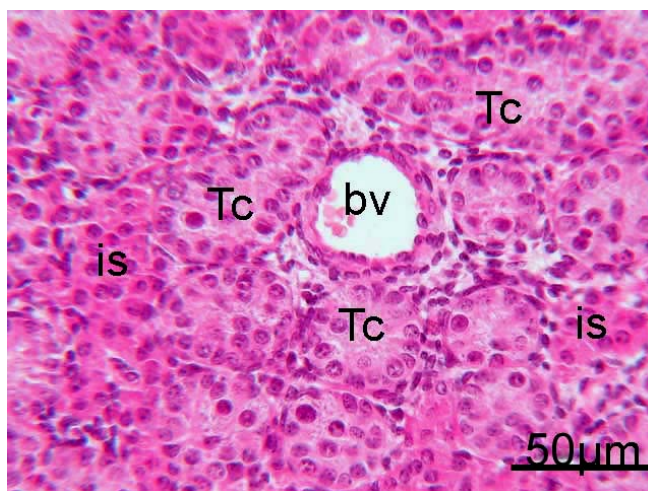
Fig 11: Within the gonadal interior, the testicular cords (Tc) are straight as indicated by numerous cross sections. The testicular interstitium (is) is expanded and contains well-constructed blood vessels (bv). Bovine fetus with 14 cm CRL, H.E.

As a consequence of the relative expansion in the interstitium, the seminiferous cords are progressively separated from each other. The cords/interstitium ratio has clearly shifted in favor of the latter (Fig. 11). As mentioned above, the lining cells of the seminiferous cords appear comparatively lighter than the interstitium. However, different staining intensities are additionally found between pre-Sertoli cells (dark) and prespermatogonia (light) which result in molting appearance of the cell populations within the testicular cords. Definitely, the average number of the total cells within the testicular cord cross section has considerably increased and approached their maximum at 14 cm CRL (80 dpc). The rapid and sudden

increase of these cells is associated with the germ cell maximum (table 11) and is mainly attributed to mitosis of germ cells which is evident at this stage of testicular development (Fig. 12).

Table 11: Some morphometric data of the embryonic bovine testis

| Stage of development	Age/ CRL /cm	Thickness of TA/µm	Diameter of testicular cord/µm		Average No of Leydig cells/0.03 mm^2 of testicular tissue	Average No of cells/cord cross section		
			Central	Peripheral		Sertoli cells	Germ cells	Total
Early stage	3.5	100-110	-	30	18.15 ± 5.53	2.71 ± 0.76	1.4 ± 0.50	3.67 ± 0.98
	10	125-150	35	50	30.50 ± 4.05	10.2 ± 2.91	3.10 ± 1.33	13.30 ± 3.03
	14	170-200	40	57	39.20 ± 3.77	9.36 ± 1.93	7.05 ± 1.75	16.61 ± 3.26
Mid stage	18	215-230	40	60	25.30 ± 2.06	11.64 ± 3.10	3.25 ± 0.87	14.50 ± 2.75
	23	260-300	40	60	22.50 ± 2.46	12.21 ± 2.49	3.52 ± 1.69	15.90 ± 1.67
	30	460-500	55	60	19.20 ± 2.44	12.52 ± 1.33	2.75 ± 0.72	$15.27 \pm .16$
	36	625- 650	60	60	18.55 ± 3.94	12.78 ± 1.93	2.76 ± 0.66	15.54 ± 1.90
	40	650-700	55	57	15.60 ± 2.32	12.92 ± 1.53	2.25 ± 0.46	15.17 ± 1.64
	57	750-800	53	55	14.60 ± 3.06	12.96 ± 1.57	1.71 ± 0.72	14.67 ± 1.78
Late stage	63	820-850	55	55	14.10 ± 3.51	10.85 ± 1.82	1.21 ± 0.42	11.67 ± 2.74
	80	900-950	50	50	7.00 ± 2.36	11.95 ± 1.55	1.27 ± 0.46	13.18 ± 1.70
	90	1-1.2 mm	50	50	3.38 ± 1.19	11.30 ± 1.26	1.16 ± 0.38	12.45 ± 0.93

Although the number of the prespermatogonia has significantly increased within the cords, the pre-Sertoli cells remain always predominant (Fig. 12, table 11).
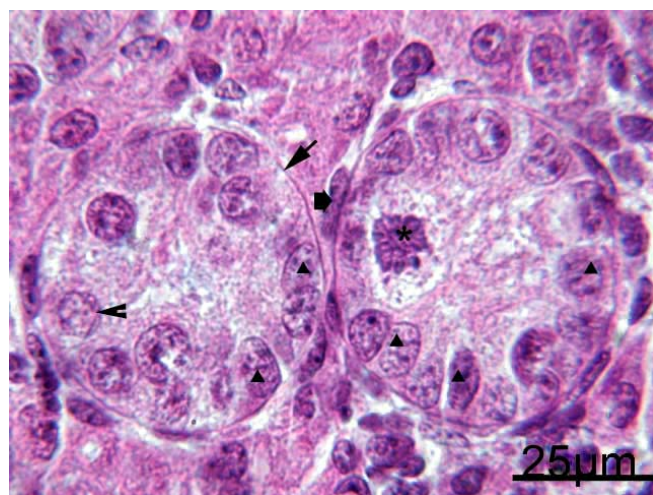
Fig 12: High magnification of the solid testicular cords of 14 cm CRL fetus. These are surrounded by well defined basal lamina (thin arrow) and peritubular cells (thick arrow) and lined by a basal row of pre-Sertoli cells (triangles) as well as prespermatogonia (notched arrowhead); some of them are in mitosis (asterisk). H.E.

Pre-Sertoli cells form a complete row at the periphery of the cords. Generally, these cells are irregular in shape and numerous but considerably smaller than the germ cells (Fig. 12). The testicular cords are enclosed by a well-developed basal lamina delineating them from the surrounding interstitium (Fig. 12). The latter has significantly expanded in this phase due to differentiation of mesenchymal cells into Leydig and peritubular cells and is shown to be composed mainly of five components: several islets or clusters of polygonal Leydig cells, 1-2

layers of peritubular flattened cells surrounding the testicular cords, loose network of undifferentiated mesenchymal cells, connective tissue cells, and numerous blood vessels (Fig. 11, 12). Nevertheless, Leydig cells constitute the largest cell population of these components and they reach their maximum at this specific age (Fig. 13, table 11).

Leydig cell developmental curve
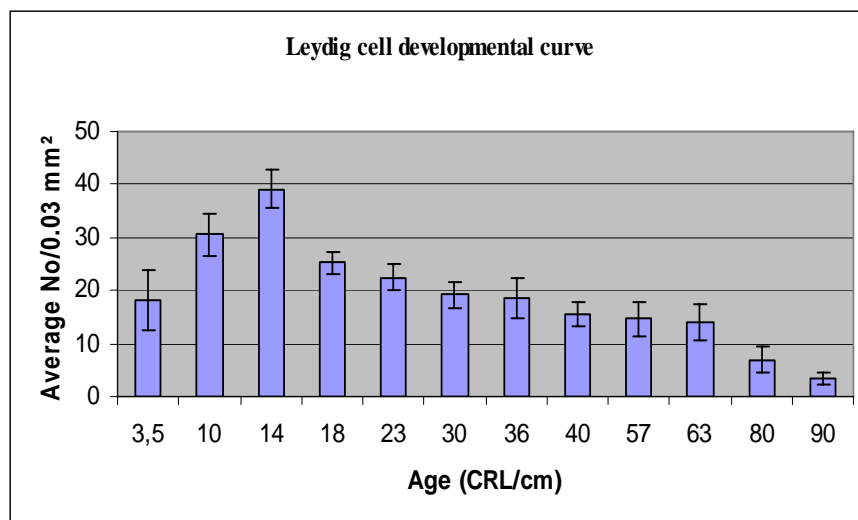
Fig 13: Diagrammatic representation of the Leydig cell developmental curve. The maximum of Leydig cells average number within the bovine testicular interstitium takes place at 14 cm CRL.

Indeed, the arrangement of Leydig cells shows no preferential position to blood capillaries. Although the intensely growing rete testis is somewhat centralized within the testicular parenchyma, some strands reach the caudal half of the testis. The organization of the rete tissue in strands is now clearly visible because they are separated by connective tissue rich in blood vessels and fibroblasts and surrounded by a continuous basal lamina (Fig. 14). Leydig cells are never seen within this area.
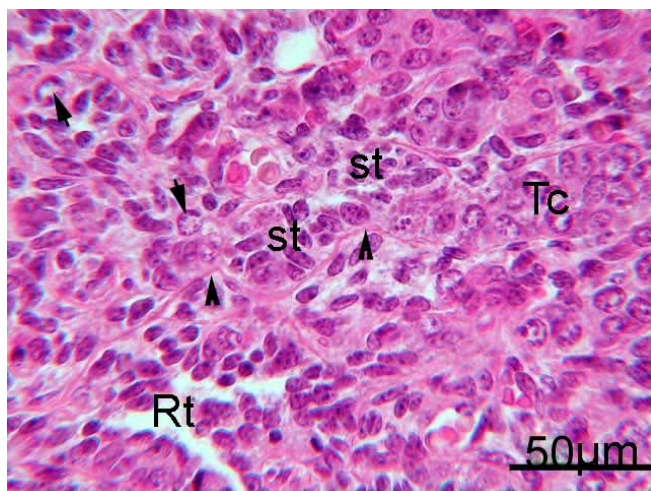
Fig 14: The initial connection between the testicular cords (Tc) and rete testis (Rt) via ill-developed straight tubules (st). Notice the continuous system of basal lamina (notched arrowheads) between the Tc and st. Some germ cells (arrows) are clearly seen within the solid st while some Rt strands are now canalized. Bovine embryo with 10 cm CRL, H.E.

A continuous system of basal lamina joining the testicular cords with rete strands is well defined (Fig. 14). This system establishes the first connection between these two testicular

components via ill-developed uncanalized straight tubules (tubuli recti). Some Pre-Sertoli cells and prespermatogonia are easily identified within this connecting part at this age (Fig. 14).

4.1.1.2. Mid stage of gestation (18-57 cm CRL/100-187 dpc)

During this stage of development, the testicular size has greatly increased and the testicular architecture becomes more differentiated. The surface epithelium constitutes a thin layer of flattened cells. TA is broader and attains 215 to 800 µm at 18 and 57 cm CRL respectively. It is moreover clearly separated in an outer tunica fibrosa with many collagen fibers and an inner tunica vasculosa with numerous blood vessels of large diameters (Fig. 15).

Fig 15: Testicular overview of 20 cm CRL bovine fetus. TA, tunica albuginea; Tp, testicular parenchyma; Rt, rete testis, H.E.
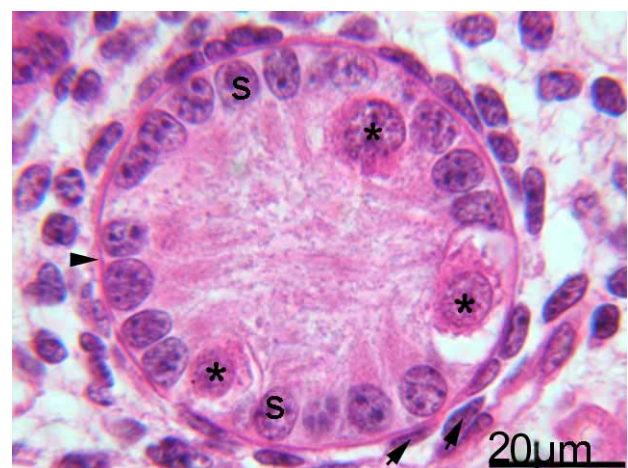
Fig 16: Solid testicular cord is surrounded by basal lamina (arrowhead), 2 layers of peritubular cells (arrows) and lined by pre-Sertoli (S) and prespermatogonia (asterisks). Fetus with 30 cm CRL. H.E

The solid testicular cords are demarcated by a well-developed basal lamina and 1-2 layers of peritubular cells, however, their diameter remain unchanged (55-60 µm) (Fig. 16). No significant differences are seen between the diameter of peripheral and central cords after the age of 23 cm CRL/110 dpc. The lining cells are always molted due to different staining intensity between pre-Sertoli cells and prespermatogonia. Prespermatogonia are present either as individual cells surrounded by pre-Sertoli cells or as adjacent pairs. Their location in relation to the basal lamina is however variable. Despite most prespermatogonia are situated in the periphery of the testicular cords (Fig. 16), some are more or less located in the center of these cords. Very rarely, prespermatogonia are directly positioned on the basal lamina because the cytoplasmic processes of pre-Sertoli cells usually separate them. Unlike

prespermatogonia, many pre-Sertoli cells nuclei are located perpendicular to basal lamina (Fig. 16). As a consequence of Leydig cells dedifferentiation in this period, the interstitium changes significantly. This character of the interstitium is clearly identified at 18 cm CRL/100 dpc when the average number of fetal Leydig cells has clearly reduced (table 11). In the subsequent stages, this feature becomes more prominent and islets of fetal Leydig cells are rarely seen. Most of these cells are recognized as solitary cells (Fig. 17, 18). Therefore, instead of large Leydig cell clusters, loose networks of undifferentiated mesenchymal cells are found (Fig. 17, 18).
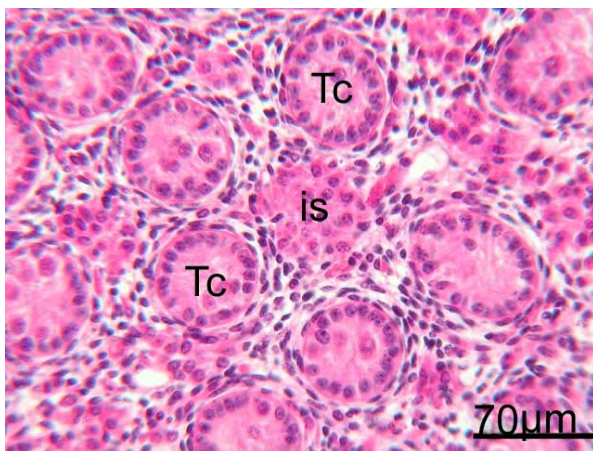
Fig 17: Testicular parenchyma of 36 cm CRL bovine fetus. The testicular cords (Tc) are widely separated due to Leydig cell dedifferentiation and to increase in the mesenchymal tissue within the interstitium (is), H.E.
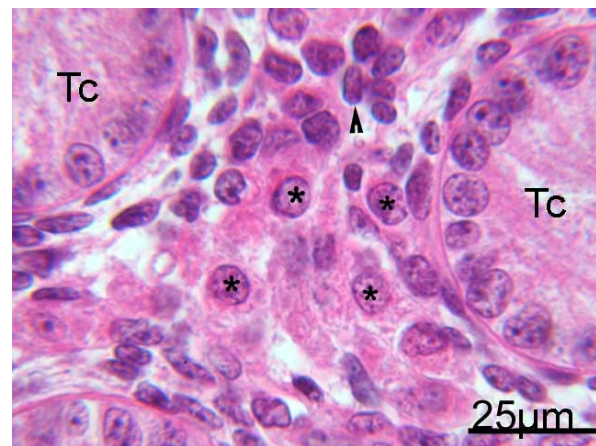

Fig 18: Leydig cells are present as isolated cells (asterisks) between the testicular cords (Tc). There is also an increase in the number of undifferentiated mesenchymal cell (notched arrowhead). Fetus with 30 cm CRL, H.E.

Toward the end of this stage, the number of Leydig cells has significantly decreased (table 11). The interstitium is additionally composed of rather undifferentiated mesenchymal cells and the testicular cords become widely separated. Simultaneously with reduction of Leydig cells, there is an increase in the fibroblasts that are located at the outer border of the peritubular cells. In addition to Leydig cells regression, connection between seminiferous cords and rete testis strands takes place at the beginning of this stage. The central rete testis strands expand toward the peripheries of the mediastinum testis to approach the thinner seminiferous cords (Fig. 19). Here, the two testicular structures come in contact to each other and their basal lamina at the attachment points begins to dissolve. Then rete testis cells invade the seminiferous cords resulting in a mixed population of germ, pre-Sertoli, and rete testis cells (Fig. 20, 21). Finally, germ and pre-Sertoli cells degenerate and the newly formed straight tubules are easily recognized (Fig. 22). Now all rete testis strands become canalized

while straight tubules still solid (Fig. 19, 20, 21, 22). Pre-Sertoli cells and prespermatogonia are only seen within the lining epithelium of these tubules at the smallest ages of this period (18-23 cm) and disappear later.
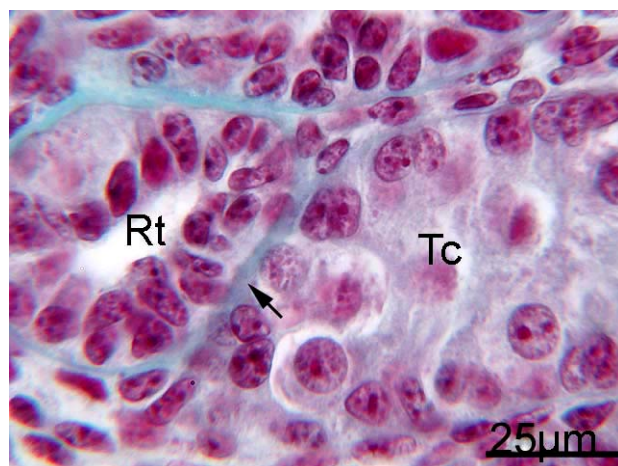

Fig 19: Beginning of connection between rete testis (Rt) and testicular cord (Tc). Their basal lamina disintegrate (arrow) to enable the invasion of Tc with the Rt cells. Fetus with 18 cm CRL, Masson-Goldner᾽s trichrome
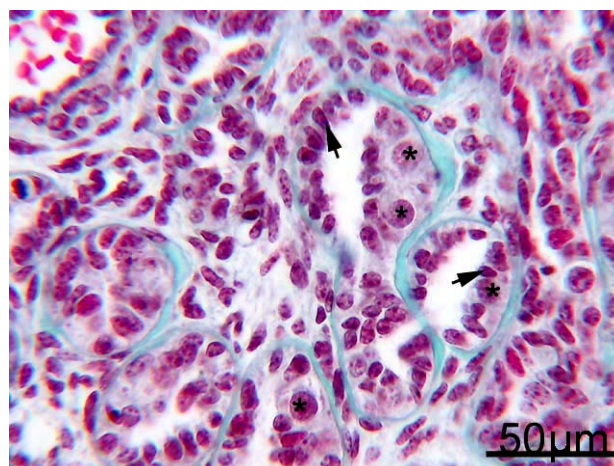
Fig 20: Invaded testicular cords are lined by a mixed population of rete testis cells (arrows), pre-Sertoli cells, and prespermatogonia (asterisks). Fetus with 18 cm CRL, Masson-Goldner᾽s trichrome
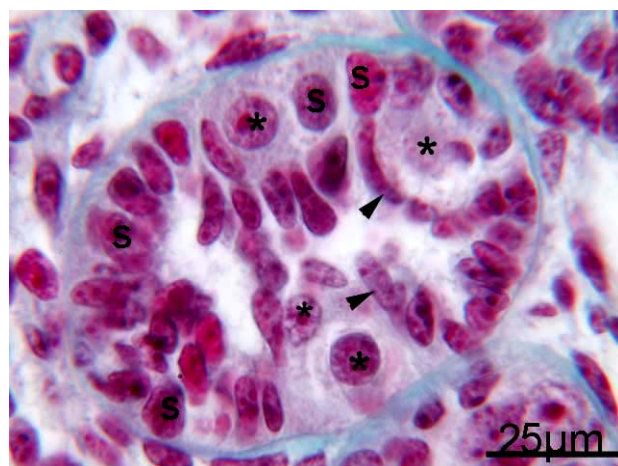

Fig 21: Higher magnification of an invaded testicular cord. Notice the mixed population of pre-Sertoli cells (s), prespermatogonia (asterisks), and rete testis epithelium (arrowheads). Fetus with 18 cm CRL, Masson-Goldner᾽s trichrome
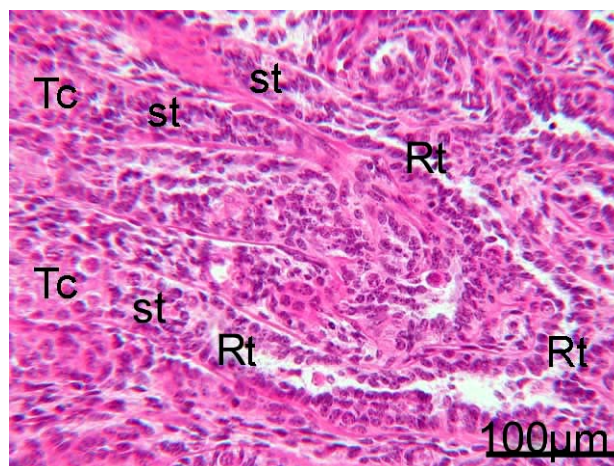
Fig 22: A well-defined connection between solid testicular cords (Tc) and canalized rete testis (Rt) via solid straight tubules (st). Fetus with 20 cm CRL, H.E.

Although no Leydig cells are seen within the mediastinum, numerous Leydig cells are observed between the invaded cords, which support the finding that straight tubules are mainly developed from the distal thin series of seminiferous cords (Fig. 23). Nevertheless,

when the connection between rete testis and testicular cords is established, these cells disappear.
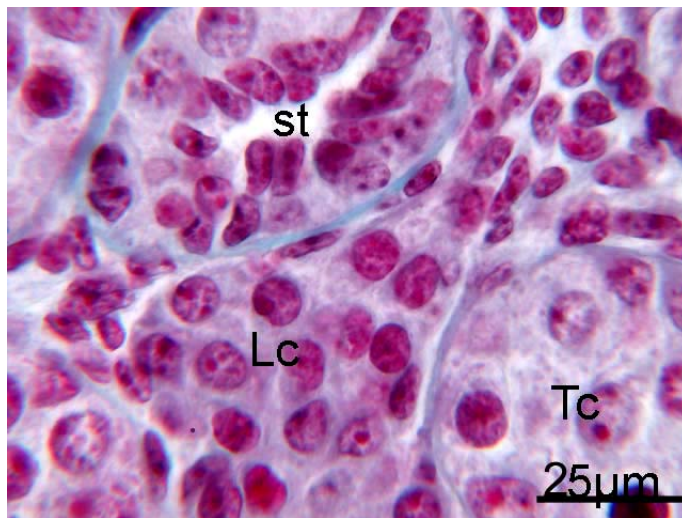
Fig 23: Fetal Leydig cells (Lc) are identified in the testicular interstitium within the area between the invaded testicular cords or future straight tubules (st) and other testicular cords (Tc) in this region. Fetus with 18 cm CRL, Masson-Goldner's trichrome

Rete testis channels are lined by simple layer of cuboidal to columnar epithelium with round nuclei occupying most of the cytoplasm; however neither pre-Sertoli cells nor prespermatogonia are found (Fig. 24). At the end of this stage (57 cm CRL/187 dpc), some cells begins to aggregate in the basal portion of the rete testis epithelium to form the short intraepithelial crypts characterizing the adult bovine rete testis (Fig. 24).
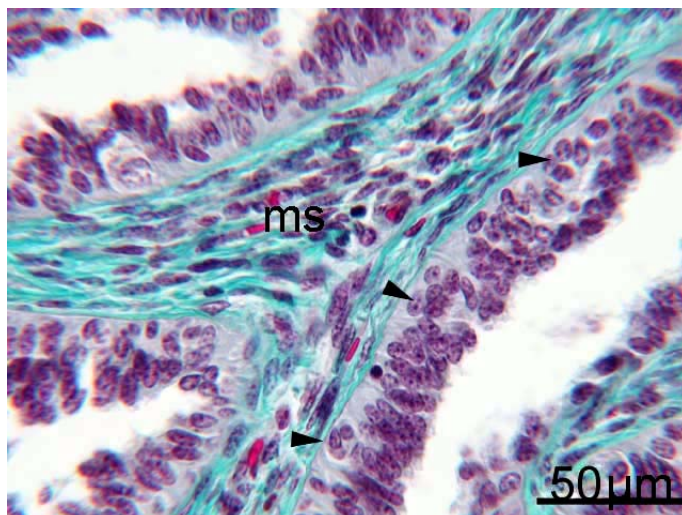

Fig 24: Rete testis channels of 57 cm CRL bovine fetus. Some cells are basally aggregated (arrows) to form the future intraepithelial crypts. The testicular mediastinum (ms) contains numerous spindle-shaped cells. Masson-Goldner's trichrome.

The initial crypts are enclosed by the basal lamina of the rete testis while the latter is surrounded by some spindle-shaped cells that may constitute the precursors of the future myofibroblasts (Fig. 24). Testicular stroma (mediastinum testis) present between rete testis channels contains both numerous spindle shape cells that are later identified as typical fibroblasts and frequent blood vessels (Fig. 24).

4.1.1.3. Late stage of gestation (63-90 cm CRL/210-285 dpc)

Although the testicular size has markedly increased during this period, no specific changes except the progressive dedifferentiation of Leydig cells are observed. As in the previous stage, the surface epithelium consists of one layer of flattened cells. TA develops into a broader band with larger diameter (table 11) and its inner vascular layer contains more differentiated blood vessels (arteries and veins in typical structure). The seminiferous cords are widely separated from each other by the continuously dedifferentiated interstitium and delimited by well definitive basal lamina as well as two layers of peritubular cells (Fig. 25). The peripheral cords are generally seen in cross or angular form while in the central area the longitudinal form is the predominant. Their diameters still within the range of 50-55 μm (table 11). Pre-Sertoli cells develop typical columnar shape while prespermatogonial mitotic division has greatly declined resulting in a striking reduction in the average number of germ cells per tubular cross section (table 11). The location and arrangement of the both cells within the testicular cords are however similar to the previous stage (Fig. 25). The interstitium has greatly changed and the connective tissue has considerably increased. Although numerous Leydig cells have disappeared, few of them are sporadically recognized. Pycnotic nuclei are only seen in very few cases.
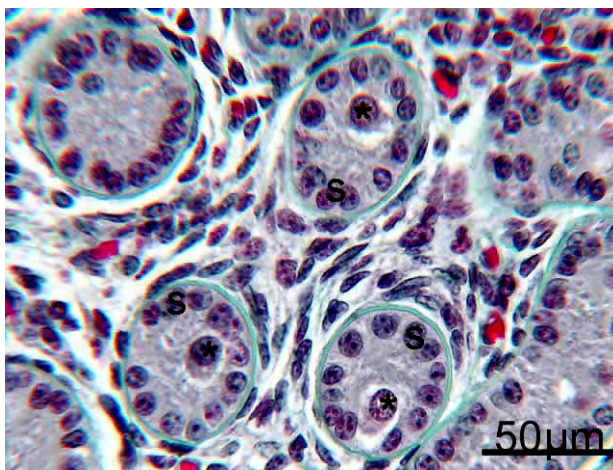
Fig 25: Testicular parenchyma of 80 cm CRL bovine fetus. The cords are lined by a basal row of pre-Sertoli cells (s) and more or less central prespermatogonia (asterisks) and are separated by undifferentiated mesenchyme. Masson-Goldner׳s trichrome
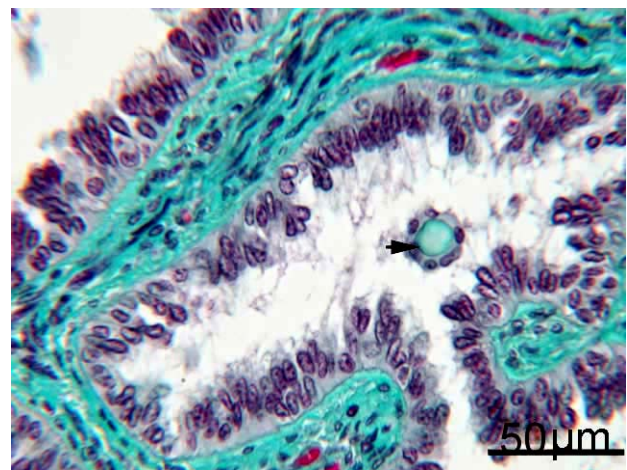
Fig 26: Rete testis of 80 cm CRL bovine fetus. The lining epithelium protrudes into the lumen and the chordae retis are clearly seen (arrow). Masson-Goldner׳s trichrome

The connecting straight tubules become longer and develop a marked lumen. The rete testis channels are irregular and show several anastomosis. The lining epithelium of these channels sometimes exhibits partial protrusions into the lumen. The chordae retis, a common feature of

the bovine rete testis, are additionally seen toward the end of gestation (Fig. 26). As in the mid stage, the mediastinum connective tissue separating the rete channels contains numerous blood capillaries and fibroblasts.

4.1.2. Adult testis: morphological overview

The histological organization of the adult bovine testis was investigated by using both light and electron microscope.

4.1.2.1. Tunica albuginea and lobuli testis

As in all species so far studied, the parenchyma of the adult bovine testis is surrounded by a thick white fibrous capsule of dense irregular connective tissue, *tunica albuginea*, which is covered by the visceral layer of the *tunica vaginalis*. Using special stains (Weigert's elastic stain and Masson-Goldner's trichrome), it can be demonstrated that TA is formed predominantly of collagen fibers and few elastic fibers. Numerous fibrocytes are also recognized within these fibrous components. In contrast to the outer zone of the TA (tunica fibrosa) that is compact and shows much fibrous elements, the inner surface (tunica vasculosa) is loose, highly vascular connective tissue. The latter is especially prominent in the bovine where large blood vessels are running in a tortuous pattern over most of the testicular surface. The inner layer of TA is additionally continuous with inconspicuous connective tissue trabeculae. As a consequence, adult bovine testis is not divided into clear pyramidal compartments, *lobuli testis* that are observed in the other species. TA is found to enclose tangential testicular parenchyma consisting of seminiferous tubules (tubuli seminiferi contorti) and interstitial compartments, and central mediastinum testis containing the excurrent duct system.

4.1.2.1.1. Tubuli seminiferi contorti

Most of the testicular parenchyma is made up of the convoluted seminiferous tubules (*Tubuli seminiferi contorti*), where the spermatozoa are formed (Fig. 27). These tubules are basically two-ended convoluted loops, with both ends opening into the rete testis via specialized terminal segments. The seminiferous tubules of sexually mature bulls are enclosed by a distinct lamina propria and are lined by two cell populations, non-proliferating Sertoli cells and highly proliferating spermatogenic cells. These structures are discussed in details in the following sections.
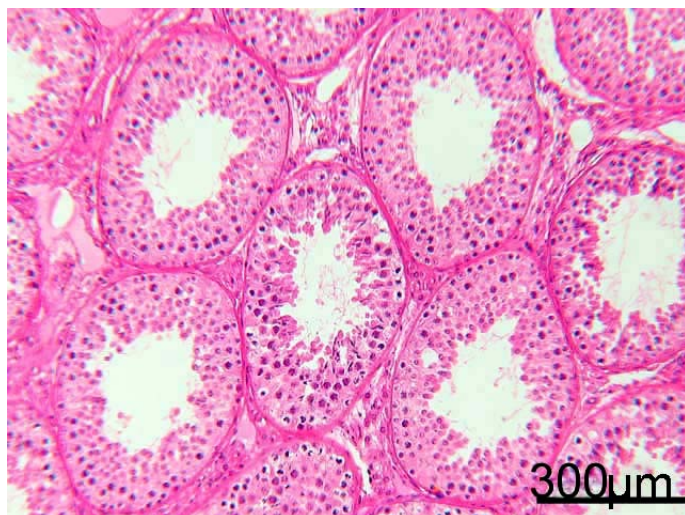
Fig 27: Most of the adult testicular parenchyma consists of convoluted seminiferous tubules, H.E.

4.1.2.1.1.1. Lamina propria

Cross section of a bovine seminiferous tubule is about 300 µm in diameter and is separated from the surrounding interstitium by a distinct lamina propria. The latter consists of a PAS positive basal lamina measuring between 0.5 and 0.8 µm (Fig. 28). It has however no or only very weak affinity for Alcian blue both at 1 and 2.5 pH. Subjacent to basal lamina, fine elastic fibers (resorcin-fuchsin positive structures) are additionally seen at the outer border of this lamina and in between the surrounding myofibroblast cell layers. Abundant cell-coat like material reacting positively with Alcian blue fills the interstices between peritubular cells and the Alcian-blue negative basal lamina.
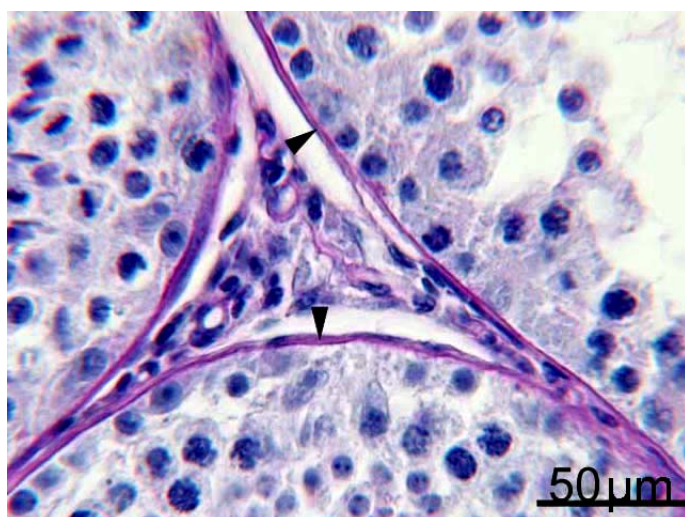

Fig 28: Tubular basal lamina (arrowheads) shows purple red staining with PAS.

Ultrastructure of the bovine lamina propria confirms the findings of the light microscope and provides more details. With EM, basal lamina of the convoluted seminiferous tubules appears as smooth surface multilayered structure that occasionally exhibits knob-like protrusions

invaginating into the basal portions of spermatogonia and Sertoli cells (Fig. 29a). At the site of these projections, the thickness of basal lamina is 1.1-1.3 μm diameters.
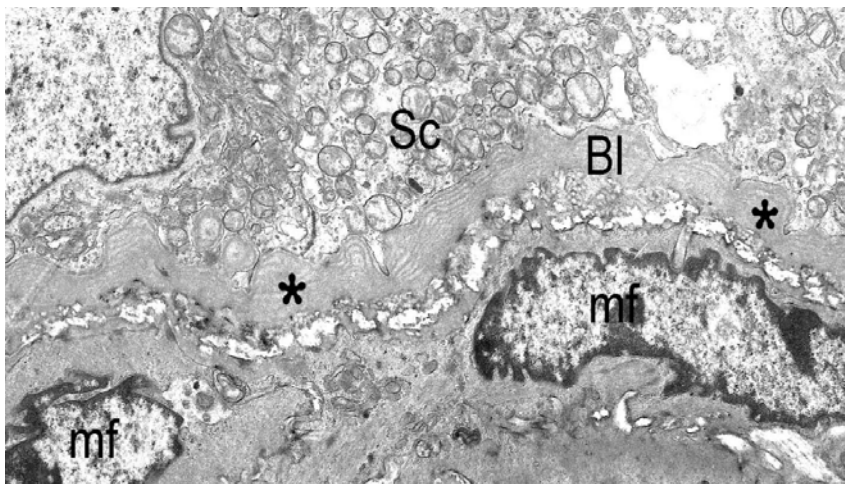
Fig 29a: Tubular basal lamina (Bl) appears as smooth surface multilayered structure that occasionally exhibits knob-like protrusions (asterisks) invaginating into the basal portions of Sertoli cells (Sc). mf are the myofibroblasts surrounding the Bl. X 3000
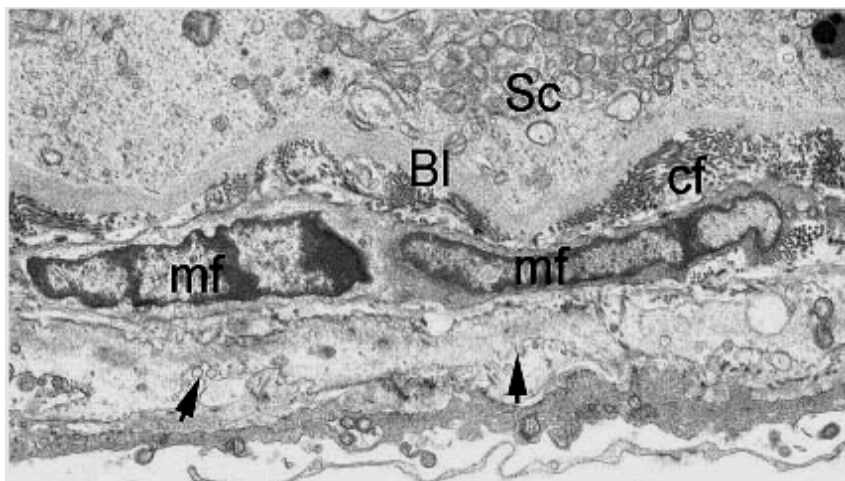

Fig 29b: Tubular lamina propria is composed of basal lamina (Bl), collagen fibrils (Cf), and myofibroblasts (mf). The cell periphery of the mf is characterized by round or pear-shaped micropinocytotic vesicles (arrows). X 3000

The basal lamina is surrounded by 3-5 layers of partially overlapping myofibroblasts covered on both sides by an inconstant basal lamina. The cytoplasmic matrix of myofibroblasts appears appreciably electron-dense and contains few mitochondria and some elongated profiles of rER. A peculiar and frequent feature of the cell membrane is round or pear-shaped micropinocytotic vesicles, which may contain a fine granular material (Fig. 29b). The nuclei of the myofibroblasts are elongated, fusiform, or rod-like and can reach a length of 15-20 μm. Collagen fibrils in various arrangements are additionally seen between the basal lamina of the seminiferous tubules and myofibroblasts as well as between the myofibroblasts themselves (Fig. 29b). However, I was unable to prove the existence of elastic fibres in the bovine lamina propria at the ultrastructural level. One to two layers of fibrocytes, collagen fibrils, and fibroblasts-like cells form the outermost border of the tubulus. Some blood vessels are also found in the lamina propria of some specimens. These vessels are situated in the zone between the layers of fibroblasts.

4.1.2.1.1.2. *Sertoli cells*

Under the light microscope, Sertoli cells are easily identifiable elements of the seminiferous epithelium. Adult Sertoli cells are large irregularly formed cells. Their broad bases rest on the basal lamina while the remaining cytoplasmic processes extend upward to the tubular lumen. Apart from their characteristic cytoplasm, they are characterized by round or oval nuclei located in the basal portion near the basal lamina of the seminiferous tubules. With higher magnification, these euchromatin-rich nuclei appear often deeply infolded or invaginated and contain large central nucleoli (Fig. 30).
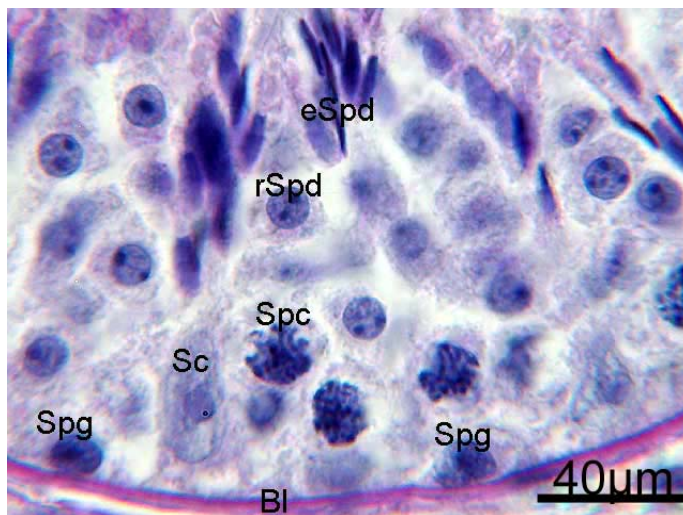

Fig 30: Overview of the adult seminiferous epithelium of bovine testis; spermatogonia (Spg), Sertoli cells (Sc), spermatocytes (Spc), round spermatids (rSpd), elongated spermatids (eSpd), and tubular basal lamina (Bl), PAS.

Fine structure of bovine Sertoli cells confirmed the irregular outline of the nucleus that showed numerous infoldings in its membrane (Fig. 31). Some organelles, such as mitochondria, free ribosomes, and cisternae of sER as well as intermediate filaments are observed in the indentation of the nucleus. The karyoplasm appears homogenous and contains little heterochromatin. The nuclear envelope has a small electron dense layer on the inner nuclear membrane. Nucleolus is a particular characteristic structure of the bovine Sertoli cell nucleus. It is composed of numerous vesicles of different sizes, tubules, and ribosomes-like structures (Fig. 31). Some vesicles contain very low electron dense material, whereas others apparently lack these contents. Frequently dark granular condensations are also seen at the outer surface of the vesicles. Generally, the position of the nucleolus is central, although some nucleolar vesicles are occasionally located close to the inner layer of the nuclear membrane. However, tubules are rarely found within this structure. Large invaginations of the nuclear envelope appear to be directed towards the nucleolus.
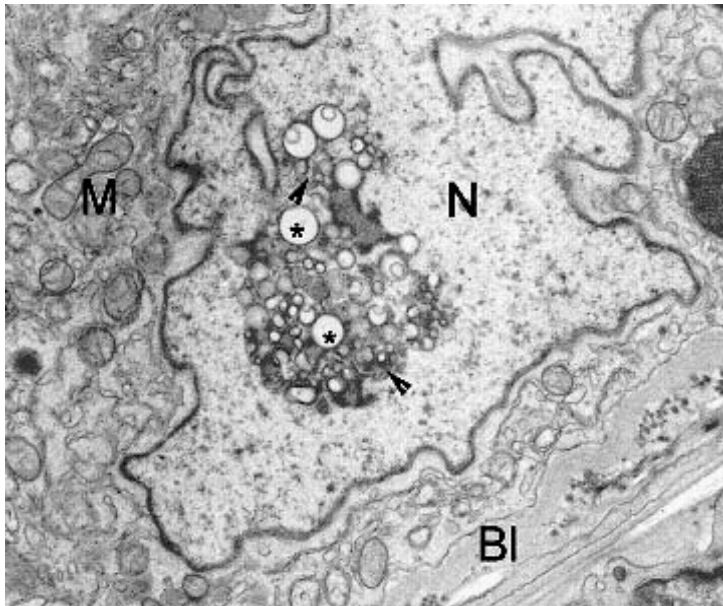
Fig 31: Electron micrograph of the nucleus (N) of adult Sertoli cell. The nuclear membrane is highly infolded. The karyoplasm appears homogenous with little heterochromatin. The nucleolus is composed of vesicles (asterisks), tubules (notched arrowhead), and ribosomes-like structures. The Sertoli cell cytoplasm contains numerous mitochondria (M) and approaches the tubular basal lamina (Bl). X 7000

The distribution of cytoplasmic organelles within the Sertoli cells shows a polar orientation with an abundance of various organelles and inclusions in the basal portion of the cell. The mitochondria in the basal part are small and round or oval in shape. They have transversely oriented cristae embedded in a relatively dense matrix (Fig. 31). In the apical cytoplasm, elongated mitochondria run along the major cell axis in this portion of the cell. The Golgi apparatus consists of a number of inconspicuous lamellar profiles, which are frequently situated near the nucleus, but some are also found in the apical cytoplasm. The endoplasmic reticulum is well developed and most of it is agranular or shows only a few ribosomes. Whorls of sER are often encountered in the bulky lateral processes in the basal part of Sertoli cells (Fig. 32).
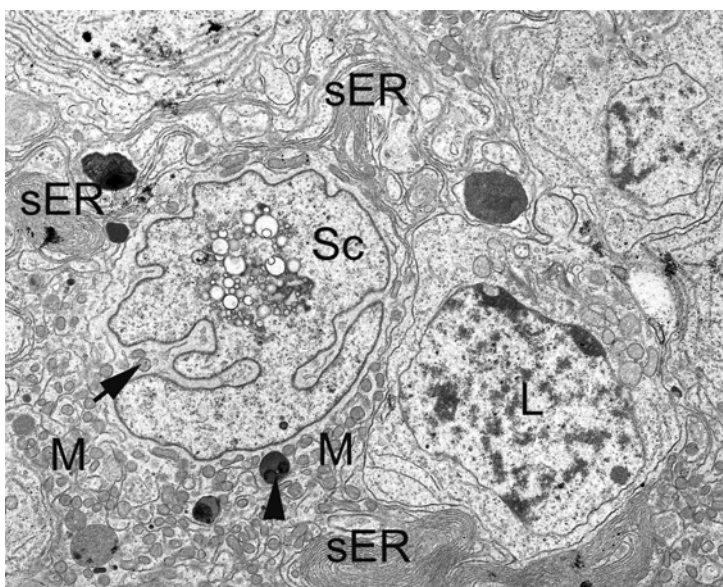
Fig 32: Electron micrograph of adult Sertoli cell (Sc). The cytoplasm contains several whorls of smooth endoplasmic reticulum (sER), some lipid droplets (arrowhead), and numerous mitochondria (M); some of them are located in the nuclear enfolding (arrow). L is a leptotene spermatocyte. X 3000

In addition, large accumulations of regularly arranged cisternae of sER are seen in those cell regions surrounding developing spermatids. These sER aggregations are firstly observed in late cap and early acrosomal phases as well as in the maturation phase. Contrary to rER that is only found in small amounts in the basal cytoplasm, free ribosomes, and polyribosomes are distributed throughout the whole cytoplasm. Dense, membrane-bounded bodies are also common in the cytoplasm. They probably represent primary and secondary lysosomes. Small numbers of lipid droplets of varying size are particularly seen in the basal cytoplasm while glycogen particles are dispersed throughout the cell. Sertoli cell cytoskeleton is shown to be well developed. Microtubules are abundant and most of them are located in the main trunk. Microfilaments occur throughout the cytoplasm and most of them constitute part of the cell contacts. Sertoli cells are known to have specialized cell junctions with other Sertoli cells and with germ cells as well. By means of these junctions, the Sertoli cells form a continuous layer dividing the seminiferous epithelium into two compartments: a basal one containing spermatogonia and preleptotene spermatocytes, and an adluminal one containing more differentiated spermatocytes and spermatids. This continuous layer comprises the ultimate and tightest part of the blood-testis barrier (Fig. 33).
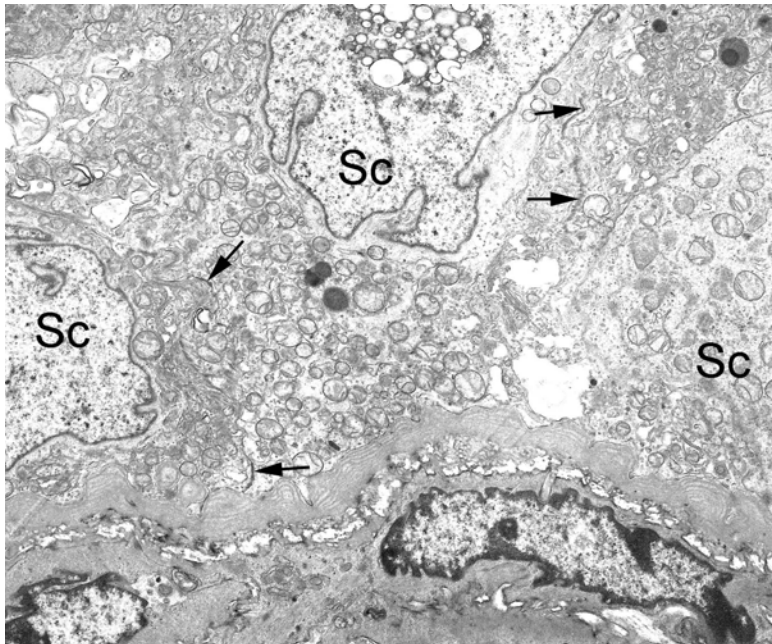
Fig 33: Electron microscope overview of the Sertoli-Sertoli cell (Sc) junctions (arrows). X 3000

The inter-Sertoli cell junctions are extensive occluding (tight) junctions (Fig. 33, 34). These are formed by fusion of the outer leaflets of opposing Sertoli cell membranes in the basal region of the seminiferous epithelium. Characteristically, bundles of microfilaments aggregated into amorphous electron-dense materials are frequently seen in the cytoplasmic

areas subjacent to the occluding junctions. Various numbers of ER cisternae (at least one) are also observed in these areas; however, actual whorls of sER are only recognized at some distances from the cisternae (Fig. 34).
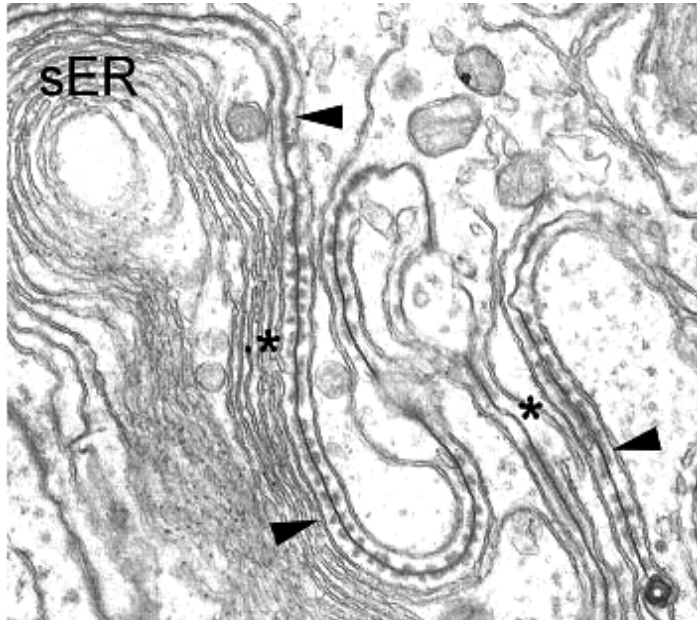
Fig 34: Higher magnification of Sertoli-Sertoli cell junctions (arrowheads). These are formed by fusion of the outer leaflets of opposing Sertoli cell membranes. Some cisternae of the sER are also observed in these areas (asterisks); however, actual whorls of sER are only seen at some distances from the cisternae. X 12000

Unlike the inter-Sertoli junctions, different types of contacts occur between Sertoli and germ cells. These include desmosome-like junctions, Sertoli ectoplasmic specializations, and tubulobulbar complexes (Fig. 35). Desmosome-like junctions are mainly seen as circumscribed contact areas between Sertoli cells and spermatogonia, spermatocytes and round spermatids. However and conversely to desmosomes, no line of dense material parallel to the cell membrane can be detected in the extracellular space.
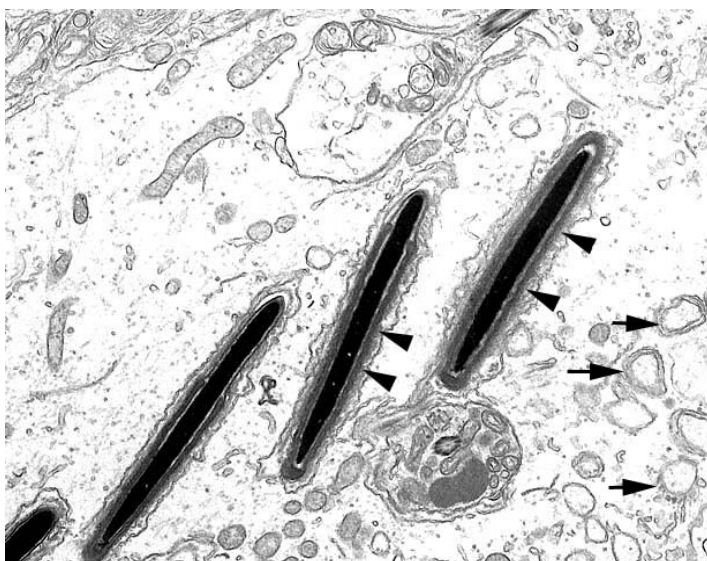
Fig 35: Electron micrograph of Sertoli cell-spermatids junctions. Sertoli ectoplasmic specializations (arrowheads) are developed in that part of Sertoli cells facing elongation and maturation-phase spermatids. Tubulobulbar complexes (arrows) are deep extension of the spermatid plasmalemma into corresponding invaginations in the Sertoli cells. X 3000

Sertoli ectoplasmic specializations are asymmetric junctional specializations, which exist only on the Sertoli cell side and consist of filaments and some cisternae of the sER. They are particularly well developed in that part of Sertoli cells facing elongation and maturation-phase spermatids and disintegrate at the time of spermiation (Fig. 35). Another peculiar cell contact is made with spermatids of the late maturation phase. These so called tubulobulbar complexes are deep extensions of the spermatid plasmalemma into corresponding invaginations in the Sertoli cells (Fig. 35).

4.1.2.1.1.3. Spermatogenic cells

In addition to Sertoli cells, tubuli seminiferi contorti are lined by germ cells in different phases of development. The exact identification of these cells under the light microscope is difficult with the conventional stains, but PAS staining, nuclei morphology and cell topography provide some help. A better distinction between the different generations of spermatogenic cells is however possible in semithin sections. Adult bovine germ cells are present in four morphologically different groups, i.e., spermatogonia, spermatocytes, spermatids, and spermatozoa (Fig. 30). Within the cell populations of the first three groups, different cell types are additionally recognized. Spermatogonia generally occupy the basal compartment while the spermatocytes and young spermatids are found in the mid and luminal portions of the tubule respectively (Fig. 30).

Spermatogonial cell population

Bovine spermatogonia multiply mitotically resulting in A-, I-(intermediate), and B-spermatogonia. A-spermatogonia (~20 μm) have the largest nuclei of spermatogonia (~12 μm) and share an extensive contact area with the basal lamina. They possess spherical or elongated nuclei with long axis parallel to the seminiferous tubule basal lamina (Fig. 36). The karyoplasm is homogenous with very little heterochromatin and contain one or more large prominent central or slightly eccentric reticulate nucleoli. The Golgi apparatus is inconspicuous and endoplasmic reticulum, most of which is agranular, is scarce. Many polymorphous mitochondria with lamellar cristae are randomly distributed in the cytoplasm. Spermatogonia intermediate types (Spg-I) resemble type A but are smaller (~16 μm). Consequently, their nuclei and contact areas with the basal lamina are small. B-spermatogonia are the smallest spermatogonia (~12 μm). They have spherical central nuclei with one or more nucleoli in a marginal position. Therefore, these nuclei appear with conventional haematoxylin and eosin stain darker than that of other spermatogonia. Although the contact

89

area of this cell with the tubular basal lamina is smaller than in type A, the organelles content of both cell types is similar.
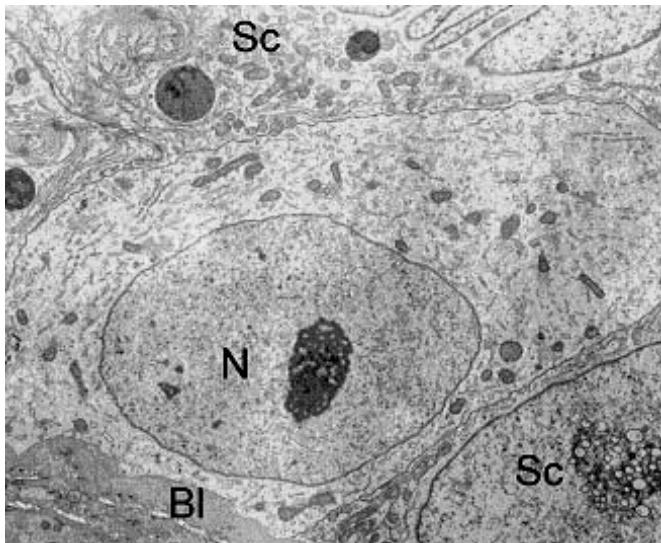
Fig 36: Electron micrograph of type A spermatogonium shows large area of contact with the basal lamina (Bl), large nucleus (N) with a prominent nucleolus and inconspicuous cytoplasmic organelles. X 3000

Spermatocytes:

Primary spermatocytes, the progenies of B-spermatogonia, are primarily located in the intermediate portion of the seminiferous epithelium. They are easily recognized by light microscope because they are the largest spermatogenic cells in the tubular epithelium (Fig. 30). However, despite the large round heterochromatin-rich nuclei of spermatocytes, it is difficult to differentiate between B-spermatogonia and the first generation of spermatocytes, *preleptotene primary spermatocytes*, with the conventional stains under light microscope. The latter, identified as spherical cells with nuclei containing thin threads of darkly stained chromatin, are observed towards the base but not in contact with the basal lamina. The subsequent stages of the prophase of first mitotic division (leptotene, zygotene, pachytene, diplotene, and diakinesis) are recognized by light microscope using either conventional stains or semithin sections.

Leptotene spermatocytes are larger than preleptotene and have a somewhat pale staining cytoplasm surrounding nuclei with deeply stained threads of chromatin. In EM, the nuclear membrane is slightly undulated and the heterochromatin begins to be displaced to one side of the nucleus. The Golgi apparatus is small and endoplasmic reticulum is scarce. More free ribosomes and polyribosomes are present than in spermatogonia. Ovoid mitochondria are found single or in cluster (Fig. 37).
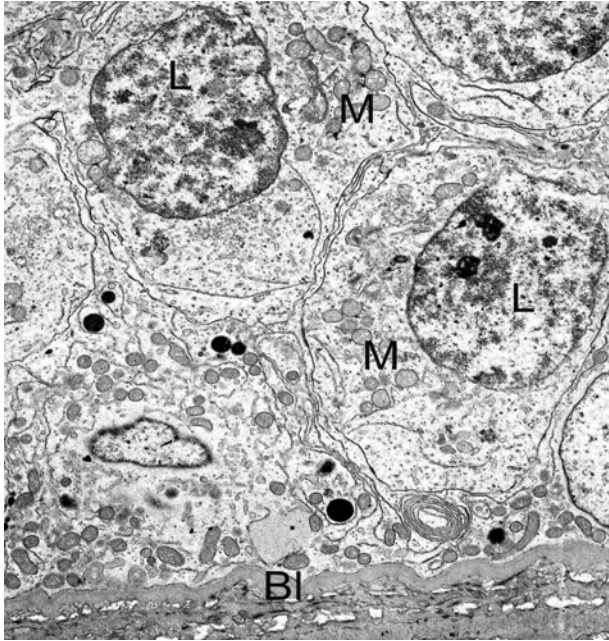
Fig 37: Primary spermatocyte in leptotene stage (L). Ovoid mitochondria (M) are found singly or in clusters and chromosome condensation has just started. Bl is the basal lamina. X 3000

In zygotene spermatocytes, both nucleus and cytoplasm have increased in size. With LM, the displacement of heterochromatin into one side of the nucleus sometimes gives it a half moon appearance. Ultrastructurally, areas of more condensed chromatin become apparent and synaptonemal complexes appear between the homologous chromosomes (Fig. 38).
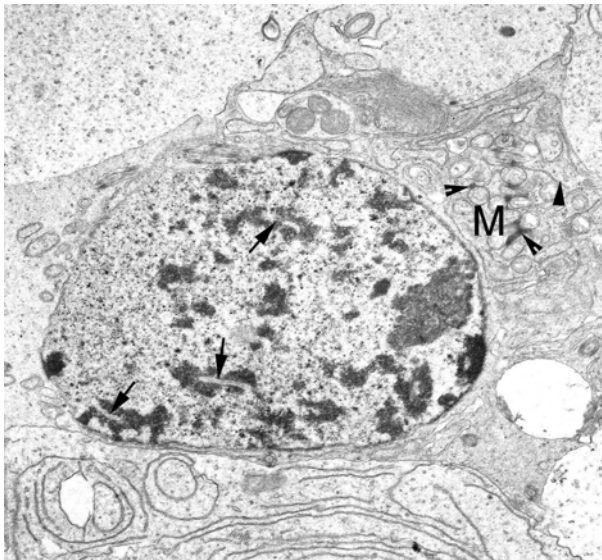
Fig 38: Primary spermatocyte in the zygotene stage. Chromosome condensation has proceeded and the individual chromosomes are more apparent. In this stage, synaptonemal complexes (arrows) appear between the homologous chromosomes. Groups of mitochondria (M) are connected by dense intermitochondrial substances (notched arrowhead). Some cisternae of rER are present between the mitochondria (arrowhead). X 4400

The Golgi apparatus is still fairly small while the rER increases further and may penetrate with narrow cisternae between clustered mitochondria (Fig. 38). Characteristically, groups of mitochondria approach each other and dense intermitochondrial substance appears.

During pachytene phase, primary spermatocytes are generally best identified in all microscopic preparations. These cells are large with equally large nuclei and prominent nucleoli. Some areas of condensed chromatin are also seen within the nuclei of these cells.
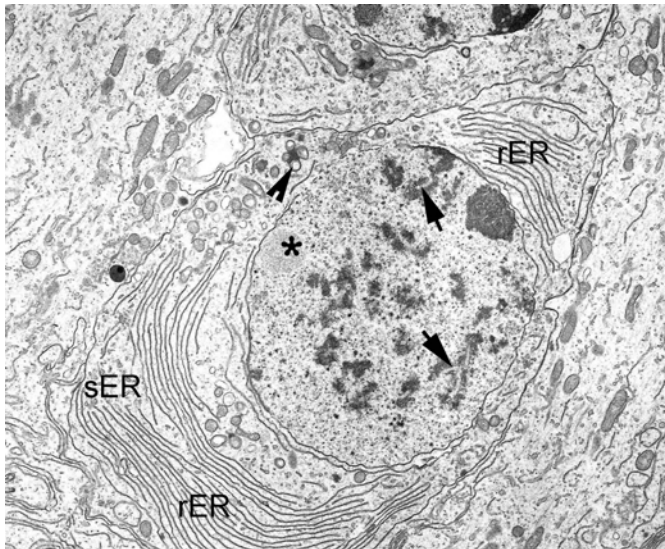
Fig 39: Late primary pachytene spermatocytes. The cell is large and the nucleus is prominent. The chromosomes are further condensed and the synaptonemal complexes (arrows) are easily recognized. Under the nuclear membrane, the sex vesicle (asterisk) appears as clear area. In the cytoplasm, the mitochondria are gathered in groups (notched arrowhead), a lot of rER occupies marginal positions and sER started to expand.
X 3000

Since chromosomes have become more contracted, areas of condensed chromatin are seen in the karyoplasm. In these areas, synaptonemal complexes are often encountered. In addition, the sex vesicle appears as a light zone just beneath the nuclear envelope (Fig. 39). Small amounts of heterochromatin accumulate at some places of the inner nuclear membrane where the reticular nucleolus is also situated. Compared to the zygotene stage, the cytoplasm contains numerous organelles. The Golgi apparatus is well developed and considerable flattened cisternae of rER elongate and form stacks of several layers in the cellular periphery (Fig. 39). In the remainder of the cytoplasm, sER is observed as irregularly arranged tubules with a cloudy content. Mitochondria are characterized by dilated cristae and are gathered in rosette-like groups holding together by dense intermitochondrial substance (Fig. 39).

Diplotene spermatocytes have deeply stained cords of chromatin some of which marginated on the nucleolar membrane. It differs from pachytene in few respects only. The cell and the nucleus are larger and synaptonemal complexes no longer persist. In the cytoplasm, some of the intermitochondrial substance separates from the mitochondria and appears free in the cytoplasm. In several diplotene spermatocytes multivesicular bodies occur.

During the prophase of the first meiotic division, the spermatocytes increase considerably in size. With the end of this division, short-lived cells, *the secondary spermatocytes*, are produced. These cells are round cells with intermediate size between diplotene spermatocytes and round spermatids and occur solely in phase 4 of the seminiferous epithelial cycle. The nucleus of the secondary spermatocyte has a relatively uniform distribution of chromatin with a thin rim of marginal heterochromatin. Just beneath the nuclear envelope, patches of very dense heterochromatin are also observed. Characteristically, the nuclear membrane of secondary spermatocytes is not smooth, but exhibits a number of slight bulges. The abundant

ER is no longer organized in stacks but in reticular partially dilated profiles. Mitochondria still display dilated cristae and are randomly distributed. The former intermitochondrial substance coalesces to form an irregular dense body in the cytoplasm. The spherical Golgi complex resembles that of primary spermatocytes but exhibits smaller dimensions (Fig. 40).
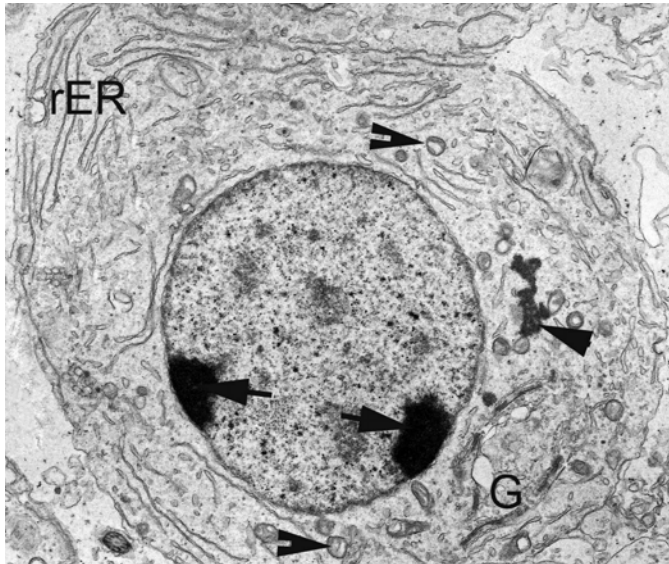
Fig 40: In secondary spermatocytes, the nucleus appear homogenous and area of marginal heterochromatin are present (arrows). Most mitochondria (notched arrowheads) have separated and lie isolated but retain their dilated cristae. The intermitochondrial substance coalesced to form irregular dense body within the cytoplasm (arrowhead). The Golgi complex (G) is also recognized and the rER is no longer organized in stacks but in reticular partially dilated profiles. X 4400

Spermatids

After the second meiotic division, secondary spermatocytes develop into round spermatids. These latter cells (round spermatids) are exclusively located in the adluminal portion of the seminiferous epithelium and undergo a complex series of cellular transformation (spermiogenesis) that finally leads to formation of mature elongated spermatids. Grossly, this process takes place via four well-defined phases termed Golgi, cap, acrosomal, and maturation phase. Under light microscope, the first and second phases are characterized by spherical nuclei whereas the third and fourth phases have elongated nuclei (Fig. 30).

During the *Golgi phase*, the cytoplasm of the newly formed spermatids exhibits a barely stained irregular zone (Golgi vesicles) containing several PAS reactive particles of various sizes, the proacrosomic granules, which locate close to the nucleus (Fig. 41). Later on, these granules coalesce to form a single structure, the acrosomic granule. The spermatid nucleus is nearly spherical and occupies a central position.

Fine structure of Golgi phase spermatid supports these findings. The nucleus has evenly distributed chromatin and a small but distinct nucleolus. Occasionally a heterochromatic body is seen beneath the nuclear envelope. The leaflets of the nuclear envelope are widely separated except in the area facing the forming acrosome. Characteristically, the spermatid cytoplasm contains a prominent Golgi apparatus comprising several dictyosomes. The length

of the cisternae within a dictyosome increases markedly from the forming to the mature side. Numerous vesicles of varying size are additionally seen as being migrated from Golgi apparatus toward the nucleus. On their way, they increase in size due to their coalescence and form one large vacuole (acrosomal vacuole) containing electron-lucent material. This vacuole is firstly attached to the nucleus and later gradually flattens and spreads over the nucleus where its content concentrates to form the comparatively electron-dense acrosomal granule.
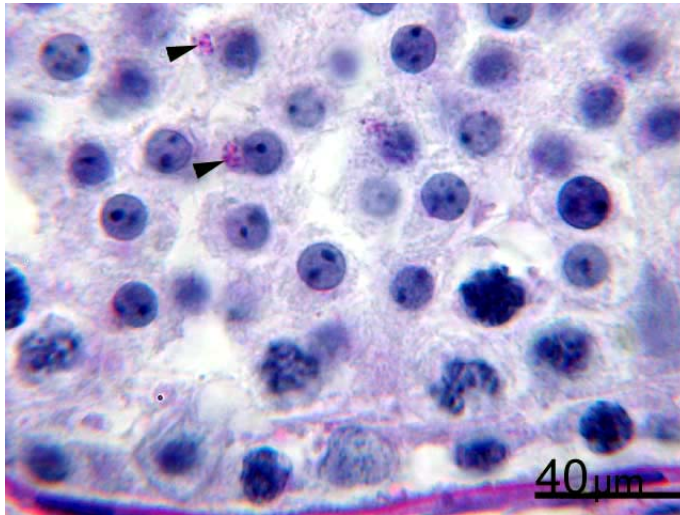
Fig 41: Golgi-phase spermatids. Their cytoplasm contains several PAS positive particles (proacrosomic granules) which are located close to their round nuclei (arrowheads).

Simultaneously with the gradual development of the acrosome, the centrioles are located near the plasmalemma in the Golgi region. From the distal centriole, the axoneme starts to develop and a plate of electron dense material appears over the proximal centriole. The centrioles begin to move into the cytoplasm and the plasmalemma, on the cytoplasmic side of which the annulus appears, invaginates to form a cytoplasmic canal. In the vicinity of the centrioles the chromatoid body and a group of vesicles are located. The cytoplasm of Golgi phase spermatid also contains randomly scattered mitochondria with dilated cristae and numerous profiles of sER.

In the subsequent stage, *cap phase*, (Fig. 42, 43) the acrosomic vacuole increases in size and flatten slightly at the surface of the nucleus. Then, it expands over the nuclear surface giving rise to a membranous structure, the head cap. The Golgi apparatus appears active and other organelles are similar to those in Golgi phase spermatids (Fig. 42)

During the next steps, the head cap enlarges and covers a third and finally a half of the nuclear surface. The acrosomal granule seems to be more electron-dense compared to the lateral parts of the head-cap (Fig. 43).
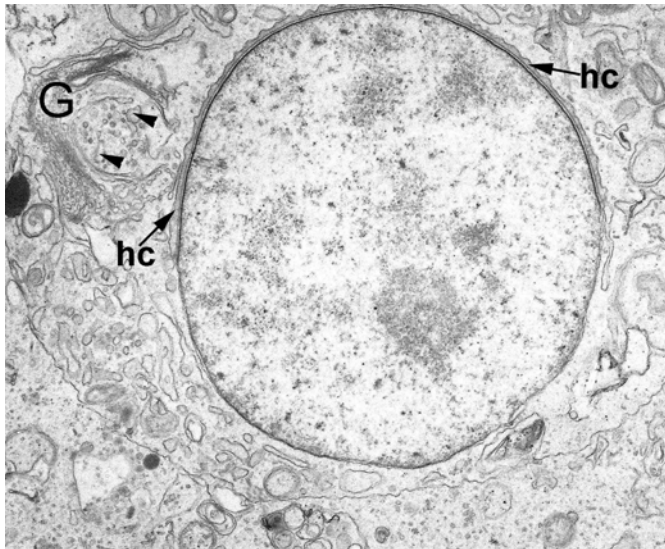
Fig 42: Early cap phase spermatids showing the presence of head cap (hc). Some vesicles (arrows) are still budding from the Golgi complex (G). X 4400
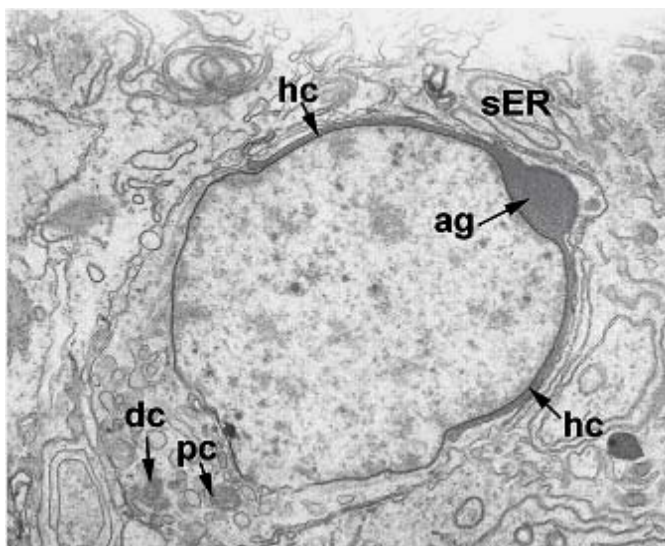
Fig 43: Electron micrograph of late cap phase spermatids. The nucleus begins to elongate, the head cap (hc) covers more than half of the nucleus and the acrosomal granule (ag) is enlarged. Some sER have begun to aggregate near the developing acrosome while the proximal (pc) and distal centrioles (dc) became adjacent to each other. X 7000

At the end of the cap phase, an aggregation of sER usually in the form of a close meshed network of anastomosing tubules is observed in the cytoplasm of the neighboring Sertoli cells that immediately surrounds the developing acrosomes (Fig. 43).

In the transition between cap and acrosome phase, the centrioles with their associated structures approach and make contact with the nucleus at the pole opposite to the acrosomal granule (Fig. 44).

As the ***acrosome phase*** starts, the acrosomic granule and head cap of spermatids are oriented toward the basal lamina. This is accompanied by a displacement of nucleus and cytoplasm toward the cell membrane. Finally, the acrosomic granule and head cap bulge on the cell surface facing outside of the tubule. Meanwhile, the acrosomal granule increase slightly in volume and protrude at the tip of the nucleus (Fig. 44). Subsequently, both the nucleus and

the acrosome are elongated whereas the latter begins to insert deeply in the Sertoli cell cytoplasm.
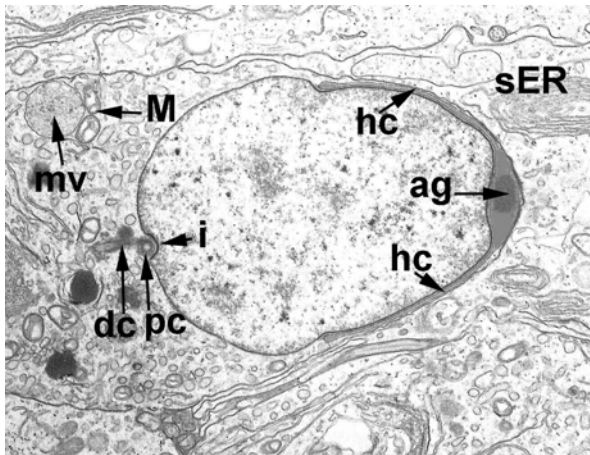
Fig 44: Very early acrosome phase spermatids. The nucleus has further elongated. Proximal (pc) and distal centriole (dc) are well embedded in the nuclear implantation fossa (i). On the other side of the nucleus, the acrosomal granule (ag) and head cap (hc) is always seen. Within the cytoplasm of spermatid, mitochondria (M) and multivesicular bodies (mv) are recognized. A whorl of sER is present in the cytoplasm of Sertoli cell. X 4400

The process of nuclear elongation is considerably complex and associated with gradual chromatin condensation. During the initial elongation, the chromatin pattern remains unchanged but later it becomes evenly distributed in form of thin threads (Fig. 45). The acrosome also undergoes several obvious rearrangements. The acrosome granule becomes more projecting and the contents of the rest of acrosome are more electron dense. As the elongation and flattening proceed, the chromatin threads are coarser and towards the end of this phase, the condensation is almost complete. Condensation starts in the peripheral part of the nucleus that is covered by the acrosome but spreads very rapidly throughout the nucleus. Definitely, the nuclear envelope does not follow the contour of the condensed chromatin and a zone of low electron density appears between the chromatin and the nuclear envelope in the postacrosomal region at the nucleus. This redundant nuclear envelope projects caudally as pockets (Fig. 45).
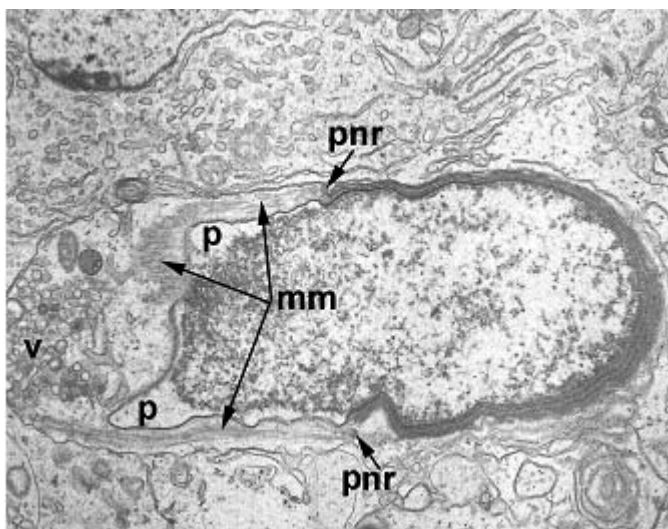
Fig 45: Electron micrograph of acrosome phase spermatid during the initial steps of elongation. The chromatin is evenly distributed in form of thin threads. The redundant nuclear envelope projects caudally as pockets (p). The microtubules manchette (mm) extends from the perinuclear ring (pnr) and comes distally into contact with numerous vesicles (v). X 7000

Remarkably, the manchette, a transient cellular structure composed of laterally associated microtubules (Fig. 45), appears immediately prior to the onset of chromatin condensation. This structure encloses the caudal part of the nucleus and has its anterior insertion in the dense material of the perinuclear ring from which it extends for some distance into the postnuclear cytoplasm. The perinuclear ring is an invagination of the plasmalemma just behind the acrosome (Fig. 45). The manchette appears to slide distally during the nuclear elongation. In the remaining cytoplasm, the organelles are randomly distributed. Numerous small vacuoles are found near the posterior end of the manchette (Fig. 45).

During the transition between acrosome and maturation phase (Fig. 46), the perinuclear ring starts its migration towards the posterior pole of the nucleus and subsequently disappears together with the microtubules of the manchette.
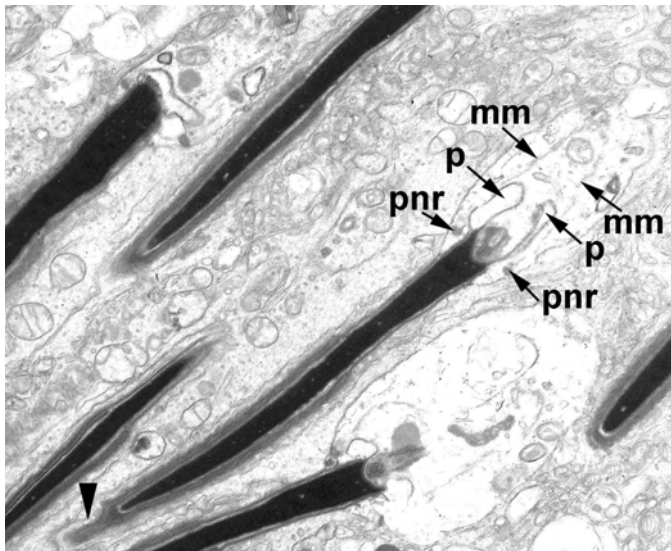
Fig 46: Transition between acrosome and maturation phase. Note the asymmetric tongue-like protrusion of the acrosome (arrowhead). The perinuclear ring (pnr) migrates towards the posterior pole of the nucleus, the redundant nuclear envelope forms very small pockets (p), and the microtubules manchette (mm) begins to disappear. X 7000

If not already completed, the final condensation of the chromatin takes place. As the perinuclear ring migrates, the postacrosomal sheath is formed and the underneath nuclear envelope becomes closely apposed to the chromatin. The bulbous swelling of the anterior part of the acrosome partly retracts, leaving an asymmetric tongue-like projection (Fig. 46). During the *maturation phase*, the spermatids complete their evolution into spermatozoa. The acrosome flattens at the apex of the head cap and the PAS reactivity of both acrosome and head cap decreases progressively. With EM, the asymmetric tongue-like projection is not evident and redundant nuclear envelope is less conspicuous while the nucleus gets the typical flattened paddle-shaped form characterizing the bovine spermatozoon (Fig. 47).
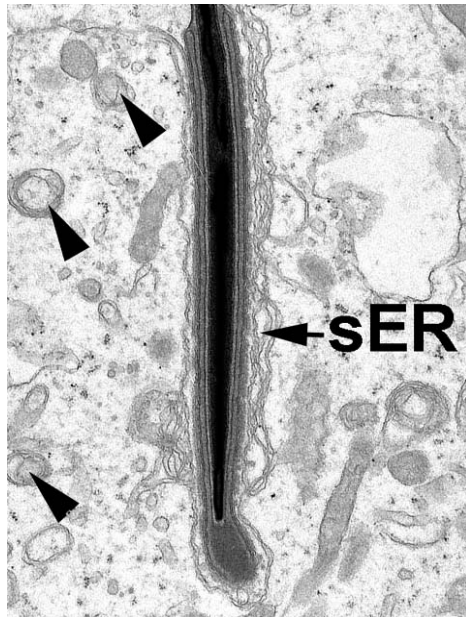
Fig 47: Maturation phase spermatid. It is embedded in the apical Sertoli cell cytoplasm and surrounded by a layer of fine filaments and subsurface cisterna of sER (ectoplasmic specialization). The arrowheads point to tubulobulbar complexes. (X 7000)

The connection between the acrosome and the spoon-shaped anterior process becomes more and more attenuated (Fig. 47). In the Sertoli cell cytoplasm adjacent to the acrosome, a layer with bundles of fine filaments followed by a single subsurface cisterna of sER is easily identifiable (this layer form what is called ectoplasmic specialization). Later in this phase, the developing tail of the bovine spermatozoon is additionally well organized and can be easily divided from proximal to distal into neck, middle piece, principle piece, and end piece. Generally, there are significant differences in the internal structure of these four segments. Toward the end of this phase, the spermatids have only little contact with the Sertoli cells and they are subsequently released into the lumen of the seminiferous tubule.

4.1.2.1.1.4. Seminiferous epithelium cycle

Stages of the seminiferous epithelium cycle are classified using changes in the germ cell nuclei as well as location and shape of spermatids. According to this method, eight stages are recognized in the seminiferous epithelium of bovine (Rüsse and Sinowatz, 1991; Wrobel, 1998). However, of the eight stages identified in this study, stage 6 and 7 are considered as a slight morphological modification of stage 5. As a result, they are combined into one main stage, stage 5-7. Consequently, the bovine seminiferous cycle is condensed into 6 main stages. The cycle begins with accomplished spermiation (stage 1) and ends with the positioning of maturation phase spermatids at the Sertoli cell apex ready for release (stage 8). The accompanying spermatogonia and spermatocytes are identified by their morphology and position in the epithelium as mentioned above. The six stages are described in details as following:

Stage 1: This stage is characterized by the absence of maturation phase spermatids on the Sertoli cell apices. Consequently, only one generation of spermatids are observed in the early stage tubules (stages 1-4). The round cap phase spermatids locate nearest to the lumen followed basally by two generations of primary spermatocytes (spc), late pachytenes, and young preleptotenes (Fig. 48).

Stage 2: During this phase, seminiferous epithelium shows flattening and elongation of both spermatids and their darkly stained nuclei. These spermatids have distinctly begun to enter the acrosomal phase. Pachytene spermatocytes are as large as in stage 1 with equally large nuclei whereas leptotene spermatocytes are transformed into zygotene spermatocytes (Fig. 49).
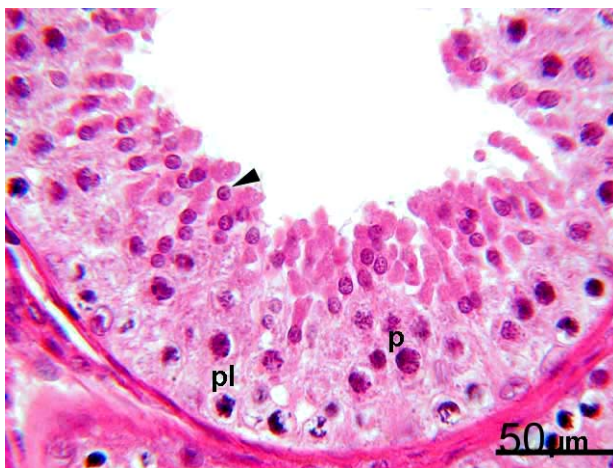
Fig 48: Stage I is characterized by one generation of round spermatids (arrowhead), pachytene (p) and preleptotene(pl) spc, H.E.

Fig 49: In stage II, the nuclei of round spermatid is elongated (arrowhead). Pachytene (p) and zygotene (Z) spc are also identified, H.E.

Stage 3: This stage of the cycle is markedly characterized by further flattening and elongation of spermatids, which are arranged in bundles in close association with the apical portion of the Sertoli cells (Fig. 50). The spermatid nucleus assumes the shape of the sperm head and although nuclear condensation is complete, tail formation is advanced but incomplete. Pachytene spermatocytes are replaced by diplotene spermatocytes while a second generation of spermatocytes in zygotene stage is located in the basal region.

Stage 4: In this stage, the first and second maturation divisions take place (Fig. 51). The nuclei of the late acrosomal and early maturation phase spermatids have, by this time, undergone advanced condensation. In addition to bundles of maturing spermatids and

zygotene spermatocytes, diplotene spermatocytes, secondary spermatocytes, or spherical spermatids are seen.
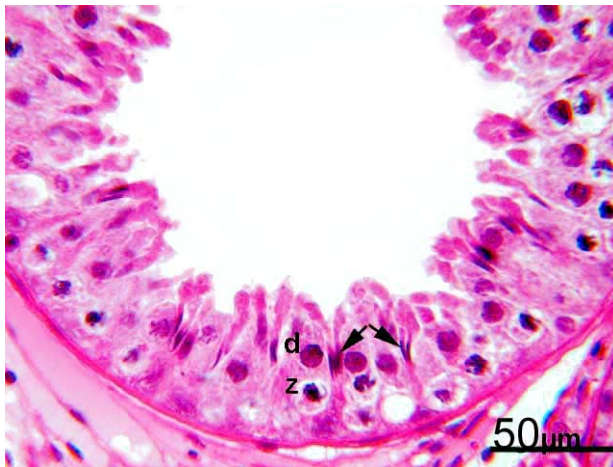
Fig 50: In stage III, the elongating spermatids are arranged in bundles (arrows) and pachytene spc are replaced by diplotene (d) spc. In the basal compartment, zygotene spc are additionally seen, H.E.

Fig 51: Stage IV is particularly characterized by the presence of second meiotic division (MII) and secondary spermatocytes (SpII). Zygotene spc (Z) are also identified , H.E.

Stage 5-7: In this stage, the association of germ cells consists of spermatogonia, only one generation of spermatocytes (pachytene spermatocytes), and two generations of spermatids (round spermatids in Golgi phase and elongated spermatids in maturation phase) (Fig. 52). Pachytene spermatocytes have shifted basally due to presence of large cell populations of round and elongated spermatids. The round spermatids are accumulated along the Sertoli cells and arranged in vertical columns of 3-4 cells, which are in the depth of columns are often separated by interconnecting Sertoli cells.

Stage 8: The last stage of the cycle is characterized by apical migration and close attachment of late maturation phase spermatids accompanied by adluminal retention of residual bodies with large dark staining inclusions (Fig. 53). This spermiation is also associated with apical shifting of pachytene spermatocytes. The remaining cells within the tubular epithelium are spherical spermatids (in changing from Golgi to cap phase) and two generation of primary spermatocytes (older pachytenes and younger preleptotenes).
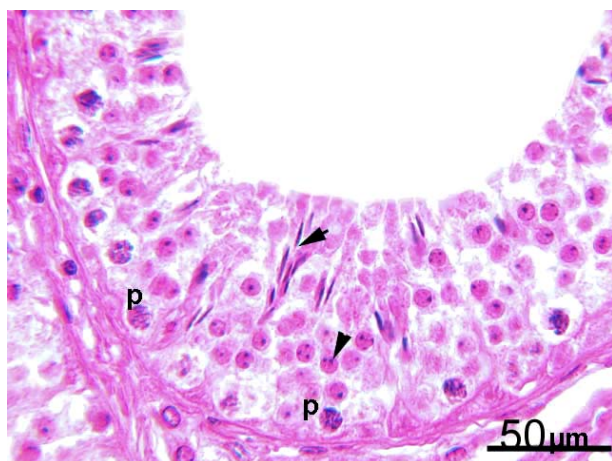
Fig 52: In Stage V-VII, two generations of spermatids are observed; elongated (arrow) and round (arrowhead), while only one generation of spc (pachytene, p) is basally located, H.E.

Fig 53: In Stage VIII, the spermiation begins and the residual bodies (arrowheads) are recognized. Pachytene spc (p) are shifted again to the mid portion of the seminiferous epithelium, H.E.

4.1.2.1.2. Intertubular compartment

The interstitial or intertubular tissue of adult bovine testis is a highly organized testicular structure. It consists either of narrow strands lodged between two adjacent seminiferous tubules or large tri-and quadrangular interstices between three to four tubules (Fig. 54). The differences between these two interstitial forms are mainly due to their constituents as the former is composed only of blood capillaries, occasional Leydig cells, and some connective tissue fibers and cells while the latter contains large vessels (blood and lymph) and numerous Leydig cells as well. Bovine Leydig cells occur in cords or clusters of varying size that appear to be random in their distribution, some being perivascular, others unrelated to vessels and still other closely associated with the lamina propria of the tubules.
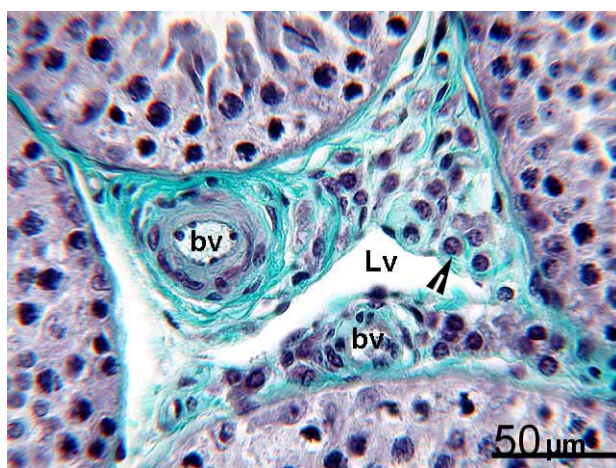
Fig 54: Organization of the interstitium of adult bovine testis. The lymph vessel (Lv) is centrally located while the blood vessels (bv) are peripherally situated and some of them come in contact with the tubular lamina propria. Some Leydig cells (notched arrowhead) are present in the vicinity of Lv, Masson-Goldner's trichrome.

Morphologically, Leydig cells are large round cells with spherical nuclei containing a small amount of peripherally disposed heterochromatin and one or two prominent nucleoli. Their cytoplasm is acidophilic in routine preparation and contains a number of empty vacuoles where lipid droplets were extracted during tissue processing. Ultrastructurally, the nucleus of bovine Leydig cells is round or oval in shape while the cytoplasmic matrix is of moderate density and contains some free ribosomes and polyribosomes. Small vesicles are additionally seen in the cell periphery. Although, sER and rER are predominant constituent of the Leydig cell cytoplasm, rER is present in relatively small quantities (Fig. 55). However, ribosome associated ER is additionally recognized. This either consists of sER profiles bearing single ribosomes or short strands of rER that are interposed in the course of the sER. In many cells, a highly organized configuration of the sER is found. Here the ER occupies extensive areas of the peripheral cellular regions in the form of concentrically arranged narrow cisternae. The mitochondria are randomly distributed and the individual mitochondrion is round to oval in shape (Fig. 55). The mitochondrial matrix is relatively dense and may contain conspicuous intramitochondrial granules. Moreover, a large number of mitochondria contains single or multiple crystalloid structures. Generally, the Golgi apparatus of bovine Leydig cell is not extensive and consists of flattened saccules and small vesicles. The amount of lipid droplets varies but is never high. The adjacent Leydig cells within cords and clusters are joined by gap junctions.
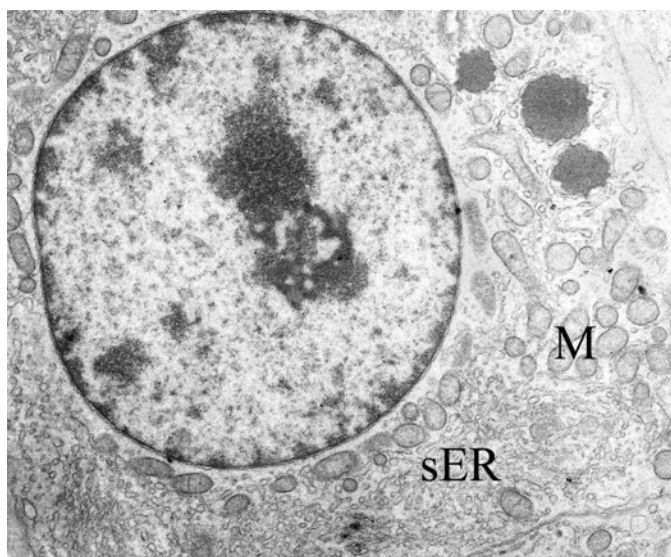
Fig 55: Electron micrograph of adult bovine Leydig cell shows numerous mitochondria (M) and sER. X 7000

As a rule, prominent lymphatic vessels are centrally located in the intertubular area (Fig. 54). Generally, one of these vessels is ever seen in each angular interspace but in some of the larger spaces, there may be two or three. The wall of the intertubular lymph vessels is only composed of uninterrupted endothelial lining whereas no typical basal lamina or associated

musculature is being seen. Bovine interstitium also contains blood vessels that are often peripheral and may be firmly attached to the lamina propria of the seminiferous tubules (Fig. 54). In addition to Leydig cells as well as blood and lymph vessels, special stains (Masson-Goldner's trichrome and Weigert's elastic) revealed the presence of some collagen and elastic fibrils within the interstitium. The latter are principally surrounding the seminiferous tubules while the former are abundant between the cords and clusters of Leydig cells. Immunohistochemically, several immune cells (macrophages and lymphocytes) are also identified within the intertubular stroma (described later). However, no cells of this compartment exhibit staining affinity for either Alcian or toluidine blue stain which may be indicatives for the absence of mast cells at least within the adult bovine interstitium.

4.1.2.1.5. Mediastinum testis

Mediastinum testis is a connective tissue zone occupying the central region of the bovine testis and is laterally and caudally surrounded by testicular parenchyma. In addition to the clearly defined contractile-elastic elements (myofibroblasts and elastin), bovine mediastinum contains rete testis channels, large blood vessels and spacious lymph vessels. However, no Leydig cells are seen in the mediastinal stroma. Occasionally straight tubules or at least their distal part are seen at the peripheries of the mediastinum which adjacent to the parenchyma. Blood vessels of the mediastinum originate from the large vessels of the tunica vasculosa of tunica albuginea where they turn into highly convoluted coils flanking the rete testis. Most of these blood vessels are associated with considerable number of toluidine blue positive cells. Numerous lymph vessels are located within the mediastinum, often in close contact to the rete channels. The wall of these vessels comprises a flattened endothelium and a discontinuous basal lamina whereas no musculature is seen. Within the mediastinal stroma, numerous immune cells especially macrophages are additionally found (described in the immunohistochemical section).

4.1.2.1.6. Intratesticular excurrent duct system

The excurrent duct system of the adult bovine testis consists of terminal segment of the convoluted seminiferous tubules, straight tubules, and rete testis. The terminal segment is a short transitional zone connects between seminiferous tubules and tubuli recti and is lined by cells designated as modified Sertoli cells (Fig. 56, 57). On the basis of regional variation in its light microscopic appearance, each terminal segment may be subdivided into a proximal (transitional) region, middle portion, and distal part (terminal plug) (Fig. 56).
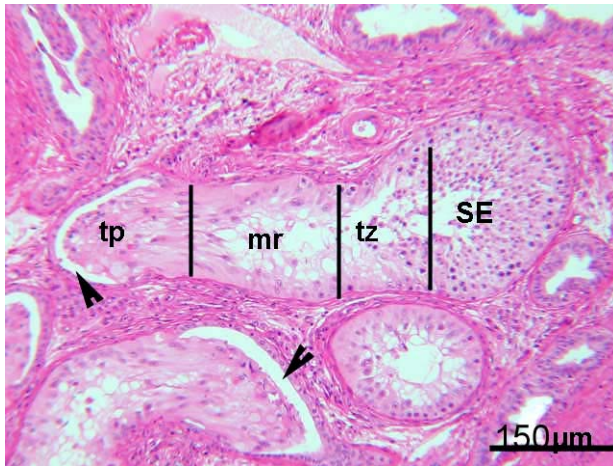
Fig 56: Overview of the bovine terminal segment. The convoluted seminiferous tubule (SE) is known to connect with straight tubule (notched arrowheads) via modified terminal segment. The latter consists of transitional zone (tz), middle region (mr), and terminal plug (tp), H.E
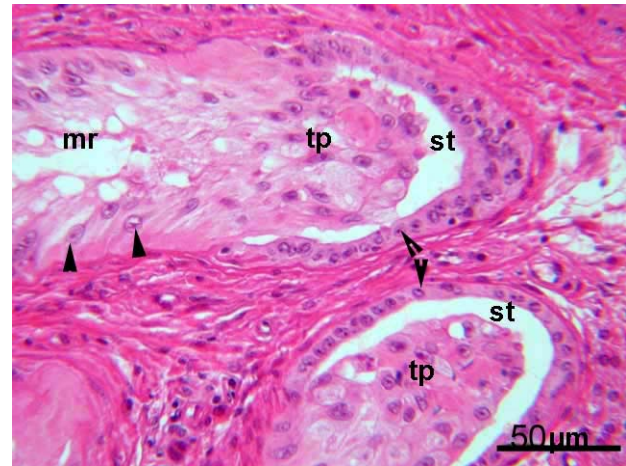
Fig 57: Middle region (mr) and terminal plug (tp) are lined mainly by modified Sertoli cells (arrowheads). The tp protruded for some distance into the proximal cup-shape region of the straight tubule (st). The latter is lined by simple cuboidal epithelium (notched arrowheads), H.E

Indeed, a gradual loss of the spermatogenic cells in a proximo-distal direction is observed through the three regions of these segments. In the transitional zone, spermatozoa and spermatids disappear first, followed by a reduction in the number of spermatocytes whereas the population of spermatogonia remains relatively constant. In this area, the tubular diameter decreases from about 250 μm to approximately 150 μm. The supporting cells of the transitional region are typical Sertoli cells which are distinguished by a round or oval nuclei situated basal to the level of primary spermatocytes. In the middle zone, early spermatogenic cells (spermatogonia and primary spermatocytes) are rarely seen (Fig. 57). Isolated germinative cells in all stages of spermatogenic development, however, are regularly observed within the lumen of this tubular region. Modified Sertoli cells in this area contain large clear vacuoles of varying shape and size separated by narrow strands of cytoplasm (Fig. 56, 57). The distal portion of the terminal segment forms what is called terminal plug that protrudes into the cup-shaped beginning of a tubulus rectus (Fig. 56, 57). All the modified Sertoli cells lining the distal zone incline distally and their apical cytoplasm together constitutes the terminal plug. Large vacuoles are also apparent in the supranuclear cytoplasm of some of the cells contributing to the plug. Nuclei are seen at two levels within the terminal plug; most of them are basal while others are located at a higher level of the cells including the club-shaped apices (Fig. 57). The central tubular lumen of the terminal plug narrows gradually whereas the club-shaped apices of opposite supporting cells coming in close proximity. As a consequence, at the tip of the terminal segment a central lumen cannot be identified light microscopically

with certainty (Fig. 57). Several small lumina are however seen by electron microscope. Bovine terminal segment is markedly surrounded by a vascular plexus in a sleeve-like manner. This plexus composed of arterioles, capillaries, venules, and small lymph vessels (Fig. 58). In the intravascular stroma and the area surrounding the plexus less collagen material and more cellular elements are observed than found in the rest of the testicular stroma. Fibroblasts and many free cells such as lymphocytes, monocytes, and plasma cells constitute this cellular aggregation.

In my study, the term tubulus rectus (straight tubule) is restricted to that region which connects the terminal segment of the seminiferous tubules to rete testis channels. The tubulus rectus of adult bovine testis is composed of three morphologically different regions: proximal cup-shaped region (Fig. 57), middle narrow stalk (Fig. 58), and distal festooned portion (Fig. 59).
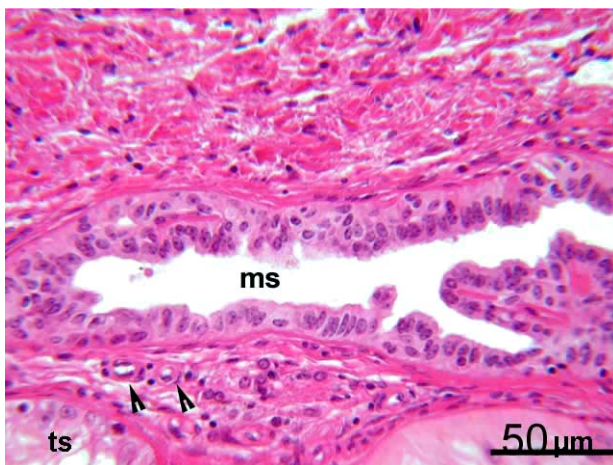
Fig 58: Middle narrow stalk (ms) of the bovine straight tubule showing smooth lumen surface and lined by single layer of cuboidal cells. The vascular plexus (notched arrowhead) is seen in adjacent to the terminal segment (ts), H.E.
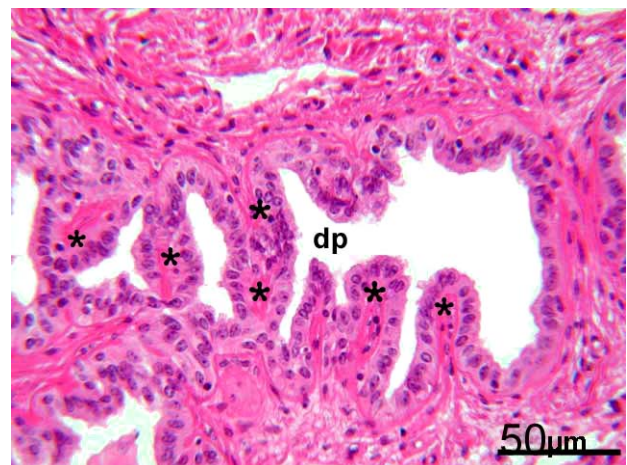
Fig 59: Distal festooned portion (dp) of the bovine straight tubule with its folded epithelium (asterisks) and uneven lumen, H.E.

The proximal cup-shaped region is lined with a single layer of flat to low cuboidal cells (Fig. 57). Tubuli recti, when seen in cross section at this part, contain a central cellular mass of the apical portions of the terminal plug separated by a narrow space from the lining epithelium of the straight tubule. Similarly, the narrow stalk is lined by a single layer of low to high cuboidal cells (Fig. 58). Characteristically, both proximal and middle regions of the straight tubules are shown to have a smooth lumen surface. Conversely, the remainder of these tubules (distal region) has a peculiar appearance. This area is distinguished by a folded epithelium,

giving the lumen a characteristic festooned form with a considerable reduction of the lumen (Fig. 59). This folded region is also lined by monolayered cuboidal epithelium and opens into a short lateral funnel-sized rete extension of varying width. Generally, the course of the tubuli recti is straight and approximately at a right angle to the long axis of the mediastinum, however, in some cases the course shows a sharp bending. In electron micrographs, the cells of the proximal region contain few organelles. Mitochondria are small in size and Golgi apparatus is inconspicuous. A few long cisternae of rER are also seen. The free border of the cells shows short microvilli while the elongated or round nuclei occupy a central position. In the middle narrow part, the mitochondria has tendency to form basal and/or adluminal aggregations and the Golgi apparatus is well developed. Numerous coated vesicles are observed in the vicinity of the Golgi apparatus and in the upper half of the cell. Many long cisternae of rER, free ribosomes, multivesicular bodies, lipid droplets, microtubules, and microfilaments are found as well. The luminal border shows microvilli, which are sometimes branched. In the festooned region, the cells are columnar and their nuclei are elongated and situated towards the lumen. A few cuboidal cells with round nuclei are observed near the basal lamina. Microfilaments and microtubules are quite abundant particularly in the basal part of the cell and around the nucleus. Many dark structures, resembling lysosomes, are common in this region. The epithelial lining of the tubuli recti is actively phagocytic. This is shown by the presence of various parts of spermatozoa and degenerated material in the cytoplasm.

The last member of the bovine excurrent duct system, the rete testis, is a complicated centrally positioned meshwork of intercommunicating channels that lies within the mediastinum testis parallel to the long axis of epididymis (Fig. 60). However, the superficial rete lying at the surface of the testis immediately beneath the tunica albuginea is not evident in bovine. Rete channels have smooth surface and numerous anastomoses. Considerably, larger channels are often traversed by epithelium-covered cords of connective tissue, chordae retis, a characteristic feature of the bovine rete testis (Fig. 60). The rete channels are lined by a simple cuboidal or columnar epithelium. At certain sites, it appears stratified due to the existence of short intraepithelial crypts (Fig. 61). The latter often form acute angle with the basal lamina; their lumina are generally narrow and slit-like, so that they may escape from the light microscopical detection (Fig. 61). Rete channels are surrounded by mediastinal stroma containing myofibroblasts, blood and lymphatic vessels and connective tissue fibers and cells (Fig. 60).
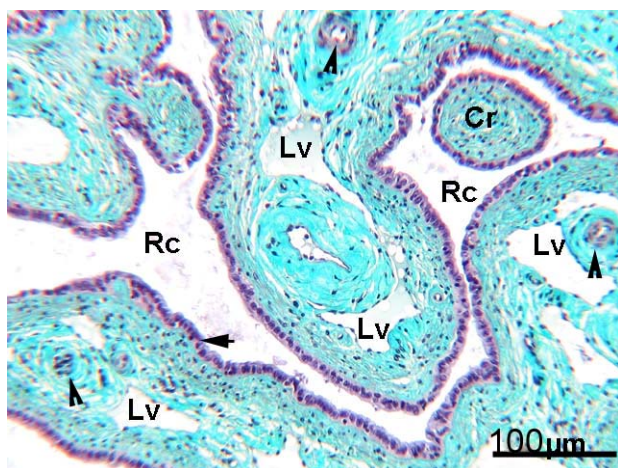
Fig 60: Overview of adult bovine rete testis. The rete channels (Rc) are lined by simple cuboidal epithelium (arrow). The lumen of the large channel is traversed by chordae retis (Cr). Within the mediastinum, numerous lymph (Lv) and blood vessels (notched arrowheads) are found, Masson-Goldner's trichrome.
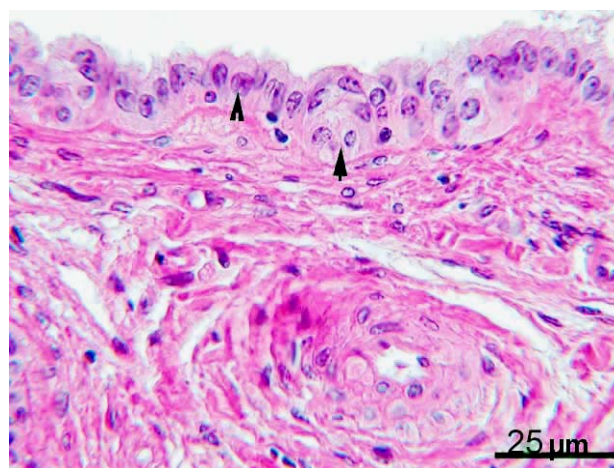
Fig 61: Higher magnification of bovine rete testis epithelium. Although it is mainly simple (notched arrowhead), appears at certain sites stratified due to the presence of short intraepithelial crypts (arrow), H.E.

Fine structure of the rete testis epithelium reveals extensive junctional complexes connect adjacent epithelial cells at the luminal border and seal the intracellular spaces against the crypts (Fig. 62). The lateral plasmalemma display interdigitations at the level of the nuclei or supranuclearly. The basal epithelial border is rather irregular with many projections into the folded basal lamina. Here many hemidesmosomes are developed.
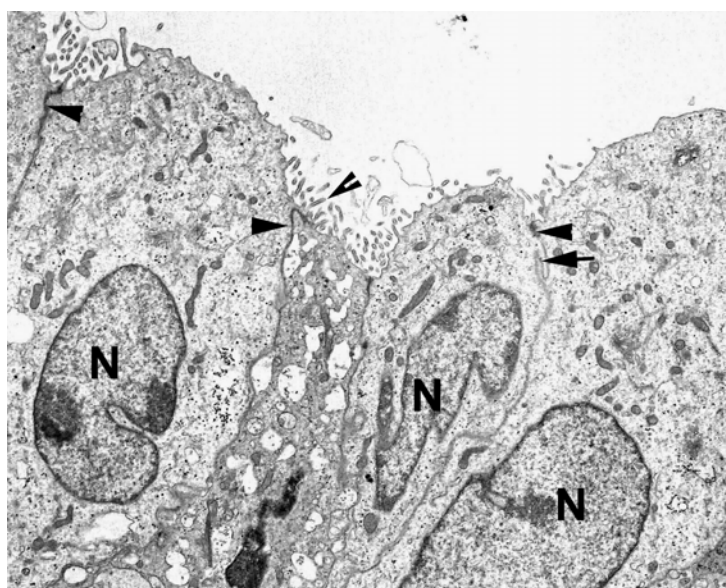
Fig 62: Electron micrograph of rete testis epithelium showing extensive junctional complexes at the luminal surface. Tight junctions (arrowheads) and lateral interdigitations (arrow) are usually seen at the level of nuclei (N) or supranuclearly. The cellular organelles are always inconspicuous while the cellular surface carries short microvilli (notched arrowhead). X 3000

The nuclei occupy the middle of the cell and are often indented (Fig. 62). Short microvilli project from the apical surface and into the crypts. The cells bear a single very long cilium, showing the usual 9+2 pattern. The inventory of organelles is rather inconspicuous (Fig. 62).

Small mitochondria are distributed at random while ER is scarcely developed. Free ribosomes and polyribosomes are however, abundant. A small Golgi and some multivesicular bodies are also present. Like the tubuli recti, rete testis epithelium has the ability to phagocytose spermatozoa. Many free mononuclear cells, mostly macrophages, to lesser degree lymphocytes, are localized in the basal half of the bovine rete epithelium.

4.2. Glycohistochemistry (table 12, 13)

The cellular distribution of glycoconjugates within the fetal and adult bovine testis was investigated using thirteen (ConA, PSA, LCA, PNA, GSA-I, ECA, DBA, SBA, HPA, VVA, WGA, UEA-I, LTA) different fluorescein isothiocyanate (FITC) conjugated lectins (shown in tables 12- 13). These lectins represent five groups (mannose-, galactose-, N-acetylgalactosamine (GalNAc)-, N-acetylglucosamine (GlcNAc)-, and fucose-binding lectins) of the known seven lectin binding groups described in my review (table 2). In fetal testis, five lectins showed positive reaction while the others were not detectable (tables 12). In adult animals, detection of sugar moieties by lectins was carried out on both Bouin′s-fixed paraffin-embedded and acetone-fixed frozen sections and showed slight difference between the two methods of fixation. However, an excellent histological morphology was generally obtained after fixation in Bouin′s fluid. These results are described in details as following:

4.2.1. Mannose-binding lectins

Of this group, PSA, LCA, and Con A were investigated (table 12). In fetal testis, PSA specific to α-D-mannose showed moderate reaction in Leydig cells while weak staining in the basal lamina of solid testicular cords and blood vessels was observed (Fig. 63). Despite distinct staining was additionally seen in the mediastinum testis particularly in the mid stage of pregnancy (20-36 cm CRL/108-141 dpc), no PSA affinity was recorded in the rete testis epithelium. Contrary to PSA, LCA that also binds α-D-mannose was not evident in the embryonic testis at all. In adult, mannose-binding lectins showed a wider pattern of distribution. PSA exhibited weak staining in some spermatogonia, apical cytoplasm of some Sertoli cells and Leydig cells (Fig. 71). Moreover, both PSA and LCA moderately stained the acrosome of round and elongated spermatids (Fig. 71, 72). Apical Sertoli cell processes, spermatocytes, Leydig cells, and basal lamina of the seminiferous tubules were LCA positive as well (Fig. 72). Conversely, Con A specific for α-D-mannose and α-D-glucose was negative in the Leydig cells and basal lamina of the seminiferous tubules, while faintly localized to Sertoli cell processes and acrosome of round spermatids. In frozen sections, Con

108

A staining was observed in the spermatids acrosome, blood vessels, interstitial extracellular matrix, tubular basal lamina, mediastinum testis and rete testis epithelium (table 13).

4.2.2. Galactose-binding lectins

This group represented by PNA, GSA-I, and ECA was identified in both fetal and adult bovine testis. PNA, binding to α-D-galactose and β-D-galactose β (1→3)-D-N-acetylgalactosamine, was observed in the coelomic epithelium of the fetal testis (2.5-3.5 cm CRL/43-50 dpc), in the Golgi region of germ cells (PGCs and the subsequent prespermatogonia) during early stage of pregnancy (2.5-14 cm CRL/43-80 dpc), and in the rete testis (Fig. 64). Some cells (mostly blood cells) were shown to have high PNA affinity shortly after the testicular differentiation (2.5-3.5 cm CRL/43-50 dpc). However, these cells were undetectable thereafter. Despite GSA-I, which binds to α-D-galactose and α-D-N-acetylgalactosamine, was found exclusively on blood vessels, Golgi region of PGCs showed transient positive reaction in the early stage of gestation (3.5- 10 cm CRL/50-75 dpc) (Fig. 65, 66). In adult testis, PNA displayed strong reaction only in the cytoplasm and acrosome of round and elongated spermatids, whereas the other constituents of the testicular tissues remained completely unstained (Fig. 73). While insignificant differences were found in the spermatids PNA staining between paraffin-embedded and frozen sections, the basal lamina of the seminiferous tubules and of the interstitial blood vessels were weakly stained in the latter (Fig. 74). In paraffin embedded testicular tissue, the affinity for GSA-I was weak in spermatid acrosomes and marked in blood vessels. In frozen sections, the acrosomes and tubular basal lamina exhibited moderate reaction while the interstitial connective tissue was weakly stained. A positive ECA reaction, specific for galactose-β (1→4)–N-acetylglucosamine, was solely seen in the spermatids acrosome (Fig. 75). Like PNA, no variation was seen in the spermatids staining between the two methods of tissue processing and fixation while the interstitial tissue showed positive reaction in frozen sections (table 13).

4.2.3. N-acetylgalactosamine (GalNAc)-binding lectins

Although both HPA and DBA are specific for α-D-N-acetylgalactosamine, they showed different pattern of distribution in fetal and adult testis (table 12, 13). HPA was not observed in fetal testis at all while DBA was seen in the Golgi region of prespermatogonia at the end of early gestation period and onward (14-63 cm CRL/80-210 dpc) (Fig. 68). In the interstitial compartment, marked DBA staining was localized solely to the cytoplasm of Leydig cells

from the beginning of their differentiation (3.5 cm CRL/50 dpc) (Fig. 67, 68, 69). In adult testis, weak DBA reaction was detected in spermatogonia, acrosome of spermatids and Leydig cells whereas HPA was indistinctly expressed in acrosomes. Other lectins of this category, SBA and VVA, were investigated in adult testis as well. In both paraffin and frozen sections, striking positive SBA reaction, specific for α- and β-D-N- acetylgalactosamine residues, was recognized in the spermatids acrosome (Fig. 76, 77). In frozen sections, some spermatogonia and spermatocytes were additionally stained while the other elements of the testicular tissue had no affinity (Fig. 77). The staining pattern of VVA that is specific for α-D-N- acetylgalactosamine was very similar to that of SBA. In paraffin section, VVA staining was seen only in the spermatids acrosome (Fig. 78) whereas moderate VVA staining was detected in the Golgi complex of spermatogonia and spermatocytes as well as in basal lamina of frozen section (Fig. 79).

4.2.4. N-acetylglucosamine (GlcNAc)-binding lectins

In fetal testis, the WGA reaction, specific for galactose-β (1→4)–N-acetylglucosamine, α-D-N- acetylglucosamine and neuraminic acid, was widely distributed. Moderate WGA staining was seen in the coelomic epithelium of the early testis (2.5-6 cm CRL/43-60 dpc), in the basal lamina of the newly organized seminiferous cords and in the Leydig cells particularly in the mid gestation period (20-36 cm CRL/108-141 dpc). Weak reaction was moreover observed in PGCs, prespermatogonia, and blood vessels while striking positive staining was found in the mediastinum but not in the rete testis epithelium (Fig. 70). In adult, spermatid acrosomes, basal lamina of the seminiferous tubules, interstitial blood vessels, and connective tissue exhibited weak reaction with WGA in the paraffin-embedded tissues. The only significant difference in the WGA staining between Bouin᾽s- and acetone-fixed tissues was observed on the basal lamina and interstitial connective tissue (Fig. 80).

4.2.5. Fucose-binding lectins

The lectins of this group represented by UEA-I and LTA are shown to bind to α-L-fucose. Although they were undetectable in paraffin sections of fetal and adult testis, UEA-I but not LTA weakly stained the interstitial blood vessels and basal lamina of the acetone-fixed frozen sections.

Controls

None of the negative control sections that were performed by omission of the lectin showed positive reactions while the use of sugar inhibitors revealed some staining affinity especially

with WGA, GSA-I, and PNA. These data may indicate that some lectins could bind more than one sugar.
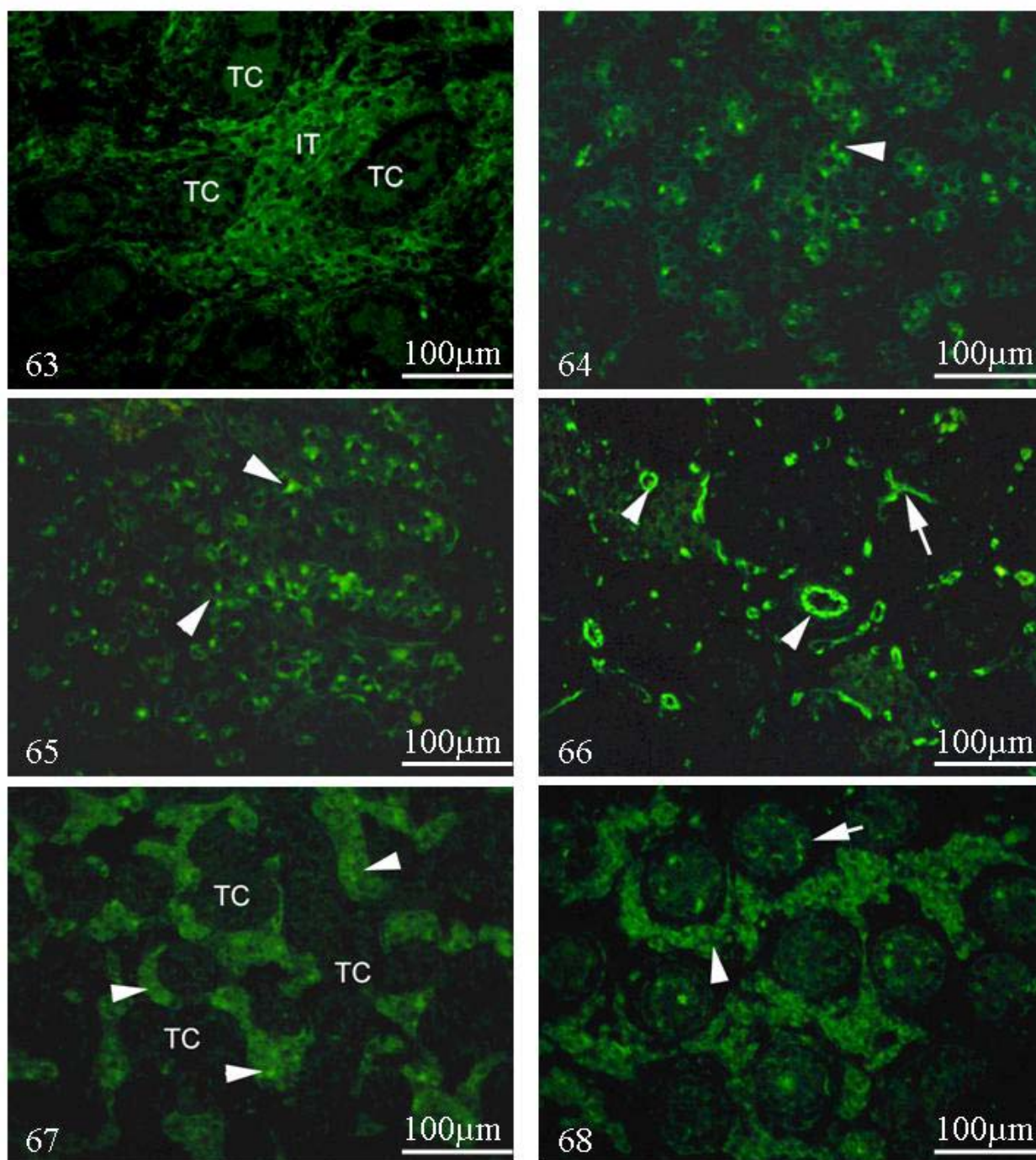
Figs 63-80: FITC- lectin labeling of fetal and adult testis of bovine. **Fig 63:** PSA labeled the testicular interstitium (IT) of 57 cm CRL embryo, no reaction was seen in testicular cords (TC). **Fig 64**: PNA marked the prespermatogonia (10 cm CRL) (arrowhead). **Fig 65:** GSA-I stained the Golgi apparatus of prespermatogonia (10 cm CRL) (arrowheads). **Fig 66:** GSA-I characterized testicular blood vessels (36 cm CRL). **Fig 67:** DBA bounded to fetal Leydig cells (arrowheads) (10 cm CRL). **Fig 68:** DBA labeled both Leydig cells (arrowhead) and prespermatogonia (arrow) (36 cm CRL).
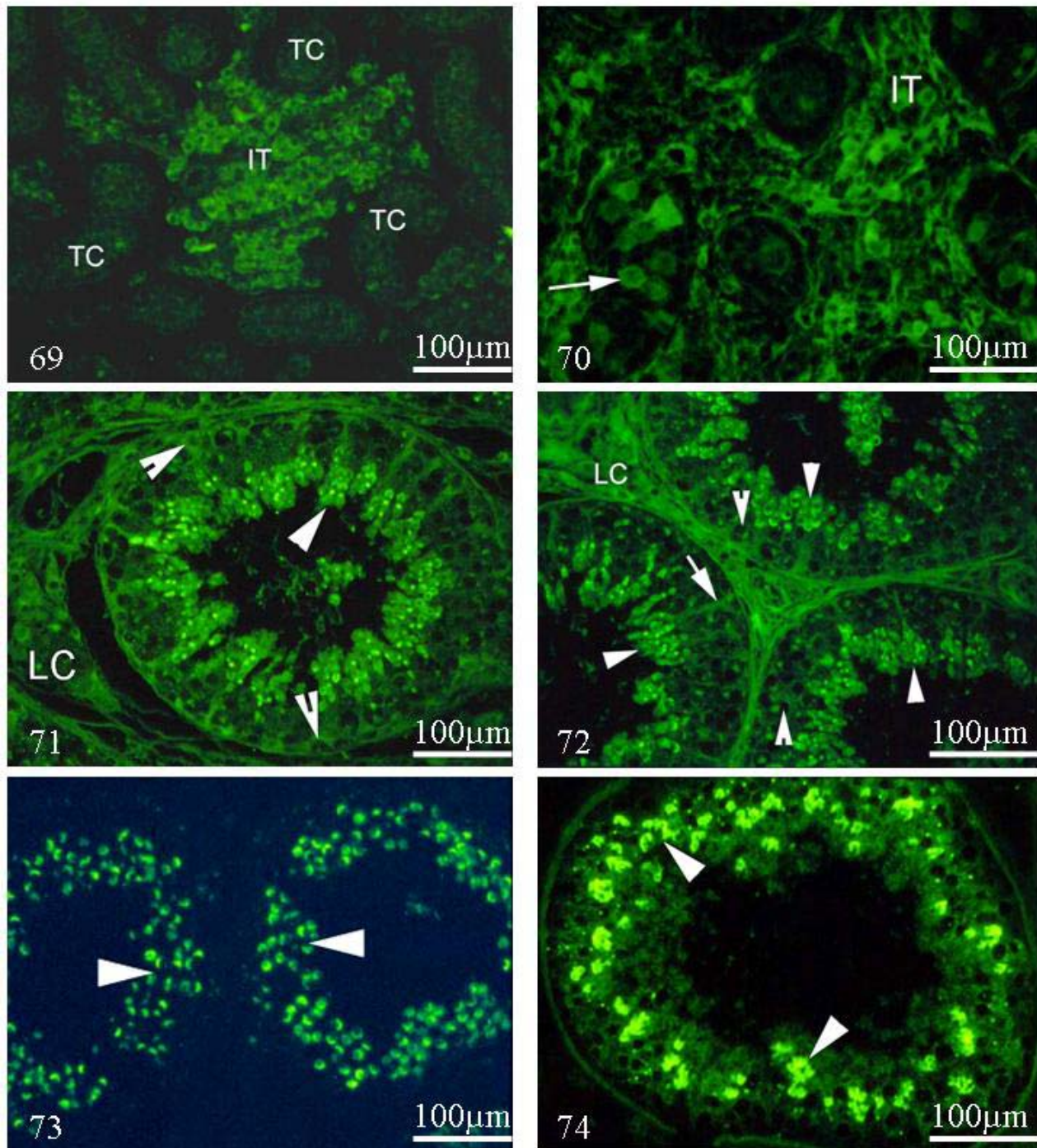
Fig 69: DBA stained the Leydig cells of the testicular interstitium (IT) of 63 cm CRL bovine embryo, however, no reaction was observed in the testicular cords (TC). **Fig 70:** WGA labeled both interstitium (IT) and prespermatogonia (36 cm CRL). **Fig 71:** PSA showed marked reaction in spermatogonia (notched arrowhead), spermatids (arrowhead), and Leydig cells (LC) of adult testis. **Fig 72:** LCA exhibited distinct reaction in spermatocytes (notched arrowhead), spermatids (arrowhead), Sertoli cell processes (arrow), and Leydig cells (LC). **Fig 73 and 74:** Striking staining of spermatids acrosome with PNA (arrowheads) in paraffin and frozen section of adult bovine testis respectively. However, acrosomes had poorly preserved morphology in the frozen section **(Fig 74)**.
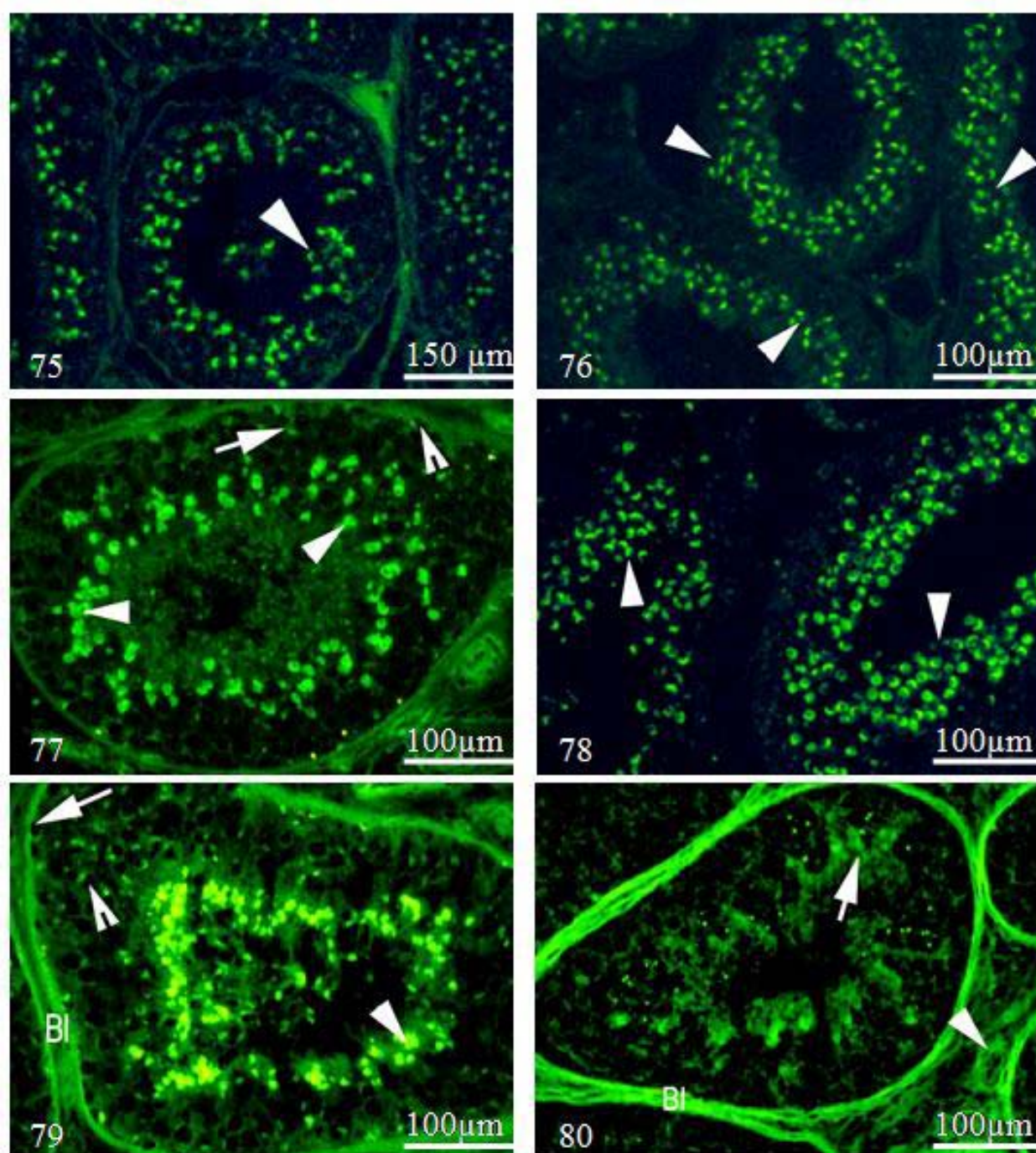
Fig 75: Marked staining of acrosomes with ECA (arrowhead). **Fig 76 and 77:** SBA exclusively marked the spermatids acrosome (arrowhead) in the paraffin sections (76) and additionally stained spermatogonia (notched arrowhead) and spermatocytes (arrow) in the frozen sections (77). **Fig 78 and 79:** VVA showed distinct reaction in the spermatids acrosome (arrowheads) in the paraffin sections (78) whereas spermatogonia (arrow), spermatocytes (notched arrowhead), spermatids acrosome (arrowhead), and basal lamina (Bl) were stained in the frozen section (79). **Fig 80:** Staining of spermatids (arrow), basal lamina (Bl), and blood vessels (arrowhead) with WGA in the frozen section but with poorly preserved morphology.

Table 12: Lectin binding sites in the fetal bovine testis (paraffin sections)

Lectin		CRL/cm	Tunica albuginea		Sex cords			Interstitial tissue		Rete testis	
			CE	Ct/Bv	Bl	Gc	Sc	Lc	Bv	RTE	MT
Mannose-binding lectins	PSA	2.5	−	−	−	−	−	−	−	−	−
		3.5	−	−	+	−	−	−	−	−	−
		6	−	−	+	−	−	−	−	−	−
		10	−	−	+	−	−	+	−	−	+
		14	−	−	−	−	−	+	−	−	+
		18	−	−	−	−	−	+	−	−	++
		20	−	−	−	−	−	+	−	−	++
		23	−	+	−	−	−	+	−	−	++
		30	−	+	−	−	−	+	−	−	++
		36	−	+	−	−	−	+	+	−	++
		56	−	+	−	−	−	+	+	−	+
		63	−	+	−	−	−	+	+	−	+
	LCA	2.5	−	−	−	−	−	−	−	−	−
		3.5	−	−	−	−	−	−	−	−	−
		6	−	−	−	−	−	−	−	−	−
		10	−	−	−	−	−	−	−	−	−
		14	−	−	−	−	−	−	−	−	−
		18	−	−	−	−	−	−	−	−	−
		20	−	−	−	−	−	−	−	−	−
		23	−	−	−	−	−	−	−	−	−
		30	−	−	−	−	−	−	−	−	−
		36	−	−	−	−	−	−	−	−	−
		56	−	−	−	−	−	−	−	−	−
		63	−	−	−	−	−	−	−	−	−
Galactose-binding lectins	PNA	2.5	+	−	−	+	−	−	−	−	−
		3.5	+	−	−	+	−	−	−	−	−
		6	−	−	−	+	−	−	−	−	−
		10	−	−	−	+	−	−	−	+	−
		14	−	−	−	+	−	−	−	+	−
		18	−	−	−	−	−	−	−	+	−
		20	−	−	−	−	−	−	−	+	−
		23	−	−	−	−	−	−	−	+	−
		30	−	−	−	−	−	−	−	+	−
		36	−	−	−	−	−	−	−	+	−
		56	−	−	−	−	−	−	−	−	+
		63	−	−	−	−	−	−	−	−	+
	GSA-I	2.5	−	+	−	−	−	−	+	−	−
		3.5	−	+	−	+	−	−	+	−	−
		6	−	+	−	+	−	−	+	−	−
		10	−	+	−	+	−	−	+	−	−
		14	−	+	−	−	−	−	+	−	−
		18	−	+	−	−	−	−	+	−	−
		20	−	+	−	−	−	−	+	−	−
		23	−	+	−	−	−	−	+	−	−
		30	−	+	−	−	−	−	+	−	−
		36	−	+	−	−	−	−	+	−	−
		56	−	+	−	−	−	−	+	−	−
		63	−	+	−	−	−	−	+	−	−

CE: coelomic epithelium, Ct: connective tissue, Bv: blood vessels, Bl: basal lamina, Gc: germinal cells,
Sc: Sertoli cells, Lc: Leydig cells, MT: mediastinum testis, RTE: rete testis epithelium.
Staining degree: - negative; + weak; ++ moderate; +++ strong.

Table 12: Lectin binding sites in the fetal bovine testis (paraffin sections) (continued)

Lectin		CRL/cm	Tunica albuginea		Sex cords			Interstitial tissue		Rete testis	
			CE	Ct/Bv	Bl	Gc	Sc	Lc	Bv	RTE	MT
N-acetylgalactosamine (GalNAc)–binding lectins	DBA	2.5	–	–	–	–	–	–	–	–	–
		3.5	–	–	–	–	–	+	–	–	–
		6	–	–	–	–	–	+	–	–	–
		10	–	–	–	–	–	++	–	–	–
		14	–	–	–	+	–	++	–	–	–
		18	–	–	–	+	–	++	–	–	–
		20	–	–	–	+	–	++	–	–	–
		23	–	–	–	+	–	++	–	–	–
		30	–	–	–	+	–	++	–	–	–
		36	–	–	–	+	–	++	–	–	–
		56	–	–	–	+	–	++	–	–	–
		63	–	–	–	+	–	++	–	–	–
	HPA	2.5	–	–	–	–	–	–	–	–	–
		3.5	–	–	–	–	–	–	–	–	–
		6	–	–	–	–	–	–	–	–	–
		10	–	–	–	–	–	–	–	–	–
		14	–	–	–	–	–	–	–	–	–
		18	–	–	–	–	–	–	–	–	–
		20	–	–	–	–	–	–	–	–	–
		23	–	–	–	–	–	–	–	–	–
		30	–	–	–	–	–	–	–	–	–
		36	–	–	–	–	–	–	–	–	–
		56	–	–	–	–	–	–	–	–	–
		63	–	–	–	–	–	–	–	–	–
N-acetylglucosamine (GlcNAc)-binding lectins	WGA	2.5	++	+	+	+	–	–	+	–	–
		3.5	++	+	+	+	–	–	+	–	–
		6	++	+	+	+	–	–	+	–	–
		10	–	+	+	+	–	–	+	–	++
		14	–	+	+	+	–	–	+	–	++
		18	–	+	+	+	–	+	+	–	+++
		20	–	+	+	+	–	++	+	–	+++
		23	–	+	+	+	–	++	+	–	+++
		30	–	+	+	+	–	++	+	–	+++
		36	–	+	+	+	–	++	+	–	+++
		56	–	+	+	+	–	+	+	–	+++
		63	–	+	+	+	–	+	+	–	+++
Fucose-binding lectins	UEA-I	2.5	–	–	–	–	–	–	–	–	–
		3.5	–	–	–	–	–	–	–	–	–
		6	–	–	–	–	–	–	–	–	–
		10	–	–	–	–	–	–	–	–	–
		14	–	–	–	–	–	–	–	–	–
		18	–	–	–	–	–	–	–	–	–
		20	–	–	–	–	–	–	–	–	–
		23	–	–	–	–	–	–	–	–	–
		30	–	–	–	–	–	–	–	–	–
		36	–	–	–	–	–	–	–	–	–
		56	–	–	–	–	–	–	–	–	–
		63	–	–	–	–	–	–	–	–	–
	LTA	2.5	–	–	–	–	–	–	–	–	–
		3.5	–	–	–	–	–	–	–	–	–
		6	–	–	–	–	–	–	–	–	–
		10	–	–	–	–	–	–	–	–	–
		14	–	–	–	–	–	–	–	–	–
		18	–	–	–	–	–	–	–	–	–
		20	–	–	–	–	–	–	–	–	–
		23	–	–	–	–	–	–	–	–	–
		30	–	–	–	–	–	–	–	–	–
		36	–	–	–	–	–	–	–	–	–
		56	–	–	–	–	–	–	–	–	–
		63	–	–	–	–	–	–	–	–	–

Table 13: Lectin binding sites of adult bovine testis (paraffin and frozen sections)

Lectins		Paraffin sections								Frozen sections							
		Seminiferous epithelium					Interstitial tissue			Seminiferous epithelium					Interstitial tissue		
		Spg	Spc	Spd	Sc	Bl	Lc	Bv	Ct	Spg	Spc	Spd	Sc	Bl	Lc	Bv	Ct
Mannose-binding lectins	Con A	−	−	+/−	+/−	−	−	−	−	−	−	+	−	++	−	++	++
	PSA	+	−	++	+	−	+	−	−	NI	NI	NI	NI	NI	NI	NI	NI
	LCA	−	+	++	+	+	+	−	−	NI	NI	NI	NI	NI	NI	NI	NI
Galactose-binding lectins	PNA	−	−	+++	−	−	−	−	−	−	−	+++	−	+	−	+	−
	GSA-I	−	−	+	−	−	−	+++	−	−	−	++	−	+	−	+++	++
	ECA	−	−	++	−	−	−	−	+	−	−	++	−	+/−	−	−	++
N-acetylgalactosamine (GalNAc)-binding lectins	DBA	+	−	+	−	−	+	−	−	NI	NI	NI	NI	NI	NI	NI	NI
	SBA	−	−	+++	−	−	−	−	−	++	++	+++	−	−	−	−	−
	HPA	−	−	+	−	−	−	−	−	NI	NI	NI	NI	NI	NI	NI	NI
	VVA	−	−	+++	−	−	−	−	−	++	++	+++	−	+	−	−	−
N-acetylglucosamine (GlcNAc)-binding lectins	WGA	−	−	+	−	+	−	+	+	−	−	+	−	++	−	−	+++
Fucose-binding lectins	UEA-I	−	−	−	−	−	−	−	−	−	−	−	−	+	−	+	−
	LTA	−	−	−	−	−	−	−	−	−	−	−	−	−	−	−	−

Spg: spermatogonia, Spc: spermatocytes, Spd: spermatids, Sc: Sertoli cells, Bl: basal lamina, Lc: Leydig cells, Bv: blood vessels, Ct: connective tissue. NI: not investigated
Staining degree: - negative; + weak; ++ moderate; +++ strong

4.3. Immunohistochemistry

In the present investigation, 12 different proteins (FGF-1, FGF-2, S100, laminin, αSMA, Cx43, VEGF, CD4, CD8, CD68, GalTase, and ACE) were analyzed by immunohistochemistry in the fetal and adult bovine testis.

4.3.1. Fibroblast growth factors (FGF-1 and FGF-2)

4.3.1.1. Localization of FGF-1 and FGF-2 in the fetal testis (table 14)

In embryonic bovine testis, FGF-1 and FGF-2 were shown to be expressed in a cellular- and time-specific way. At the first age of the early gestation period (2.5 cm CRL/43 dpc), marked FGF-1 immunostaining was seen as dark brown granules in the cytoplasm of pre-Sertoli cells. One week later (3.5 cm CRL/50 dpc), FGF-1 staining was additionally observed in the

interstitial compartment, particularly in fetal Leydig cells. While FGF-1 immunostaining was found in pre-Sertoli cells throughout the whole embryonic period, no reaction was seen in germ cells (Fig. 81). Toward the end of early pregnancy (from 10 cm CRL/ 75 dpc, onward) moderate to distinct immunostaining was also found in the epithelium of the newly differentiated straight tubules and rete testis (Fig. 82). Further on, the endothelium of the newly formed blood vessels (arteries) was shown to localize FGF-1 protein from the mid pregnancy (30 cm CRL/ about 130 dpc) and onwards.
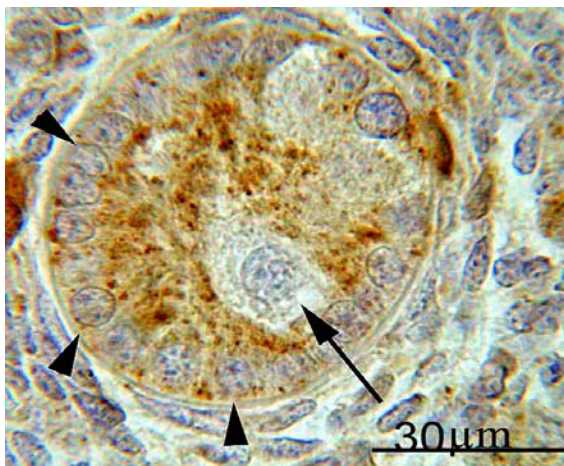
Fig 81: Localization of FGF-1 in the pre-Sertoli cell cytoplasm (arrowheads). No staining was found in prespermatogonia (arrow). Fetus with 36 cm CRL
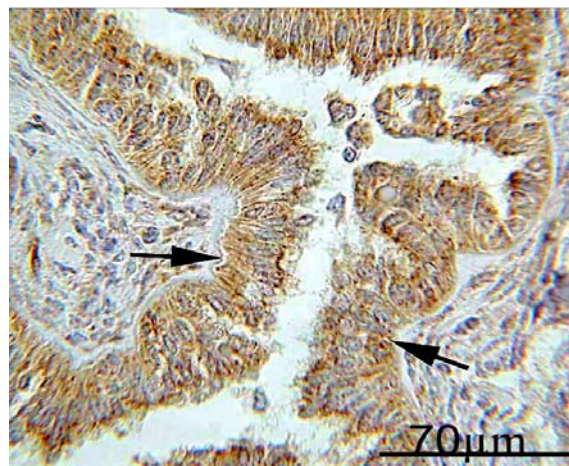
Fig 82: FGF-1 is also detected in the rete testis epithelium (arrows). Bovine fetus with 63 cm CRL

Unlike FGF-1, FGF-2 protein was not detected during the early phase of testicular differentiation. The first FGF-2 immunostaining was observed at 6 cm CRL (60 dpc). It attained a maximum at 14 cm CRL (80 dpc), markedly declined at 30 cm CRL (130 dpc) and disappeared completely thereafter. During this limited period of expression, distinct FGF-2 immunostaining was only found in the nucleus of fetal Leydig cells (Fig. 83). Although the presence of scattered Leydig cells in mid and late stages of gestation, demonstrated FGF-2 positive Leydig cells were not seen after 30 cm CRL (130 dpc). No FGF-2 immunoreactivity was found in the seminiferous cords or in other cells of the interstitium.

Despite the rete testis channels were shown to differentiate at the end of the early gestation (10-14 cm CRL), FGF-2 immunoreactivity in their epithelium was detected shortly after its disappearance from Leydig cells nuclei (at 36 cm CRL/141 dpc). With beginning of late pregnancy (63 cm CRL/ 210 dpc, on), striking nuclear staining was seen in the rete testis epithelium (Fig. 84) as well as in the endothelium of the blood vessels, principally of arteries. By the end of pregnancy (90 cm CRL/ 285 dpc), FGF-2 immunostaining was predominantly

localized to tubulus rectus and rete testis epithelium, to endothelium and tunica media of blood vessels especially that of the tunica albuginea, and to some peritubular cells surrounding the seminiferous cords.
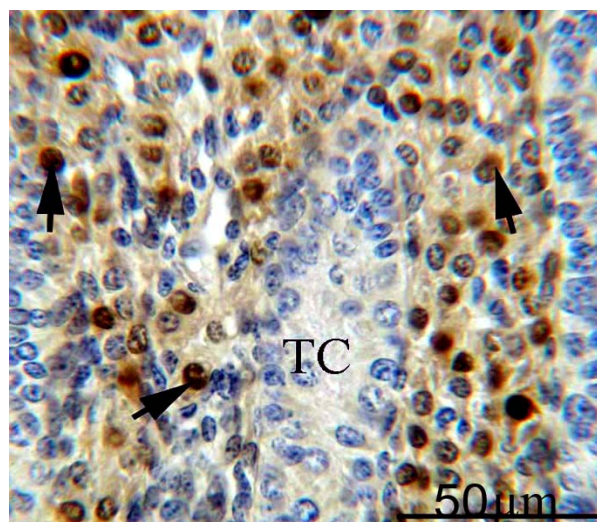
Fig 83: FGF-2 staining is exclusively found in the fetal Leydig cell nuclei (arrows) while no reaction is seen in the testicular cords (TC). Fetus with 14 cm CRL.
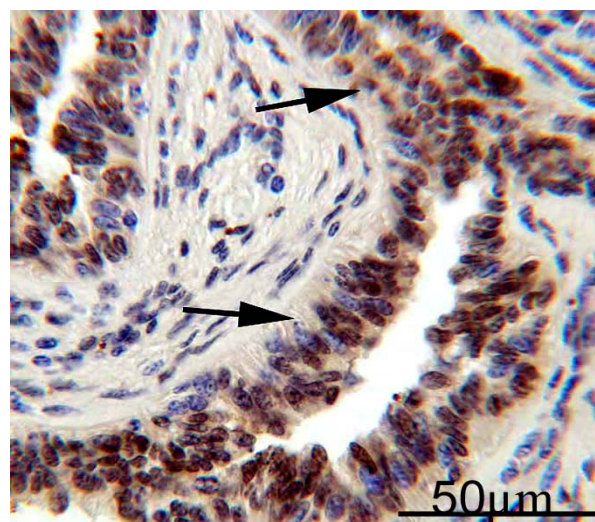
Fig 84: Striking positive staining of the rete testis epithelium with FGF-2 (arrows). Fetus with 63 cm CRL.

Table 14: Localization of FGF-1 and FGF-2 in the fetal bovine testis

Stage of development	Age CRL/cm	FGF-1							FGF-2						
		Sc	Gc	Lc	Bv	Pc	St	Rt	Sc	Gc	Lc	Bv	Pc	St	Rt
Early	2.5	++	–	–	–	–	–	–	–	–	–	–	–	–	–
	3.5	+++	–	+	–	–	–	–	–	–	–	–	–	–	–
	6	+++	–	+	–	–	–	–	–	–	+	–	–	–	–
	10	+++	–	+	–	–	+	+	–	–	++	–	–	–	–
	14	+++	–	++	–	–	+	+	–	–	+++	–	–	–	–
Mid	18	+++	–	+	–	–	+	+	–	–	+++	–	–	–	–
	20	+++	–	+	–	–	+	+	–	–	++	–	–	–	–
	23	+++	–	+	–	–	++	++	–	–	++	–	–	–	–
	30	+++	–	+	+	–	++	++	–	–	+	–	–	–	–
	36	+++	–	+	+	–	++	++	–	–	–	–	–	++	++
	40	+++	–	+	+	–	++	++	–	–	–	–	–	++	++
	57	+++	–	+	+	–	++	++	–	–	–	–	–	++	++
Late	63	+++	–	+	+	–	++	++	–	–	–	++	–	+++	+++
	80	+++	–	–	+	–	++	++	–	–	–	++	–	+++	+++
	90	+++	–	–	+	–	++	++	–	–	–	++	+	+++	+++

Sc, pre-Sertoli cells; Gc, germ cells; Lc, Leydig cells; Bv, blood vessels; St, straight tubules; Rt, rete testis

4.3.1.2. Expression, quantification, and localization of FGF-1 and FGF-2 in the adult testis

In adult animals, the presence of FGF-1 and FGF-2 in the testis was investigated by real time RT-PCR, in situ hybridization, and immunohistochemistry.

4.3.1.2.1. Real time PCR

In real time RT-PCR, amplification plots of FGF-1 and FGF-2 cDNA (Fig. 85a, b) were assembled from fluorescence emission data collected during PCR amplification. Negative controls and 18S control gene did not reveal any significant genomic DNA contamination or pipetting errors, respectively.
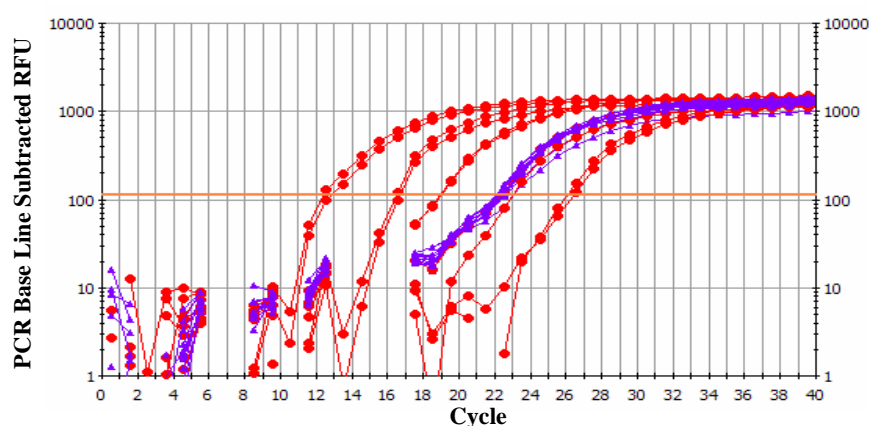
Fig 85a: Amplification plots of FGF-1. The horizontal orange line is the baseline from which the C_T was calculated. The gene under investigation (blue curves) falls within the range of standards (red curves).
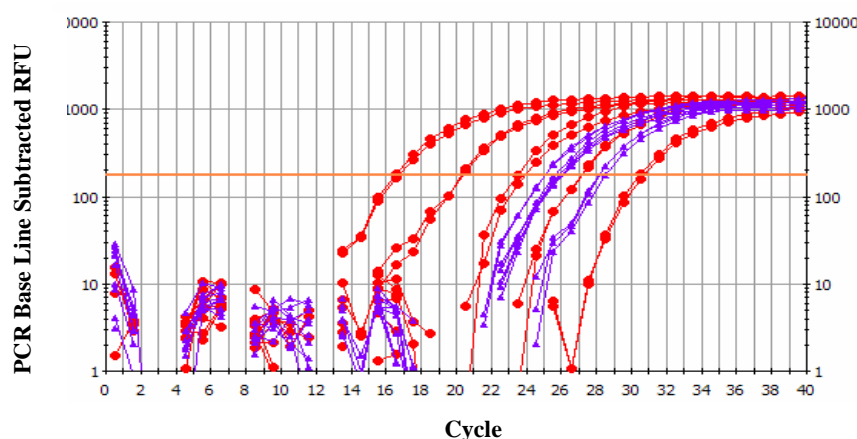
Fig 85b: Amplification plots of FGF-2. The horizontal orange line is the baseline from which the C_T was calculated. The gene under investigation (blue curves) falls within the range of standards (red curves).

Specificity of PCR product for both genes in testis, as confirmed by melt curve analysis, revealed the presence of a single peak for each amplicon. This peak was identified in the melt curve (Fig. 86a, b) at a melting temperature of 85.5°C for FGF-1 and 79.5°C for FGF-2. Furthermore, the routine agarose gel electrophoresis showed the existence of a single PCR

band of the expected molecular weight, i.e., 189 and 236 base pairs for FGF-1 and FGF-2 respectively (Fig 87).
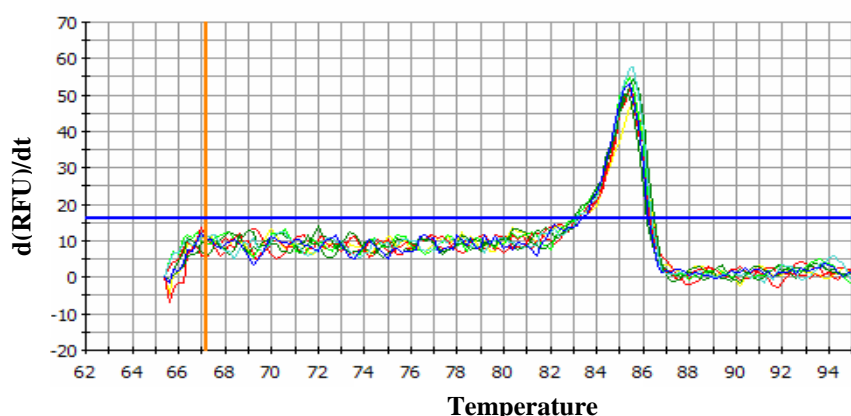
Fig 86a: Melt curve of FGF-1 showing a single melting peak at a temperature of 85.5 °C.
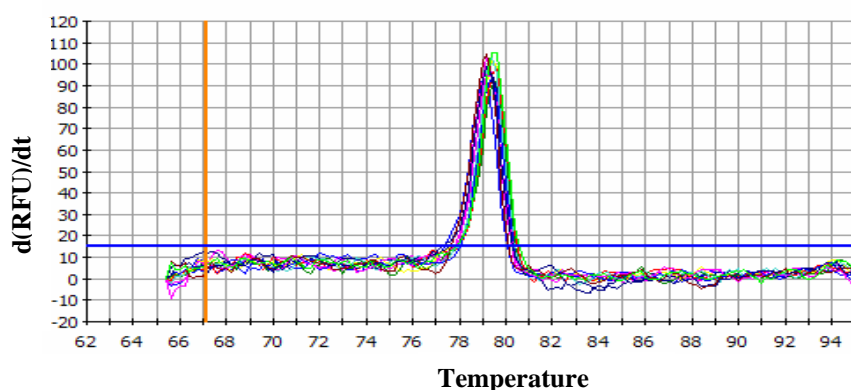
Fig 86b: Melt curve of FGF-2 showing a single melting peak at a temperature of 79.5 °C.
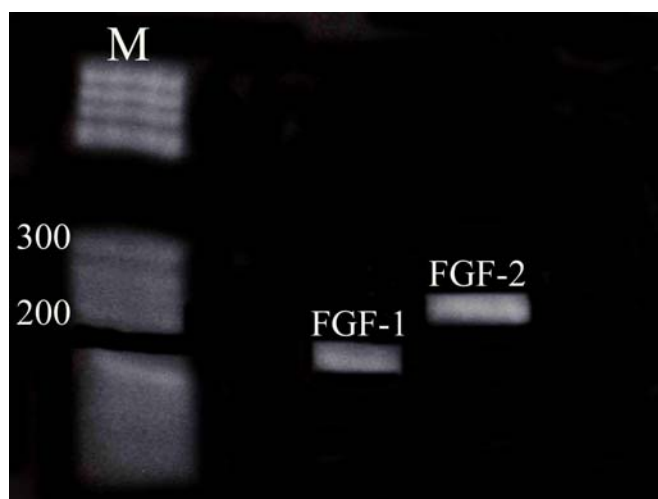
Fig 87: Agarose gel electrophoresis indicates the specificity of the PCR product (M is the molecular ladder). FGF-1 and FGF-2 were detected at the expected base pairs, i.e., 189 bp for FGF-1 and 236 bp for FGF-2.

Our gene quantification result demonstrated that FGF-1 was transcribed about 10 times higher than FGF-2 by the presence of 4500-6500 (FGF-1 mRNA) and 300-600 (FGF-2 mRNA) molecules/10 ng total RNA. The standard curves (Fig. 88a, b) displayed a linear relationship, i.e., inverse correlation, between the starting copy numbers and the C_T for each standard curve over the five $\log_{10}$ dilution. This strongly indicates that the detection limit for both genes was

the same. Moreover, the standard curves showed a correlation coefficient close to 1 for both genes, i.e., 0.997 and 1.000 for FGF-1 and FGF-2 respectively. The PCR efficiency values were also close to optimal PCR conditions as revealed by 99.6% for FGF-1 and 93.7% for FGF-2 (Fig. 88a, b).
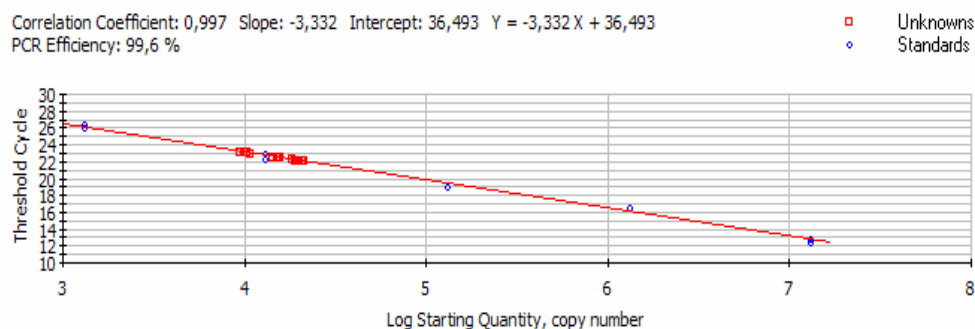
Fig 88a: Standard curve of FGF-1 generated by the iCycler software from data in figure 85a.
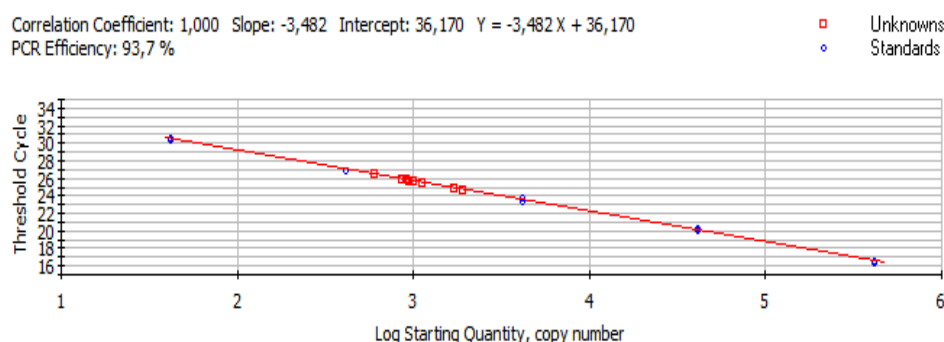
Fig 88b: Standard curve of FGF-2 generated by the iCycler software from data in figure 85b.

4.3.1.2.2. In situ hybridization

By means of in situ hybridization, both FGF-1 and FGF-2 mRNA were found in Leydig and Sertoli cells (Fig. 89, 90) as well as in the modified Sertoli cells of terminal segment. FGF-1 transcripts were additionally recognized in the straight tubules and rete testis epithelium.
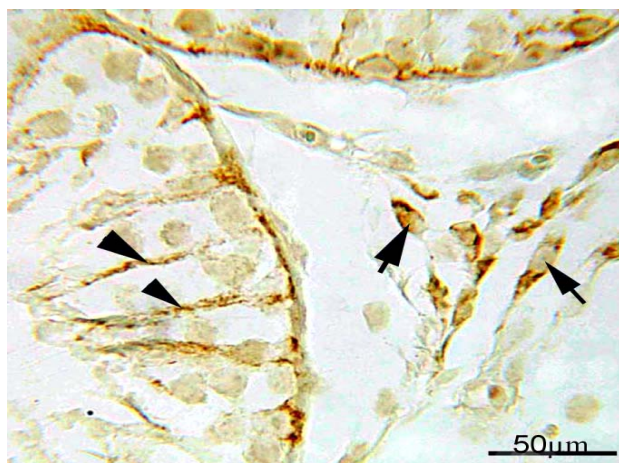
Fig 89: FGF-1 transcripts are detected in Sertoli (arrowheads) and Leydig cells (arrows).
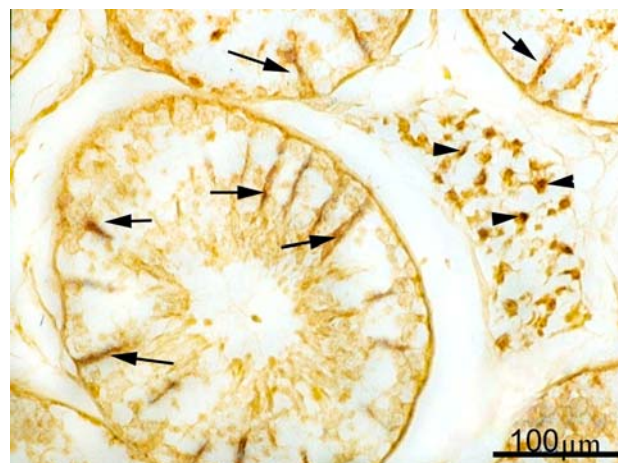
Fig 90: FGF-2 signals are found in Sertoli (arrows) and Leydig (arrowheads) cells.

4.3.1.2.3. Immunohistochemistry (table 15)

Unlike the corresponding mRNA, FGF-1 and FGF-2 protein showed a wider pattern of expression. While moderate to marked FGF-1 immunostaining was detected in the cytoplasm of spermatogonia and spermatids as well as in the cytoplasm of Sertoli and Leydig cells (Fig. 91, 92), no FGF-2 immunoreactivity was seen Sertoli cells and germ cells other than spermatogonia. Alternatively, moderate FGF-2 protein expression was detected in the cytoplasm of Leydig cells and some spermatogonia (Fig. 93, 94). FGF-2 immunostaining was also seen in cytoplasm and nuclei of myofibroblasts (Fig. 94). Several cells in the interstitial tissue other than Leydig cells and in the mediastinum testis (mostly stromal fibroblast and tissue macrophage) showed intense positive staining for FGF-1 and FGF-2. In blood vessels, the endothelium and vascular smooth muscle cells (tunica media of the medium and small sized blood vessels) were markedly stained for FGF-1 and FGF-2. Lymph vessels however were always negative for both. In modified Sertoli cells lining the terminal segment, FGF-1 reaction showed a characteristic localization. It was not evenly distributed in the cytoplasm as seen in the epithelium of straight tubules and rete testis, but was localized in the form of basal dark brown granules located between the nucleus and basal lamina (Fig. 95). FGF-1 protein expression was seen in the cytoplasm of simple cuboidal epithelium of straight tubules and rete testis (Fig. 96). Some of cells of rete testis epithelium, probably immune cells, were negative. Contrary to the cytoplasmic reaction for FGF-1 in rete testis and straight tubules epithelium, FGF-2 immunostaining was mostly nuclear and more intense (Fig. 97).

Table 15: Localization of FGF-1 and FGF-2 in the adult bovine testis

Testicular cells	Spg	Spd	Sc	Lc	Mf	Bv	Lv	Smc	MSc	St	Rt
FGF-1	++	++	++	++	—	+++	—	+	++	+++	+++
FGF-2	++	—	—	++	++	+++	—	+	—	+++	+++

Spg, spermatogonia; Spd, Spermatids; Sc, Sertoli cells; Lc, Leydig cells; Mf, myofibroblasts; Bv, blood vessels; Lv, lymph vessels; Smc, stromal cells; MSc, modified Sertoli cells; St, straight tubules; Rt, rete testis
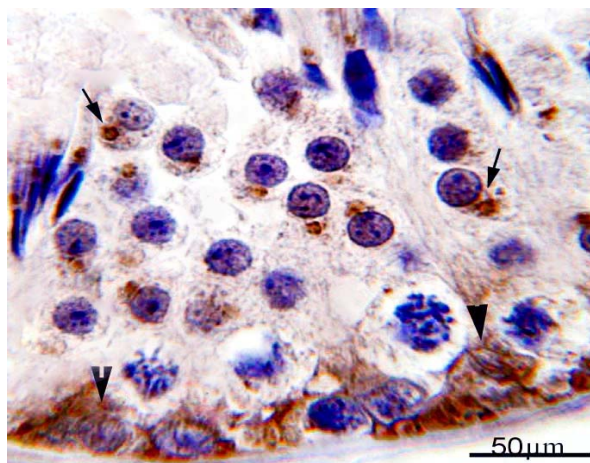
Fig 91: Localization of FGF-1 in Sertoli cell (arrowhead), spermatogonia (notched arrowhead), and spermatids (arrows).
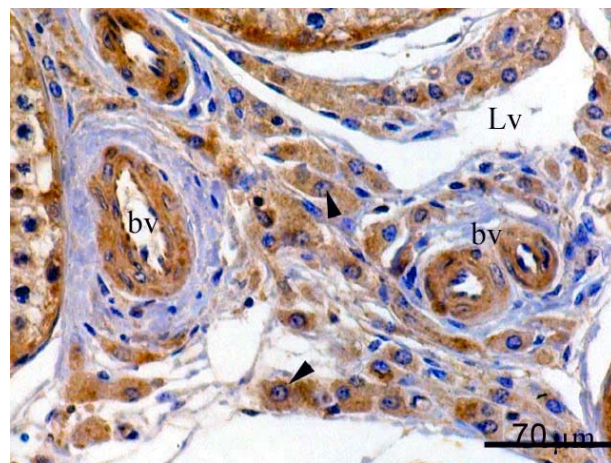
Fig 92: Immunolocalization of FGF-1 in the Leydig cells (arrows) and testicular blood vessels (bv). Lymphatic vessels (Lv) have no FGF-1 affinity.
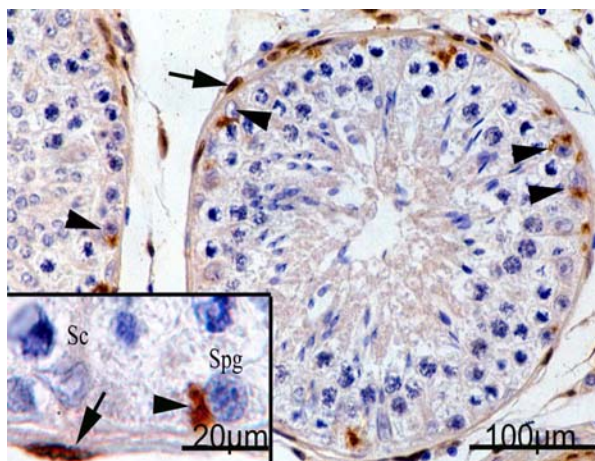
Fig 93: Immunostaining of some spermatogonia (Spg) (arrowheads) and myofibroblasts (arrows) with FGF-2. Sertoli cells (Sc) did not exhibit any immunostaining.
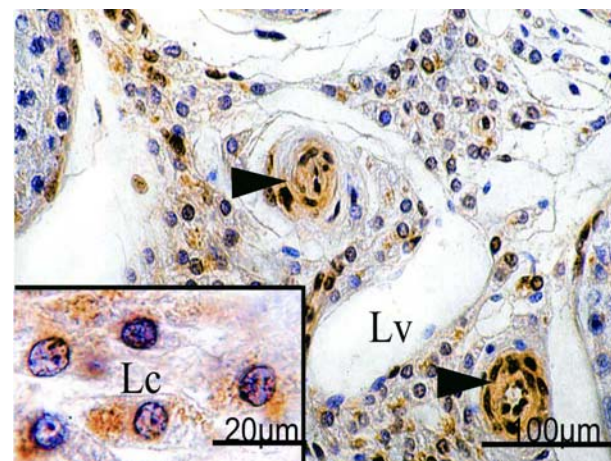
Fig 94: Marked staining of Leydig cells (Lc), and blood vessels (arrowheads), with FGF-2. However, lymph vessels (Lv) have no affinity.
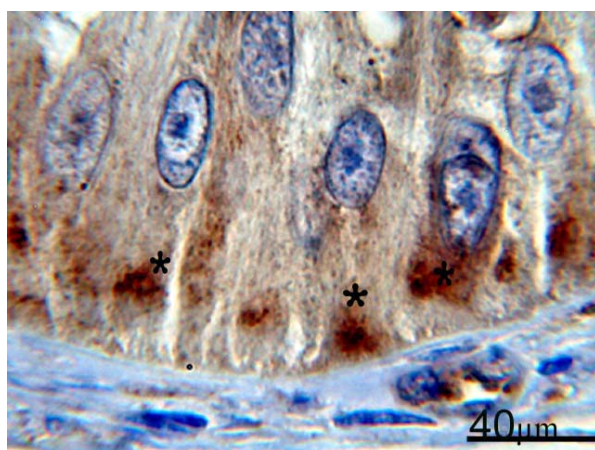
Fig 95: Localization of FGF-1 in the basal portion of the modified Sertoli cells of terminal segment (asterisks).

123
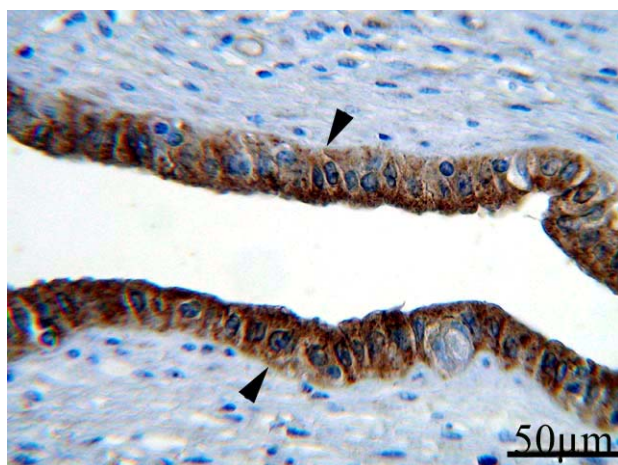
Fig 96: Intensive cytoplasmic staining of the rete testis epithelium (arrows) with FGF-1.
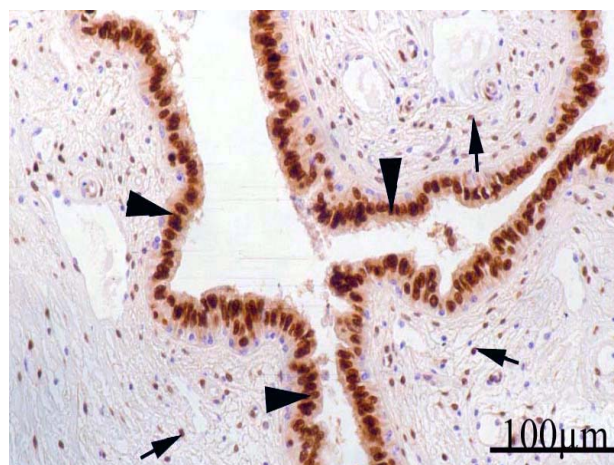
Fig 97: Strong reaction for FGF-2 in the nuclei of the rete testis epithelium (arrowheads), and some of stromal cell nuclei (arrows).

4.3.2. S100 (table 16)

Shortly after the testicular differentiation (2.5 cm CRL/43 dpc), a particular strong reaction of S100 protein was detected in the cytoplasm and nucleus of pre-Sertoli cells. Germ and Leydig cells, on the contrary, exhibited no immunostaining. S100 immunolocalization was cell- but not time-specific as it was seen during the whole period of prenatal testicular development (Fig. 98). In mid pregnancy (from 23 cm CRL/110 dpc, on), moderate S100 reaction was also found in the lining epithelium of the differentiated straight tubules, in the rete testis epithelium and in the endothelium of blood and lymph vessels (Fig. 99). Blood vessels of tunica albuginea were shown to express S100 earlier than those inside the testicular parenchyma (from 6 cm CRL/60 dpc, on). The intensity of S100 protein expression in blood vessels, tubulus rectus and rete testis was reported to increase with age.

In adult testis, immunostaining for S100 was observed in the Sertoli cells of the bovine seminiferous tubules (Fig. 100). Immunoreactive S100 appeared to be widely distributed within the cytoplasm filling the thin cytoplasmic projections that are closely associated with various stages of germinal cells. However, the intensity of immunostaining was somewhat dependent upon the cyclic variation within the seminiferous epithelium. Comparatively strong reaction was seen in all stages associated with the elongation of spermatids. Adult Sertoli cell nuclei were S100 positive as well. A particular marked reaction was seen in the modified Sertoli cells of terminal segment and in epithelial cells of straight testicular tubules and rete testis (Fig. 101, 102). Additional immunoreactivity was also found in endothelial cells of capillaries, veins, and lymphatic vessels. In contrast, the endothelial cells of preterminal arterioles did not react with the antiserum. Spermatogonia, spermatocytes in the different

phases of meiosis, spermatids, and spermatozoa did not show immunostaining for S100 proteins, nor did Leydig cells, myofibroblast cells, and intraepithelial macrophages of the rete testis.
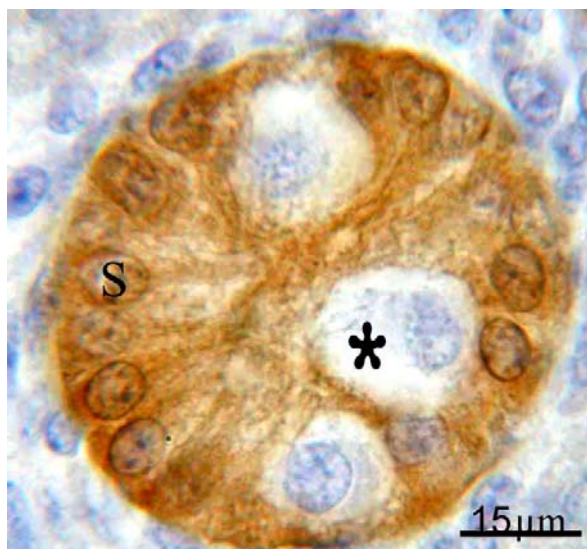
Fig 98: S100 was localized in pre-Sertoli cells (S) while the prespermatogonia showed no staining (asterisk). Fetus with 23 cm CRL
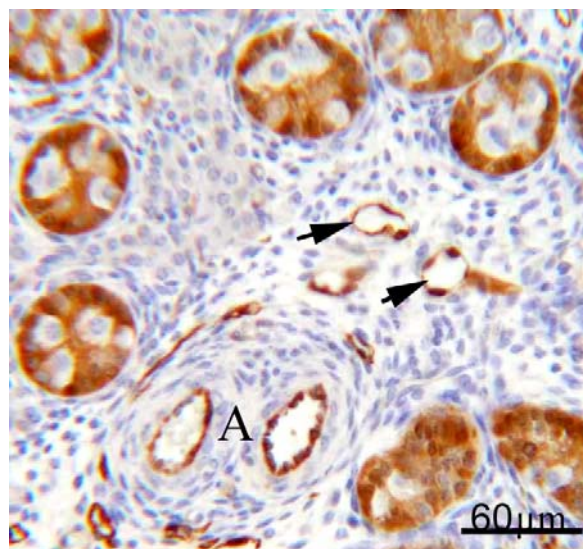
Fig 99: Localization of S100 in the endothelium of testicular arteries (A) and capillaries (arrows). No staining was found in the interstitial cells. Fetus with 36 cm CRL
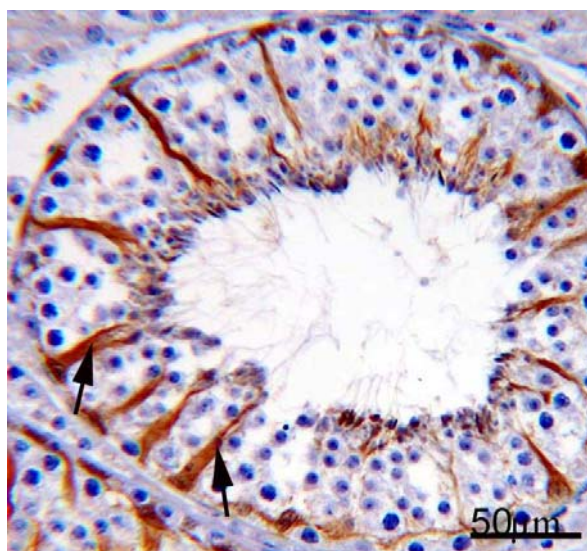
Fig 100: Localization of S100 in the adult Sertoli cells (arrows).
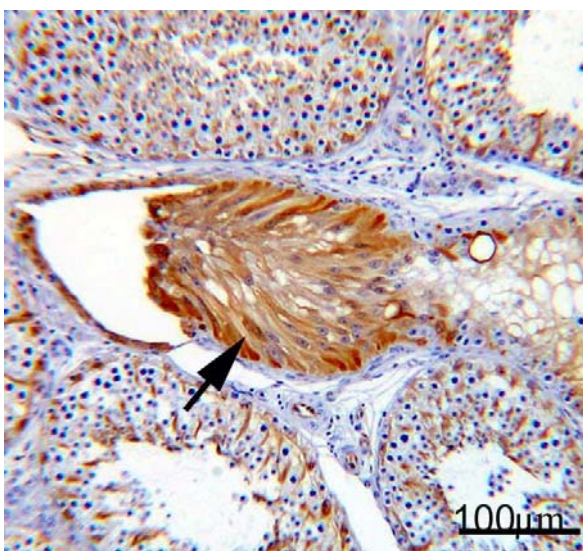
Fig 101: Immunostaining of modified Sertoli cell of the terminal segment (arrow) with S100
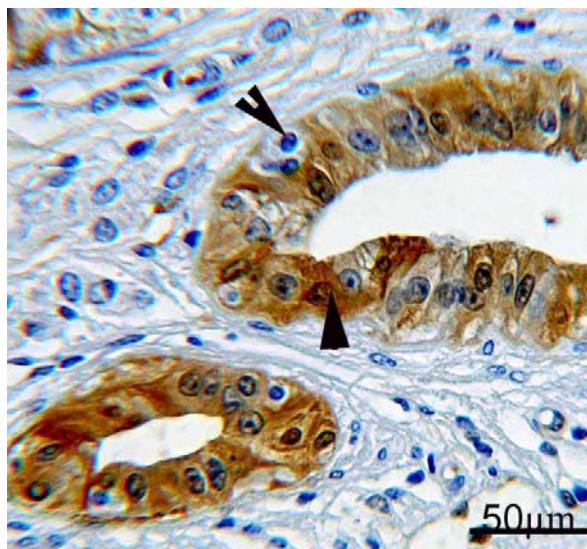
Fig 102: In rete testis, S100 is localized in the epithelium (arrowhead), while the intraepithelial macrophages show no staining (notched arrowhead).

Table 16: Immunohistochemical Localization of S100 in the prenatal and adult bovine testis

Stage of development	Early stage					Mid stage							Late stage			Adult testis
Age (CRL/cm)	2.5	3.5	6	10	14	18	20	23	30	36	40	57	63	80	90	
Sc	+++	+++	+++	+++	+++	+++	+++	+++	+++	+++	+++	+++	+++	+++	+++	+++
Gc	–	–	–	–	–	–	–	–	–	–	–	–	–	–	–	–
Lc	–	–	–	–	–	–	–	–	–	–	–	–	–	–	–	–
Pc	–	–	–	–	–	–	–	–	–	–	–	–	–	–	–	–
Bv	–	–	±	±	+	+	+	++	++	++	++	++	++	+++	+++	+++
MSc	?	?	?	?	?	?	?	?	?	?	?	?	?	?	?	+++
St	–	–	–	–	–	+	+	++	++	+++	+++	+++	+++	+++	+++	+++
Rt	–	–	–	–	–	+	+	++	++	+++	+++	+++	+++	+++	+++	+++

Sc, Sertoli cells; Gc, germ cells; Lc, Leydig cells; Pc, peritubular cells; Bv, blood vessels; MSc, modified Sertoli cells (developed in the postnatal life); St, straight tubules; Rt, rete testis.

4.3.3. Laminin

With the incipient differentiation of bovine testes (2.5 cm CRL/43 dpc), laminin immunoreactivity was evident both in the basal lamina that delineates the differentiating sexual cords and below the thickened surface epithelium of tunica albuginea. Initially (2.5 cm CRL/43 dpc), a discontinuous layer of laminin was demonstrated in these structures. A few days later (3.5 cm CRL/50 dpc), the basal lamina completely enclosed the testicular cords and the laminin immunostaining became more intense particularly in the tunica albuginea and around the blood vessels. Subsequently (6 cm CRL/60 dpc), short laminin positive filament-like structures were found around the cellular aggregates of rete testis. Toward the end of the early pregnancy (10 cm CRL/75 dpc), a connection between the laminin positive basal lamina of seminiferous cords and rete testis was detectable. Proceeding with age (18 cm CRL/100 dpc and onwards), the deposited layer of laminin increased in thickness and appeared to be

separated in several layers especially around blood vessels and rete testis as well as in the inner layer of the tunica albuginea (Fig. 103).

Fig 103: Localization of laminin in the basal lamina of testicular cords (arrows) and in the blood vessels (arrowhead). Fetus with 36 cm CRL.

In the testis of adult animals, a marked positive reaction was localized to the basal lamina of the seminiferous tubules and of the myofibroblast cell layers. In most seminiferous tubules, laminin appeared as a diffuse staining in the basal lamina (Fig. 104), but in some tubules, particularly at the level of terminal segments, the laminin deposits formed invaginations into the seminiferous epithelium. This pattern of arrangement results in striated appearance of the modified Sertoli cells basal portion (Fig. 105).

Fig 104: Basal lamina of the adult seminiferous tubules (arrowhead) and blood vessels (arrow) is distinctly stained with laminin
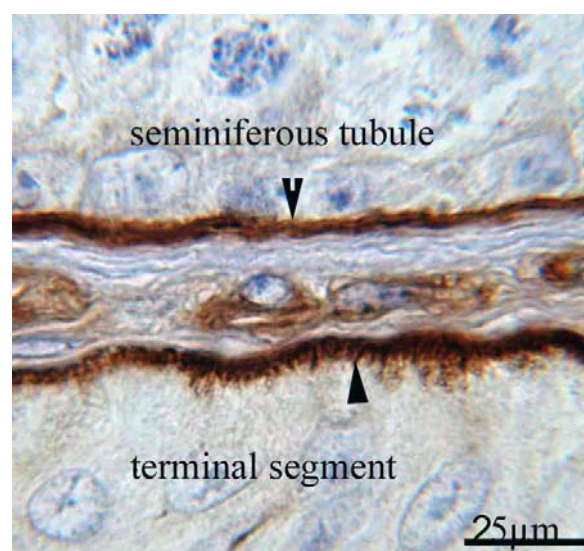
Fig 105: Laminin demonstrated a diffuse staining in the basal lamina of seminiferous tubules (notched arrowhead), but at the level of terminal segments, the laminin deposits formed invaginations into the seminiferous epithelium (arrowhead).

127

The vasculature of the adult bovine testis also exhibited intense laminin immunostaining, especially in the muscular layer of the medium sized vessels and in the basal lamina of the endothelium. Localization of laminin was present in the basal lamina of the rete testis epithelium and myofibroblast cell layers located in the mediastinum of the adult testis as well.

4.3.4. Alpha Smooth muscle actin (αSMA)

α-smooth muscle actin (αSMA) was only detectable in the blood vessels of the embryonic bovine testis. No αSMA immunostaining was found either in the fetal tunica albuginea or other testicular structures including the peritubular cells (Fig. 106).

Fig 106: Immunostaining of the vascular smooth muscle with αSMA (arrow) while the peritubular cells exhibited no affinity (arrowhead). Bovine fetus with 36 cm CRL.

αSMA was exclusively expressed in the tunica albuginea blood vessels at early stage of development (3.5 cm CRL/50 dpc) but not within the testicular parenchyma. Later on (10 cm CRL/75 dpc), the parenchymal blood vessels exhibited marked staining. The localization of αSMA in the blood vessels was originally seen in the arteries at 3.5 cm CRL/50 dpc, and one month later in the veins (14 cm/80 dpc). The intensity of αSMA immunoreaction as well as the number of blood vessels showing positive staining has increased with age. At the end of mid pregnancy (57 cm /187 dpc), αSMA was additionally localized to some cells surrounding the rete testis.

In adult, striking αSMA expression was found in the myofibroblasts delineating the seminiferous tubules (Fig. 107). Distinct reaction was observed in the testicular blood vessels as well. Likewise, several layers of αSMA positive cells were seen beneath the rete testis epithelium (Fig. 108).

Fig 107: Distinct staining of the myofibroblasts of the adult seminiferous tubules (arrowhead) and vascular smooth muscle (arrow) with αSMA
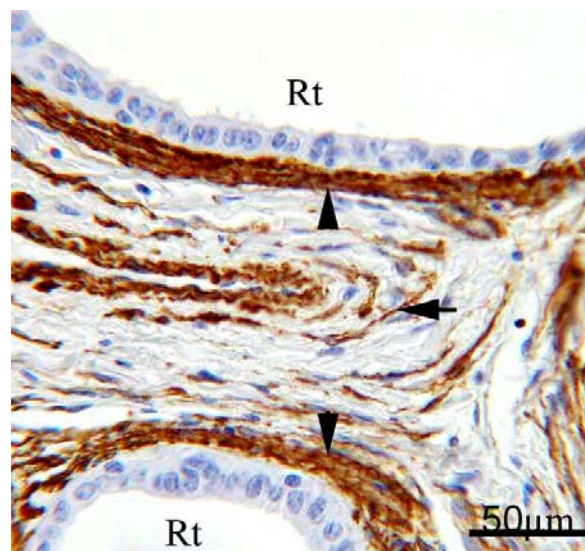
Fig 108: Immunolocalization of αSMA in the myofibroblasts under the rete testis (Rt) epithelium (arrowheads) and within the mediastinum (arrow)

4.3.5. Vascular endothelial growth factor (VEGV)

My immunohistochemical data of adult bovine testis showed a limited expression of VEGF. No VEGF immunostaining was found in Sertoli cells and germ cells other than some specific stages of spermatids. Likewise, no cells of the interstitial compartment and rete testis epithelium displayed any VEGF positive reaction. Round and early elongating spermatids at the first three stages of the seminiferous epithelial cycles showed a distinct reaction at the site of the future acrosomes (Fig. 109, 110).
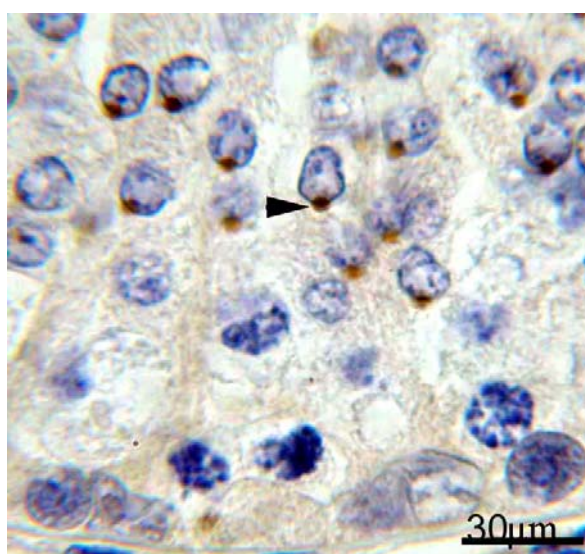
Fig 109: Localization of VEGF in the cap and early acrosomal phase spermatids. The reaction was only found in the acrosomal granule (arrowhead).
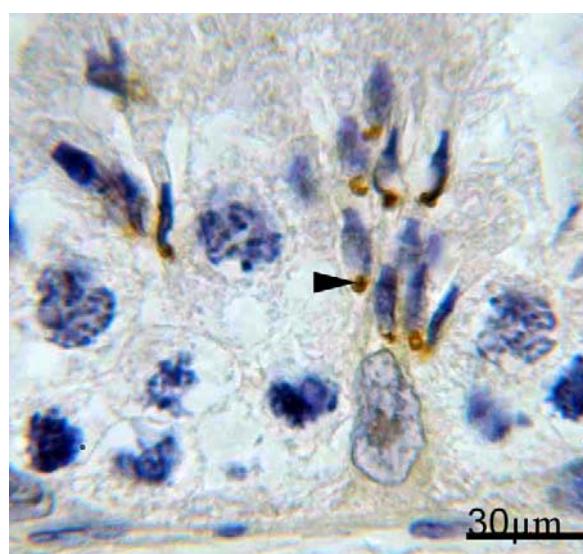
Fig 110: Distinct positive VEGF staining in the acrosomal phase spermatids (arrowhead).

129

Moderate immunostaining for VEGF was seen in modified Sertoli cells of the terminal segment especially at the terminal plug. In blood vessels, although no VEGF immunostaining was found in the endothelium, a punctate reaction was seen in the smooth muscle cells (tunica media) of the medium and small sized arteries.

4.3.6. Connexin 43 (Cx43)

Cx43 was seen at early stage of the testicular development (3.5 cm CRL/50 dpc). All the Cx43 immunostained cells are localized in the interstitial compartment and identified as Leydig cells according to their characteristic morphology. Immunostaining of Cx43 was generally punctate or circumscribed and appeared as brown dots on the cellular membrane between adjacent Leydig cells (Fig. 111). Expression of Cx43 was markedly parallel to the developmental pattern of the Leydig cells. Cx43 immunostained Leydig cells increased gradually with age until 14 cm CRL where they attained their maximal number. Thereafter (18 cm CRL, onward), it was usual to see some focal areas of the interstitium free from Cx43 immunopositive Leydig cells. This feature increased gradually and became more prominent with the beginning of the late gestation period (63 cm CRL/210 dpc, on) where the Leydig cell number has considerably reduced (table 11). Although strong punctate immunostaining Cx43 was observed between the cells of the rete testis in the period between 3.5 cm and 23 cm/CRL, no positive reaction was seen within the solid seminiferous cords throughout the whole embryonic period of this investigation (Fig. 111).

In adult bovine testis, the immunohistochemistry revealed a focal to linear localization of Cx43 protein on the plasma membrane of the neighboring Leydig cells. Occasionally, fine immunostained dots were also seen within the cytoplasm of adult Leydig cells. Contrary to seminiferous cords in the fetal period, a strong immunoreaction was seen within the adult seminiferous tubules of bovine testis. Although Cx43 immunoreaction was observed within the seminiferous tubules nearly throughout the 8 stages, its intensity was mainly stage-dependent. Cx43 immunostaining reduced greatly during stages II, III, and IV, thereafter, it increased again through stages V, VI, and VII to attain its maximum at stage VIII and stage I. Within the seminiferous tubules, the Cx43 protein localization was mainly detected in the basal compartment, apical to spermatogonia and basal to spermatocytes (Fig. 112). This site of localization coincided with the location of Sertoli cells junctional complexes that form the blood-testis barrier. In addition, occasional dark brown dots were also seen in the adluminal compartment toward the tubular lumen between Sertoli cells and spermatocytes as well as between the newly formed round spermatids (Fig. 112).
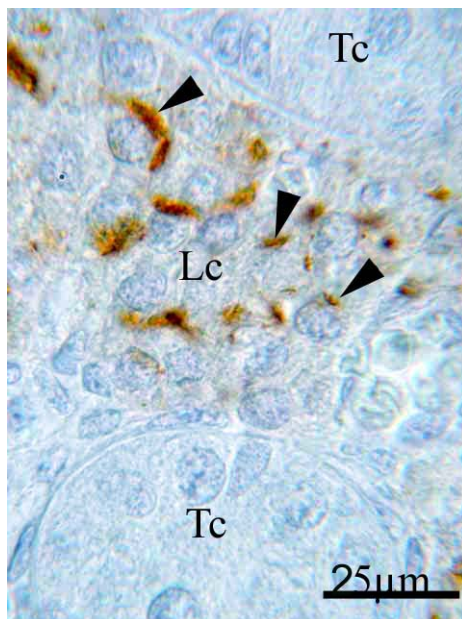
Fig 111: localization of Cx43 (arrowheads) between fetal Leydig cells (Lc). No immunostaining was found within the testicular cords (Tc). Fetus with 14 cm CRL.
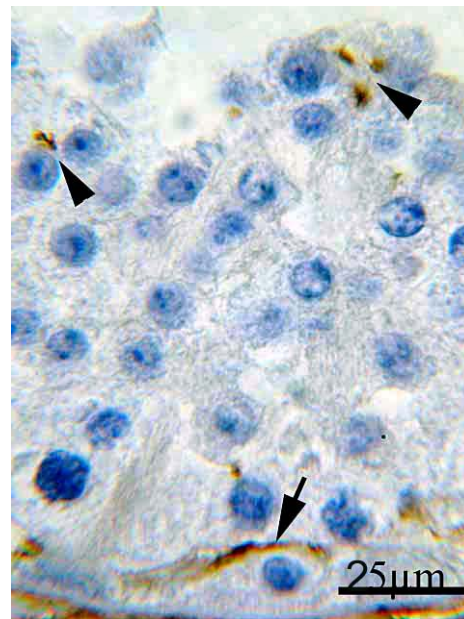
Fig 112: Within the adult seminiferous tubules, Cx43 was seen in the basal compartment, apical to spermatogonia and basal to spermatocytes (arrows). It was also detected in the apical compartment between the round spermatids (arrowheads)

4.3.7. CD68, CD4, and CD8

The CD68 (EBM11) identifying resident macrophages, was not detectable in the fetal bovine testis. However, CD68 positive cells were clearly seen within the interstitial testicular compartment of the adult animals (Fig. 113). These cells were randomly distributed within the interstitium being sometimes near Leydig cells, myofibroblast cells, blood vessels or present directly under the basal lamina of seminiferous tubules but never within the lumen of seminiferous tubules. CD68 immunostaining was mainly granular and either localized to the cytoplasm or to the cellular process (revealed by thin filamentous reaction extended from the cell body). Despite the presence of CD68 positive staining within the mediastinum, no reaction was found in any of the cells lining rete testis. In the straight tubules, CD68 expression was detected in the lining epithelium of a single straight tubule while the others exhibited negative reaction (Fig. 114). The other tested CD68 clone (KP1) was not reactive in the bovine testis at all. In a similar way CD4 and CD8 positive cells were, albeit few, recognized in the interstitial tissue of adult testis (Fig. 115, 116). CD4 positive cells were mostly small, round with spherical nuclei and present mainly as single cells. Most of the interstitium was free of these cells and it was very rare to see a few positive cells within the

same area. CD4 immunoreaction was observed in the cuboidal cells of the rete testis, but this may be unspecific. In contrast to CD4, very few CD8 positive cells were detected in the interstitium (2-5 cells per testicular section)
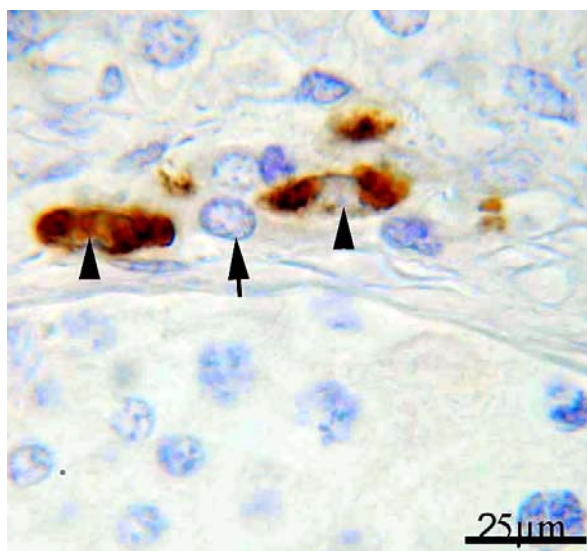
Fig 113: CD68 positive cells are seen within the adult bovine interstitium (arrowheads). Some Leydig cells (arrow) are present in contact with these cells.
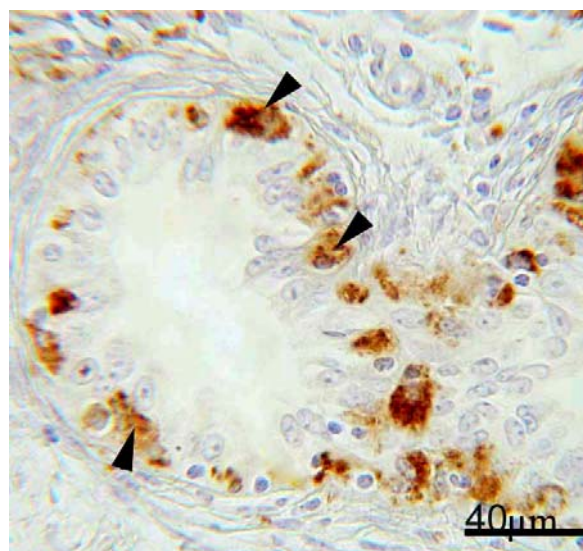
Fig 114: CD68 positive cells are found in the basal portion of an individual straight tubule (arrowheads).
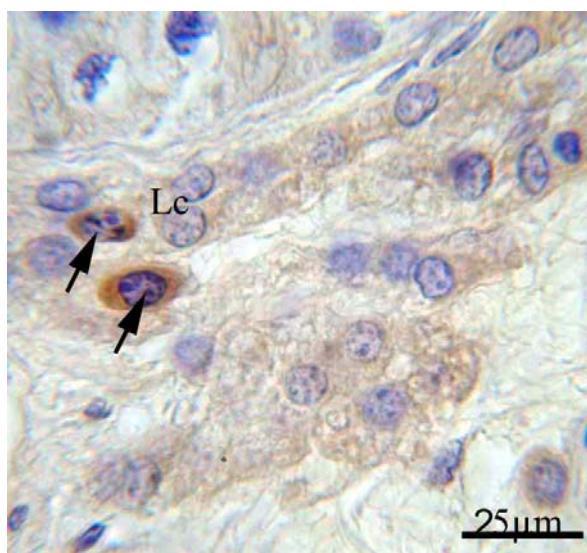
Fig 115: CD4 positive cells (arrows) are seen near the adult Leydig cells (Lc) of bovine testis.
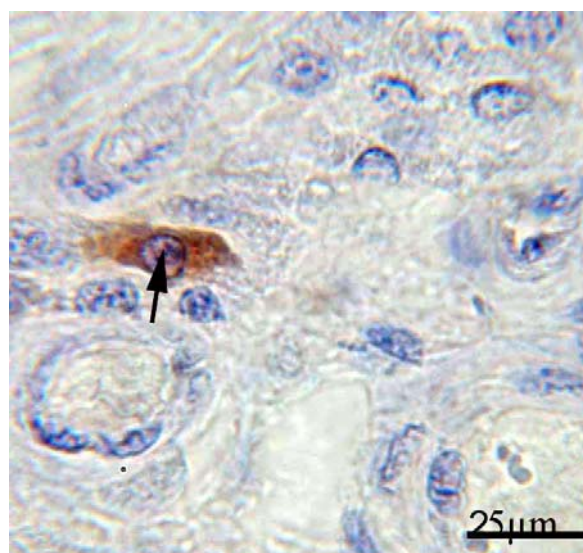
Fig 116: Very few CD8 positive cells (arrow) are located near the blood vessels and adult Leydig cells.

4.3.8. Galactosyltransferase (GalTase) (table 17)

The immunolocalization of galactosyltransferase (GalTase) was exclusively seen in the cytoplasm of fetal Leydig cells in an area corresponding to Golgi apparatus (Fig. 117) and at the cell surface of rete testis epithelium of prenatal bovine testis. The intensity of reaction

within the fetal Leydig cells Golgi apparatus was found to increase through the early pregnancy period. Despite, the presence of isolated Leydig cells in the mid and late stages of pregnancy, the number of GalTase immunopositive fetal Leydig cells was markedly decreased in the mid pregnancy (from 23 cm CRL/110 dpc, on) and they disappeared completely in the late stage (63 cm CRL/210 dpc). Contrary to Leydig cells, immunostaining of the rete testis epithelium was detected at 14 CRL (80 dpc) and simultaneously increased with age. No GalTase protein localization was observed in fetal Sertoli and germ cells. Similarly, blood and lymph vessels did not exhibit any reaction.
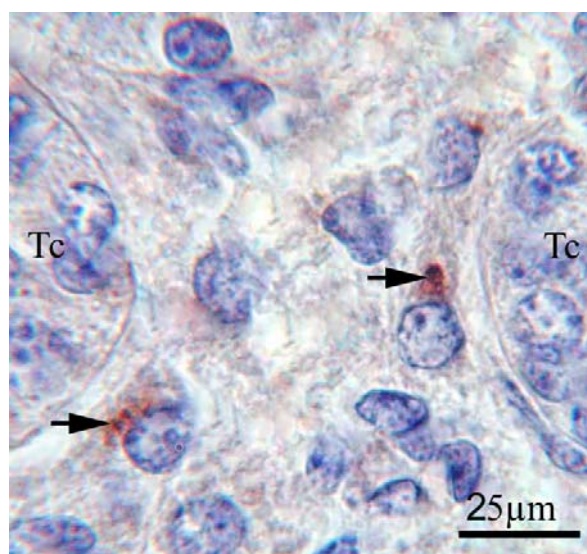
Fig 117: Localization of GalTase in the Golgi apparatus of fetal Leydig cells (arrows). Fetus with 10 cm CRL.

In the adult testis, distinct immunostaining was seen in the Golgi complex of Sertoli and Leydig cells (Fig. 118). GalTase was also detected in the Golgi apparatus of some spermatocytes and at the head surface of the elongating spermatids (Fig. 119) while no immunostaining was observed in the spermatogonia. Marked immunostaining of GalTase was additionally observed in straight tubule and rete testis epithelium (Fig. 120). As in fetal testis, blood and lymph vessels, as well as peritubular myofibroblast cells showed negative reaction.

Table 17: Localization of GalTase in the prenatal and adult bovine testis

Stage of development	Early stage					Mid stage							Late stage			Adult testis
Age (CRL/cm)	2.5	3.5	6	10	14	18	20	23	30	36	40	57	63	80	90	
Sc	–	–	–	–	–	–	–	–	–	–	–	–	–	–	–	++
Gc	–	–	–	–	–	–	–	–	–	–	–	–	–	–	–	++
Lc	–	+	+	++	++	++	++	++	+	+	+	–	–	–	–	++
Pc	–	–	–	–	–	–	–	–	–	–	–	–	–	–	–	–
Bv	–	–	–	–	–	–	–	–	–	–	–	–	–	–	–	–
St	–	–	–	–	–	+	+	++	++	++	++	++	++	++	++	+++
Rt	–	–	–	–	–	+	+	++	++	++	++	++	++	++	++	+++

Sc, Sertoli cells; Gc, germ cells; Lc, Leydig cells; Pc, peritubular cells; Bv, blood vessels; St, straight tubules; Rt, rete testis.

Fig 118: Immunolocalization of GalTase in the Golgi apparatus (arrows) of adult Leydig cells.
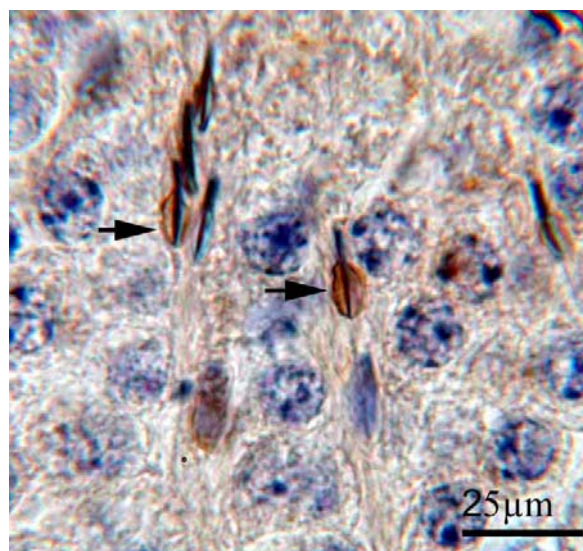
Fig 119: GalTase was additionally detected in the elongating spermatids (arrows).

Fig 120: Localization of GalTase in the apical area of rete testis epithelium (arrowheads) and within the Golgi apparatus (arrows).

4.3.9. Angiotensin-converting enzyme (ACE) (table 18)

In fetal testis, ACE was found exclusively within the testicular cords. Prespermatogonia exhibited a transient expression of ACE in 6 and 10 cm CRL (60-75 dpc) but immunostaining was no longer detected in the subsequent stages of testicular development (Fig. 121). Moderate reaction was also seen in the endothelium of the newly formed blood vessels. The ACE positive reaction of endothelium was first detected by 18 cm CRL (100 dpc) and increased concurrently with age (Fig. 122).
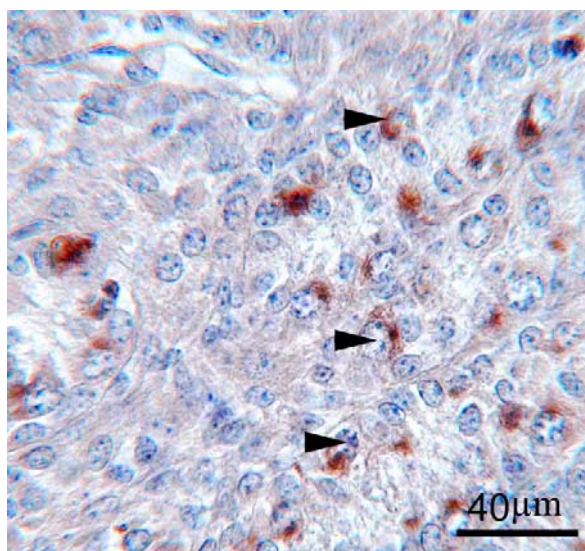
Fig 121: ACE is only localized to the cytoplasm of prespermatogonia (arrowheads). Bovine fetus with 10 cm CRL.
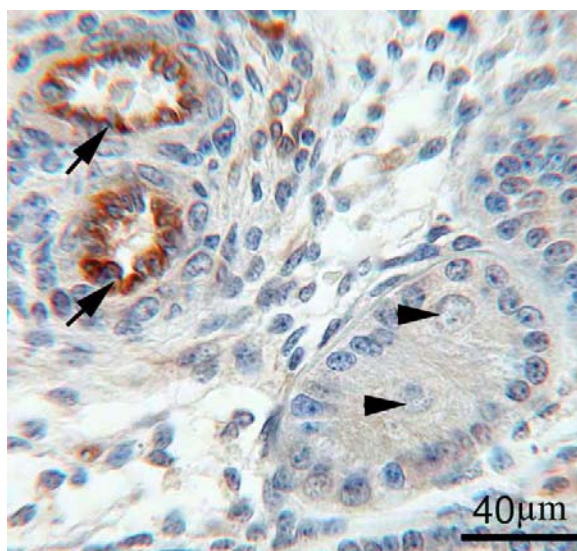
Fig 122: Immunostaining of fetal testicular blood vessels endothelium with ACE (arrows). No reaction was seen in the germ cells at this age (57 cm CRL) (arrowheads).

ACE was not evident in Sertoli, Leydig and germ cells as well as in straight tubules and rete testis epithelium of fetal and adult testis. Within the adult bovine testis, marked ACE protein expression was only observed in the endothelium of blood vessels.

Table 18: Immunohistochemical Localization of ACE in the prenatal and adult bovine testis

Stage of development	Early stage					Mid stage							Late stage			Adult testis
Age (CRL/cm)	2.5	3.5	6	10	14	18	20	23	30	36	40	57	63	80	90	
Sc	–	–	–	–	–	–	–	–	–	–	–	–	–	–	–	–
Gc	–	–	++	++	–	–	–	–	–	–	–	–	–	–	–	–
Lc	–	–	–	–	–	–	–	–	–	–	–	–	–	–	–	–
Pc	–	–	–	–	–	–	–	–	–	–	–	–	–	–	–	–
Bv	–	–	–	–	–	+	+	++	++	++	++	++	++	++	+++	+++
St	–	–	–	–	–	–	–	–	–	–	–	–	–	–	–	–
Rt	–	–	–	–	–	–	–	–	–	–	–	–	–	–	–	–

Sc, Sertoli cells; Gc, germ cells; Lc, Leydig cells; Pc, peritubular cells; Bv, blood vessels; St, straight tubules; Rt, rete testis.

5. DISCUSSION

5.1. Morphological studies of fetal and adult bovine testis

The testis is responsible for the production of functional sperm and for the secretion of hormones and factors that govern all aspects of male sexual development and reproductive function. Disturbance in prenatal development and differentiation of the testis can thus be responsible for an array of undermasculinisation syndromes, ranging from XY females to males with subnormal fertility (Tohonen et al., 2003). Proper development of testis is therefore critical to establish the male phenotype and to attain maximal reproductive capacity.

5.1.1. Testicular differentiation and morphogenesis

The differentiation and morphogenesis of bovine male gonad during prenatal development has been investigated in numerous previous (Santamarina and Reece, 1957; Schrag, 1983, Anton, 1987, Sinowatz et al., 1987, Setijanto, 1992) and recent (Wrobel and Süß, 1999, 2000; Wrobel 2000a, b) studies. Most of these investigations suggested the age of 39-40 dpc/ 2 cm CRL as the beginning of sexual differentiation in bovine. In the present study, the developmental changes of bovine fetal testis were divided into three stages: early, mid, and late stage according to crown-rump length (CRL) and the corresponding age. With the beginning of the first stage (2.5 cm CRL/43 dpc), the gonadal anlage can be identified as paired bean-shaped structures situating on either side of the dorsal mesentery medial to the mesonephros. Each initial gonad is peripherally delineated by a relatively thick layer of mesenchymal tissue characterizing the first appearance of tunica albuginea (TA), a distinct event in the pathway of testicular differentiation (Schrag, 1983). Firstly, TA is shown to be homogenous layer consists mainly of undifferentiated mesenchymal cells and is covered externally by a thin layer of coelomic epithelium. Later on, the TA increases considerably in thickness (attains about 1-1.2 mm shortly before birth) and separates in two well-defined layers: outer fibrous (tunica fibrosa) and inner cellular (tunica vasculosa). The latter is highly vascular layer and connects with inconspicuous connective tissue trabeculae, the septula testis. Collectively, the differentiated TA is markedly composed of abundant collagen fibrils, little elastic, and numerous fibroblasts. However, the fibrous and vascular contents are predominantly seen in the outer and inner layer respectively and are found to increase progressively with age. Such developmental changes are also documented in the bovine TA by previous investigators (Schrag, 1983, Anton, 1987, Setijanto, 1992). Interestingly, the

initial emergence of TA at the gonadal periphery is timely concomitant with the aggregation of somatic and primordial germ cells to form the testicular cords, the precursors of the seminiferous tubules. A similar sequence of events has been reported to take place in human testis, except that segregation of plate-like structures containing somatic cells apparently precedes their development into cords (Orth, 1993). Although the mechanisms that trigger the aggregation of somatic and germ cells are still uncertain, several local factors have recently been shown to be produced within the genital ridge at the time of testicular cord formation. Among these, numerous growth factors such as TGF-β, IGF, FGF-9, HGF, and neurotrophic factors are proposed to be possible candidates regulating testicular differentiation and morphogenesis (reviewed by Abd-Elmaksoud and Sinowatz, 2005/in press). Bovine testicular cords were firstly observed at the gonadal peripheries whereas the gonadal interior was shown to be cords-free area. However, toward the end of the early stage of development (10-14 cm CRL/75-80 dpc), the peripheral testicular parenchyma is further subdivided into two zones: a narrow outer zone containing-plate like cords with thick diameter (50-60 μm) and a large inner zone filled with a network of thinner cords (35-40 μm). In the outer region, the cords are mostly convoluted while in the inner area they are straight. These findings are supported by the results of Wrobel (2000a) who additionally reported that only the thick outer cords transform into permanent seminiferous tubules whereas the thinner ones are transitory structures that eventually disappear between 45 and 110 dpc. A similar model of arrangement has also been demonstrated in rat (Roosen-Runge, 1961) where seminiferous tubules initially form two rows of consecutive C-shaped arches, one internal to the other. This basic pattern does not change throughout the adult life, even if the C-shaped tubules no longer run a straight course, but are coiled in a number of convolutions. Although the seminiferous cords lie in a plane perpendicular to the long axis of the testis in bovine (Wrobel, 2000a) and rat (Roosen-Runge, 1961), the bovine individual cord is hairpin-shaped and all of them are grouped in a rosette-like fashion around the central testis. The forming bovine testicular cords are rapidly surrounded by a marked basal lamina and 1-2 layers of peritubular cells. Throughout the whole embryonic period, the testicular cords are always solid and lined by two types of cell population: large number of dark polygonal cells with irregular nuclei, pre-Sertoli cells and small number of large light cells with relatively round nuclei, the PGCs. Bovine pre-Sertoli cells are generally in contact with the basal lamina, despite some are sometimes displaced more centrally by the close packing of cells within the cords especially at the end of the early gestation period when the number of pre-Sertoli cells has relatively increased. They have polygonal shape with their cytoplasm oriented radially within the cords.

Their nuclei are variable in shape and rarely show indentation while the nucleoli are mostly associated with the nuclear envelop. Toward the end of gestation period, bovine pre-Sertoli cells were shown to develop columnar shape with basally situated nuclei. Mitotic figures of these cells are seen throughout the whole pregnancy period. Although Schrag (1983) identified two types (light and dark) of presumptive Sertoli cells within the fetal bovine testis, the present study recognized only one type of these cells. In most of mammals, the presence of pre-Sertoli cells is a critical event for the initial testicular cord formation. For instance, these cells are shown to appear on day 13 pc in the differentiating fetal rat testis and then aggregate to form testicular cords on the following day (Magre and Jost, 1980). The signals responsible for eliciting the appearance of pre-Sertoli cells have not been identified yet, but presumably are related to gene product, encoded on the Y chromosome (Bardin et al., 1994). Therefore, it is thought that the action of Sry (sex determining gene on Y chromosome) triggers the differentiation of the Sertoli cell lineage and that the Sertoli cells in turn direct the differentiation of the rest of the testicular somatic cells (Swain and Lovell-Badge, 1999). The origin of pre-Sertoli cells is still uncertain. Several investigations indicated that motile cells derived from mesonephros, coelomic epithelium, or pronephros/mesonephros overlapping area can contribute to the Sertoli cell population (Martineua et al., 1997; Karl and Capel, 1998; Tilmann and Capel, 1999; Wrobel and Süß, 1999, 2000). In agreement with my findings, the mitotic proliferation of pre-Sertoli cells has been reported to begin in the fetal life in all species so far studied (Schrag, 1993; Orth, 1993; Bardin et al., 1994). This division continues during postnatal life and ceases by the formation of functional blood-testis barrier prior to puberty of the animal (Sinowatz and Amselgruber, 1986). Although, the expansion of fetal Sertoli cell population depends principally on FSH, testosterone may also have a role (de Kretser and Kerr, 1994). In bovine, FSH-binding capacity is detected in the fetal testis from 60 dpc and onwards (Khalil and Hauser, 1979). Functionally, pre-Sertoli cells secrete AMH responsible for the regression of the Müllerian ducts in the male fetuses and phagocytose the degenerative germ cells (Bardin et al., 1994; de Kretser and Kerr, 1994). In addition, pre-Sertoli cells in association with peritubular cells are responsible for the process of tubulogenesis at the time of testicular differentiation (Tung and Fritz, 1980).

The early differentiation of germ cells prior to the onset of spermatogenesis has been referred to as prespermatogenesis (Hilscher and Hilscher, 1976). In bovine, this process begins with PGCs that localize the genital ridge as early as 27 dpc (Wrobel and Süß, 1998). The germ cells can be identified as polygonal cells with light cytoplasm and spherical nuclei. They are located either at the periphery of cords (not in direct contact with the basal lamina) or slightly

central. Interestingly, both in the coelomic epithelium and in the TA, some sporadic germ cells can also be identified particularly during the first half of the early gestation period (2.5-6 cm CRL/43-60 dpc), but disappear thereafter. The functional significance and the fate of these cells are unknown. Generally, the germ cells are larger than pre-Sertoli cells and are easily recognizable elements of the seminiferous epithelium. Although, mitotic figures of germ cells are predominantly found in the early stage of pregnancy especially in the period between 3.5 and 14 cm CRL (50-80 dpc), the number of presumptive Sertoli cells within an individual cord cross section is always greater than that of germ cells even at the maximum of germ cells mitosis at 14 cm CRL (table 11). After this stage, germ cell mitosis has significantly reduced. Different to my results, Schrag (1983) stated that the mitotic activity of bovine germ cells begins immediately after the seminiferous cord formation and continues until 23.5 cm CRL and then decreases. My results get support from the findings of Wrobel (2000b) who studied the proliferative pattern of bovine germ cells with monoclonal antibodies against Ki-67 and proliferating cell nuclear antigen (PCNA). As in rat and hamster (Hilscher and Hilscher, 1976, Miething, 1993, 1998), Wrobel (2000b) found that the bovine male germ cell population also shows periods of proliferative activity in the time span between testicular cord formation in the embryo and the onset of spermatogenesis in the pubertal animal. Germ cells with a high proliferation rate are observed from day 50 pc to day 80 pc whereas these cells are in transition from PGCs to prespermatogonia. After this period, the proliferation of prespermatogonia decreases continuously to arrest at day 200 pc where the germ cells enter a phase of relative mitotically quiescence lasting until the 4th postnatal week (Wrobel, 2000b). Schrag (1983) identified two different types (light and dark) of bovine germ cells and described these cells as two different cellular functional states. However, these findings are inconsistent with the results of the present study and with the data of Wrobel (2000b) and may be due to inappropriate fixation. In a recent approach, Gaskell et al. (2004) identified three types of germ cells in the human fetal testis using single, double and triple immunohistochemistry. They proposed these cells as gonocytes, intermediate germ cells, and prespermatogonia. In the first trimester, most germ cells have a gonocyte phenotype, however, from 18 week of gestation, prespermatogonia are the most abundant cell type.

In virtually all species so far investigated, recognizable steroid-secreting cells, the Leydig cells, appear in the interstitium of fetal testis shortly after the testicular cord development (Sinowatz et al., 1987; Rüsse, 1991; Orth 1993). Although the origin of fetal Leydig cells is a matter of debate, several studies have suggested a subpopulation of mesenchymal-like cells in the testis interstitium to be the source of these cells, with evidence obtained from many

mammalian species including rat, mouse, ferret, pig, bovine, and human (Habert et al., 2001; Mendis-Handagama and Ariyarante, 2001). In mammals except pig (van Vorstenbosch et al., 1984) and human (Prince, 2001), Leydig cells ontogenesis was shown to be biphasic, i.e., two generations are involved (Habert et al., 2001). The first Leydig cells generation develops during fetal life, and is responsible for the virilization of the male genital system but regresses thereafter, while the second generation appears during puberty and produce the testosterone required for the onset of spermatogenesis and maintenance of male reproductive functions (Habert et al., 2001). In pig (van Vorstenbosch et al., 1984) and human (Prince, 2001), a triphasic pattern (fetal, neonatal and adult Leydig cells) has been suggested. In bovine, Leydig cells development seems to follow the pattern of most mammalian species (biphasic) (Sinowatz et al., 1987). In the present approach, no Leydig cells were observed at the first developmental age (2.5 cm CRL/43 dpc). Clearly identifiable Leydig cells were however seen at the subsequent age (3.5 cm CRL/50 dpc). These findings confirm the results of Schrag (1983) and Sinowatz et al. (1987) who described the age of 46 dpc (3 cm CRL) to be the time at which the first bovine Leydig cells are seen. Fetal bovine Leydig cells are polygonal with large spherical nuclei that appear slightly darker than that of the pre-Sertoli and germ cells. Their nuclei contain at least two nucleoli while their cytoplasm appears mostly acidophilic in routine histological staining. These cells are grouped in clusters between the testicular cords but are never detected within the mediastinum. Leydig cells show no preferential position in relation to blood capillaries but are randomly distributed. Interestingly, they exhibit a characteristic developmental curve with a distinct peak at the end of early stage of gestation (14 cm CRL/80 dpc). The increase in Leydig cell number is mainly due to further differentiation of mesenchymal cells, whereas mitotic figures within the Leydig cell population are rarely observed. Taken into consideration that embryos of the same age may considerably differ in length, my data appear consistent with that of Schrag (1983) and Sinowatz et al. (1987) who detected this peak at 11-12 cm CRL. The level of testosterone concentration also reaches its peak with maximum development of Leydig cells at 11-12 cm CRL (Sinowatz et al., 1987). As mentioned above, the maximum of germ cells is also detected at this age (14 cm CRL). Taken together, these data raise the possibility that a paracrine relationship exists between fetal Leydig and germ cells, particularly at the early stage of pregnancy. This hypothesis is further supported by the finding that decrease in fetal Leydig cell number is also accompanied by a drop in the testicular testosterone concentration (Sinowatz et al., 1987) and this is parallel to a reduction of the average germ cell number in the cord cross section (table 11). Furthermore, the progressive decline in Leydig cells number

is always associated with a diminishing of the germ cells. In agreement with the previous studies (Schrag, 1983; Sinowatz et al., 1987), fetal bovine Leydig cells are shown to dedifferentiate, since degenerated Leydig cells with pycnotic nuclei or vacuolated cytoplasm are rarely observed. Studies in the rabbit also showed no evidence of degeneration, but rather a reversion to a less differentiated state (Gondos et al., 1976). On the contrary, the investigation of Prince (1984) in human suggested fetal Leydig cells degeneration. The actual cause and functional significance of Leydig cell regression is not known. By dedifferentiation of Leydig cells, the bovine testicular interstitium, especially shortly before birth, consists of undifferentiated mesenchymal cells, blood vessels, and connective tissue.

An interesting event in testicular development is the organization of rete testis and establishment of connection between their channels and the solid seminiferous cords. Early in the first stage of pregnancy (2.5-6 cm CRL/43-60 dpc), rete testis is represented by solid cords which initially occupy a marginal and then an eccentric position at the attached border of the testis. Shortly thereafter (from 6 cm CRL/60 dpc, on), bovine rete testis cells migrate centrally and start to acquire its definitive position by extending into the centre of the longitudinal testicular axis as far caudally as into the caudal fourth of the gonad (Wrobel, 2000a). Considerably, the organization of rete testis into solid strands becomes clearly visible toward the end of early gestation stage (10-14 cm CRL/75-80 dpc) because the strands are separated by connective tissue rich in blood vessels and are surrounded by thick basal lamina. With the beginning of the mid stage of pregnancy (18 cm CRL/100 dpc), these strands become canalized and connect to the seminiferous cords via solid tubuli recti. Although the establishment of connection commences at the end of the early stage (10-14 cm CRL/75-80 dpc), it markedly progresses and develops into easily identifiable straight tubules at the mid stage of gestation. The rete testis strands expand peripherally and come in contact with the thin testicular cords. Their cells invade these solid cords resulting in a mixed population of germ, pre-Sertoli, and rete testis cells. Then the germ and pre-Sertoli cells degenerate and the newly constructed tubuli recti turn out to be lined by rete testis cells. This mechanism may indicate that the straight tubules have two developmental origins, i.e., their basal lamina develops from the seminiferous cords while their lining epithelium is derived from the rete testis. These events also clarify why thin cords disappear; they are replaced by tubuli recti. Although, the development of bovine rete testis has been previously investigated in details by Anton (1987) and Wrobel (2000a), the findings of my work demonstrate mechanisms for connection between the rete testis and the seminiferous cords.

5.1.2. Histological organization of adult testis

The present light and ultrastructural description of the normal adult testis agrees closely with the previous investigations of the testicular morphology of the bovine (Wrobel et al., 1978, 1979, 1981, 1982, 1995a, b; Ekstedt et al., 1986; Sinowatz and Amselgruber, 1988).

As in all species so far studied, adult bovine testis is covered by a tough fibrous capsule which is often referred to as the tunica albuginea that is composed of two layers: an our layer with many fibrous elements (tunica fibrosa) and inner one containing numerous blood vessels (tunica vasculosa). The latter is particularly prominent in bovine whereas large blood vessels running in a tortuous course over most of the testicular surface. The bovine TA itself consists of fibroblasts, bundles of collagen fibers, and few elastic fibers. In some species (horse, boar, and ram) there are additionally appreciable numbers of smooth muscle cells (Bloom and Fawcett, 1986; Dyce et. al., 1987; Wrobel, 1998). Different to boar (Setchell et al., 1994), no Leydig cells are seen in the bovine TA. In addition to its influence on sperm transport in the species containing smooth muscle, testicular capsule probably plays an important role in maintaining the interstitial pressure inside the testis (Setchell et al., 1994). The inner layer of TA is continuous with inconspicuous connective tissue trabeculae that only surrounding the large intratesticular blood vessels. Adult bovine testis is therefore not subdivided into clear lobules as observed in the other species.

Histologically, the testicular tissue is composed of convoluted seminiferous tubules, interstitial compartment, and excurrent duct system. Bovine seminiferous tubules (tubuli seminiferi contorti) are shown to occupy most of the testicular parenchyma. They are basically two-ended convoluted loops with both ends opening into the excurrent duct system via specialized terminal segments. The seminiferous tubules are surrounded by a distinct lamina propria and lined by non-dividing Sertoli cells and highly proliferating spermatogenic cells. Consistent with the results of Wrobel et al. (1979) and Christl (1990), the present approach shows that the lamina propria of the bovine seminiferous tubules has some specific features although its overall construction follows the general pattern of other ruminants such as goat and sheep (Bustos-Obregon and Courot 1974; Bustos-Obregon, 1976). Generally, the lamina propria consists of 4 four layers that are designated from internal to external as basal lamina, a zone containing collagen fibrils, a layer of myofibroblasts, and a covering layer of fibroblasts. Bovine basal lamina is a smooth surface multilayered structure that occasionally shows knob-like protrusions invaginating into the basal portions of spermatogonia and Sertoli cells. A stratified organization of tubular basal lamina has also been reported for goat and ram (Bustos-Obregon, 1976). In other species, this lamina is classical one with knob-like

structures as in cat, dog, monkey, horse, and man (Bustos-Obregon, 1976) or is split into two layers as in rabbit and boar (Bustos-Obregon, 1976) or into three layers as in camel (Moniem et al., 1980). Collagen fibrils in various arrangements are found in the area between the basal lamina and myofibroblasts as well as among the myofibroblasts themselves. Although Resorcin-Fuchsin positive structures are additionally seen at the outer border of basal lamina and in between the surrounding myofibroblasts, my data do not confirm the existence of elastic fibers at the ultrastructural level. This may be due to the fact that elastic fibers in the tubular membrana propria are not easily revealed by conventional electron microscopic techniques (Wrobel et al., 1979). The basal lamina is surrounded by 3-5 layers of myofibroblasts covered on both sides by an inconstant basal lamina. These contractile cell layers vary from one layer (rat and mouse) or two (guinea pig), to up to four or more in other species (Bustos-Obregon, 1976). According to ultrastructural features and alkaline phosphatase histochemistry, Böck et al. (1972) distinguished between two types of peritubular cells, i.e., myoid cells and myofibroblasts. Myoid cells are highly differentiated and possess a continuous basal lamina as well as tightly packed parallel-oriented cytoplasmic filaments. They also exhibit a positive reaction for alkaline phosphatase. Myofibroblasts are surrounded by a discontinuous basal lamina, possess bundles of crossing cytoplasmic filaments, and lack alkaline phosphatase. The peritubular cells of the bovine seminiferous tubules are considered as myofibroblasts with a somewhat higher degree of differentiation than the postpuberal human peritubular cells. Conversely, these cells acquire all features of typical smooth muscle cells in boars (Wrobel et al., 1979; Wrobel, 1998). The covering layer of fibroblasts is proposed to renew the contractile cell layers (Bustos-Obregon, 1976). To date, our knowledge of the functional duties of the lamina propria can be summarized as follows: (a) provision of mechanical support and contractile function for the seminiferous tubules, (b) passive paracrine influence on spermatogenesis via secretory products stimulated by testosterone, (c), partial and species-specific restriction of macromolecules entering the seminiferous tubules via the intertubular tissues, (d) a source of precursor cells capable of differentiating into Leydig cells (de Kretser and Kerr, 1994).

Sertoli cells are known to be the only somatic cells within the seminiferous epithelium. Although, bovine Sertoli cells are tall cells with their broad bases resting on the basal lamina while the remaining cytoplasmic processes extend upward to the tubular lumen, their precise shape is difficult to ascertain because their form is always obscured by surrounding germ cells (Sinowatz and Amselgruber, 1988). The present study has demonstrated that the adult bovine Sertoli cells have some notable characteristics. Their nuclei are for instance characterized by

deep invaginations of the nuclear membrane. Some organelles, such as mitochondria, free ribosomes, and cisternae of sER as well as intermediate filaments are observed in the indentation of the nucleus. The karyoplasm appears homogenous and contains very little heterochromatin. The nucleolus is a particular characteristic structure of the bovine Sertoli cell nucleus. It is composed of numerous vesicles of different sizes, tubules, and ribosomes-like structures. My findings not only agree with the previous studies in bovine (Zibrin, 1972; Ekstedt et al., 1986; Sinowatz and Amselgruber, 1988) but also with data of other ruminants like goat (Jurado et al., 1994) and water buffalo (Kurohmaru et al., 1992). It is generally accepted that this structure is distinctive only in ruminants (Fawcett, 1975 and Kurohmaru et al., 1992) whereas the usual configuration of nucleolus in rat (Fawcett, 1975) and man (Schulze, 1984) resembles a tripartite structure composed of two amorphic lateral bodies and central part formed by a compact nucleolonema. As has been pointed out (Fawcett, 1975), the nucleolus is similar to the nucleolar channel system that appears in the human endometrial cell during the secretory phase of menstrual cycle. A number of hypothesis on its possible function have been proposed, for example, transport of mRNA from the nucleus to the cytoplasm, metabolism of RNA-containing materials and influence on the activity of cellular enzyme systems (More et al., 1974). Although, the nucleolus is usually central, in some nuclei, the nucleolus locates close to the inner layer of the nuclear membrane suggesting that this structure communicates with the perinuclear space or with the cytoplasm of Sertoli cells (Osman and Ploen, 1979). Bovine Sertoli cell nucleoli lack satellite heterochromatin bodies, which are common in many species, e.g. rodents (Fawcett, 1975). Intermediate filaments are widely distributed throughout the cytoplasm and are particularly abundant around the Sertoli cell nucleus and in the areas of cell contacts. They represent an important part of the Sertoli cell cytoskeleton (Sinowatz and Amselgruber, 1988), which additionally consists of microtubules and proposed to be involved in maintaining cell shape, anchoring organelles within the cytoplasm, and positioning the nucleus (Jurado et al., 1994). This dynamic cytoskeleton also allows the Sertoli cell to undergo remarkable changes in shape during spermatogenesis and to determine the position of spermatogenic cells within the seminiferous tubules (Sinowatz and Amselgruber, 1988). The endoplasmic reticulum is well developed and most of it is agranular or contains only few ribosomes. Whorls of sER are often encountered in the bulky lateral processes of the basal part of Sertoli cells. In addition, large accumulations of regularly arranged cisternae of sER are seen in those cell regions surrounding developing spermatids. These whorls are not only obvious in goat (Jurado et al., 1994) and ram (Osman and Ploen, 1979) but are also quite noticeable in rodents (Fawcett, 1975). There may be two

possibilities to explain the function of these Whorls of sER. One is that the sER probably associated with the production of steroid hormones. Although, the existence of lipid droplets seems to support this hypothesis, biochemical studies have shown that Sertoli cells cannot synthesize steroids using acetate or cholesterol as precursors (Fawcett, 1975; de Kretser and Kerr, 1994; Jurado et al., 1994). The other is supported by the finding that spermatocytes and Sertoli cells can transform testosterone into its 5α-reduced metabolites. These data support the idea that the considerable sER, which accumulates in the basal part of Sertoli cells, may play a role in hormone production and transformation (Sinowatz and Amselgruber, 1988), thereby creating a local microenvironment high in androgen concentration, which could be important for certain aspects of sperm differentiation. Sertoli cell cytoplasm also contains mitochondria, an inconspicuous Golgi apparatus, little rER, free ribosomes, polyribosomes, lysosomes and lipid inclusions, however, Charcot-Böttcher crystalloids, a typical constituent of human Sertoli cells (Schulze, 1984), are not evident in bovine.

Importantly, Sertoli cells are known to have specialized cell junctions with other Sertoli cells and with germ cells. By means of these junctions, the Sertoli cells form a continuous layer dividing the seminiferous epithelium into two compartments: a basal one containing spermatogonia and preleptotene spermatocytes, and an adluminal one containing more differentiated spermatocytes and spermatids. This continuous layer comprises the ultimate and tightest part of the blood-testis barrier. The Sertoli-Sertoli cell junctions which have been described in various mammalian species (Russell and Peterson, 1985), including bull (Ekstedt et al., 1986; Sinowatz and Amselgruber, 1988) and non-mammalian species, consist of numerous tight junctions with associated microfilaments and endoplasmic reticulum (Gilula et al., 1976; Osman and Ploen, 1978a). Contrary to inter-Sertoli junctions, different types of specializations occur between Sertoli and germ cells. These include desmosome-like junctions, Sertoli ectoplasmic specializations, and tubulobulbar complexes. Sertoli-germ cell specializations have been proposed to function in the adhesion, orientation, and positioning of the developing spermatids as well as in the release of mature sperm cells from the seminiferous epithelium (Sinowatz and Amselgruber, 1988). In addition to nutritive, protective and supportive functions, several other pivotal roles for Sertoli cells are now well established (these are reviewed under Sertoli cell functions in the first part of this work). Adult bovine germ cells are present in four morphologically different groups, i.e., spermatogonia, spermatocytes, spermatids, and spermatozoa. Generally spermatogonia are present within the basal compartment while the spermatocytes and young spermatids are found in the mid and luminal portions of the tubule respectively. Importantly, the bovine

spermatogonia are currently known to have two separate populations, i.e., stem and spermatogonia precursor cell line as well as cycling spermatogonia involved in spermatogenesis (Wrobel et al., 1995a, b). The former are classified as basal stem cells (BSC), aggregated spermatogonia precursor cells (ASPC), and committed spermatogonia precursor cells (CSPC). Stem cells and spermatogonia precursor cells are morphologically similar to spermatogonia but differ in size, shape, and immunoreactivity. The self-renewing BSC give rise to ASPC, which in turn develop to CSPC. These latter cells transform into new type A spermatogonia (A_1-Sg). The exact demarcation between CSPC and A_1-Sg is defined as the moment when CSPC enter S-phase in preparation for the first A-Sg mitosis (Wrobel et al., 1995a, b). The cycling population of bovine spermatogonia multiply mitotically resulting in A-, I-(intermediate), and B-spermatogonia. In the present investigation, these cells are morphologically identified according to their nuclear shape, cytoplasmic organelles, and contact area with the basal lamina. The mitotic division culminates in the production of preleptotene primary spermatocytes, which no longer divide mitotically but undergo meiotic division resulting in a fourfold increase in the number of germ cells. Preleptotene spermatocytes are documented to pass through a long prophase of the first meiotic division consisting of leptotene, zygotene, pachytene, diplotene, and diakinesis stages. During these stages, spermatocytes increase considerably in size. As a result of this division, short-lived cells "secondary spermatocytes" are produced which go through a second meiotic division to develop finally into round spermatids. Round spermatids are exclusively located in the adluminal part of the seminiferous epithelium and undergo a complex series of cellular transformation (spermiogenesis). This process takes place via four well-defined phases, termed Golgi, cap, acrosomal, and maturation phase. Under light microscope, the first and second phases are characterized by spherical nuclei whereas the third and fourth phases have elongated nuclei. Ultrastructurally, the spermatids have been subdivided into 15 distinctive steps represented by Arabic numerals (1-15). Obviously, the most important morphologic changes during spermiogenesis are formation of the acrosome, condensation of the nuclear chromatin, outgrowth of a motile tail, and loss of excess spermatid cytoplasm not necessary for the later spermatozoon. These findings confirm the conclusions of the previous studies on bovine testis (Sinowatz and Wrobel, 1981; Ekstedt et al., 1986; Wrobel et al., 1995a, b; Wrobel, 1998).

Currently there are two main views on the criteria for staging the seminiferous cycle. The first is based on the development of the acrosomic system of spermatids beginning with the appearance of young spermatids (Leblond and Clermont, 1952), while the second one

depends on the morphological changes of germ cell nuclei and begins after the release of spermatozoa into the tubular lumen (Ortavant, 1958). Thus, in conformity with the definition of the seminiferous cycle as a series of changes occurring in a cell line up to the re-emergence of the same phase at a given point in the tubule, both these methods trace these cyclic events in particular cell lines: the former in the spermatids and the latter in various germ cells. The first method has largely been applied in rodents where it often yields comparatively more stages (Leblond and Clermont, 1952) than the second one. However, the second method has found wide application in domestic animals. This study therefore used the second method where eight such stages are identified. This compares favorably with what has been reported in other domestic species such as the boar (Wrobel, 1998), ram (Wrobel et al., 1995c), donkey (Nipken and Wrobel 1997), goat (Onyango et al., 2000) and their close relatives like buffalo (Wrobel and Pawar, 1992) where a cycle of 8 stages is the standard. Of the eight stages identified in this study, stage 6 and 7 were of relatively short duration and therefore considered as slight morphological variations of stage 5. As a result, they are combined with stage 5 to form one main stage, stage 5-7. Consequently, bovine seminiferous cycle is condensed into 6 main divisions. This practice has previously gained wide application in bovine (Wrobel and Schimmel, 1989), goat (Onyango et al., 2000), ram (Wrobel et al., 1995c), and buffalo (Wrobel and Pawar, 1992).

In general, the interstitial compartment is defined as the tissue that fills up the interstices between the seminiferous tubules and contains in addition to the steroid secreting cells, blood and lymph vessels, as well as nerves of the testicular parenchyma (Fawcett et al., 1973; Setchell et al., 1994). In the present approach, the bovine interstitium appears to consist of either narrow strands being lodged between two adjacent seminiferous tubules or large tri-and quadrangular areas between three to four tubules. The variation between these forms of interstitium are mainly due to their constituents as the former is composed only of blood capillaries, occasional Leydig cells, and some connective tissue fibers and cells while the latter contains large vessels (blood and lymph) and numerous Leydig cells as well. Bovine Leydig cells occur in cords or clusters of varying size that appear to be random in their distribution, some being perivascular, others unrelated to vessels and still other closely associated with the lamina propria of the tubules. However, unlike cat (Wrobel and Hees, 1987), and dog (Montkowski, 1992), no heterotopic Leydig cells were identified neither in the mediastinum nor in the tunica albuginea. Morphologically, bovine Leydig cells are characterized by the same cytological features as the Leydig cells of other mammalian species. Conversely, in some aspects a structural specificity of bovine Leydig cells prevails

and is documented by a relative abundance of a ribosome-associated ER, by a relative paucity of lysosomes and lipid droplets, and by intramitochondrial crystalloids. Previously these findings have also been reported in bovine by Wrobel et al. (1981), who described the ribosome-associated ER as a mixed type of the endoplasmic reticulum (mER). This peculiar feature is however unlike most of mammals whereas the ER of the Leydig cells is predominantly of the typical smooth type (Schulze, 1984; Setchell et al., 1994). It moreover appears to be unusual for an active testosterone-producing cell, since the enzymes related to decisive steps of androgen synthesis are localized within the sER (Murota et al., 1965). Therefore, Wrobel et al. (1981) have stated that the membranes of the mER may carry out the same functions of the pure sER in Leydig cells of the other species. They also denoted that the presence of granular tubular ER in steroid-secreting cells may reflect involvement in enzyme and membrane formation and may be related to the production of a carrier protein for steroids. In addition to Leydig cells, the bovine interstitium is shown to include fine collagen and elastic fibers and several immune cells (discussed under CD4, CD8, and CD 68 section) as well as blood and lymph vessels. Although, blood vessels are often peripheral and may be attached to lamina propria of the seminiferous tubules, lymphatic vessels are centrally located in the intertubular area. Generally, at least one of the lymphatic vessels is always seen in each angular interspace but in some of the larger spaces, there may be two or three. Such arrangement has already been reported for ram and bull (Fawcett et al., 1973; Wrobel et al., 1981). Although, the lymph vessels are a common feature of the testicular intertubular spaces in mammals (Fawcett et al., 1973), a broad range of variation is found in the relative proportion of the principal components of the interstitial tissue. Three more or less distinct patterns of testicular interstitial organization have been distinguished (Fawcett et al., 1973). In the first category are those animals, which have a relatively small volume of Leydig cells (1-5 % of the testicular volume) and a minimum of interstitial connective tissue. A considerable part of the intertubular area in these animals is occupied by extensive peritubular lymphatics. This category includes guinea pig, chinchilla, rat, and mouse. In the second group are those species in which clusters of Leydig cells are widely scattered in a very loose connective tissue stroma drained by conspicuous lymphatic vessels. These lymphatic vessels are bounded by continuous, unbroken endothelial cells and, together with Leydig cells, are supported by variable quantities of collagen and fibroblasts. To this category belong ram, bull, elephant, monkey, and man. The relative paucity of Leydig cells in this group together with their wide separation from blood vessels suggest that steroids secreted from Leydig cells must gain access to the seminiferous tubules and venous system via diffusion through the edematous

loose connective tissues. In the third group, closely packed Leydig cells are the dominant component of the interstitium (20-60% of the testicular volume). They fill nearly all of the intertubular area whereas the interstitial connective tissue is very little and the lymphatics are very few and of small calibre. This group includes domestic boar, warthog, zebra, and naked mole rat (Fawcett et al., 1973). No explanation has been advanced for these differences in the testicular interstitium, but it is interesting that in two species with abundant large Leydig cells (the pig and the horse), the testis secretes large amount of oestrogens (Setchell et al., 1994). The excurrent duct system of the adult bovine testis is composed of terminal segment of the convoluted seminiferous tubules, straight tubules, and rete testis. The terminal segment is a short transitional zone between seminiferous tubules and tubuli recti and is lined by cells designated as modified Sertoli cells. Although, the terminal segment is topographically located at the end of the convoluted seminiferous tubules, it is considered as a part of the intratesticular excurrent duct system because spermatozoa are no longer produced there (Wrobel et al., 1982). Based on regional variation in its light microscopic appearance, each terminal segment is subdivided into a transitional region, middle portion, and terminal plug. In fact, a gradual loss of the spermatogenic cells in a proximo-distal direction is observed through these three regions. In the transitional zone, spermatozoa and spermatids disappear first, followed by a reduction in the number of spermatocytes whereas the population of spermatogonia remains relatively constant. The supporting cells of the transitional region are typical Sertoli cells that are distinguished by round or oval nuclei usually situated basal to the level of primary spermatocytes. In the middle zone, early spermatogenic cells (spermatogonia and primary spermatocytes) are rarely observed. Isolated germinative cells in all stages of spermatogenic development, however, are regularly seen within the lumen of this tubular region. Modified Sertoli cells in this area contain large clear vacuoles of varying shape and size separated by narrow strands of cytoplasm. The terminal plug forms the distal portion of the terminal segment and protrudes into the cup-shaped beginning of the tubulus rectus. A central lumen is clearly visible in the transitional region and middle portion while further distally, the lumen narrows more and more, and near the tip of the terminal segment no permanent central lumen appears to be present. The bovine terminal segment is markedly surrounded by a vascular plexus in a sleeve-like manner. This plexus is composed of arterioles, capillaries, venules, and small lymph vessels. Fibroblasts and many free cells such as lymphocytes, monocytes, and plasma cells constitute this cellular aggregation. Similar findings have previously been described in ram and goat (Osman and Ploen, 1979; Ezeasor, 1986) as well as in bull (Osman and Ploen, 1979; Wrobel et al., 1982). Although, the

functional significance of the terminal segment is not fully clarified, Wrobel et al. (1982) have stated that in bull the terminal plug may function as a valve-like device preventing a reflux of spermatozoa and tubulus rectus fluid under normal conditions. They added that modified Sertoli cells of the terminal segment could play a role in the spermatophagy within the excurrent duct system. Such claims have also been proposed in goat (Ezeasor, 1986), monkey (Dym 1974), and boar (Osman, 1978b). The terminal segment is joined to the rete testis by a tubulus rectus, which is a narrow extension of the rete testis proper. Tubulus rectus of adult bovine testis is composed of three morphologically different regions: a proximal cup-shaped region, a middle narrow stalk, and a distal festooned portion. The significant differences between these regions are mainly seen in the lumen surface, i.e., the first two segments are characterized by smooth lumen surface while the last one is distinguished by a folded epithelium, giving the lumen a characteristic festooned form with a considerable reduction of the lumen. These results confirm the previous investigation of Osman and Ploen (1978b) and Hees et al. (1987) who also reported the presence of three different segments of the bovine tubuli recti. The rete testis is a complicated network of intercommunicating channels that lies in the mediastinum of the testis parallel to the axis of the epididymis (de Kretser and Kerr, 1994). In bovine, rete channels have smooth surface and numerous anastomoses. Although, these are lined by a simple cuboidal or columnar epithelium, they appear stratified at certain sites due to the existence of short intraepithelial crypts. Large channels are often traversed by epithelium-covered cords of connective tissue, *chordae retis*, a characteristic feature of the bovine rete testis. However, chordae retis have been described so far for the human (Roosen-Runge and Holstein, 1978) and for the monkey (Burgos et al., 1979), and probably represent common and characteristic features of the rete testis in many other species (Hees et al., 1987). Rete channels are surrounded by mediastinal stroma containing myofibroblasts, blood and lymphatic vessels and connective tissue. Topographically, the rete testis may be either superficial (marginal) as in rat, mice, hamster, and man (Dym, 1976; Roosen-Runge and Holstein, 1978) or axial (central) as found in the monkey, cat, dog, guinea pig, ram, rabbit, and bull (Dym, 1976; Hees et al., 1987). Further on, Roosen-Runge and Holstein in man (1978) as well as Goyal and Williams in goat (1987) have divided the rete testis into septal, mediastinal and extratesticular rete. The septal rete testis consists of the zone of the tubuli recti that drain the seminiferous tubules. My findings in the fetal testis support the latter classification. Therefore, the term septal rete or straight part of the rete testis is more appropriate than the term straight tubule. This assumption gets further support from the ultrastructural results of the lining epithelium of straight tubules and mediastinal rete. No

considerable differences were found between them as both are lined by simple cuboidal epithelium with inconspicuous organelles and extensive lateral junctional complexes. Many free mononuclear cells, mostly macrophages, and to lesser degree lymphocytes, are localized in the basal half of the bovine straight tubules and rete testis epithelium. Additionally, the lining epithelium of both has the ability to phagocytose spermatozoa (Sinowatz et al., 1979). Immunohistochemically, tubulus rectus and rete testis show the same degree of reaction for many antigens (discussed latter). Consequently, these tubules can be viewed as a part of the rete testis and not as a separate structure. Because an extratesticular rete is not observed in bovine (Dym, 1976; Hees et al., 1989), the bovine rete testis can therefore be divided into septal and mediastinal rete testis. A peculiar feature of the bovine mediastinum is the presence of conspicuous lymph vessels. Generally, there is a close association between the cranial part of the rete testis and adjacent large, thin-walled lymphatics. It has been suggested that this arrangement may facilitate transfer of androgen into rete testis fluid (Hees et al., 1987)

5.2. Glycohistochemistry

Over the last two decades, an impressive variety of regulatory processes including cell growth and apoptosis, folding and routing of glycoproteins and cell adhesion/migration have been unraveled and found to be mediated or modulated by specific protein-carbohydrate interactions (Gabius, 2001). This protein-carbohydrate partnership also determines conformation, function, turnover, solubility, targeting, and sorting of many molecules (Töpfer-Peterson, 1999). In proteins, oligosaccharides that are linked by a N-acetylglucosamine residue to asparagine are termed N-glycans. These oligosaccharides exhibit high content of terminal mannose and/or neuraminic acids residues (Spicer and Schulte, 1992; Wheatley and Hawtin, 1999). Other oligosaccharides attach to serine or threonine amino acids via a N-acetylgalactosamine residue. These O-linked glycans contain galactosyl, fucosyl, N-acetylneuraminc, and N-acetylglucosamine residues (Wheatley and Hawtin, 1999). Fucosyl residues are present in glycans that participate in cell-cell adhesion (Blackmore and Eisoldt, 1999; Töpfer-Peterson, 1999) and in the regulation of substrate diffusion between cells (Spicer and Schulte, 1992). Glucose and mannose residues are abundant in compounds with ion transport functions (Spicer and Schulte, 1992; Blackmore and Eisoldt, 1999); moreover, α-D-N- acetylglucosamine residues regulate membrane interactions and membrane permeability (Blackmore and Eisoldt, 1999; Töpfer-Peterson, 1999). Galactose residues are important for cell-cell adhesions (Spicer and Schulte, 1992; Töpfer-Peterson, 1999) and are also considered markers of cell differentiation (Spicer and

Schulte, 1992). Galactose-β (1→3)−D−N-acetylgalactosamine complexes participate in the transport of fluids and ions (Spicer and Schulte, 1992).

Lectins have a specific binding affinity for the sugar residues of glycoconjugates. Therefore they are used as histochemical reagents to investigate the distribution of glycoconjugates in various tissue including testis (Arya and Vanha-Perttula,1984, 1986; Lee and Damjanov, 1984, 1985; Soderstrom et al., 1984;Wollina et al., 1989; Malmi et al., 1990; Ballesta et al., 1991; Kurohmaru, 1991; Ertl and Wrobel, 1992; Montkowski, 1992; Prem, 1992; Jones et al., 1993; Arenas et al., 1998; Martinez-Menargues et al., 1999; Cavola et al., 2000; Verini-Supplizi et al., 2000; Pinart et al., 2001, 2002; Gheri et al., 2003). Lectin histochemistry can also be used to detect the minute changes in the composition of the cellular glycoconjugates and to follow these changes during normal cellular differentiation and during malignant transformation of cells (Malmi and Söderström, 1988). In my study, the sugar residues of glycoconjugates in the fetal and adult bovine testis were investigated using thirteen (ConA, PSA, LCA, PNA, GSA-I, ECA, DBA, SBA, HPA, VVA, WGA, UEA-I, LTA) different fluorescein isothiocyanate (FITC) conjugated lectins. These lectins represent five groups (mannose-, galactose-, N-acetylgalactosamine (GalNAc)-, N-acetylglucosamine (GlcNAc)-, and fucose-binding lectins) of the known seven lectin-binding groups. In fetal testis, five lectins (PSA, PNA, GSA-I, DBA, WGA) showed a positive reaction while the others were undetectable. PNA, GSA-I, DBA, and WGA were detected in the germ cells (PGCs and their subsequent prespermatogonia) whereas PSA, DBA and WGA labeled fetal Leydig cells. None of the lectins used were bound to pre-Sertoli cells. Further on, some lectins have affinity to tunica albuginea (PSA, PNA, GSA-I, WGA), basal lamina of testicular cords (PSA, WGA), interstitial blood vessels (PSA, GSA-I, WGA), mediastinum testis (PSA, PNA, WGA) and rete testis epithelium (PNA). These findings suggest the presence of binding sites containing galactose (PNA and GSA-I labeled), GalNAc (DBA labeled) and GlcNAc (WGA labeled) but not α-L-fucose in the bovine PGCs and prespermatogonia as well as the existence of mannose (PSA labeled), GalNAc, and GlcNAc residues in the fetal Leydig cells. Interestingly, galactose binding-lectins (PNA and GSA-I) are mainly localized to germ cells during the early stage of gestation (up to 14 cm CRL/ 100 dpc for PNA and 10 cm CRL/ 75 dpc for GSA-I) and disappear thereafter while GalNAc (DBA) is seen later (14 cm CRL/ 80 dpc) and sustains to late stage of gestation (63 cm CRL/210 dpc). However, GlcNAc (WGA), albeit weak, is found during the entire period of pregnancy. My results confirm the findings of Wrobel and Süß (1998) who detected GSA-I, DBA, and WGA affinity in bovine embryonic germ cells. Conversely and may be in species-specific manner, PSA, LCA and WGA showed

a positive reaction in the plasma membrane and cytoplasm of gonocytes, Sertoli cells and other somatic cells in mouse while PNA, GSA-I, and DBA showed no definite reaction throughout prespermatogenesis (Nagano et al., 1999). In human fetal testis, pre-Sertoli cells, PGCs and Leydig cells were characterized by presence of D-galactose-(β1$\rightarrow$3)–D–N-acetylgalactosamine in terminal and/or in subterminal positions, sialic acids, D-N-acetylglucosamine, and α-D-mannose (Gheri et al., 2003). As pointed out above, galactose residues are important for cell-cell adhesions (Spicer and Schulte, 1992; Töpfer-Peterson, 1999) and are considered markers of cell differentiation (Spicer and Schulte, 1992). Galactose-β (1$\rightarrow$3)–D–N-acetylgalactosamine complexes also participate in the transport of fluids and ions (Spicer and Schulte, 1992). Consistent with these reports galactose residues may be expressed in the fetal bovine germ cells very early during their differentiation to facilitate their adhesion to the Sertoli cells and/or to basal lamina. Moreover, persistence of WGA binding to germ cells during the whole gestation period supports the finding that α-D-N- acetylglucosamine residues may regulate membrane interactions and membrane permeability (Blackmore and Eisoldt, 1999; Töpfer-Peterson, 1999). Since glucose and mannose residues are abundant in cells with ion transport functions (Spicer and Schulte, 1992; Blackmore and Eisoldt, 1999), mannose present in fetal Leydig cells could be involved in inducing and maintaining the cellular activity of these cells (Gheri et al., 2003).

In adult bovine testis, detection of sugar moieties by lectins was performed on both Bouin′s-fixed paraffin-embedded and acetone-fixed frozen sections and showed slight difference between the two methods of fixation. Nevertheless, the preservation of testicular morphology was better with Bouin than with acetone. Careful analysis of sugar binding-lectins in the adult animals revealed the presence of mannose (PSA, LCA) and GalNAc (DBA, SBA, VVA) residues in the bovine spermatogonia and spermatocytes. Importantly, binding sites to SBA and VVA in spermatogonia and spermatocytes were only evident in the frozen sections (discussed below). All lectins investigated except fucose-binding lectins (UEA-I and LTA) were bound to the acrosome of round and elongated spermatids. These findings clearly indicate that the acrosome of spermatids contain mannosyl, galactosyl, and glucosly residues. Apical Sertoli cells processes and Leydig cells were weakly stained with the mannose-binding lectins PSA and LCA as well. DBA was additionally seen in the Leydig cells. Although previous studies have reported the presence of these sugar residues in the bovine testis (Arya and Vanha-Perttula, 1985; Ertl and Wrobel 1992), a clear discrepancy was observed between these approaches in the cellular distribution of these glycoconjugates (table 6). In contrast to Arya and Vanha-Perttula (1985), who did not succeed to demonstrate lectin staining in male

153

postnatal prepuberal bovine germ cells and discussed a cyclic affinity of the Sertoli cells for some of the lectins, Ertl and Wrobel (1992) emphasized that lectin affinity in developing testicular tubules of bull testis was restricted to the germ cell line, while the Sertoli cells and their precursors remained completely unstained. Although, DBA served as a selective marker for prespermatogonia, this lectin stained Golgi complexes of most germ cell stages after the gradual onset of spermatogenesis (Ertl and Wrobel, 1992). Inner and outer membranes of the acrosomal complex of spermatids, especially during Golgi and cap phase of spermiogenesis, were intensely stained with PNA, RCA-I, and SBA. In the intertubular tissue BS-I, RCA-I, and UEA-I bound to vascular endothelia. Compartments of the intertubular extracellular matrix were stained with ConA, RCA-I, UEA-I, and WGA but no reaction was recorded with the Leydig cells (Ertl and Wrobel, 1992). Conversely, Arya and Vanha-Perttula (1985) reported that the Sertoli cells display a staining pattern, which varied with the stages of the spermatogenic cycle. A moderate staining of the Sertoli cell processes around the spermatogenic cells was found with PNA, RCA-I, ConA and WGA. After the release of the mature spermatozoa, the apical cytoplasmic extensions of the Sertoli cells were strongly stained with the same lectins. At a later stage of the cycle, staining was located in the body of these cells and eventually in the basal portion of the Sertoli cells (Arya and Vanha-Perttula, 1985). My results are therefore fairly consistent with that of Ertl and Wrobel (1992) since the germ cells, particularly spermatids, were the most clearly lectin-binding cells in the adult bovine testis. These data are substantiated by the fact that the acrosomes of spermatids contain several enzymes, such as acid phosphatase, acrosin, and hyaluronidase, which are glycoproteins or closely associated with complex saccharide moieties that are essential for fertilization (Gould and Bernstein, 1975). Similar to my findings, acrosomes of adult boar spermatids exhibited no affinity for lectins that detect α-L-fucose residues (Cavola et al., 2000; Pinart et al., 2001). Probably these residues are masked by the immediate addition of other sugars in the subsequent glycosylation steps of acrosin (Peterson et al., 1992). Lectin histochemistry was widely investigated in many mammalian species including rats (Arya and Vanha-Perttula, 1984; Söderstrom et al., 1984; Malmi et al., 1990; Jones et al., 1993; Martinez-Menargues et al., 1999), mice (Lee and Damjanov, 1984; Arya and Vanha-Perttula, 1986), hamsters (Ballesta et al., 1991), cat (Prem, 1992), dog (Montkowski, 1992), goats (Kurohmaru, 1991), horse (Verini-Supplizi et al., 2000), boar (Cavola et al., 2000; Pinart et al., 2001,2002) and humans (Wollina et al., 1989; Arenas et al., 1998). My findings in the adult bovine testis are compatible with the results of these studies where the spermatogenic cells were also the most reactive cells in all species so far studied (table 5). Generally,

carbohydrate residues in germ cell plasma membranes are needed for Sertoli-germ cell interactions during spermatogenesis and, later on, for interactions with the male excurrent duct epithelia, and cell surfaces in the female genital tract (Ertl and Wrobel, 1992). Recently, this notion is further supported by the finding that target disruption of Man2a2, a gene encoding α-mannosidase IIx (MX), an enzyme that forms intermediate asparagine-linked carbohydrate (N-glycans), results in Man2a2 null males that are nearly infertile (Akama et al., 2002). Man2a2 null spermatogenic cells fail to adhere to Sertoli cells and are prematurely released from the testis to epididymis. These data clearly show that successful spermatogenesis may mainly depend on specific type of carbohydrates. Further on, it has been suggested that glycoconjugates of spermatogonia and spermatocytes are implicated in substrate and ion transport, and in regulation of membrane permeability (Jones et al., 1992; Jegou et al., 1995). Low content of adhesion molecules in spermatocytes could be explained by the fact that they are migrating cells moving from the basal compartment to the apical compartment of the seminiferous epithelium (Jones et al., 1992; Griswold, 1995). Spermatid glycans participate in ion transport and in adhesion and interaction with the neighboring Sertoli cells (Jegou et al., 1995; Santi et al., 1998). Galactose residues are abundant in glycans that intervene in formation of anchoring structures and in transport of fluids and ions, but they are also considered markers of acrosomal differentiation (Jones et al., 1992). The residues of α-D-glucose and α-D-mannose of the Sertoli cell apical cytoplasm are additionally considered as markers of the compounds that participate in differentiation of the acrosomes in spermatids (Ballesta et al., 1991). The differences in cellular distribution of lectins between fetal and adult bovine testis are firmly supported by the conclusion that specific carbohydrate expression patterns may exhibit striking changes related to cell differentiation (Roth, 1996). In addition, recent advances in glycan research have shown that cell surface proteoglycans are implicated in cell development and differentiation (Iozzo, 1998; Lander and Selleck, 2000). Results obtained by lectin histochemistry are considerably influenced by the mode of fixation used and that the difference in lectin staining after different fixation methods can be marked (Malmi and Söderstrom, 1988). Generally, an excellent result of lectin stain of testicular tissue is obtained after fixation in the Bouin's fluid or formaldehyde with acetic acid while poor results are obtained after the fixation in non-buffered formaldehyde (Malmi and Söderstrom, 1988). The effects of fixation and tissue processing on lectin staining are probably mediated via two mechanisms: the fixative employed may alter the sugars responsible for the specific lectin binding or the glycoproteins in tissues may be dissolved and lost during the fixation or other tissue processing. In this approach, the most obvious

differences between Bouin's-and acetone-fixed testicular tissues were seen for SBA and VVA. These lectins solely stained spermatids acrosomes in the paraffin-embedded tissue while additionally labeled spermatogonia and spermatocytes in the frozen sections. These results show that the fixative and the embedding processes have a considerable effect on the staining pattern of lectins. Moreover, it was evident that the effect of fixative was also influenced by the type of lectin, i.e., some lectins are rather insensitive to the method of fixation (e.g., PNA, ECA and WGA) compared to others. These results are substantiated by the conclusion of Malmi and Söderström (1988) who stated that SBA staining pattern is dependent on the fixation method. Interestingly, they also added that if the cells contain large amounts of glycoconjugates, the staining pattern would not be considerably influenced by the method of fixation. This supports my results as SBA and VVA were identified in small compartment of the spermatogonia and spermatocytes cytoplasm (Golgi complexes). The basal lamina of the seminiferous tubules and blood vessels showed different affinity according to the fixative used. In Bouin's-fixed tissue, the basal lamina was only labeled with LCA and WGA while in acetone-fixed sections most lectins including the constantly negative fucose binding-lectins UEA-I was detectable. In the same way, testicular blood vessels were markedly stained with GSA-I in the paraffin sections however, similar results to that of the basal lamina were seen in the frozen sections. In addition to fixation, lectin binding to sugars of similar composition may be influenced by sugar configuration (α or β) and localization of the specific sequence (terminal vs. internal) (Walker, 1988). This can explain the diverse staining results of the same group of sugar binding-lectin and with the employment of different fixation methods. For instance, PSA and LCA of the mannose group as well as DBA and HPA of the GalNAc group showed different results in the fetal testis. Several examples are also available in the adult (table 13). Furthermore, the reactive behavior of the adjacent structures may impede or facilitate the recognition of lectin binding to certain structures. Therefore, it is always recommended to use a battery of lectins for the study of one sugar (Walker, 1988). In addition to the aforementioned factors, lectin concentration, temperature of incubation, time of incubation, and pH value play an important role and greatly affect the result of lectins staining (Dulaney, 1979; Roth, 1983; Allison, 1987; Malmi and Söderstrom, 1988).

5.3. Immunohistochemistry

In this thesis, 12 different proteins (FGF-1, FGF-2, S100, laminin, α-SMA, VEGF, Cx43, CD4, CD8, CD68, ACE, and GalTase) have been investigated in the bovine testis. Fibroblast growth factors (FGFs) are a family of heparin-binding proteins with key roles in a variety of developmental events and possible importance for maintaining normal tissue homeostasis (Ornitz and Itoh, 2001). In vertebrates, the FGF family comprises to date 23 (FGF-1 to FGF-23) structurally related heparin-binding polypeptide mitogens. The members of FGF family range in molecular mass from 17 to 34 kDa and share 13-71% amino acid identity (Ornitz and Itoh, 2001). A common feature of all members of the FGF family is their high affinity to glycosaminoglycan heparin and structurally related cell surface as well as extracellular matrix heparan-sulfates (Givol and Yayon, 1992; Ornitz and Itoh, 2001). FGFs act at least through three distinct types of receptors (Szebenyi and Fallon, 1999) and are produced by many cell types and tissues, including testis (Ueno et al., 1987; Mayerhofer et al., 1991; Mullaney and Skinner, 1992; Han et al., 1993; Steger et al., 1998; Cancilla et al., 2000; Wagener et al., 2000, 2003; Wahlgren, 2003). FGF-1 and FGF-2 are closely related polypeptide proteins with a predominant length of 140 and 146 AA respectively. However, both shorter and longer forms with a length of 134 &155 AA for FGF-1 and 131 &155 AA for FGF-2 have also been described (Gospodarowicz, 1992). Several forms of FGF-1, varying in size from 16 to 18 kDa, were generated by proteolysis during purification (McKeehan and Crabb, 1987). Similarly, FGF-2 exists in five isoforms with molecular masses of 18, 22, 22.5, 24, and 34 kDa (Arnaud et al., 1999). Although the 18 kDa FGF-2 is localized primarily in the cytoplasm, it has also been detected at the cell surface and in the extracellular matrix (Bikfalvi et al., 1997). The other forms with higher molecular weight are predominantly localized in the nucleus (Bikfalvi et al., 1997; Arnaud et al., 1999). It has been suggest that different molecular weight forms of FGF-2 have distinct functions (Bikfalvi et al., 1997). The 18 KDa form promotes cell migration and mitogenesis, whereas higher molecular weight FGF-2 controls the cell growth (Bikfalvi et al., 1997). On protein level, FGF-1 is 55% homologous to FGF-2, and both bind to the same receptors. Although the prototypes FGF-1 and FGF-2 lack conventional secretory signal sequence and the mechanism of release from cells remains unclear, they are highly abundant in ECM and on the cell surface of a variety of embryonic and adult tissues (Givol and Yayon, 1992, Ornitz and Itoh, 2001). Functionally, FGFs are shown to regulate cell survival, apoptosis, proliferation, differentiation, matrix composition, chemotaxis, cell adhesion, migration, motility, and growth of cell processes (Gospodarowicz et al., 1987; Bikfalvi et al., 1997; Szebenyi and Fallon, 1999). In the testis, several putative

functions have additionally been proposed for FGFs. These include testicular angiogenesis, prepubertal Sertoli cell and germ cell proliferation, mediating Sertoli-germinal cell interaction, initiation of spermatogenesis, and Leydig cell steroidogenesis (Jaillard et al., 1987; Fauser et al., 1988; Murono et al., 1992; Van Dissel-Emiliani et al., 1996; Laslett et al., 1997; Wagener et al., 2003; Wahlgern, 2003). In the present study, FGF-1 and FGF-2 were expressed in a cellular- and stage-specific manner within the embryonic bovine testis. FGF-1 immunostaining was localized to the cytoplasm of the pre-Sertoli cells in the seminiferous cords and to the cells in the interstitial compartment, especially to fetal Leydig cells. Interestingly, while the FGF-1 immunostaining was observed in the pre-Sertoli cells through the entire embryonic period, no reaction was found in the germ cells. Toward the end of early pregnancy (from 10 cm CRL/ 75 dpc, onward), FGF-1 immunostaining was also recognized in the epithelium of the newly differentiated straight tubules and rete testis. Further on, the endothelium of the newly formed blood vessels (arteries) was shown to localize FGF-1 protein from the mid pregnancy (30 cm CRL/130 dpc) and onwards. Contrary to my findings in bovine fetal testis, FGF-1 immunostaining has previously been detected in the gonocytes of the fetal rat testis while no reaction was reported within the pre-Sertoli cells (Cancilla et al., 2000). However, the fetal Leydig cells of the rat testis are also FGF-1 positive cells. While the role of FGF-1 in the pre-Sertoli and germ cells development is uncertain, its role in Leydig cells steroidogenesis appears rather established. In rat, immunostaining for FGF-1 in immature adult-like Leydig cells and peritubular cells co-localizes with FGFRs1-4 (Cancilla and Risbridger, 1998), suggesting that FGF-1 can act through all these receptors in the interstitium (Cancilla et al., 2000). An autocrine action is consistent with FGF-1 modulation of fetal Leydig cell steroidogenesis (Laslett et al., 1997). FGF-1 has been shown to stimulate testosterone production by fetal Leydig cells and 5α-androstane 3α, 17 β-diol production by immature Leydig cells in a cultured interstitial cell preparation in the absence of LH (Laslett et al., 1997).

Unlike FGF-1, FGF-2 could not be demonstrated by immunohistochemistry during early testicular differentiation but was identified somewhat later. FGF-2 immunostaining was first observed at 6 cm CRL (60 dpc), reached a maximum at 14 cm CRL (80 dpc), markedly declined at 30 cm CRL (130 dpc), and disappeared completely thereafter. Importantly, during this limited period of expression, distinct FGF-2 immunostaining was only localized in the nucleus of fetal Leydig cells. Unexpectedly, although the presence of scattered Leydig cells in mid and late stages of gestation, no FGF-2 positive Leydig cells have been demonstrated after 30 cm CRL (130 dpc). No immunostaining was also found in seminiferous cords or in

other cells of the interstitium. In late pregnancy, FGF-2 immunostaining was predominantly localized to tubulus rectus and rete testis epithelium, to endothelium and tunica media of blood vessels especially that of the tunica albuginea and to some peritubular cells surrounding the seminiferous cords. In rat fetal testis, FGF-2 was detected in germ, Leydig, and peritubular cells (Gonzalez et al., 1990; Koike and Noumura, 1994). As mentioned above, Leydig cells have been morphologically recognized in the present study at 3.5 cm CRL and reached their maximum level of development at 14 cm CRL (80 dpc). Later they begin to dedifferentiate. In addition, the level of testosterone concentration within the testis is simultaneously increased with Leydig cells development to reach its peak with their maximum at 88 dpc. Thereafter and in parallel to the process of Leydig cells dedifferentiation, rapid decrease in the testosterone concentration takes place (Sinowatz et al., 1987). Taken together, the stage-specific immunolocalization of FGF-2 is nearly concurring with developmental changes of bovine fetal Leydig cells as well as with the changes in the testosterone concentration. These data indicate that FGF-2 could be involved in Leydig cells steroidogenesis during the fetal period. Such claim gets further support from the finding that no FGF-2 positive Leydig cells were seen after the reduction in testicular testosterone concentration despite the presence of scattered Leydig cells within the testicular tissue at the late stage of gestation (table 11). Consistent with my suggestion, several approaches have shown that FGF-2 is able to modulate Leydig cell steroidogenesis (Fauser et al., 1988; Murono et al., 1992; Laslett et al., 1997).

In adult bovine testis, the presence of FGF-1 and FGF-2 in the testis was investigated by Real time RT-PCR, in situ hybridization, and immunohistochemistry. Absolute mRNA quantification was done using real time RT-PCR that is regarded as a very sensitive method for quantification of low level mRNA in biological specimens (Bustin, 2000; Ginzinger, 2002). In this technique, amplicons are measured as they accumulate during the exponential phase of the reaction. This makes quantification much more accurate than methods that depend mainly on the end-point measurements. In the present study, 10 fold serial dilutions of the standard cDNA template of both factors resulted in slopes of -3.33 and -3.48 for FGF-1 and FGF-2 respectively. These values are fairly close to the theoretical ideal values of -3.32 (Ginziger, 2002). Moreover, the PCR efficiencies (defined as the factor by which the amplicon concentration is multiplied at each cycle) showed an acceptable percentage (99.6% for FGF-1 and 93.7% for FGF-2). The calculated copy numbers mainly depend on slope and PCR efficiency. An ideal slope should be -3.32 for 100% efficiency (Ginziger, 2002). Transcription of FGF-1 about 10 times higher than that of FGF-2 may not be an absolute

value because the PCR efficiency was not the same. To ensure specificity of the PCR products, melt curve analysis was performed immediately after amplification. The melt curves of this study showed a single peak for each growth factor. In addition, the agarose gel electrophoresis revealed a single PCR band, which ensures the specificity of amplification. A drawback of real time quantification is that it cannot offer an accurate quantification for the actual copy number of molecules of unknown samples (Yin et al., 2001; Ginzinger, 2002). This mainly attributes to several reasons. Quantification does not take account of the original sample's RNA purification efficiency or of cDNA synthesis during reverse transcription. Moreover, it does not consider the difference in amplification efficiency between sample cDNA and PCR products of the standard (Yin et al., 2001; Ginzinger, 2002). For these reasons, the term "absolute quantification" may not be fully appropriate as long as these problems are not solved.

By means of in situ hybridization, both FGF-1 and FGF-2 signals were found in Leydig and Sertoli cells as well as in the modified Sertoli cells of terminal segment. FGF-1 transcripts were additionally recognized in the straight tubules and rete testis epithelium. Immunohistochemically, FGF-1 protein was localized in the cytoplasm of spermatogonia and spermatids as well as in the cytoplasm of Sertoli and Leydig cells while FGF-2 protein was only seen in the cytoplasm of some spermatogonia and in myofibroblasts. The discrepancies between in situ hybridization and immunohistochemical results may indicate a difference in the sites of synthesis and utilization of FGF-1 and FGF-2 within the bovine testis, which may point to a paracrine action of these growth factors.

Previously similar data have also been reported in the other mammals. FGF-1 was detected in the rat spermatogonia (Wahlgren, 2003) and roe deer spermatids (Schön and Blottner, 2004). Localization of FGF-1 in Sertoli and Leydig cells was additionally found in adult rat (Cancilla et al., 2000) and roe deer (Wagener et al., 2003) testis. Furthermore, FGF-2 was seen in the cytoplasm of spermatogonia in adult rodent (Mayerhofer et al., 1991; Wahlgren, 2003), human (Steger et al., 1998) and roe deer testis (Wagener et al., 2003) as well as in the Sertoli, Leydig, and peritubular cells of rat (Mullany and Skinner, 1992; Han et al., 1993). A recent paper of Schön and Blottner suggested that FGF-1 may be involved in the Sertoli cell-spermatid communication and could serve as a survival factor for somatic cell populations within the testis. In contrast to FGF-1, FGF-2 has been intensively studied. Earlier investigations have suggested that FGF-2 is an important factor for the regulation of Sertoli cell functions in pig (Jaillard et al., 1987) and for the initiation and regulation of spermatogenesis in rat (Mayerhofer et al., 1991; Mullaney and Skinner, 1992, Han et al.,

1993, Van Dissel-Emiliani et al., 1996). Moreover, it was proposed that FGF-2 is involved in autocrine and paracrine regulation of the proliferation and differentiation of spermatogonia and spermatocytes in human testis (Steger et al., 1998). Consistent with this assumption, more recent data emphasized that FGF-1 and FGF-2 have stimulatory effects on spermatogonia type A and type B proliferation via a direct effect on premitotic DNA synthesis (Wahlgren, 2003). This effect is stage specific (stage I only), which indicates mitogenic as well as survival actions of both factors on germ cells. As demonstrated in human and various animals model, localization of FGF-1 and FGF-2 in bovine spermatogonia suggests a role of these growth factors in spermatogonial proliferation. My results, moreover, propose that FGF-1 and FGF-2 may modulate the testicular hormonal profiles via autocrine actions on adult Leydig cells. This hypothesis is partially substantiated by findings of in vitro studies (Fauser et al., 1988; Murono et al., 1992; Laslett et al., 1997), which have demonstrated a positive influence for FGF-2 on the Leydig cell steroidogenesis.

In this study, blood vessels endothelium and vascular smooth muscle cells (tunica media of the medium and small sized blood vessels) were markedly stained with FGF-1 and FGF-2. Interestingly, previous investigators have proposed that FGF-2 could be involved in the regulation of blood pressure and improvement of blood flow (reviewed by Bikfalvi et al., 1997). Further on, it has been shown that factors inducing vascularization improve the spermatogenic and steroidogenic functions of the varicocelized rat testis (Isoyama and Sofikitis, 1999). A more recent study has additionally emphasized that local release of FGF-2 significantly improves testicular blood flow and morphology after ligation of testicular vessels in rat (Guler et al., 2004). FGF-2 may therefore play a role in the local control of blood flow within the bovine testis. Nevertheless, additional experiments are necessary to clarify the functional role of FGF-1 and FGF-2 in testicular blood flow.

Although, FGF-2 has been detected in the rete testis fluid of rat and ram and has been proposed to be produced in the testis and act upon the initial segment of the epididymis to regulate gamma-glutamyl transpeptidase (Lan et al., 1998; Kirby et al., 2003), the functional significance of intense localization of FGF-1 and FGF-2 in the bovine rete testis and straight tubule epithelium requires further investigations to be elucidated.

S-100 proteins, named for their solubility in a 100% saturated solution of ammonium sulphate at neutral pH, is a group of closely related, small, acidic, water-soluble, Ca^{2+}-binding proteins (Donato, 1986; Zimmer et al., 1995). S-100 belongs to the family of Ca^{2+}-binding protein, which includes calmodulin, calcyclin, troponin c, parvalbumin, light chain of myosin and

intestinal calcium-binding protein (Isobe et al., 1982). To date, some 20 different proteins have been assigned to S-100 family. They show different degree of homology, ranging from 25% to 65% identity at the amino acid level. Altogether, they represent the largest subgroup in the EF-hand Ca^{2+}-binding protein family (Schafer and Heizmann, 1996; Heizmann et. al., 2002). Structurally, S-100 proteins are dimers of at least two types of subunits (α and β) with different amino acid composition. These subunits are selectively expressed by specific cell types in the form of either homodimers ($\alpha\alpha$ and $\beta\beta$) or heterodimers ($\alpha\beta$). In resting cells, S-100 proteins are localized in specific cellular compartments from which some of them relocate upon cellular stimulation and even are secreted exerting extracellular, cytokine-like activities (Heizmann et. al., 2002). Therefore, S-100 proteins display the unusual property of acting both, within cells as Ca^{2+} sensor proteins implicated in Ca^{2+} signal transduction and, outside cells as ligands for specific cell surface receptors on an increasingly larger number of cell types. It is thought that this group of proteins carries out their intracellular functions by interacting with specific target proteins. The list of these target proteins now includes a number of types (up to 40 types) e.g. desmin, vimentin, tubulin, p53, etc. (Heizmann and Cox, 1998; Donato, 2001). Additionally, it has been reported that some S-100 proteins (after secretion) can have paracrine effects on neighboring cells and that the extracellular concentrations play a crucial role in the physiological response. It has recently been found that, some S-100 proteins have also the capability to interact with the newly discovered RAGE surface receptors (Receptor for Advanced Glycation End Product) to exert their function but it is not known whether RAGE is a universal S-100 receptor or S-100 members also interact with other cell surface receptors (Donato, 2001; Heizmann et al., 2002; Hsieh et al., 2002). Initially S-100 protein was found in glial elements of the brain and in Schwann cells of the peripheral nervous system. It had therefore long been considered specific to the nervous tissue (Bock, 1978). However, subsequent immunohistochemical and biochemical studies have revealed the presence of S-100 protein in tissues other than the nervous system, particularly in the testis (Girod et al., 1986; Haimoto et al., 1987; Amselgruber et al., 1992, 1994; Cruzana et al., 2000; Cruzana et al., 2003). In my thesis, S100 has been detected in the embryonic and adult bovine testis. In the prenatal testis, it was demonstrated in the cytoplasm and nucleus of pre-Sertoli cells. Germ and Leydig cells exhibited no immunostaining. During mid pregnancy (from 23 cm CRL/110 dpc, on), moderate S100 reaction was also found in the lining epithelium of the newly differentiated straight tubules, in rete testis epithelium and in the endothelium of blood and lymph vessels.

In adult bovine testis, specific immunoreactivity for S100 was observed in Sertoli cells, modified Sertoli cells of the terminal segments and in epithelial cells of the straight testicular tubules and rete testis. Additional S100 immunostaining was found in the endothelial cells of capillaries, veins, and lymphatic vessels. No S100 immunoexpression was observed in different stages of germ cells, Leydig and myofibroblast cells, and intraepithelial macrophages of the rete testis. Immunohistochemical localization of S-100 in the testis has previously been reported in the fetal testis of rat (Kagi et al., 1988) and bovine (Setijanto, 1992) as well as in the adult testis of different mammalian species including rat (Michetti et al., 1985, Amselgruber et al., 1994), cat (Amselgruber et al., 1994; Cruzana et al., 2000), European bison (Czykier et al., 1999), ram, boar, horse, dog, and bull (Amselgruber et al., 1992,1994), buffalo (Cruzana et al., 2003), monkey (Girod et al, 1986), and human (Michetti et al., 1985; Haimoto et al., 1987). My findings in bovine fetal testis are consistent with the results of Setijanto (1992) who has also observed S100 immunostaining in the pre-Sertoli cells, endothelium of blood and lymph vessels and rete testis epithelium. Conversely, Kagi and colleagues (1988) have detected S100 in the Leydig cells, fetal spermatogonia and endothelial cells of prenatal rat testis. S-100 protein was seen in the cytoplasm and nuclei of Sertoli cells in adult monkey (Girod et al, 1986), ram, bull, boar, cat, horse (Amselgruber et al., 1994; Cruzana et al., 2000), and buffalo (Cruzana et al., 2003) testes. With the exception of monkey in the abovementioned animals, a particular intense staining was seen in the modified Sertoli cells of the terminal tubular segment (Girod et al., 1986; Amselgruber et al., 1992, 1994; Cruzana et al., 2000, 2003). Leydig cells were found to be strongly positive for S-100 protein in rat, cat, and human testis and to a lower degree in pig and horse testis (Michetti et al., 1985; Girod et al, 1986; Amselgruber et al., 1994; Cruzana et al., 2000). Endothelial cells of capillaries, veins, and lymphatic vessels were regularly S-100 protein immunoreactive in rat, boar, ruminants, and human (Michetti et al., 1985; Amselgruber et al., 1992, 1994; Cruzana et al., 2003). A distinct immunostaining of peritubular cells was only found in the testis of dog, cat, and rat (Amselgruber et al., 1994; Cruzana et al., 2000). S-100 protein immunoreactivity was additionally detected in the epithelial cells of the straight tubules and in the epithelial cells of rete testis in bull, ram, boar and buffalo (Amselgruber et al., 1992, 1994; Cruzana et al., 2003). In the European bison, immunoreactivity for S-100 protein was observed in the endothelial cells of arteries, veins, capillaries, and lymphatic and a weak reaction was also found in the smooth muscle of arteries and veins. No reaction was detected in Sertoli cells and/or Leydig cells (Czykier et al., 1999). Therefore, the S100 protein immunoreactivity in the adult testis of my research supported the findings of Amselgruber et

al. (1992) on bovine and showed a parallel result with that of sheep (Amselgruber et al. 1994) and buffalo (Cruzana et al., 2003). A great body of evidence suggests that S-100 could be viewed as a multifunctional subfamily of Ca^{2+}-binding proteins of the EF-hand type. A large number of diverse functions is attributed to S-100 proteins, ranging from calcium-buffering through intracellular (e.g., modulation of enzyme activities, energy metabolism, motility, and secretion) and nuclear (e.g., transcription and apoptosis) functions to extracellular activities (e.g., secretion, neurite extension, and chemotaxis) (Donato, 1999, 2001; Schafer and Heizmann, 1996; Heizmann and Cox, 1998; Heizmann et. al., 2002). Despite all of these proposed functions, the exact biological role of this protein in the testis is not yet known. However, S-100 protein in the different cell types of the testis supports the hypothesis that this protein is a multifunctional protein (Donato, 1986; Haimoto et al., 1987; Amselgruber et al., 1992). The expression of S100 in fetal bovine testis points to a pivotal role of this protein in Sertoli cell morphology. S100 proteins have also been implicated in the regulation of cell cycle due to the stimulation of Ndr, a nuclear serine/threonine protein kinase important in the regulation of cell division and cell morphology, in a Ca^{2+}-dependent manner (Donato, 2001). Additionally, one of the best-characterized functions of S100 proteins is the regulation of cell morphology, the dynamics of certain cytoskeleton constituents, and the reciprocal relationships of cytoskeleton element via direct and/or indirect interactions with microtubules, intermediate filaments, microfilaments, myosin, and /or tropomyosin (Donato, 2001). Although the exact testicular function of S100 is yet unclear, it is striking to note that the bulk of the cell types staining positive for S100 exhibit special morphological features (Michetti et al., 1985) such as Sertoli cells (Amselgruber et al., 1992). S100 protein in the Sertoli cells is assumed to be involved in the microtubule assembly-disassembly system (Amselgruber et al., 1992). Further on, the protein may play a role in the secretory and absorptive functions in the intratesticular excurrent duct system and may be involved in establishing the blood-testis barrier (Amselgruber et al., 1994; Cruzana et al., 2003).

The role of basal lamina (BL) in the embryonic development and in the functions of adult tissues has been inferred from a number of observations. For instance, BL components promote cell adhesions and modulate the in vitro phenotype of the cells. BL also serves as depositories of growth factor (e.g., FGF), and may thereby modulate access to, and activity of, such growth factors. In addition, several groups have shown that disruption of the cell adhesion to extracellular matrix in vitro can induce programmed cell death (reviewed by Engvall, 1995). A growing body of evidence supports the notion that extracellular matrix

(ECM) molecules and mesenchymal cells influence Sertoli and spermatogenic cells (Dym, 1994). The interest in the seminiferous tubule ECM components stems partially from observations that male infertility is associated with abnormal thickening in the lamina propria of the seminiferous tubules (Salomon and Hedinger, 1982; Davidoff et al., 1990).

As pointed out in my review, the lamina propria is composed of both peritubular myoid cells and ECM material including a basal lamina. Previous approaches have shown that this lamina contains laminin, type IV collagen, heparan sulfate proteoglycans, fibronectin, and nidogen/entactin (Dym, 1994; Erickson and Couchman, 2000). Laminins, prominent glycoproteins in basal lamina, are large complexes composed of a heavy α chain, and the light β and γ chains. To date, there is evidence of 12 different laminin isoforms in vivo (six α-, three β- and three γ-laminin). Several biologically important activities of laminin have been suggested, including cell adhesion, growth, morphology, differentiation, and migration (Kleinman et al., 1985).

In the bovine fetal testis, positive immunostaining for laminin was initially detected in the basal lamina that delineates the differentiating sexual cords and below the thickened surface epithelium of tunica albuginea at 2.5 cm CRL (43 dpc). In the subsequent stages of testicular development, laminin positive basal lamina completely enclosed the testicular cords and became evident around the blood vessels and beneath the rete testis epithelium. Importantly, toward the end of the early pregnancy (10 cm CRL/75 dpc), a connection between the laminin positive basal lamina of seminiferous cords and rete testis was detectable. In the testis of adult animals, marked laminin positive reaction was also localized in basal lamina of the seminiferous tubules and myofibroblast cell layers. In most seminiferous tubules, laminin showed a diffuse staining of the basal lamina, but in some tubules, particularly at the level of terminal segments, the laminin deposits formed invaginations into the seminiferous epithelium. This pattern of arrangement results in striated appearance of the modified Sertoli cells basal portion. Laminin was also detected in the adult basal lamina of the vascular endothelium, of smooth muscle cells of blood vessels, of the rete testis epithelium and of the myofibroblasts. These findings are consistent with numerous approaches that have studied the localization of laminin in fetal and adult testis of several mammalian species including mouse (Enders et al., 1995; Frojdman et al., 1995; Pelliniemi and Frojdman, 2001), rat (Hadley and Dym, 1987; Gelly et al., 1989; El Quali et al., 1991; Yazama et al., 1997; Pelliniemi and Frojdman, 2001), dog (Benazzi et al., 1995) and human (Pollanen et al., 1985; Davidoff et al., 1990; Santamaria et al., 1990; Virtanen et al., 1997; Gulkesen et al., 2002). Nevertheless, laminins are not exclusively localized to basal lamina. El Quali et al. (1991) identified the

165

laminin as being expressed in Sertoli cells, gonocytes, and peritubular cells during rat testicular development. These data may be partially substantiated by the fact that laminin is released from cultured rat Sertoli cells (Skinner et al., 1985) and is synthesized and secreted by both Sertoli and peritubular cells in human (Pollanen et al., 1985). Although Wrobel (2000a) demonstrated that the first connection between the seminiferous tubules and rete testis via short straight testicular tubules occurred after 85 dpc, my result detected an earlier connection through the basal lamina (10 cm CRL/75 dpc). The early expression of laminin in the bovine fetal testis may suggest a functional role in the process of testicular cord morphogenesis. This assumption has been substantiated by several observations. First, laminin secreted by gonocytes has been proposed to play an important role in adhesion of gonocytes to the basal lamina and adjacent Sertoli cells (El Quali et al., 1991). Second, laminin probably mediates connection between the Sertoli cells and the basal lamina, since antibodies to laminin inhibit Sertoli cell attachment to reconstituted basal lamina (Tung and Fritz, 1993). This attachment is important for the morphology of Sertoli cells and for the in vitro differentiation of cords composed of Sertoli cells (Hadley et al., 1990). Finally, some isoforms of laminin (laminin α 5) has recently been designated as an early molecular marker for sexual differentiation, which may be regulated by the testis-determining factors (Frojdman et al., 1999). In mature testis, Tung and Fritz (1993) concluded that laminin regulates the Sertoli-Sertoli tight junctions and the blood testis barrier via a transmembrane link between the extracellular laminin and the Sertoli cell cytoskeleton. Morphologically, invaginations of the tubular basal lamina towards the seminiferous epithelium have been described earlier in the literature (Bustos-Obregon, 1976; Wrobel et al., 1979) and recently by this study. This morphology seems to be the reason of laminin deposit invaginations within the seminiferous tubules particularly at the terminal segment. Similar to my observation, laminin deposits has been shown to form small invaginations into the seminiferous epithelium in adult human testis (Pollanen et al., 1985; Santamaria et al., 1990; Gulkesen et al., 2002).

Actin is one of the most conserved eukaryotic proteins present in the cytoskeleton of all cells (Schlatt et al., 1993). Actin occurs as cardiac muscle actin, skeletal muscle actin, smooth muscle actin, and structural F-actin (Steger and Wrobel, 1994; Steger et al., 1994). Since α-smooth muscle actin (αSMA) is known as a specific marker of the final smooth muscle cell differentiation (Skalli et al., 1986), it was expected to be solely expressed in the differentiated smooth muscle cells of bovine testis. No αSMA immunoreaction was seen in tunica albuginea or in peritubular cells during the whole period of bovine testis development. These findings

are completely related to the observation of Wrobel et al. (1988) who stated that the differentiation of peritubular cells commences in the proliferative phase (8th -20th week) of the postnatal bovine testis and is completed in the subsequent prepubertal phase (20th -32nd week) when the transformation of peritubular cells to myofibroblast cells that can be clearly separated by light microscope from other derivates of the mesenchymal-like cell line takes place. My results are additionally consistent with that in the rat (Palombi et al., 1992), monkey (Schlatt et al., 1993), and human (Holstein et al., 1996; Jezek et al., 1996) where αSMA is expressed in adult but is never observed in fetal peritubular cells. αSMA was exclusively expressed in the blood vessels at early stage of development (3.5 cm CRL/50 dpc). The expression of αSMA in the blood vessels was originally seen in the arteries at 3.5 cm CRL/50 dpc, while one month later in the veins (14 cm/80 dpc). The intensity of αSMA immunoreaction as well as the number of blood vessels showing positive staining has increased with age. The early differentiation of vascular smooth muscle cells in the embryonic male gonad suggests a critical role of differentiated blood vessels in the embryonic development. This idea is supported by the proposal that elaboration of the arterial system increases blood flow through the testis to promote the efficient export of testosterone from the early testis, a processes that is crucially important for the virilization of the embryo (secondary sex determination) (Brennan and Capel, 2004). In adult bovine testis, marked αSMA expression was found in the myofibroblasts demarcating the seminiferous tubules. Distinct reaction was observed in the testicular blood vessels as well. Several layers of αSMA positive cells were also seen beneath the rete testis epithelium. Similarly, previous studies have detected αSMA in the adult testis of rat (Palombi et al., 1992), monkey (Schlatt et al., 1993), ram (Steger and Wrobel, 1994; Steger et al., 1994), bull (Steger et al., 1994) and human (Holstein et al., 1996). Indeed, the myoid or myofibroblast cells have been shown to be contractile elements, responsible for the peristaltic activity of the tubules transporting spermatozoa and testicular fluid towards the rete testis and epididymis (Roosen-Runge, 1951; Bock et al., 1972). This fact may justify the absence of αSMA expression in the undifferentiated peritubular cells of fetal testis, as no spermatozoa are available, i.e., there is no need for the contractility. More recently, αSMA has been shown to signal the beginning of blood-testis barrier formation rather than its completion (Holt et al., 2004). Away from its contractile ability, peritubular myoid cells are known to stimulate total protein production by Sertoli cells and to increase the Sertoli cell production of ABP and transferrin. They produce a protein named P-mod-S that has been shown to be an important regulator of Sertoli cell

function in vitro (Anthony et al., 1991). They are also considered to modulate the effects of androgens on the seminiferous tubule and therefore upon spermatogenesis.

Vascular endothelial growth factor (VEGF), a basic heparin-binding homodimeric glycoprotein of 45 KDa, is an endothelial cell-specific mitogen and an angiogenic inducer in a variety of in vivo models. There are at least four different human VEGF isoforms, which result from differential splicing of the mRNA. These isoforms are proteins containing 121, 165, 189, and 206 amino acid residues (Ferrara, 2004). In my work, no VEGF immunostaining was seen in Sertoli cells and spermatogenic cells other than specific stages of spermatids. Similarly, no cells of the interstitial compartment and rete testis epithelium showed any VEGF positive reaction. Interestingly, round and early elongating spermatids at the first three stages of the seminiferous epithelial cycle exhibited a marked reaction at the site of the forming acrosomes. Additionally, moderate immunostaining for VEGF was found in the modified Sertoli cells of the terminal segment especially in the terminal plug. In blood vessels, despite no VEGF immunoreactivity was observed in the endothelium, a punctate reaction was seen in smooth muscle cells (tunica media) of medium and small sized arteries. VEGF and their receptors were recently detected in the testis of rat (Anand et al., 2003; Rudolfsson et al., 2004; Zhang et al., 2004), mouse, (Young and Nelson, 2000; Anand et al., 2003; Nalbandian et al., 2003) and human (Ergun et al., 1997). Sertoli and Leydig cells expressed VEGF both at mRNA and protein level in these species. In an interesting approach, Zhang et al. (2004) have recently shown that the expression pattern of VEGF in the spermatids is different in the 14 stages of rat seminiferous cycle and a strong immunopositive reaction is mainly found in the forming acrosomes of round and elongated spermatids and in spermiogenic residual bodies. These data have led to the assumption that VEGF may play an important role in the processes of spermatogenesis and spermiogenesis, particularly in the acrosomal developing process (Zhang et al., 2004). That VEGF can be involved in regulating transport of important blood borne factors has been supported by a recent report showing that VEGF plays a major role in the cellular transport of blood glucose (Sone et al., 2000). Therefore, it is conceivable that VEGF plays a pertinent role in the maintenance of testicular functions by its ability to facilitate transport of blood borne hormones and nutritional elements (Anand et al., 2003). However, a recent approach has reported that VEGF does not appear to regulate testicular blood flow and it is not involved in inducing the hCG-induced inflammation-like response in the testicular microvasculature. Moreover, the permeability-increasing effect of VEGF is low in the testis under basal conditions but appeared to be up-

regulated by hCG treatment (Rudolfsson et al., 2004). The notion that VEGF may play a crucial role in the testis physiology is supported by the findings that overexpression of this factor either leads to complete infertility (Korpelainen et al., 1998) or at least reduces the male fertility due to impaired spermiogenesis (Huminiecki et al., 2001). Nevertheless, in an apparent conflict to these findings, Obermair and co-workers (1999) reported that VEGF is not associated with male factor infertility and does not improve fertilization.

Gap junctions are now known to be dynamic, multifunctional membrane channels that are implicated in a wide variety of biological processes. In mammals, gap junctions are composed of two hemi-channels, termed connexons, each provided by one of the two neighboring cells. Two connexons interact and dock end-to-end in the extracellular space to form a tightly sealed double-membrane intercellular channel. Structural analyses have shown that each connexon is composed of six polytopic trans-membrane protein subunits, termed connexins (Cx). The central pore of the gap junction channels allows the exchange of nutrients, metabolites, ions and small biological molecules such as second messengers (cAMP, IP3, Ca^{+2}) up to 1 KDa (for reviews see Saez et al., 2003; Segretain and Falk, 2004).

To date, the connexin gene family comprises 20 and 21 members in the mouse and human genome respectively (Sohl and Willecke, 2004). However, their current nomenclature is based on the molecular weights (Willecke et al., 2002). The importance of gap junctions is underscored by the fact that Cx genes contain internal ribosome entry site (IRES) elements, which are typically found in genes of transcription factors, growth factors, and other genes that need to be specifically regulated independently of cell cycle (reviewed by Harris, 2001). Apart from their role in channel formation, Cx could exert other functions including signal transduction and linkage to cytoskeleton through Cx-partner protein interactions (Duffy et al., 2002). Recent data showed that Cx43 is tightly associated with ZO-1 in Sertoli cells (Defamie et al., 2001). Thus, it is likely that alterations of one of these proteins could perturb either their classical functions (cell adhesions, formation of tight or gap junctions) or their newly postulated functions (signal transduction) leading to disturbed germ cell development and infertility (Fiorini et al., 2004). As discussed before, my study confirms previous investigations that reported the presence of gap junctions between adjacent Sertoli cells in the adult bovine seminiferous tubules (Ekstedt et al., 1986) as well as between neighboring Leydig cells in both fetal (Schrag, 1983; Sinowatz et al., 1987) and adult (Wrobel et al., 1981) bovine testis. In order to characterize these gap junctions, I have investigated the immunolocalization of Cx43 in fetal and adult bovine testis. My finding showed that Cx43 is

localized to the gap junctions between Leydig cells of embryonic and adult testis and to Sertoli-Sertoli cell junctions of the seminiferous epithelium apical to spermatogonia and basal to spermatocytes. In the fetal period, the localization of Cx43 was markedly parallel to the developmental pattern of the Leydig cells discussed above in the morphological section (table 11). The number of Cx43 immunopositive Leydig cells increased gradually with age until 14 cm CRL where it attains its maximum. Thereafter (18 cm CRL, onward), it was usual to see some focal areas of the interstitium free of Cx43 immunopositive Leydig cells. This feature increased gradually and became more prominent with the beginning of the late gestation period (63 cm CRL/210 dpc, on) where the Leydig cell number has considerably reduced (table 11). The variation in the Cx43 immunolocalization nearly follows ontogenesis and developmental changes of bovine fetal Leydig cells as well as changes in testosterone concentration reported by Sinowatz et al. (1987). This observation is further supported by the data that gap junctions between steroidogenic cells are subjected to changes consistent with alterations of the functional status (Wrobel et al., 1981). Cx43 immunoreactivity between fetal Leydig cells has also been detected in mouse (Perez-Armendariz et al., 2001) and guinea pig (Pelletier, 1995). The fact that Cx43 is expressed between Leydig cells before it is seen in the seminiferous tubules may be a reflection that optimal hormone levels would be required among a greater number of Leydig cells to ensure normal development of the testis and adequate timing of the onset of spermatogenesis (Pelletier, 1995). Furthermore, expression of Cx43 between adjacent interstitial Leydig cells from the earliest stage of testicular differentiation may suggest a role for this protein in the control of developmental processes required to regulate testosterone production, secretion or both (Bravo-Moreno et al., 2001; Perez-Armendariz et al., 2001). One possible mechanism by which gap junctions may enhance testosterone release is by transfer of cAMP (Murray and Fletcher, 1984) which amplifies the transcription of cAMP-dependent steroidogenic enzymes (Payne and Youngblood, 1995) as well as synchronizes testosterone release by adjacent Leydig cells. Interestingly, knock-in mice in which the Cx40-or Cx32-coding region was substituted for Cx43 survive to adulthood but show disturbed spermatogenesis (Plum et al., 2000). Whether alterations in testosterone levels at this developmental stage contribute to the failure of differentiation of germinal cells in these mice remains to be determined. In the adult bovine testis, Cx43 is localized between Leydig cells as found in man (Steger et al., 1999), rodent (Risely et al., 1992; Perez-Armendariz et al., 1994; Varanda and de Carvalho, 1994; You et al., 2000; Bravo-Moreno et al., 2001), guinea pig, and mink (Pelletier, 1995). Because not all adult bovine Leydig cells are situated in close contact to capillaries or venules (Wrobel et al.,

1981), my results propose that gap junctions may play a role in conveying nutrients, metabolites, ions, and small biological molecules such as second messengers (cAMP, IP3, Ca^{+2}) to Leydig cells away from the blood vessels.

Within the seminiferous tubules, Cx43 immunopositive reaction is found within the basal compartment apical to spermatogonia and basal to spermatocytes in a stage-dependent manner. It has greatly reduced during stages II, III, and IV. Thereafter, it increased again through stages V, VI, and VII to attain its maximum at stage VIII and stage I. Similar findings have been reported in rodents (Risely et al., 1992; Batias et al., 1999; Decoury et al., 2004) and human (Sterger et al., 1999). The localization of Cx43 in the area of Sertoli-Sertoli cell contact reinforces the presence of Sertoli cell gap junctions as demonstrated by ultrastructural analysis (Ekstedt et al., 1986). Such location correlates with Sertoli-Sertoli cell junctions responsible for the blood testis-barrier formation (Wrobel and Schimmel, 1989). Stage dependent changes of Cx43 expression concurs with cyclic variations of Sertoli-Sertoli cell junctions. The blood testis-barrier in the bovine seminiferous epithelium is especially tight in stages I and VIII, as compared with stages II through VII where basal Sertoli-Sertoli contacts are less developed (Wrobel and Schimmel, 1989). The decrease of Cx43 at stage II, III, and VI may be linked to germ cell passage (preleptotene spermatocytes) from the basal location to the adluminal position, which temporarily modifies the blood testis barrier (Russell, 1978). In rodents, subsequent formation of gap junctions at stage XI regulates germ cell multiplication and meiosis of spermatocytes (Decoury et al., 2004). Recently, it has been shown that intercellular communication via gap junction represents a bidirectional way between adjacent Sertoli cells and unidirectional means from Sertoli cells to spermatogonia and spermatocytes. This functional coupling is, however, associated only with the presence of Cx43 isoform of Cx (Decoury et al., 2004). In addition to localization of Cx43 in the basal compartment, occasional dark brown dots were seen in the adluminal compartment toward the tubular lumen (between Sertoli cells/ spermatocytes and spermatids). The presence of these Cx43 positive gap junctions in the adluminal compartment make the seminiferous epithelium to look like a syncytium, but such ideas need further studies to be confirmed. In adult, the hypothesis that Cx43 mediated gap junction intercellular communication is absolutely required for spermatogenesis is supported by the conclusion that Cx43 gene targeted deletion results in male infertility (Plum et al., 2000) and altered Cx43 expression is correlated with impaired human fertility (Defamie et al., 2003), and testicular dysfunction (Brehm et al., 2002).

The fact that majority of males do not develop immunity to their own germ cells has led to the conclusion that testis is one of the "immunologically privileged" tissues of the body (Hedger, 2002). In addition to Leydig cells, the testicular interstitium contains connective tissue cells, vascular and lymphatic endothelial cells, and immune cells (Hedger, 1997). Prominent among these latter are the resident macrophages, which show species-specific variation in their relative numbers. They are particularly numerous in rat and mouse testis (Hutson, 1994; Wang et al., 1994; Itoh et al., 1995). Studies in these species have established that the resident testicular macrophages play an important role in Leydig cell development, and steroidogenesis in the adult (Bergh et al., 1993; Gaytan et al., 1994). In my study, the lysosomal marker CD68 (EBM11) that identifies bovine resident macrophages (Ackermann et al., 1994) was not detectable in the fetal testis. However, CD68 positive cells were clearly seen within the interstitial testicular compartment of the adult animals. These cells are randomly distributed within the interstitium being sometimes located near to Leydig cells, myofibroblasts, blood vessels, or present directly under the tubular lamina propria. Nevertheless, they were never seen within the lumen of seminiferous tubules. CD68 immunostaining was mainly granular and localized to the cytoplasm. In straight tubules, CD68 expression was detected in the lining epithelium of a single straight tubule while the others exhibited negative reaction. Despite the presence of CD68 positive staining within the mediastinum, no reaction was found in any of the cells lining rete testis. Unlike CD68 (EBM11), CD68 (KP1) immunostaining was not demonstrable in the bovine testis. The present report is in accordance with several previous approaches that have detected the resident macrophages in the testis of rodent (Hutson, 1994; Wang et al., 1994; Itoh et al., 1995), sheep (Pollanen and Maddocks, 1988), and human (Pollanen and Niemi, 1987; El-Demiry and James, 1988; Frungieri et al., 2002). CD68 antigen is not only expressed by macrophages but also by monocytes, dendritic cells, neutrophiles, basophiles, and large lymphocytes (Pulford et al., 1990; Bukovsky et al., 2001). Therefore, it is difficult to quantify the testicular macrophages with this marker alone. Although earlier electron microscopic studies revealed the presence of macrophages as regular constituents of the bovine rete epithelium (Wrobel et al., 1978), no CD68 positive cells were seen in this work within the lining epithelium of rete. These results are concomitant with the findings that not all macrophage population of rat testis expresses resident macrophage markers (Wang et al., 1994; Gerdprasert et al., 2002). The functional significance of CD68 localization in a single straight tubule is not clear. A close functional association between the Leydig cell and macrophages is indicated by several lines of evidence (reviewed by Hedger, 2002). These

include the existence of specialized interdigitations between the two cell types implying the potential for a direct exchange of information and materials, and parallel changes in morphology and cell volume that occur in several experimental models. Moreover, macrophage depletion prior to testicular maturation in the immature rat and in the ethane dimethane sulphonate (EDS)-treated adult rat severely inhibits Leydig cell development or recovery in these models. These data indicate that, not only testicular macrophage development is influenced by the Leydig cells, but also that Leydig cell development is profoundly influenced by the presence of macrophage (Hedger, 2002). This surprising concept has been given a further support by the poor Leydig cell functions of macrophage-deficient MCSF-deficient mice (Cohen et al., 1996). Recently, testicular interstitial macrophages have been shown to produce and secrete 25-hydroxycholesterol that causes direct stimulation of Leydig cell steroidogenic functions (Nes et al., 2000; Lukyanenko et al., 2001). Testicular macrophages are also potential sources for several growth and differentiation factors (reviewed by Hales, 2002). Of these, three well-known macrophage cytokines–TNFα, IL1α, and IL1β– have been reported to be secreted from rat testicular macrophages (Kern et al., 1995; Hayes et al., 1996, Soder et al., 2000). Although the role of these cytokines in the bovine testis is still uncertain, several reports indicate a modulatory effect of IL1 and TNFα on steroidogenesis (see Hales, 2002; Hedger and Meinhardt, 2003). The available reports are contradictory, showing both inhibitory and stimulatory effects of IL1 and TNFα on androgen synthesis depending on the experimental conditions. Khan et al. (1992) described an important role for IL1 in proliferation of Leydig cells. TNFα enhances expression of growth factors in Sertoli cells and production of metabolites important for germ cells. IL1 regulates nitric oxide production, gamma-glutamyl transpeptidase, and lactate generation in Sertoli cells (reviewed by Hedger and Meinhardt, 2003). In addition to the modulatory action exerted by macrophages and their secretory products on steroidogenesis and Sertoli cell activity, testicular macrophages secrete pro-inflammatory as well as anti-inflammatory cytokines and exert an important trophic and/or scavenger role in tissue morphogenesis and function (reviewed by Hedger and Meinhardt, 2003). Macrophages also produce reactive oxygen species (ROS) such as hydrogen peroxide, which inhibits Leydig cell functions. ROS appears to act by perturbing Leydig cell mitochondria resulting in the inhibition of steroidogenic acute regulatory (StAR) protein expression (Hales, 2002).

Like macrophages, T lymphocytes or T cells are important cells in the immune response. They are also distributed throughout the interstitial tissue of the normal adult testis (Pollanen and Niemi, 1987; Pollanen and Maddocks, 1988; Wang et al., 1994; Hedger et al., 1998;

Hedger and Meinhardt, 2000). T cells that express the surface molecule CD4 are mostly regulatory or helper cells and can be activated by professional MHC class II-bearing antigen-presenting cells. However, T cells that exhibit the CD8 surface marker are generally cytotoxic and are activated when they come in contact with antigen presented on the surface of cells expressing MHC class I molecules (Hedger, 1997). Since nearly all somatic cells exhibit MHC class I molecules on their surface, the CD8$^+$ T cells play an important role in protection against viral infections and transformed (tumourigenic) cells (Hedger, 1997). CD4 and CD8 were previously detected in fixed and paraffin embedded bovine tissue using a range of antigen recovery and signals amplification techniques (Gutierrez et al., 1999). In my report, CD4 and CD8 are, albeit few, recognized in the interstitial tissue of adult bovine testis. CD4 positive cells were mostly small, round with spherical nuclei and present mainly as single cells. Most of the interstitium was free of these cells and it was very rare to see pair of cells within the same area. Unexpectedly, CD4 immunoreaction was observed in the cuboidal cells of the rete testis but this may be unspecific. In contrast to CD4, very few CD8 positive cells were detected in the interstitium (2-5 cells per testicular section). Localization of these cells in the bovine testis is concomitant with the previous approaches that detected helper (CD4) and cytotoxic (CD8) T cells in the rat (Wang et al., 1994; Hedger et al., 1998; Hedger and Meinhardt, 2000), mouse (Mukasa et al., 1995) and human (Pollanen and Niemi, 1987) testis. Conversely, El-Demiry et al. (1987) failed to observe any intratesticular T cells under normal conditions in human. Parallel to my results, Mukasa et al. (1995) reported that the mouse testis contains much lower numbers of T cells. However, Hedger and coworkers (1998) have found that the T cells in the rat testis are predominately CD8 immunopositive cells. This discrepancy may be due to species differences but it is equally likely that differences in T cell numbers are related to past exposure to infections or other immune events (Picker and Butcher, 1992). In general, T cells appear to have relatively free access to the rat testis (Pollanen and Maddocks, 1988; Wang et al., 1994). Importantly, away from the species variations, the inconsistency of my data with the results described in rat could be due to differences in tissue fixation and immunohistochemical technique employed. CD4 and CD8 epitopes were shown to be the most difficult to immunostain and demonstration of these epitopes was not achieved in formalin fixed tissue (Rathkolb et al., 1997; Gutierrez et al., 1999). Additionally, the microwave pre-treatment appears to be essential for the antigen retrieval especially for the CD4 epitope (Gutierrez et al., 1999). Any way, in normal non-inflamed testis, it seems that T cells numbers are determined by normal T cell re-circulation mechanisms, by past immune activation events, and by local regulatory mechanisms

involving the Leydig cells and resident macrophages that induce the preferential accumulation of CD8 positive T cells (Hedger and Meinhardt, 2000). As pointed out above, the CD4 T cells are activated by professional antigen-presenting cells, such as macrophages, and direct the subsequent pattern and intensity of the immune response, but do not usually function as immune effector cells (Kaye, 1995). On the other hand, CD8 plays a key role in protection against tumor development and viral infections as well as in graft rejection response (Hedger et al., 1998). Clearly, these two subsets will have very different influence on the development of immune response within the testis. Collectively, the presence of testicular macrophages, T-helper and T-cytotoxic cells suggest that the testis may possess enhanced innate immunoprotection. This could be a compensatory mechanism to limit tumor development or potential infections by microorganisms entering via the genital tract (Hedger, 1997).

Galactosyltransferase (GalTase) is one member of a functional family of intracellular, membrane-bounded enzymes that participate in the biosynthesis of carbohydrate moieties of glycoproteins and glycolipids. This enzyme catalyzes the transfer of galactose from UDPgalactose to the acceptor sugar N-acetylglucosamine. In mammals, 19 distinct GalTase enzymes have been characterized to date (Hennet, 2002). In those species analyzed so far, the gene for GalTase encodes two proteins, both of which have a type II membrane conformation, analogous to all other glycosytransferase cloned so far. The two GalTase proteins (short and long isoform) have identical catalytic and transmembrane domains but differ in their cytoplasmic domains (Shur et al., 1998). A number of observations show that the short GalTase isoform is normally confined to the Golgi complex where it serves a purely biosynthetic function. In contrast, the long GalTase isoform can function both biosynthetically in the Golgi complex and due to its additional cytoplasmic domain, can also function as a signal-transducing receptor on the cell surface (Shur et al., 1998). In this preliminary study, the immunostaining of galactosyltransferase (GalTase) was found exclusively in the Golgi apparatus of Leydig cells and at the cell surface of rete testis epithelium of fetal bovine testis. Although, scattered Leydig cells were present in mid and late stages of pregnancy, the GalTase immunopositive fetal Leydig cells have markedly reduced in mid pregnancy (from 23 cm CRL/110 dpc, on) and disappeared completely in late stage (63 cm CRL/210 dpc, on). Unlike Leydig cells, surface immunostaining for GalTase in the rete testis epithelium was detected at 14 CRL (80 dpc) and increased with age. No GalTase protein localization was however observed in fetal Sertoli and germ cells. Similarly, blood and lymph vessels did not exhibit any reaction. While Northern blot analysis revealed a developmental

expression of GalTase mRNA in the newborn mouse testis (Zhu et al., 2003), no data are available on the cellular localization of this enzyme in embryonic and postnatal testis. The expression of the short GalTase isoform in the Golgi apparatus of fetal Leydig cells is correlated with the localization of some lectins (PSA, WGA, and DBA) in these cells during prenatal period (table 12). Further on, the abundance of short GalTase isoform in Leydig raises the possibility that it may function in the glycoprotein biosynthesis of the extracellular matrix. This suggestion is substantiated by previous studies (Denduchis et al., 1996), which proposed that Leydig cells in culture are able to synthesize ECM proteins (laminin and type IV collagen) and express ECM receptors (integrins), as well as cell-to-cell adhesion molecules such as N-CAM and N-cadherin. In addition, cell lines with an abundant Golgi complex actively involved in the elaboration of an extracellular matrix show proportionally more short transcript than long transcript (Lopez et al., 1991; Kudo and Narimatsu, 1995). Unlike Leydig cells, surface immunostaining of the rete testis epithelium is detected at 14 CRL (80 dpc) and increased with age. There is some evidence that surface GalTase participates in cell interactions during embryogenesis (Shur et al., 1998). The GalTase functions on the embryonic cells as a receptor for glycoside ligands in the basal lamina. Cells initially adhere to basal lamina components in a GalTase-independent manner, which is presumably mediated by the integrins. Signals induced by the basal lamina, perhaps via integrins, result in increased GalTase expression on the cell surface, which becomes associated with the cytoskeleton and localizes to the newly formed leading edge of the cell (Shur et al., 1998). The binding site for GalTase in the basal lamina has been identified as N-linked oligosaccharides within the E8 domain of laminin. This is the same domain that is responsible in large part for cell migration and neurite outgrowth properties of laminin (Shur et al., 1998). In summary, these findings suggest that surface GalTase may participate in the rete testis morphogenesis and canalization during mid and late stages of testicular development.

In the adult bovine testis, distinct immunostaining was seen in the Golgi complex of Sertoli and Leydig cells. GalTase was also detected in the Golgi apparatus of some spermatocytes and at the head surface of the elongating spermatids while no immunostaining was observed in the spermatogonia. Marked surface and cytoplasmic expression of the GalTase was also detected in the straight tubules and rete testis epithelium. As in the fetal testis, blood and lymph vessels and peritubular myofibroblast cells have no GalTase reactivity. Although mammalian testes are found to be rich in various glycoconjugates with distinct differentiation-related changes in their distribution (Malmi et al., 1990; Ertl and Wrobel; 1992), limited data

are generally available about the immunohistochemical localization of GalTase in the adult mammalian testis (Pratt et al., 1993). Northern blot, S1 nuclease analysis, and in situ hybridization revealed the expression of GalTases mRNA in adult mouse testis (Shaper et al., 1990; Pratt and Shur, 1993; Zhu et al., 2003). These studies detected the GalTase mRNA and its corresponding protein at the surface of Sertoli and spermatogenic cells. In addition, immunoelectron microscopy confirmed the localization of GalTases to spermatogonia, late stage spermatids, Sertoli cell surface membrane, and interstitial Leydig cells of adult rat testis (Suganuma et al., 1991). Generally, GalTase has been widely accepted as a marker enzyme for the Golgi complex (Navaratnam et al., 1988). In this situation, the fact that GalTase was localized only to adult but not fetal bovine Sertoli cells may suggest some associations between this enzyme and bovine spermatogenesis. Moreover, the localization of GalTase within the Sertoli cells Golgi apparatus may indicate the involvement of this organelle in the secretory activities of Sertoli cells. This supposition is however contradictory to the view of some authors (Bloom and Fawcett, 1986; de Kretser and Kerr, 1994) who stated that Golgi apparatus of Sertoli cells have no morphological indication of involvement in secretory pathways. The latter observation may be true in rodents whereas GalTase is evident only at the Sertoli cells surface but not within the Golgi apparatus (Shaper et al., 1990; Suganuma et al., 1991; Pratt and Shur, 1993; Raychoudhury and Millette, 1993). These investigations proposed that the cell surface GalTase might be involved in the Sertoli cell function during spermatogenesis. The modification of oligosaccharide moieties of glycoprotein on the sperm surface is one of the biochemical changes believed to be important in the production of functionally mature spermatozoa (Tulsiani et al., 1993). In spermatogenic cells, GalTase mRNA accumulated during the maturation of primary spermatocytes, reached peak level prior to meiosis, and decreased at meiosis (Pratt and Shur, 1993). Germ cell surface GalTase is found to facilitate their adhesion to Sertoli cells (Pratt and Shur, 1993). As spermatogenic cell develop, GalTase is redistributed to the anterior aspect of the sperm head, possibly by association with the action of the cytoskeleton (Scully et al., 1987). In the cauda epididymis, the glycoconjugates secreted by the epididymis mask the sperm GalTase-binding sites. During capacitation, these competitive glycoconjugates are shed from the sperm surface, making GalTase available to bind its oligosaccharide ligand (O-liked oligosaccharides on the ZP3 glycoprotein) in the zona pellucida (Miller et al., 1992). The presence of GalTase on the plasma membrane of bovine sperm (Fayrer-Hosken et al., 1991) confirms my findings of the localization of GalTase in the spermatocyte Golgi apparatus and at the head surface of the elongating spermatids since sperms no longer synthesize glycoprotein and no longer have

need for a Golgi complex (Shur and Neely, 1988). As demonstrated in rodent, localization of GalTase at the surface of the bovine elongating spermatids may facilitate their adhesion to Sertoli cells.

Immunoelectron microscopy verified the precise localization of the enzyme in the trans-Golgi stacks of adult rat Leydig cells (Suganuma et al., 1991). As pointed out in the glycohistochemical part of this thesis, some sugar residues (mannose and N-acetylgalactosamine, table 13) are detected in the adult Leydig cells of bovine testis. These data may clarify the intensive localization of GalTase in the Golgi complex of Leydig cells. Although GalTase has previously been detected in the rete testis fluid (RTF) of ram and boar (Tang, 1998), the physiological function of its existence is not well understood. Several studies have reported that the RTF provides a favorable environment for GalTase activity due to the low pyrophosphatase and phosphatase activity (Hamilton, 1980; Tang, 1998). The localization of GalTase in modified Sertoli cells of the terminal segment, in straight tubules and in rete testis epithelium may suggest that specific glycosylation of sperm surface glycoproteins may occur at multiple sites in the male reproductive tract. Oligosaccharides on cell surface glycoproteins have also been proposed to act as essential functional groups required for appropriate biological activities in the reproductive system (Dell et al., 1999; Hennet and Ellies, 1999).

Angiotensin-converting enzyme (ACE, CD143) is a zinc-containing dipeptidylcarboxypeptidase that has important functions in the renin-angiotensin system for the regulation of blood pressure as well as fluid and electrolyte regulation. Although this enzyme is associated most commonly with the regulation of blood pressure, there is considerable evidence for the potential role of ACE in the reproductive function (Speth et al., 1999). In mammals, the enzyme occurs in two isoforms encoded by a single gene. The larger isoform, somatic form (sACE), is found in blood and several other tissues including the vascular endothelial cells, renal epithelial cells and testicular Leydig cells (Sibony et al., 1993; Esther et al., 1997), while the testis-specific form (tACE) is expressed only in post-meiotic spermatogenic cells and sperm (Langford et al., 1993; Sibony et al., 1994; Sabeur et al., 2001; Ball et al., 2003; Pauls et al., 2003). In my investigation, the fetal bovine germ cells (prespermatogonia) showed a transient expression of ACE in 6 and 10 cm CRL (60-75 dpc) whereas no immunostaining was detected in the subsequent stages of testicular development. Additionally, moderate reaction was seen in the endothelium of the blood vessels. The ACE positive reaction of endothelium was firstly detected by 18 cm CRL (100 dpc) and increased

simultaneously with age. Similarly, in adult bovine testis, marked ACE protein expression was only observed in the endothelium of blood vessels. However, ACE was not evident in Sertoli, Leydig and germ cells as well as in straight tubules and rete testis epithelium of fetal and adult testis.

Immunohistochemically, the cellular distribution of ACE has previously been studied in the testis of rat (Sibony et al., 1994), mice (Langford et al., 1993; Sibony et al., 1994), dog, (Sabeur et al., 2001), and human (Pauls et al., 2003). In the present study, I found that ACE is localized to the cytoplasm of fetal germ cells between 60 and 75 dpc, a period wherein germ cells have a high proliferation rate and are in transition from PGCs to prespermatogonia (Wrobel, 2000b). Recently, Pauls et al. (2003) have detected the sACE in the human gonocytes especially between 18th and 22nd gestation week, a period in which prespermatogonia of the late M-and T1-types predominates (Wartenberg, 1981; Hilscher, 1991). The assignment of sACE to this particular stage of prespermatogonial differentiation and its complete down-regulation in the subsequent stages of testicular development led to the supposition that sACE may play a role in the human germ cell development and ontogenesis of human testis (Pauls et al., 2003). Somatic ACE was also localized to the fetal and adult Leydig cells as well as vascular endothelium of different mammalian testis (Pandey et al., 1984; Pauls et al., 1999; Pauls et al., 2003). Although the endothelial sACE may participate in regulating the vasculature tone (Franke et al., 2003), its physiological role in the Leydig cells needs to be addressed. In the adult testis, tACE is expressed in a stage-specific manner in rodent (Langford et al., 1993; Sibony et al., 1994), dog (Sabeur et al., 2001), and human (Pauls et al., 2003). In man, ACE was initially found in post-meiotic step 3 spermatids and increased markedly during differentiation and strictly localizing to the adluminal membrane site of elongating spermatids (Pauls et al., 2003). In mouse and rat testis, the highest level of expression tACE was associated with elongated spermatids (acrosome phase) at step 10-11 (Sibony et al., 1994). Close correlation between the germ cell specific formation of tACE and maturation of germ cell exists, but the significance of this correlation remains obscure, although studies with ACE-deficient mice demonstrated reduced male fertility in homozygous mutants (Krege et al., 1995). In the male reproduction, some investigators have suggested that ACE may play a role in capacitation, hyperactivation, or acrosomal exocytosis of spermatozoa. In human sperm, ACE is released during capacitation in vitro (Kohn et al., 1995) and inhibition of ACE via the specific inhibitor, captopril, reduced both acrosomal exocytosis and hamster ova penetration rates by human spermatozoa (Foresta et al., 1991). However, other investigations did not identify any effect of inhibition of ACE on the ability

of sperm to bind the zona pellucida (Kohn et al., 1998; Metayer et al., 2001). In mice in which both the sACE and tACE have been eliminated by homologous recombination, homozygous mutant males demonstrated normal histological features of the seminiferous tubules epithelium and normal seminal parameters; however, these males have a reduced fertility associated with a reduction in the ability to fertilize oocytes and a reduced number of spermatozoa present in the oviduct of mated females (Krege et al., 1995; Esther et al., 1996; Hagaman et al., 1998). Although these studies have not identified the specific role of ACE, they do indicate a potentially critical role of tACE in normal reproductive function.

On the other hand, Liao and Roy (2002) did not recently find any association between known polymorphisms in the tACE gene and male infertility in an Asian population. Concerning these contradictory data, the potential role of ACE in male reproduction is still uncertain.

In conclusion, the stage- and cellular-specific expression of some sugar moieties and of some cellular proteins within fetal and adult bovine testis may indicate different cellular requirements during testicular development as well as during spermatogenesis.

6. SUMMARY

Morphological, Glycohistochemical, and Immunohistochemical Studies on the Embryonic and Adult Bovine Testis

In the present study, the testes of 32 bovine embryos with different crown-rump length (2.5-90 cm CRL) and of 15 sexually mature bulls (Deutsches Fleckvieh) were investigated using light- and electron microscope as well as glycohistochemical and immunohistochemical methods. The gestation period was divided into 3 stages; early, mid, and late gestation. Developmental changes in the testicular morphogenesis were therefore analyzed in details during these phases.

Generally, embryonic development of bovine testis involves the same mechanism described in other mammals. At the first stage of this study (2.5 cm CRL/43 dpc), the anlage of the testes protruded to the coelomic cavity as paired bean-shaped structures on either side of the dorsal mesentery medial to the mesonephros. It consists of primitive testicular cords, interstitium, and rete testis blastema. Proceeding with fetal age, these basic testicular structures are further differentiated. The tunica albuginea is separated into two layers: an outer fibrous layer (tunica fibrosa) with some mesenchymal cells, numerous fibroblast, and much fibrous content and an inner cellular layer with several blood vessels (tunica vasculosa). The testicular cords are surrounded by a marked basal lamina and peritubular cells and lined by two types of cells: a large number of dark polygonal cells with irregular nuclei, pre-Sertoli cells and small number of large light round cells with relatively round nuclei, the prespermatogonia. The average number of the germ cells per cross section of cord increases, particularly form 3.5 to 14 cm CRL, resulting in a germ cell maximum at the end of this stage (14 cm CRL). Although most of the germ cells are located toward the periphery of the cord, some are also found in the center. Pre-Sertoli cells form a complete layer at the periphery of the cords. Generally, these cells are irregular in shape and numerous but considerably smaller than the germ cells. Unlike prespermatogonia, mitotic figures are seen in pre-Sertoli cells during the whole embryonic life. As a consequence of the expansion in the interstitium, the seminiferous cords are progressively separated from each other. The testicular interstitium is rapidly differentiated and is composed of several islets or clusters of polygonal Leydig cells, peritubular flattened cells surrounding the testicular cords, connective tissue cells, and numerous blood vessels. In the present study, fetal Leydig cells were first recognized at 3.5 cm CRL. Thereafter, the average number of these cells is rapidly increased to attain their

maximum with the end of the first gestation period (14 cm CRL). This generation of Leydig cells however dedifferentiates progressively with developmental age. A continuous system of basal lamina joins the testicular cords with rete strands from 10 cm CRL and onwards. This system establishes the first connection between these two testicular components via ill-developed uncanalized straight tubules (tubuli recti). Rete testis channels are lined by simple layer of cuboidal epithelium with round nuclei occupying most of the cytoplasm and enclosed by well-defined basal lamina.

The adult bovine testis is enclosed by a connective tissue capsule, tunica albuginea, composed predominantly of collagen fibers and few elastic fibers. Most of the testicular parenchyma is made up of the convoluted seminiferous tubules (tubuli seminiferi contorti), two-ended convoluted loops, with both ends opening into the rete testis via specialized terminal segments. The seminiferous tubules of sexually mature bulls are enclosed by a distinct lamina propria and are lined by two cell populations, non-proliferating Sertoli cells and highly proliferating spermatogenic cells. The bovine lamina propria consists of basal lamina, collagen and elastic fibers, and 3-5 layers of partially overlapping myofibroblasts. Additionally, fibrocytes, collagen fibrils, and fibroblasts-like cells form the outermost border of the tubulus. Sertoli cells are easily identifiable elements of the seminiferous epithelium. Adult Sertoli cells are large irregularly shaped cells with their broad bases resting on the basal lamina while the remaining cytoplasmic processes extend upward to the tubular lumen. They are characterized by round or oval euchromatin-rich nuclei situating in the basal portion near the basal lamina of the seminiferous tubules. Adult bovine germ cells are present in four morphologically different groups, i.e., spermatogonia, spermatocytes, spermatids, and spermatozoa. The seminiferous cycle stages are identified using changes in the germ cell nuclei as well as location and shape of spermatids. According to this method, eight stages are defined in the seminiferous epithelium of bovine. The interstitial or intertubular tissue of adult bovine testis consists of Leydig cells, macrophages, scattered lymphocytes and plasma cells, and contains numerous blood and lymph vessels. Not all Leydig cells have contact to blood or lymph capillaries.

The excurrent duct system of the adult bovine testis consists of terminal segment of the convoluted seminiferous tubules, straight tubules, and rete testis. The terminal segment can be further subdivided into a proximal (transitional) region, middle portion, and distal part (terminal plug). The proximal region is lined by typical Sertoli cells while the last two parts are lined by modified Sertoli cells. The tubulus rectus of adult bovine testis is composed of

three morphologically different regions: a proximal cup-shaped region, a middle narrow stalk, and a distal festooned portion. The rete testis is a complicated centrally positioned meshwork of intercommunicating channels that lies within the mediastinum testis parallel to the long axis of epididymis. The simple cuboidal epithelium of straight tubules and rete testis is shown to contain some lymphocytes and macrophages.

The cellular distribution of glycoconjugates within the fetal and adult bovine testis was investigated using thirteen (ConA, PSA, LCA, PNA, GSA-I, ECA, DBA, SBA, HPA, VVA, WGA, UEA-I, LTA) different fluorescein isothiocyanate (FITC) conjugated lectins. In fetal testes, detection of sugar moieties by lectins was carried out on Bouin's-fixed paraffin-embedded sections while in adult it was performed on both Bouin's-fixed paraffin-embedded and acetone-fixed frozen sections. Only five lectins (PSA, PNA, GSA-I, DBA, WGA) showed a positive reaction in the embryonic testes. PNA, GSA-I, DBA, and WGA were detected in the germ cells whereas PSA, DBA and WGA labeled the fetal Leydig cells. None of the lectins used was observed in the pre-Sertoli cells. Further on, some lectins were seen in tunica albuginea (PSA, PNA, GSA-I, WGA), basal lamina of testicular cords (PSA, WGA), interstitial blood vessels (PSA, GSA-I, WGA), mediastinum testis (PSA, PNA, WGA) and rete testis epithelium (PNA). In adult animals, spermatogonia and spermatocytes were positively stained with PSA, LCA, DBA, SBA, and VVA. All the lectins investigated except that of the fucose-binding lectin (UEA-I and LTA) were definitely detected in the acrosome of round and elongated spermatids. These results indicate a role for carbohydrates in spermiogenesis. Apical Sertoli cells processes and Leydig cells were weakly stained with PSA and LCA as well. DBA binding sites were also seen in the Leydig cells.

Immunohistochemical studies were performed using the Avidin-Biotin-Peroxidase Complex (ABC) method for localization of fibroblast growth factor-1 (FGF-1), fibroblast growth factor-2 (FGF-2), S-100, laminin, alpha-smooth muscle actin (α-SMA), vascular endothelial growth factor (VEGF), connexin 43 (Cx43), CD4, CD8, CD68, angiotensin-converting enzyme (ACE), and galactosyltransferase (GalTase) in the bovine testis. The expression of FGF-1 and FGF-2 was further investigated in the adult bovine testis using in situ hybridization and PCR. Immunohistochemically, FGF-1 was seen in the Sertoli cells, Leydig cells, endothelium of the blood vessels, and epithelium of straight tubules and rete testis of fetal and adult testis. It was additionally detected in spermatogonia and spermatids of sexual mature animals. FGF-2 exhibited a striking positive reaction in fetal (from 6 to 30 cm CRL)

and adult Leydig cells. Moreover, it showed marked reaction in the endothelium of blood vessels and in the epithelium of tubulus rectus and rete testis. FGF-2 was also localized in some spermatogonia, and myofibroblasts. By means of in situ hybridization, FGF-1 and FGF-2 mRNA were found in Leydig and Sertoli cells as well as in the modified Sertoli cells of the terminal segment. FGF-1 transcripts were additionally recognized in the straight tubules and rete testis epithelium. Distinct S100 immunostaining was observed in the Sertoli cells, endothelium of blood vessels and in the rete testis epithelium of fetal and adult testis. Laminin was localized to the basal lamina of seminiferous tubules, blood vessels, myofibroblasts, and rete testis. Although α-SMA was detected in smooth muscle cells of the blood vessels, no immunoreactivity was seen in the peritubular cells during the whole gestation period. The myofibroblasts surrounding the seminiferous tubules and rete testis showed intense positive reaction for α-SMA in the adult testis. VEGF was detected in the acrosomes of the elongating spermatids. Connexin 43 was localized to gap junctions between Leydig cells in the fetal and adult life as well as to the seminiferous epithelium apical to spermatogonia and basal to spermatocytes, a position correlating with Sertoli-Sertoli cell junctions. The detection of cells positive for CD4, CD8, CD68 within the adult testis interstitium clearly indicate the presence of lymphocytes and macrophages within this testicular compartment. GalTase showed striking positive reaction in the Golgi complex of Sertoli cells, Leydig cells, and some spermatocytes as well as at the cell membrane of elongating spermatids and in the simple cuboidal epithelium of rete testis. ACE positive reaction was found in the prespermatogonia (only at 6-10 cm CRL) and in fetal and adult testicular blood vessels. The functional significance of these immunocytochemically-demonstrated proteins is discussed.

7. ZUSAMMENFASSUNG

Morphologische, glykohistochemische und immunohistochemische Studien am fetalen und geschlechtsreifen Hoden des Rindes (*Bos taurus*)

In der vorliegenden Arbeit wurden die Hoden 32 fetaler Rinder underschiedlicher Scheitel-Steiß-Längen (SSL 2.5-90 cm) und von 15 geschlechtsreifen, klinisch gesunden Rindern (Deutsches Fleckvieh) mit licht-und elektronmikroskopischen sowie glykohistochemischen und immunohistochemischen Methoden untersucht. In Abhängigkeit von der SSL wurde die Trächtigkeit in drei (Früh-, Mittel-, und Spätgestationsperiode) Phasen unterteilt.

Bei den jüngsten der untersuchten Embryonen (2.5 cm SSL/43 Tage P.c.) erscheint die Hodenanlage als eine in die Zölomhöhle vorspringende, beidseits medial der Urniere gelegene, bohnenförmige Struktur. Sie besteht aus soliden Hodensträngen zwischen einem noch wenig differenziertem Interstitium. Die Tunica albuginea erfährt kurze Zeit später eine deutliche Differenzierung und ihre Schichtdicke nimmt zu. Mit 3.5 cm SSL können in den Hodensträngen zwei unterschiedliche Zelltypen unterschieden werden: große, rundliche Präspermatogonien und etwas kleinere, polymorphe Zellen, die Vorläufer der Sertoli-Zellen. Die Samenkanälchen verlaufen vom Rete testis, mit dem sie ab der Entstehung der Hodenstränge verbunden sind, gestreckt zur Peripherie der Gonade. Dort werden sie breiter und knäulen sich auf. Die Zahl der großen Keimzellen nimmt zwischen 3.5 cm SSLund 14 cm SSL deutlich zu. Das Maximum der pränatalen Keimzellbildung wird mit einer SSL von 14 cm erreicht. Die meisten Keimzellen sind nun in der Tubulusperipherie lokalisiert. Prä-Sertoli-Zellen sind insgesamt unregelmäßig geformt, sehr zahlreich und wesentlich kleiner als die Keimzellen. Während des gesamten Fetallebens teilen sie sich mitotisch und stellen den Hauptteil der Tubuluszellen dar.

Mit zunehmendem fetalen Alter dehnt sich auch das Interstitium stark aus. Dies ist vor allem auf eine Zunahme der Leydig-Zellen zurückzuführen. In der vorliegenden Arbeit sind die fetalen Leydig-Zellen des Rindes erstmals ab 3.5 cm SSL erkennbar. Sie treten hauptsächlich in Form von Zellclustern auf. Ein erstes Maximum der Differenzierung der Leydig-Zellen wird bei Feten mit einer SSL von 14 cm (ca. 80 Tag p.c.) erreicht. Diese erste Generation von Leydig-Zellen wird jedoch zum Geburtstermin hin immer mehr zurückgebildet. Ab einer SSL von 10 cm treten die Keimstränge über gerade verlaufende Anschlußstücke mit dem Rete testis in Verbindung.

Der Aufbau des Hodens von geschlechtsreifen Rindern gleicht in vielen Aspekten dem der anderen Haussäugetiere. Er wird von einer Tunica albuginea umschlossen, die außen von einer Serosa umgeben wird. Die Tunica albuginea stellt eine bindegewebige Organkapsel dar, die überwiegend aus straffen kollagenen Fasern und wenigen elastischen Fasern besteht. Die Tubuli seminiferi contorti stellen sich als gewundene Kanälchen dar. Sie setzen sich aus der Membrana propria, den Sertolizellen und der Keimzellpopulation zusammen. Die Membrana propria ist die äußere Umhüllung des Keimepithels. Sie besteht aus einer Basallamina, sowie aus einer Schicht kollagener und elastischer Fasern, an die sich peritubuläre Zellen (Myofibroblasten) anlagern. Das Keimepithel wird von Sertoli- und Keimzellen gebildet. Die Sertoli-Zellen weisen eine typische, mit anderen Spezies vergleichbare Form auf. Morphologische Kritieren für eine Unterscheidung von Subtypen, wie sie in anderen Untersuchungen beschrieben werden, konnte ich nicht beobachten. Der Keimepithelzyklus des Rinds wurde, wie auch bei anderen Spezies üblich, anhand der Kernmorphologie der Keimzellen sowie anhand ihrer Lage im Keimepithel eingeteilt. Dabei können acht verschiedene Phasen differenziert werden.

Das intertubuläre Stroma des Rinderhodens besteht vor allem aus Leydig-Zellen und Makrophagen sowie vereinzelten Lymphozyten und Plasmazellen. Weiter enthält das Interstitium zahlreiche Blut- und Lymphgefäße. Leydig-Zellen liegen in Strängen oder kleinen Aggregaten zwischen den Tubuli seminiferi. Nicht jede Leydig-Zelle grenzt dabei an eine Blut-oder Lymphkapillare. Am Ausführungangsystem des geschlechtsreifen Bullen lassen sich drei Bestandteile (Terminalsegment, Tubulus rectus, und Rete testis) unterscheiden. Dabei kann das Terminalsegment ebenfalls in drei Abschnitte, nämlich in die Übergangsregion, in den Mittelabschnitt und in den terminalen Pfropf, eingeteilt werden. Während in der Übergangsregion normale Sertoli-Zellen der Basalmembran senkrecht aufsitzen, werden der Mittelabschnitt und der terminale Pfropf von modifizierten Sertoli-Zellen gebildet. Jedes Terminalsegment wird von einem Gefäßplexus manschettenartig umgeben. An den Tubulus seminiferus schließt sich der Tubulus rectus an. Der Tubulus rectus beginnt mit einer kelchartigen Erweiterung, die den terminalen Pfropf umfasst. Er verjüngt sich dann zum engen, glattwandigen Kelchstiel. Retewärts vom Kelchstiel ist er durch die Ausbildung von intraepithelialen Invaginationen gekennzeichnet und mündet schließlich in das Rete testis.

Das Rete testis befindet sich eingebettet im Mediastinum in der Hodenachse und mündet in den Nebenhodenkopf. Extratestikuläre Rete-Anteile wurden nicht beobachtet. Das einschichtige Epithel von Tubulus rectus und Rete testis enthält teilweise zahlreiche freie

Zellen (Lymphozyten und Makrophagen). Im subepithelialen Stroma des Rete testis liegen flache kontraktile Zellen (Myofibroblasten) sowie reichlich elastische Fasern.

Mit 13 verschiedenen Fluoreszeinisothiocyanat (FITC)-markierten Lektinen (ConA, PSA, LCA, PNA, GSA-I, ECA, DBA, SBA, HPA, VVA, WGA, UEA-I, LTA) wurde die Topographie von Kohlenhydratstrukturen im Hoden untersucht. Diese FITC- markierten Lektine wurden an Bouin-Lösung fixierten Proben von fetalen Rindernhoden und an Aceton fixierten Gefrierschnitten sowie an Bouin-Lösung fixierten Proben aus adulten Hoden eingesetzt. Für fünf FITC- markierte Lektine (PSA, PNA, GSA-I, DBA, WGA) konnten nur im fetalen Hoden Bindungstellen nachgewiesen werden. Keimzellen reagierten mit PNA, GSA, DBA, und WGA, wohingegen Leydig-Zellen Bindungsstellen für PSA, DBA, und WGA aufwiesen.

Bei geschlechtsreifen Bullen war eine Reaktion der Spermatogonien und der Spermatozyten mit PSA, LCA, DBA, SBA und VVA erkennbar. Akrosomen von sich differenzierenden Spermatiden färbten sich mit Ausnahme von UEA-I und LTA mit allen Lektinen deutlich an. Zudem wurden PSA- und LCA-Bindungsstellen in Sertolizellen und Leydigzellen und DBA-Bindung in Leydig-Zellen nachgewiesen.

Immunohistochemische Untersuchungen mit der "Avidin-Biotin-Complex" Methode wurden zur Lokalisation von FGF-1, FGF-2, S-100, Laminin, α-SMA, VEGF, Connexin 43, CD4, CD8, CD68, ACE, und von GalTase im Hoden eingesetzt. Außerdem wurde die Expression der mRNA von FGF-1 und FGF-2 mittels in situ Hybridisierung und PCR im adulten Hoden untersucht. Beim immunohistochemischen Nachweis von FGF-1 im fetalen Hoden des Rindes ergab sich eine positive Immunoreaktivität in den Prä-Sertoli-Zellen, in den Leydig-Zellen sowie im Endothel der Blutgefäße und im Epithel der Tubuli recti und im Rete testis. Zusätzlich konnte immunhistochemisch eine deutliche Reaktion mit FGF-1-Antikörpern in Spermatogonien und Spermatiden geschlechtsreifer Tiere nachgewiesen werden. FGF-2 Antikörper hingegen reagierte mit fetalen Leydig-Zellen (von 6 bis 30 cm SSL), mit dem Endothel der Blutgefäße (ab 63 cm SSL) sowie in den Tubuli recti und im Epithel des Rete testis (ab 36 cm SSL). Im adulten Hoden kam FGF-2 in Spermatogonien, in Leydig-Zellen und in Myofibroblasten vor. Mit in situ Hybridisierung waren FGF-1 und FGF-2 mRNA in den Sertoli- und Leydig-Zellen sowie in den modifizierten Sertoli-Zellen der terminalen Pfropfes nachweisbar. Eine intensive S100 Immunfärbung wurde in Sertoli-Zellen, im Endothel der Blutgefäße und im Reteepithel fetaler und geschlechtsreifer Hoden beobachtet. Laminin zeigte eine positive Reaktion mit der Basallamina der Tubuli seminiferi contorti und

mit der Basallamina der Blutgefäße und der peritubulären Muskelzellen (Myofibroblasten). Eine deutliche Immunreaktivität auf α-SMA war in den glatten Muskelzellen der fetalen Blutgefäße nachweisbar, während in den peritubulären Zellen bei allen untersuchten Stadien keine Reaktion für α-SMA festgestellt werden konnte. Im Gegensatz dazu zeigten die Muskelzellen (Myofibroblasten) der Tubuli seminiferi contorti und des Rete testis im adulten Hoden eine intensive Immunreaktion mit α-SMA-Antikörpern. VEGF Immunreaktivität wurde nur in den elongierende Spermatiden beobachtet. Gap junctions zwischen Leydig-Zellen waren durch eine deutliche Immunfärbung mit Connexin 43-Antikörper darstellbar. Auch das Epithel der Tubuli seminiferi contorti in Höhe der Sertoli-Sertoli Zellverbindung stellte sich in dieser Untersuchung positiv dar. Im Interstitium traten Zellen auf, die mit CD4, CD8, und CD68 eine positive Immunreaktion zeigten. Die GalTase reagierte jeweils in der Golgi-Zone der Sertoli-Zellen, der Leydig-Zellen, einiger Spermatozyten und des Rete testis sowie an der Oberfläche der elongierenden Spermatiden und des Rete testis. ACE wurde außer im Gefäßendothel noch in den Präspermatogonien (nur bei 6-10 cm SSL) nachgewiesen.

8. REFERENCES

Abd-Elmaksoud A, Sinowatz F (2005).
Expression and localization of growth factors and their receptors in the mammalian testis. Review/Part I.
Anat. Histol. Embryol. In press.

Abdel-Raouf M (1960).
The postnatal development of the reproductive organs in bulls with special reference to puberty (incluing growth of the hypophysis and the adrenals).
Acta Endocrinol (Copenh). 34 (Suppl 49):1-109.

Ackermann MR, DeBey BM, Stabel TJ, Gold JH, Register KB, Meehan JT (1994).
Distribution of anti-CD68 (EBM11) immunoreactivity in formalin-fixed, paraffin-embedded bovine tissues.
Vet. Pathol. 31: 340-8.

Akama TO, Nakagawa H, Sugihara K, Narisawa S, Ohyama C, Nishimura S, O'Brien DA, Moremen KW, Millan JL, Fukuda MN (2002).
Germ cell survival through carbohydrate-mediated interaction with Sertoli cells.
Science 295: 124-7.

Allison RT (1987).
The effects of various fixations on subsequent lectin binding to tissue sections.
J. Histochem. 19: 65-74

Amselgruber W, Sinowatz F, Schams D, Lehmann M (1992).
S-100 protein immunoreactivity in bovine testis.
Andrologia 24: 231-5.

Amselgruber WM, Sinowatz F, Erhard M (1994).
Differential distribution of immunoreactive S-100 protein in mammalian testis.
Histochemistry 102: 241-5.

Anand RJ, Paust HJ, Altenpohl K, Mukhopadhyay AK (2003).
Regulation of vascular endothelial growth factor production by Leydig cells in vitro: the role of protein kinase A and mitogen-activated protein kinase cascade.
Biol Reprod. 68: 1663-73.

Anthony CT, Rosselli M, Skinner MK (1991).
Actions of the testicular paracrine factor (P-Mod-S) on Sertoli cell transferrin secretion throughout pubertal development.
Endocrinology 129: 353-60.

Anton H (1987).
Vergleichende Untersuchungen über die Entwicklung des Rete testis und Rete ovarii beim Rind (*Bos primigenius taurus f. taurus*).
Thesis, Institute of Veterinary Anatomy II, Faculty of Veterinary Medicine, LMU ,Munich, Germany

Arenas MI, Madrid JF, Bethencourt FR, Fraile B, Paniagua R (1998).
Lectin histochemistry of the human testis.
Int. J. Androl. 21: 332-342

Arnaud E, Touriol C, Boutonnet C, Gensac MC, Vagner S, Prats H, Prats AC (1999).
A new 34-kilodalton isoform of human fibroblast growth factor 2 is cap dependently synthesized by using a non-AUG start codon and behaves as a survival factor.
Mol. Cell Biol. 19: 505-14.

Arya M, Vanha-perttula T (1984).
Distribution of lectin-binding in rat testis and epididymis.
Andrologia 16: 495-508

Arya M, Vanha-perttula T (1985).
Lectin binding pattern of bull testis and epididymis.
J. Androl. 6: 230-242

Arya M, Vanha-perttula T (1986).
Comparison of lectin-staining pattern in testis and epididymis of gerbil, guinea pig, mouse, and nutria.
Am. J. Anat. 175: 449-469

Ashwell G, Morell AG (1977).
Membrane glycoproteins and recognition phenomena.
Trends Biochem. Sci. 2: 76-78

Ball BA, Gravance CG, Wessel MT, Sabeur K (2003).
Activity of angiotensin-converting enzyme (ACE) in reproductive tissues of the stallion and effects of angiotensin II on sperm motility.
Theriogenology 59: 901-14.

Ballesta J, Martinez-Menarguez JA, Pastor LM, Aviles M, Madrid JF, Castells MT (1991).
Lectin binding pattern in the testes of several tetrapode vertebrates.
Eur. J. Basic Appl. Histochem. 35:107-17.

Bardin CW, Cheng CY, Mustow NA, Gunsalus GL (1994).
The Sertoli cells. In: Knobil E, Neill JD (eds.), The Physiology of Reproduction, 2nd ed. New York: Raven Press, 1291-1334.

Barker SG, Kendall MD (1984).
A study of the rete testis epithelium in several wild birds.
J. Anat. 138: 139-52.

Batias C, Defamie N, Lablack A, Thepot D, Fenichel P, Segretain D, Pointis G (1999).
Modified expression of testicular gap-junction connexin 43 during normal spermatogenic cycle and in altered spermatogenesis.
Cell Tissue Res. 298: 113-21.

Benazzi C, Sarli G, Preziosi R, Marcato PS (1995).
Laminin expression in testicular tumours of the dog.
J. Comp. Pathol. 112: 141-50.

Bergh A (1985).
Effect of cryptorchidism on the morphology of testicular macrophages: evidence for a Leydig cell-macrophage interaction in the rat testis.
Int. J. Androl. 8: 86-96.

Bergh A, Damber JE, van Rooijen N (1993).
Liposome-mediated macrophage depletion: an experimental approach to study the role of testicular macrophages in the rat.
J. Endocrinol. 136: 407-13.

Berndtson WE, Igboeli G, Pickett BW (1987).
Relationship of absolute numbers of Sertoli cells to testicular size and spermatogenesis in young beef bulls.
J. Anim. Sci. 64: 241-6.

Berthold, R.D (1849).
Transplantation der Hoden.
Arch. Anat. physiol. u. wissensch. Med. 42-46

Bikfalvi A, Klein S, Pintucci G, Rifkin DB (1997).
Biological roles of fibroblast growth factor-2.
Endocr. Rev. 18: 26-45.

Blackmore PF, Eisoldt S (1999).
The neoglycoprotein mannose-bovine serum albumin, but not progesterone, activates T-type calcium channels in human spermatozoa.
Mol. Hum. Reprod. 5: 498-506.

Bloom W, Fawcett DW (1986).
Male reproductive system. In: A Textbook of Histology. 11th ed. W.B. Saunders Company, Philadelphia, London, Toronto, 796-835.

Bock E (1978).
Nervous system specific proteins.
J. Neurochem. 30: 7-14.

Böck P, Breitenecker G, Lunglmayr G (1972).
Contractile fibroblasts (myofibroblasts) in the lamina propria of human seminiferous tubules.
Z. Zellforsch. Mikrosk. Anat. 133: 519-27.

Boyed WC, Shapleigh E (1954).
Antigenic relations of blood group antigens as suggested by testes with lectins.
J. Immunol.73: 226-231

Bravo-Moreno JF, Diaz-Sanchez V, Montoya-Flores JG, Lamoyi E, Saez JC, Perez-Armendariz EM (2001).
Expression of connexin 43 in mouse Leydig, Sertoli, and germinal cells at different stages of postnatal development.
Anat. Rec. 264: 13-24.

Brehm R, Mark A, Rey R, Kliesch S, Bergmann M, Steger K (2002).
Altered expression of connexins 26 and 43 in Sertoli cells in seminiferous tubules infiltrated with carcinoma-in-situ or seminoma.
J. Pathol. 197: 647-53.

Brennan J, Capel B (2004).
One tissue, two fates: molecular genetic events that underlie testis versus ovary development.
Nat. Rev. Genet. 5: 509-21.

Brennan J, Karl J, Capel B (2002).
Divergent vascular mechanisms downstream of Sry establish the arterial system in the XY gonad.
Dev. Biol. 244: 418-28.

Brennan J, Karl J, Martineau J, Nordqvist K, Schmahl J, Tilmann C, Ung K, Capel B (1998).
Sry and the testis: molecular pathways of organogenesis.
J. Exp. Zool. 281: 494-500.

Bukovsky M, Koscova H, Dubnickova M, Sirotkova L (2001).
Comparative study of disintegrated cells influence of Staphylococcus aureus, Escherichia coli and Candida albicans on human and mouse immune mechanisms.
Bratisl. Lek. Listy. 102: 314-7.

Burgos MH, Cavicchia JC, Einer-Jensen N (1979).
Electron microscopy (SEM and TEM) of the rete testis in the monkey.
Int. J. And. 2: 559-571

Burgos M H, Vitale-Calpe R, Aoki A (1970).
Fine structure of the testis and its functional significance. In: Johnson AD, Gomes WR, Vandemark NL (Eds). The testis. Academic Press. New York. London. pp. 451- 649.

Bustin SA (2000).
Absolute quantification of mRNA using real-time reverse transcription polymerase chain reaction assays.
J. Mol. Endocrinol. 25: 169-93.

Bustos-Obregon E (1976).
Ultrastructure and function of the lamina propria of mammalian seminiferous tubules.
Andrologia 8: 179-85.

Bustos-Obregon E, Courot M (1974).
Ultrastructure of the lamina propria in the ovine seminiferous tubule. Development and some endocrine considerations.
Cell Tissue Res. 150: 481-92.

Byskov AG (1986).
Differentiation of mammalian embryonic gonad.
Physiol. Rev. 66: 71-117.

Byskov AG, Hoyer PE (1994).
Embryology of mammalian gonads and ducts. In: Knobil E, Neill JD (eds.), The Physiology of Reproduction, 2nd ed. New York: Raven Press; 1994: 487-540.

Cancilla B, Davies A, Ford-Perriss M, Risbridger GP (2000).
Discrete cell- and stage-specific localisation of fibroblast growth factors and receptor expression during testis development.
J. Endocrinol. 164: 149-59.

Cancilla B, Risbridger GP (1998).
Differential localization of fibroblast growth factor receptor-1, -2, -3, and -4 in fetal, immature, and adult rat testes.
Biol. Reprod. 58:1138-45.

Capel B (2000).
The battle of the sexes.
Mech. Dev. 92: 89-103.

Capel B, Albrecht KH, Washburn LL, Eicher EM (1999).
Migration of mesonephric cells into the mammalian gonad depends on Sry.
Mech. Dev. 84: 127-31.

Cavola A, Pastor LM, Bonet S, Pinart E, Ventura M (2000).
Characterization of the glycoconjugates of boar testis and epididymis.
J. Reprod. Fert. 120: 325-335

Christl HW (1990).
The lamina propria of vertebrate seminiferous tubules: a comparative light and electron microscopic investigation.
Andrologia 22: 85-94.

Chung KW (1974).
Fine structure of Sertoli cells and myoid cells in mice with testicular feminization.
Fertil. Steril. 25: 325-35.

Cohen PE, Chisholm O, Arceci RJ, Stanley ER, Pollard JW (1996).
Absence of colony-stimulating factor-1 in osteopetrotic (csfmop/csfmop) mice results in male fertility defects.
Biol. Reprod. 55: 310-7.

Cruzana BC, Hondo E, Kitamura N, Matsuzaki S, Nakagawa M, Yamada J (2000).
Differential localization of immunoreactive alpha- and beta-subunits of S-100 protein in feline testis.
Anat. Histol. Embryol. 29: 83-6.

Cruzana MB, Budipitojo T, De Ocampo G, Sasaki M, Kitamura N, Yamada J (2003).
Immunohistochemical distribution of S-100 protein and subunits (S100-alpha and S100-beta) in the swamp-type water buffalo (*Bubalus bubalis*) testis.
Andrologia 35: 142-5.

Czykier E, Sawicki B, Zabel M (1999).
Immunocytochemical localization of S-100 protein in the European bison testis and epididymis.
Folia Histochem. Cytobiol. 37: 83-4.

Damjanov I (1987).
Biology of diseases. Lectin cytochemistry and histochemistry.
Lab. Invest. 57: 5-20

Davidoff MS, Breucker H, Holstein AF, Seidl K (1990).
Cellular architecture of the lamina propria of human seminiferous tubules.
Cell Tissue Res. 262: 253-61.

de Kretser DM, Kerr JB (1994).
The cytology of the testis. In: Knobil E, Neill JD (eds.), The Physiology of Reproduction, 2nd ed. New York: Raven Press, 1177-1290.

Decrouy X, Gasc JM, Pointis G, Segretain D (2004).
Functional characterization of Cx43 based gap junctions during spermatogenesis.
J. Cell Physiol. 200: 146-54.

Defamie N, Mograbi B, Roger C, Cronier L, Malassine A, Brucker-Davis F, Fenichel P, Segretain D, Pointis G (2001).
Disruption of gap junctional intercellular communication by lindane is associated with aberrant localization of connexin 43 and zonula occludens-1 in 42GPA9 Sertoli cells.
Carcinogenesis 22:1537-42.

Defamie N, Berthaut I, Mograbi B, Chevallier D, Dadoune JP, Fenichel P, Segretain D, Pointis G (2003).
Impaired gap junction connexin 43 in Sertoli cells of patients with secretory azoospermia: a marker of undifferentiated Sertoli cells.
Lab. Invest. 83: 449-56.

Dell A, Morris HR, Easton RL, Patankar M, Clark GF (1999).
The glycobiology of gametes and fertilization.

Biochim. Biophys. Acta 1473: 196-205.

Denduchis B, Schteingart H, Cigorraga S, Vianello SE, Casanova MB, Lustig L (1996).
Immunodetection of cell adhesion molecules and extracellular matrix proteins in rat Leydig cell cultures.
Int. J. Androl. 19: 353-61.

Desjardins C (1993).
Design and function of the microcirculation. In: Desjardins C, Ewing LL (Eds). Cell and Molecular Biology of the Testis. Oxfor. Uni. Press, Oxford.

Donato R (1986).
S-100 proteins.
Cell Calcium 7: 123-45.

Donato R (1999).
Functional roles of S100 proteins, calcium-binding proteins of the EF-hand type.
Biochim. Biophys. Acta 1450: 191-231.

Donato R (2001).
S100: a multigenic family of calcium-modulated proteins of the EF-hand type with intracellular and extracellular functional roles.
Int. J. Biochem. Cell Biol. 33: 637-68.

Duffy HS, Sorgen PL, Girvin ME, O'Donnell P, Coombs W, Taffet SM, Delmar M, Spray DC (2002).
pH-dependent intramolecular binding and structure involving Cx43 cytoplasmic domains.
J. Biol. Chem. 277: 36706-14.

Dulaney JT (1979).
Binding interactions of glycoproteins with lectins.
Mol. Cell Biochem. 21: 43-61

Dyce KM, Sack WO, Wensing CJG (1987).
The pelvis and reproductive organs of the male ruminants. In: Textbook of Veterinary Anatomy. W.B. Saunders Company, Philadelphia, London, Toronto, Montreal, Sydney, Tokyo, 678-686.

Dym M (1973).
The fine structure of the monkey (Macaca) Sertoli cell and its role in maintaining the blood-testis barrier.
Anat. Rec. 175: 639-56.

Dym M (1974).
The fine structure of monkey Sertoli cells in the transitional zone at the junction of the seminiferous tubules with the tubuli recti.
Am. J. Anat. 140: 1-25.

Dym M (1976).
The mammalian rete testis-a morphological examination.
Anat. Rec. 186: 493-523.

Dym M (1994).
Basement membrane regulation of Sertoli cells.
Endocr. Rev. 15: 102-15.

Dym M, Fawcett DW (1970).
The blood-testis barrier in the rat and the physiological compartmentation of the seminiferous

epithelium.
Biol. Reprod. 3: 308-26.

Eicher EM, Shown EP, Washburn LL (1995).
Sex reversal in C57BL/6J-YPOS mice corrected by a Sry transgene.
Philos. Trans. R. Soc. Lond. B. Biol. Sci. 350: 263-169.

Ekstedt E, Soderquist L, Ploen L (1986).
Fine structure of spermatogenesis and Sertoli cells (*Epitheliocytus sustentans*) in the bull.
Anat. Histol. Embryol. 15: 23-48.

El Ouali H, Leheup BP, Gelly JL, Grignon G (1991).
Laminin ultrastructural immunolocalization in rat testis during ontogenesis.
Histochemistry 95: 241-6.

El-Demiry M, James K (1988).
Lymphocyte subsets and macrophages in the male genital tract in health and disease. A monoclonal antibody-based study.
Eur. Urol. 14: 226-35.

El-Demiry MI, Hargreave TB, Busuttil A, Elton R, James K, Chisholm GD (1987).
Immunocompetent cells in human testis in health and disease.
Fertil. Steril. 48: 470-9.

Enders GC, Kahsai TZ, Lian G, Funabiki K, Killen PD, Hudson BG (1995).
Developmental changes in seminiferous tubule extracellular matrix components of the mouse testis: alpha 3(IV) collagen chain expressed at the initiation of spermatogenesis.
Biol. Reprod. 53: 1489-99.

Engvall E (1995).
Structure and function of basement membranes.
Int. J. Dev. Biol. 39: 781-7.

Ergun S, Kilic N, Fiedler W, Mukhopadhyay AK (1997).
Vascular endothelial growth factor and its receptors in normal human testicular tissue.
Mol. Cell Endocrinol. 131: 9-20.

Erickson AC, Couchman JR (2000).
Still more complexity in mammalian basement membranes.
J. Histochem. Cytochem. 48: 1291-306.

Ertl C, Wrobel KH (1992).
Distribution of sugar residues in the bovine testis during postnatal ontogenesis demonstrated with lectin-horseradish peroxidase conjugates.
Histochemistry 97: 161-71.

Esther CR Jr, Howard TE, Marino EM, Goddard JM, Capecchi MR, Bernstein KE (1996).
Mice lacking angiotensin-converting enzyme have low blood pressure, renal pathology, and reduced male fertility.
Lab. Invest. 74: 953-65.

Esther CR, Marino EM, Howard TE, Machaud A, Corvol P, Capecchi MR, Bernstein KE (1997).
The critical role of tissue angiotensin-converting enzyme as revealed by gene targeting in mice.
J. Clin. Invest. 99: 2375-85.

Ezeasor DN (1986).
Ultrastructural observations on the terminal segment epithelium of the seminiferous tubule of West African dwarf goats.
 J. Anat. 144: 167-79.

Faraggiana T, Malchiodi F, Prado A, Churg J (1982).
Lectin peroxidase conjugates reactivity in normal human kidney.
J.Histochem. Cytochem. 30: 451-458

Fauser BC, Baird A, Hsueh AJ (1988).
Fibroblast growth factor inhibits luteinizing hormone-stimulated androgen production by cultured rat testicular cells.
Endocrinology 123: 2935-41

Fawcett DW (1975).
Observations on the organization of the interstitial tissue of the testis and on the occluding cell junctions in the seminiferous epithelium.
Adv. Biosci. 10: 83-99.

Fawcett DW, Neaves WB, Flores MN (1973).
Comparative observations on intertubular lymphatics and the organization of the interstitial tissue of the mammalian testis.
Biol. Reprod. 9: 500-32.

Fayrer-Hosken RA, Caudle AB, Shur BD (1991).
Galactosyltransferase activity is restricted to the plasma membranes of equine and bovine sperm.
Mol. Reprod. Dev. 28: 74-8.

Ferrara N (2004).
Vascular endothelial growth factor: basic science and clinical progress.
Endocr. Rev. 25: 581-611.

Fiorini C, Tilloy-Ellul A, Chevalier S, Charuel C, Pointis G (2004).
Sertoli cell junctional proteins as early targets for different classes of reproductive toxicants.
Reprod. Toxicol. 18: 413-21

Foresta C, Mioni R, Rossato M, Varotto A, Zorzi M (1991).
Evidence for the involvement of sperm angiotensin converting enzyme in fertilization.
Int. J. Androl. 14: 333-9.

Franke FE, Pauls K, Metzger R, Danilov SM (2003).
Angiotensin I-converting enzyme and potential substrates in human testis and testicular tumours.
APMIS. 111: 234-244

Freeman B (2003).
The active migration of germ cells in the embryos of mice and men is a myth.
Reproduction 125: 635-43.

Frojdman K, Ekblom P, Sorokin L, Yagi A, Pelliniemi LJ (1995).
Differential distribution of laminin chains in the development and sex differentiation of mouse internal genitalia.
Int. J. Dev. Biol. 39: 335-44.

Frojdman K, Miner JH, Sanes JR, Pelliniemi LJ, Virtanen I (1999).
Sex-specific localization of laminin alpha 5 chain in the differentiating rat testis and ovary.
Differentiation 64: 151-9.

Frungieri MB, Calandra RS, Lustig L, Meineke V, Kohn FM, Vogt HJ, Mayerhofer A (2002).
Number, distribution pattern, and identification of macrophages in the testes of infertile men.
Fertil. Steril. 78: 298-306.

Fujimoto T, Yoshinaga K, Kono I (1985).
Distribution of fibronectin on the migratory pathway of primordial germ cells in mice.
Anat. Rec. 211: 271-8.

Gabius HJ (2001).
Glycohistochemistry: the why and how of detection and localization of endogenous lectins.
Anat. Histol. Embryol. 30: 3-31.

Gabius HJ (1987).
Vertebrate lectins and their possible role in fertilization, development, and tumor biology.
In Vivo 1: 75-83.

Gallagher JT (1984).
Carbohydrate-binding properties of lectins: A possible approach to lectin nomenclature and classification.
Bios. Reports 4: 621-632

Garcia-Castro MI, Anderson R, Heasman J, Wylie C (1997).
Interactions between germ cells and extracellular matrix glycoproteins during migration and gonad assembly in the mouse embryo.
J. Cell Biol. 138: 471-80.

Gaskell TL, Esnal A, Robinson LL, Anderson RA, Saunders PT (2004).
Immunohistochemical profiling of germ cells within the human fetal testis: identification of three subpopulations.
Biol. Reprod. 71: 2012-21.

Gaytan F, Bellido C, Aguilar E, van Rooijen N (1994).
Requirement for testicular macrophages in Leydig cell proliferation and differentiation during prepubertal development in rats.
J. Reprod. Fertil. 102: 393-9.

Gelly JL, Richoux JP, Leheup BP, Grignon G (1989).
Immunolocalization of type IV collagen and laminin during rat gonadal morphogenesis and postnatal development of the testis and epididymis.
Histochemistry 93: 31-7.

George FW, Wilson JD (1994).
Sex determination and differentiation. In: Knobil E, Neill JD (eds.), The Physiology of Reproduction, 2nd ed. New York: Raven Press, 3-28.

Gerdprasert O, O'Bryan MK, Muir JA, Caldwell AM, Schlatt S, de Kretser DM, Hedger MP (2002).
The response of testicular leukocytes to lipopolysaccharide-induced inflammation: further evidence for heterogeneity of the testicular macrophage population.
Cell Tissue Res. 308: 277-85.

Gheri G, Vannelli GB, Marini M, Zappoli Thyrion GP, Sgambati E (2003).
Lectin binding in the human foetal testis.
Histol. Histopathol. 18: 735-40.

Gier HT, Marion GB (1970).
Development of the mammalian testis. In: Johnson AD, Gomes WR, Vandemark NL (Eds). The

testis. Vol I Ch.I. 1st ed. Academic press., New York, USA

Gilula NB, Fawcett DW, Aoki A (1976).
The Sertoli cell occluding junctions and gap junctions in mature and developing mammalian testis.
Dev. Biol. 50: 142-68.

Ginzinger DG (2002).
Gene quantification using real-time quantitative PCR: an emerging technology hits the mainstream.
Exp. Hematol. 30: 503-512.

Girod C, Durand N, Raccurt M (1986).
A comparative study of immunocytochemical localization of S-100 protein in the monkey (*Macaca irus*) and the albino rat testes.
Biomed. Res. 7: 333-337

Givol D, Yayon A (1992).
Complexity of FGF receptors: genetic basis for structural diversity and functional specificity.
FASEB J. 6: 3362-9.

Goldstein IJ, Hayes CE (1978).
The lectins: carbohydrate-binding proteins of plants and animals.
Adv. Carhydr. Chem. Biochem. 35: 127-340

Goldstein IJ, Poretz RD (1986).
Isolation, physicochemical characterization, and carbohydrate- binding specificity of Lectins. In: Liener IE, Sharon N, Goldstein IJ (Eds). The Lectins: properties, functions, and applications in biology and medicine. Acad. Press, New York, London. 35-244.

Goldstein IJ, Hughes RC, Monsigney M, Osawa T, Sharon N (1980).
What should be called a lectin?
Nature 285: 66.

Gondos B, Renston RH, Goldstein DA (1976).
Postnatal differentiation of Leydig cells in the rabbit testis.
Am. J. Anat. 145: 167-81.

Gondos B (1977).
Testicular development. In: Johnson AD, Gomes WR (Eds). Testis. Academic press, New York.

Gonzalez AM, Buscaglia M, Ong M, Baird A (1990).
Distribution of basic fibroblast growth factor in the 18-day rat fetus: localization in the basement membranes of diverse tissues.
J. Cell Biol. 110: 753-65.

Gospodarowicz D (1992).
Fibroblast growth factors. In Aggarwal BB, Gutterman UJ (Eds). Human cytokines (Handbook for basic and clinical research). Berlin: Blackwell Scientific Publications pp: 329-352

Gospodarowicz D, Ferrara N, Schweigerer L, Neufeld G (1987).
Structural characterization and biological functions of fibroblast growth factor.
Endocr. Rev. 8: 95-114.

Gould SF, Bernstein MH (1975).
The localisation of bovine sperm hyaluronidase.
Differentiation 3: 123-32.

Goyal HO, Dhingra LD (1973).
Postnatal study on the histology and histochemistry of mediastinum testis in buffalo (*Bubalus bubalis*) from birth to one year.
Acta Anat. 86: 65-70.

Goyal HO, Williams CS (1987).
The rete testis of the goat, a morphological study.
Acta Anat. 130: 151-7.

Griswold MD (1995).
Interactions between germ cells and Sertoli cells in the testis.
Biol. Reprod. 52: 211-6.

Griswold MD (1998).
The central role of Sertoli cells in spermatogenesis.
Semin. Cell Dev. Biol. 9: 411-6.

Gubbay J, Collignon J, Koopman P, Capel B, Economou A, Munsterberg A, Vivian N, Goodfellow P, Lovell-Badge R (1990).
A gene mapping to the sex-determining region of the mouse Y chromosome is a member of a novel family of embryonically expressed genes.
Nature 346: 245-50.

Guler F, Bingol-Kologlu M, Yagmurlu A, Guven C, Hasirci N, Kucuk O, Aytac S, Dindar H (2004).
The effects of local and sustained release of fibroblast growth factor on testicular blood flow and morphology in spermatic artery-and vein-ligated rats.
J. Pediatr. Surg. 39: 709-716.

Gulkesen KH, Erdogru T, Sargin CF, Karpuzoglu G (2002).
Expression of extracellular matrix proteins and vimentin in testes of azoospermic man: an immunohistochemical and morphometric study.
Asian J. Androl. 4: 55-60.

Gutierrez M, Forster FI, McConnell SA, Cassidy JP, Pollock JM, Bryson DG (1999).
The detection of CD2+, CD4+, CD8+, and WC1+ T lymphocytes, B cells and macrophages in fixed and paraffin embedded bovine tissue using a range of antigen recovery and signal amplification techniques.
Vet. Immunol. Immunopathol. 71: 321-34.

Gutierrez-Adan A, Behboodi E, Murray JD, Anderson GB (1997).
Early transcription of the SRY gene by bovine preimplantation embryos.
Mol. Reprod. Dev. 48: 246-50.

Habert R, Lejeune H, Saez JM (2001).
Origin, differentiation, and regulation of fetal and adult Leydig cells.
Mol. Cell Endocrinol. 179: 47-74.

Hadley MA, Dym M (1987).
Immunocytochemistry of extracellular matrix in the lamina propria of the rat testis: electron microscopic localization.
Biol. Reprod. 37: 1283-9.

Hadley MA, Weeks BS, Kleinman HK, Dym M (1990).
Laminin promotes formation of cord-like structures by Sertoli cells in vitro.
Dev. Biol. 140: 318-27.

Hagaman JR, Moyer JS, Bachman ES, Sibony M, Magyar PL, Welch JE, Smithies O, Krege JH, O'Brien DA (1998).
Angiotensin-converting enzyme and male fertility.
Proc. Natl. Acad. Sci. U S A 95: 2552-7.

Haimoto H, Hosoda S, Kato K (1987).
Differential distribution of immunoreactive S100-alpha and S100-beta proteins in normal nonnervous human tissues.
Lab. Invest. 57: 489-98.

Hakomori S (1981).
Glycosphingolipids in cellular interaction, differentiation, and oncogenesis.
Annu. Rev. Biochem. 50: 733-64.

Hales DB (2002).
Testicular macrophage modulation of Leydig cell steroidogenesis.
J. Reprod. Immunol. 57: 3-18.

Hall PF (1994).
Testicular steroid synthesis: Organization and regulation. In: Knobil E, Neill JD (eds.), The Physiology of Reproduction, 2nd ed. New York: Raven Press, 1335-1362.

Hamilton DW (1980).
UDP-galactose: N-acetylglucosamine galactosyltransferase in fluids from rat rete testis and epididymis.
Biol. Reprod. 23: 377-85.

Han IS, Sylvester SR, Kim KH, Schelling ME, Venkateswaran S, Blanckaert VD, McGuinness MP, Griswold MD (1993).
Basic fibroblast growth factor is a testicular germ cell product which may regulate Sertoli cell function.
Mol. Endocrinol. 7: 889-97.

Harris AL (2001).
Emerging issues of connexin channels: biophysics fills the gap.
Q. Rev. Biophys. 34: 325-472.

Hayes R, Chalmers SA, Nikolic-Paterson DJ, Atkins RC, Hedger MP (1996).
Secretion of bioactive interleukin 1 by rat testicular macrophages in vitro.
J. Androl. 17: 41-9.

Hedger MP (1997).
Testicular leukocytes: what are they doing?
Rev. Reprod. 2: 38-47.

Hedger MP (2002).
Macrophages and the immune responsiveness of the testis.
J. Reprod. Immunol. 57: 19-34.

Hedger MP, Meinhardt A (2000).
Local regulation of T cell numbers and lymphocyte-inhibiting activity in the interstitial tissue of the adult rat testis.
J. Reprod. Immunol. 48: 69-80.

Hedger MP, Meinhardt A (2003).
Cytokines and the immune-testicular axis.
J. Reprod. Immunol. 58: 1-26.

Hedger MP, Wang J, Lan HY, Atkins RC, Wreford NG (1998).
Immunoregulatory activity in adult rat testicular interstitial fluid: relationship with intratesticular CD8$^+$ lymphocytes following treatment with ethane dimethane sulfonate and testosterone implants.
Biol. Reprod. 58: 935-42.

Hees H, Wrobel KH, Kohler T, Abou Elmagd A, Hees I (1989).
The mediastinum of the bovine testis.
Cell Tissue Res. 255: 29-39.

Hees H, Wrobel KH, Kohler T, Leiser R, Rothbacher I (1987).
Spatial topography of the excurrent duct system in the bovine testis.
Cell Tissue Res. 248: 143-51.

Heizmann CW, Cox JA (1998).
New perspectives on S100 proteins: a multi-functional Ca (2+)-, Zn (2+) - and Cu (2+)-binding protein family.
Biometals 11: 383-97.

Heizmann CW, Fritz G, Schafer BW (2002).
S100 proteins: structure, functions, and pathology.
Front. Biosci. 7: d1356-68.

Hennet T (2002).
The galactosyltransferase family.
Cell Mol. Life Sci. 59: 1081-95.

Hennet T, Ellies LG (1999).
The remodeling of glycoconjugates in mice.
Biochim. Biophys. Acta 1473: 123-36.

Hilscher W (1991).
The genetic control and germ cell kinetics of the female and male germ line in mammals including man.
Hum. Reprod. 6: 1416-25.

Hilscher W, Hilscher B (1976).
Kinetics of the male gametogenesis.
Andrologia 8: 105-16.

Holstein AF, Maekawa M, Nagano T, Davidoff MS (1996).
Myofibroblasts in the lamina propria of human seminiferous tubules are dynamic structures of heterogeneous phenotype.
Arch. Histol. Cytol. 59: 109-25.

Holt WV, Waller J, Moore A, Jepson PD, Deaville R, Bennett PM (2004).
Smooth muscle actin and vimentin as markers of testis development in the harbour porpoise (*Phocoena phocoena*).
J. Anat. 205: 201-11.

Hsieh HL, Schafer BW, Cox JA, Heizmann CW (2002).
S100A13 and S100A6 exhibit distinct translocation pathways in endothelial cells.
J. Cell Sci. 115: 3149-58.

Hsu, S.M., Raine, L, Fanger H (1981).
Use of avidin-biotin-peroxidase complex (ABC) in immunoperoxidase techniques: a comparison between ABC and unlabeled antibody (PAP) procedures.
J. Histochem. Cytochem. 29: 577-580.

Huminiecki L, Chan HY, Lui S, Poulsom R, Stamp G, Harris AL, Bicknell R (2001).
Vascular endothelial growth factor transgenic mice exhibit reduced male fertility and placental rejection.
Mol. Hum. Reprod. 7: 255-64

Hutson JC (1992).
Development of cytoplasmic digitations between Leydig cells and testicular macrophages of the rat.
Cell Tissue Res. 267: 385-9.

Hutson JC (1994).
Testicular macrophages.
Int. Rev. Cytol. 149: 99-143.

Iozzo RV (1998).
Matrix proteoglycans: from molecular design to cellular function.
Annu. Rev. Biochem. 67: 609-52.

Isobe T, Ishioka N, Kocha T, Okuyama T (1982).
In: Peeters H (eds), Protides of the biological fluids, vol 30. Pergamon Press, pp 21-24

Isoyama T, Sofikitis N (1999).
Factors inducing vascularization improve the spermatogenic and steroidogenic function of the varicocelized testis.
Yon. Acta Med. 42: 41-49

Itoh M, De Rooij DG, Jansen A, Drexhage HA (1995).
Phenotypical heterogeneity of testicular macrophages/dendritic cells in normal adult mice: an immunohistochemical study.
J. Reprod. Immunol. 28: 217-32.

Jaillard C, Chatelain PG and Saez JM. (1987).
In vitro regulation of pig Sertoli cell growth and function: effects of fibroblast growth factor and somatomedin-C.
Biol. Reprod. 37: 665-74.

Jegou B, Cudicini C, Gomez E, Stephan JP (1995).
Interleukin-1, interleukin-6, and the germ cell-Sertoli cell cross-talk.
Reprod. Fertil. Dev. 7: 723-30.

Jezek D, Schulze W, Rogatsch H, Hittmair A (1996).
Structure of small blood vessels in the testes of infertile men.
Int. J. Androl. 19: 299-306.

Johnson L, Nguyen HB. (1986).
Annual cycle of the Sertoli cell population in adult stallions.
J. Reprod. Fertil. 76: 311-6.

Jones CJ, Morrison CA, Stoddart RW (1993).
Histochemical analysis of rat testicular glycoconjugate. 3. Non-reducing terminal residues in seminiferous tubules.
Histochem. J. 25: 711-718

Jones CJ, Morrison CA, Stoddart RW (1992).
Histochemical analysis of rat testicular glycoconjugates. 2. Beta-galactosyl residues in O- and N-linked glycans in seminiferous tubules.
Histochem. J. 24: 327-36.

Jost A, Vigier B, Prepin J, Perchellet J (1973).
Studies on sex differentiation in mammals.
Recent Prog. Horm. Res. 29: 1–41.

Jurado SB, Kurohmaru M, Hayashi Y (1994).
An ultrastructural study of the Sertoli cell in the Shiba goat.
J. Vet. Med. Sci. 56: 33-8.

Kagi U, Chafouleas JG, Norman AW, Heizmann CW (1988).
Developmental appearance of the $Ca2^+$-binding proteins parvalbumin, calbindin D-28K, S-100 proteins and calmodulin during testicular development in the rat.
Cell Tissue Res. 252: 359-65.

Kamachi Y, Uchikawa M, Kondoh H (2000).
Pairing SOX off: with partners in the regulation of embryonic development.
Trends Genet. 16: 182-7.

Karl J, Capel B (1998).
Sertoli cells of the mouse testis originate from the coelomic epithelium.
Dev. Biol. 203: 323-33.

Karnovsky MJ (1965).
A formaldehyde-glutaraldehyde fixative of high osmolality for use in electron microscopy.
J. Cell Biol. 27: 137A-138A

Kaufman MH (1992).
Atlas of the development of the mouse. Academic Press, San Diego, London

Kaye PM (1995).
Costimulation and the regulation of antimicrobial immunity.
Immunol. Today 16: 423-7.

Kern S, Robertson SA, Mau VJ, Maddocks S (1995).
Cytokine secretion by macrophages in the rat testis.
Biol. Reprod. 53: 1407-16.

Khalil IA, Hauser EH (1979).
Testis morphology and gonadotropin hormones binding in fetal calves. 71st Annual meeting of the American society of animal science. Tuscon, Arizona, USA.

Khan SA, Khan SJ, Dorrington JH (1992).
Interleukin-1 stimulates deoxyribonucleic acid synthesis in immature rat Leydig cells in vitro.
Endocrinology 131: 1853-7.

Kirby JL, Yang L, Labus JC, and Hinton BT (2003).
Characterization of fibroblast growth factor receptors expressed in principal cells in the initial segment of the rat epididymis.
Biol. Reprod. 68: 2314-21.

Kleinman HK, Cannon FB, Laurie GW, Hassell JR, Aumailley M, Terranova VP, Martin GR, DuBois-Dalcq M (1985).
Biological activities of laminin.
J. Cell Biochem. 27: 317-25.

Kocourek J, Horejsi V (1983).
A note of the recent discussion on definition of the term ″Lectin″. In: T.C. Bog Hansen and G.A

Spengler (Eds.). Lectins. Vol.3.De Guyter, Berlin, New York, 3-6

Kohn FM, Miska W, Schill WB (1995).
Release of angiotensin-converting enzyme (ACE) from human spermatozoa during capacitation and acrosome reaction.
J. Androl. 16: 259-65.

Kohn FM, Muller C, Drescher D, Neukamm C, el Mulla KF, Henkel R, Hagele W, Hinsch E, Habenicht UF, Schill WB (1998).
Effect of angiotensin converting enzyme (ACE) and angiotensins on human sperm functions.
Andrologia 30: 207-15.

Koike S, Noumura T (1994).
Cell- and stage-specific expression of basic FGF in the developing rat gonads.
Growth Regul. 4: 77-81.

Koopman P, Gubbay J, Vivian N, Goodfellow P, Lovell-Badge R (1991).
Male development of chromosomally female mice transgenic for Sry.
Nature 351: 117-21.

Kormano M (1967).
Dye permeability and alkaline phosphatase activity of testicular capillaries in the postnatal rat.
Histochemie 9: 327-38.

Korpelainen EI, Karkkainen MJ, Tenhunen A, Lakso M, Rauvala H, Vierula M, Parvinen M, Alitalo K (1998).
Overexpression of VEGF in testis and epididymis causes infertility in transgenic mice: evidence for nonendothelial targets for VEGF.
J. Cell Biol. 143: 1705-12.

Krege JH, John SW, Langenbach LL, Hodgin JB, Hagaman JR, Bachman ES, Jennette JC, O'Brien DA, Smithies O (1995).
Male-female differences in fertility and blood pressure in ACE-deficient mice.
Nature 375: 146-8.

Kudo T, Narimatsu H (1995).
The beta 1,4-galactosyltransferase gene is post-transcriptionally regulated during differentiation of mouse F9 teratocarcinoma cells.
Glycobiology 5: 397-403.

Kurohmaru M, Yamashiro S, Azmi TI, Basrur PK (1992).
An ultrastructural study of the Sertoli cell in the water buffalo (*Bubalus bubalis*).
Anat. Histol. Embryol. 21: 82-90.

Kurohmaru M (1991).
Lectin-binding patterns in the spermatogenic cells of the shiba goat testis.
J. Vet. Med. Sci. 53: 893-897

Lan ZJ, Labus JC, Hinton BT (1998).
Regulation of gamma-glutamyl transpeptidase catalytic activity and protein level in the initial segment of the rat epididymis by testicular factors: role of basic fibroblast growth factor.
Biol. Reprod. 58: 197-206.

Lander AD, Selleck SB (2000).
The elusive functions of proteoglycans: in vivo veritas.
J. Cell Biol. 148: 227-32.

Langford KG, Zhou Y, Russell LD, Wilcox JN, Bernstein KE (1993).
Regulated expression of testis angiotensin-converting enzyme during spermatogenesis in mice.
Biol. Reprod. 48: 1210-8.

Laslett AL, McFarlane JR, Risbridger GP (1997).
Developmental response by Leydig cells to acidic and basic fibroblast growth factor.
J. Steroid Biochem. Mol. Biol. 60: 171-9.

Leblond CP, Clermont Y (1952).
Definition of the stages of the cycle of the seminiferous epithelium in the rat.
Ann. N Y Acad. Sci. 55: 548-73.

Lee MC, Damjanov I (1984).
Anatomic distribution of lectin-binding sites in mouse testis and epididymis.
Differentiation 27: 74-81

Lee MC, Damjanov I (1985).
Lectin binding sites on human sperm and spermatogenic cells.
Anat Rec. 212: 282-7.

Leeson, T, Leeson R (1970).
The male reproductive system. In. Histology. 2nd ed. W.B. Saunders Company, Philadelphia, London, Toronto.

Liao WX, Roy AC (2002).
Lack of association between polymorphisms in the testis-specific angiotensin converting enzyme gene and male infertility in an Asian population.
Mol. Hum. Reprod. 8: 299-303.

Liener IE, Sharon N, Goldstein IJ (1986).
The Lectins: properties, functions, and applications in biology and medicine. Academic Press, New York, London.

Lindner SG (1982).
On the morphology of the transitional zone of the seminiferous tubule and the rete testis in man.
Andrologia 14: 352-62.

Lis H, Sharon N (1986).
Lectins as molecules and as tools.
Ann. Rev. Biochem. 55: 35-67

Lopez LC, Youakim A, Evans SC, Shur BD (1991).
Evidence for a molecular distinction between Golgi and cell surface forms of beta 1,4-galactosyltransferase.
J. Biol. Chem. 266: 15984-91.

Lukyanenko YO, Chen JJ, Hutson JC (2001).
Production of 25-hydroxycholesterol by testicular macrophages and its effects on Leydig cells.
Biol. Reprod. 64: 790-6.

Maddocks S, Setchell BP (1988).
The physiology of the endocrine testis.
Oxf. Rev. Reprod. Biol. 10: 53-123.

Maekawa M, Kamimura K, Nagano T (1996).
Peritubular myoid cells in the testis: their structure and function.

Arch. Histol. Cytol. 59: 1-13.

Magre S, Jost A (1980).
The initial phases of testicular organogenesis in the rat. An electron microscopy study.
Arch. Anat. Microsc. Morphol. Exp. 69: 297-318.

Main SJ, Waites GM (1978).
The blood-testis barrier and temperature damage to the testis of the rat.
J. Reprod. Fertil. 51: 439-450.

Malmi R, Frojdman K, Soderstrom KO (1990).
Differentiation-related changes in the distribution of glycoconjugates in rat testis.
Histochemistry 94: 387-95.

Malmi R, Söderström KO (1988).
Effects of fixation on lectin histochemistry. Application on normal testicular tissue and seminoma. In Bog Hansen TC and Freed DLJ (Eds). Lectins: biology, biochemistry, clinical biochemistry.Vol.6.Sigma Chem. Co., St. Louis, Missouri, USA. 601-614

Malmi R, Kallajoki M, Suominen J (1987).
Distribution of glycoconjugates in human testis. A histochemical study using fluorescein- and rhodamine-conjugated lectins.
Andrologia 19: 322-32.

Marker PC, Donjacour AA, Dahiya R, Cunha GR (2003).
Hormonal, cellular, and molecular control of prostatic development.
Dev. Biol. 253:165-74.

Martineau J, Nordqvist K, Tilmann C, Lovell-Badge R, Capel B (1997).
Male-specific cell migration into the developing gonad.
Curr. Biol. 7: 958-68.

Martinez-Menargues JA, Abascal I, Aviles M, Castells MT, Ballesta J (1999).
Cytochemical and western blot analysis of the subcompartmentalization of the acrosome in rodents using soybean lectin.
Histochem. J. 31: 29-37

Mayerhofer A, Bartke A, Amador AG, Began T (1989).
Histamine affects testicular steroid production in the golden hamster.
Endocrinology 125: 2212-4.

Mayerhofer A, Russell LD, Grothe C, Rudolf M, Gratzl M (1991).
Presence and localization of a 30-kDa basic fibroblast growth factor-like protein in rodent testes.
Endocrinology 129: 921-4.

McCarrey J R (1993).
Development of the germ cell. In: Desjardins C, Ewing LL (Eds). Cell and Molecular Biology of the Testis. Oxford Uni. Press, Oxford.

McKeehan WL, Crabb JW (1987).
Isolation and characterization of different molecular and chromatographic forms of heparin-binding growth factor 1 from bovine brain.
Anal. Biochem. 164: 563-9.

McLaren A (1988).
Somatic and germ-cell sex in mammals.
Philos. Trans. R. Soc. Lond. B. Biol. Sci. 322: 3-9.

McLaren A (1995).
Germ cells and germ cell sex.
Philos. Trans. R. Soc. Lond. B. Biol. Sci. 350: 229-33.

McLaren A (2000).
Germ and somatic cell lineages in the developing gonad.
Mol. Cell Endocrinol. 163: 3-9.

McLaren A (2003).
Primordial germ cells in the mouse.
Dev. Biol. 262: 1-15.

Mendis-Handagama SM, Ariyaratne HB (2001).
Differentiation of the adult Leydig cell population in the postnatal testis.
Biol. Reprod. 65: 660-71.

Metayer S, Dacheux F, Guerin Y, Dacheux JL, Gatti JL (2001).
Physiological and enzymatic properties of the ram epididymal soluble form of germinal angiotensin I-converting enzyme.
Biol. Reprod. 65: 1332-9.

Michetti F, Lauriola L, Rende M, Stolfi VM, Battaglia F, Cocchia D (1985).
S-100 protein in the testis. An immunochemical and immunohistochemical study.
Cell Tissue Res. 240: 137-42.

Miething A (1993).
Proliferative activity of the developing seminiferous epithelium during prespermatogenesis in the golden hamster testis measured by bromodeoxyuridine labeling.
Anat. Embryol. 187: 249-58.

Miething A (1998).
The establishment of spermatogenesis in the seminiferous epithelium of the pubertal golden hamster (*Mesocricetus auratus*).
Adv. Anat. Embryol. Cell Biol. 140: 1-92.

Miller DJ, Macek MB, Shur BD (1992).
Complementarity between sperm surface beta-1, 4-galactosyltransferase and egg-coat ZP3 mediates sperm-egg binding.
Nature 357: 589-93.

Miller SC, Bowman BM, Rowland HG (1983).
Structure, cytochemistry, endocytic activity, and immunoglobulin (Fc) receptors of rat testicular interstitial-tissue macrophages.
Am. J. Anat. 168: 1-13.

Moniem kA, Tingari MD, Künzel E (1980).
The fine structure of the boundary tissue of the seminiferous tubule of the camel (Camelus dromedarius).
Acta anat. 107: 169-176

Montkowski A (1992).
Lichtmikroskopische, ultrastrukturelle, und glykohistochemische Untersuchungen am Hoden des Hundes.
Thesis, Institute of Veterinary Anatomy II, Faculty of Veterinary Medicine, LMU ,Munich, Germany

More IA, Armstrong EM, McSeveney D, Chatfield WR (1974).
The morphogenesis and fate of the nucleolar channel system in the human endometrial glandular cell.
J. Ultrastruct. Res. 47: 74-85.

Mukasa A, Hiromatsu K, Matsuzaki G, O'Brien R, Born W, Nomoto K (1995).
Bacterial infection of the testis leading to autoaggressive immunity triggers apparently opposed responses of alpha beta and gamma delta T cells.
J. Immunol. 155: 2047-56.

Mullaney BP, Skinner MK (1992).
Basic fibroblast growth factor (FGF-2) gene expression and protein production during pubertal development of the seminiferous tubule: follicle-stimulating hormone-induced Sertoli cell FGF-2 expression.
Endocrinology 131: 2928-34.

Murono EP, Washburn AL, Goforth DP, Wu N (1992).
Evidence for basic fibroblast growth factor receptors in cultured immature Leydig cells.
Mol. Cell Endocrinol. 88: 39-45.

Murota S, Shikita M, Tamaoki B (1965).
Intratesticular distribution of the enzyme related to androgen formation in mouse testes.
Steroids 5:409-43

Murray SA, Fletcher WH (1984).
Hormone-induced intercellular signal transfer dissociates cyclic AMP-dependent protein kinase.
J. Cell Biol. 98: 1710-9.

Nagano R, Sun X, Kurohmaru M, Hayashi Y (1999).
Changes in lectin binding patterns of mouse male germ cells (gonocytes) during prespermatogenesis.
J. Vet. Med. Sci. 61: 465-70.

Nalbandian A, Dettin L, Dym M, Ravindranath N (2003).
Expression of vascular endothelial growth factor receptors during male germ cell differentiation in the mouse.
Biol. Reprod. 69: 985-94

Navaratnam N, Ward S, Fisher C, Kuhn NJ, Keen JN, Findlay JB (1988).
Purification, properties, and cation activation of galactosyltransferase from lactating-rat mammary Golgi membranes.
Eur. J. Biochem. 171: 623-9.

Nes WD, Lukyanenko YO, Jia ZH, Quideau S, Howald WN, Pratum TK, West RR, Hutson JC (2000).
Identification of the lipophilic factor produced by macrophages that stimulates steroidogenesis.
Endocrinology 141: 953-8.

Nickel R, Schummer A, Seiferle E (1999).
Männliche Geschlechtsorgane der Wiederkäuer. In. Lehrbuch der Anatomie der Haustiere , Band II. 5. Auflage, Paul Parey Verlag, Berlin und Hamburg

Nipken C, Wrobel KH (1997).
A quantitative morphological study of age-related changes in the donkey testis in the period between puberty and senium.
Andrologia 29: 149-61.

Noden DM, de Lahunta A (1985).
The embryology of domestic animals. Developmental mechanisms and malformations. 1st ed.

Williams and Wilkins Baltimore. London. Los Angeles, Sydney.

Obermair A, Obruca A, Pohl M, Kaider A, Vales A, Leodolter S, Wojta J, Feichtinger W (1999).
Vascular endothelial growth factor and its receptors in male fertility.
Fertil. Steril. 72: 269-75.

Onyango DW, Wango EO, Otiang'a-Owiti GE, Oduor-Okelo D, Werner G (2000).
Morphological characterization of the seminiferous cycle in the goat (*Capra hircus*): a histological and ultrastructural study.
Anat. Anz. 182: 235-41.

Ornitz DM, Itoh N (2001).
Fibroblast growth factors.
Genome Biol. 2: 1-12

Ortavant R (1958).
Study of spermatogonial generations in the ram.
C. R. Seances Soc. Biol Fil. 148: 1958-61.

Orth JM (1993).
Cell biology of testicular development in the fetus and neonate. In: Desjardins C, Ewing LL (Eds).
Cell and Molecular Biology of the Testis. Oxford Uni. Press, Oxford.

Osman DI (1978a).
The terminal segment of the seminiferous tubules in the rat.
J. Ultrastruct. Res. 63:96-97

Osman DI (1978b).
On the ultrastructure of modified Sertoli cells in the terminal segment of seminiferous tubules in the boar.
J. Anat. 127: 603-13.

Osman DI and Ploen L (1978a).
Ultrastructure of Sertoli cells in the boar.
Int. J. Androl. 1: 162-179.

Osman DI, Ploen L (1978b).
The mammalian tubuli recti: ultrastructural study.
Anat. Rec. 192: 1-17.

Osman DI (1979).
A comparative ultrastructural study on typical and modified Sertoli cells before and after ligation of the efferent ductules in the rabbit.
Anat. Histol. Embryol. 8: 114-123.

Osman DI, Ploen L (1979).
Fine structure of the modified Sertoli cells in the terminal segment of the seminiferous tubules of the bull, ram, and goat
Anim. Reprod. Sci. 2: 343-351

Palombi F, Farini D, Salanova M, de Grossi S, Stefanini M (1992).
Development and cytodifferentiation of peritubular myoid cells in the rat testis.
Anat. Rec. 233: 32-40.

Pandey KN, Misono KS, Inagami T (1984).
Evidence for intracellular formation of angiotensins: coexistence of renin and angiotensin-converting

enzyme in Leydig cells of rat testis.
Biochem. Biophys. Res. Commun. 122: 1337-43.

Pauls K, Fink L, Franke FE (1999).
Angiotensin-converting enzyme (CD143) in neoplastic germ cells.
Lab. Invest. 79: 1425-35.

Pauls K, Metzger R, Steger K, Klonisch T, Danilov S, Franke FE (2003).
Isoforms of angiotensin I-converting enzyme in the development and differentiation of human testis
and epididymis.
Andrologia 35: 32-43.

Pawar HS, Wrobel KH (1991).
Quantitative aspects of water buffalo (*Bubalus bubalis*) spermatogenesis.
Arch. Histol. Cytol. 54: 491-509.

Payne AH, Youngblood GL (1995).
Regulation of expression of steroidogenic enzymes in Leydig cells.
Biol. Reprod. 52: 217-25.

Pelletier RM (1995).
The distribution of connexin 43 is associated with the germ cell differentiation and with the
modulation of the Sertoli cell junctional barrier in continual (guinea pig) and seasonal breeders'
(mink) testes.
J. Androl. 16: 400-9.

Pelliniemi LJ, Frojdman K (2001).
Structural and regulatory macromolecules in sex differentiation of gonads.
J. Exp. Zool. 290: 523-8.

Perey B, Clermont Y, Leblond CP (1961).
The wave of the seminiferous epithelium in the rat.
Am. J. Anat. 108: 47-75

Perez-Armendariz EM, Romano MC, Luna J, Miranda C, Bennett MV, Moreno AP (1994).
Characterization of gap junctions between pairs of Leydig cells from mouse testis.
Am. J. Physiol. 267: C570-80.

**Perez-Armendariz, EM, Lamoyi E, Mason JI, Cisneros-Armas D, Luu-The V, Bravo Moreno
JF (2001).**
Developmental regulation of connexin 43 expression in fetal mouse testicular cells.
Anat. Rec. 264: 237- 46.

Peterson RN, Bozzola J, Polakoski K (1992).
Protein transport and organization of the developing mammalian sperm acrosome.
Tissue Cell 24: 1-15.

Picker LJ, Butcher EC (1992).
Physiological and molecular mechanisms of lymphocyte homing.
Annu. Rev. Immunol. 10: 561-91.

Pinart E, Bonet S, Briz M, Pastor LM, Sancho S, Garcìa N, Badia E, Bassol J (2001).
Lectin affinity of the seminiferous epithelium in healthy and cryptorchid post-pubertal boars.
Int. J. Androl. 24: 153-164

Pinart E, Bonet S, Briz M, Pastor LM, Sancho S, Garcìa N, Badia E, Bassol J (2002).
Histochemical study of the interstitial tissue in scrotal and abdominal boar testes.

Vet. J. 163: 68-76

Plum A, Hallas G, Magin T, Dombrowski F, Hagendorff A, Schumacher B, Wolpert C, Kim J, Lamers WH, Evert M, Meda P, Traub O, Willecke K (2000).
Unique and shared functions of different connexins in mice.
Curr. Biol. 10: 1083-91.

Pollanen P, Maddocks S (1988).
Macrophages, lymphocytes and MHC II antigen in the ram and the rat testis.
J. Reprod. Fertil. 82: 437- 45.

Pollanen P, Niemi M (1987).
Immunohistochemical identification of macrophages, lymphoid cells and HLA antigens in the human testis.
Int. J. Androl. 10: 37-42.

Pollanen PP, Kallajoki M, Risteli L, Risteli J, Suominen JJ (1985).
Laminin and type IV collagen in the human testis.
Int. J. Androl. 8: 337-47.

Pratt SA, Scully NF, Shur BD (1993).
Cell surface beta 1, 4 galactosyltransferase on primary spermatocytes facilitates their initial adhesion to Sertoli cells in vitro.
Biol. Reprod. 49: 470-82.

Pratt SA, Shur BD (1993).
Beta-1, 4-galactosyltransferase expression during spermatogenesis: stage-specific regulation by t alleles and uniform distribution in + -spermatids and t-spermatids.
Dev. Biol. 156: 80-93.

Prem J (1992).
Histologische, ultrastrukturelle und histochemische Untersuchungen an Hoden und Nebenhoden der Katze (Felis silvestris "familiaris").
Thesis, Institute of Veterinary Anatomy II, Faculty of Veterinary Medicine, LMU, Munich, Germany.

Prince FP (1984).
Ultrastructure of immature Leydig cells in the human prepubertal testis.
Anat. Rec. 209: 165-76.

Prince FP (2001).
The triphasic nature of Leydig cell development in humans, and comments on nomenclature. J. Endocrinol. 168: 213-6.

Pulford KA, Sipos A, Cordell JL, Stross WP, Mason DY (1990).
Distribution of the CD68 macrophage/myeloid associated antigen.
Int. Immunol. 2: 973-80.

Rathkolb B, Pohlenz JF, Wohlsein P (1997).
Identification of leucocyte surface antigens in paraffin-embedded bovine tissues using a modified formalin dichromate fixation.
Histochem. J. 29: 487-93.

Raychoudhury SS, Millette CF (1993).
Surface-associated glycosyltransferase activities in rat Sertoli cells in vitro.
Mol. Reprod. Dev. 36: 195-202.

Reynolds EG (1963).
The use of lead citrate at high pH as an electron-opaque stain in electron microscopy.
J. Cell Biol. 17: 208-212

Risley MS, Tan IP, Roy C, Saez JC (1992).
Cell-, age- and stage-dependent distribution of connexin43 gap junctions in testes.
J. Cell Sci. 103: 81-96.

Rodger JC (1982).
The testis and its excurrent ducts in American caenolestid and didelphid marsupials.
Am. J. Anat. 1982 163: 269-82.

Romeis B (1989).
Mikroskopische Technik. Urban und Schwarzenberg, 17.Auflage. München/ Wien/ Baltimore.

Roosen-Runge EC (1951).
Quantitative studies on spermatogenesis in the albino rat. II. The duration of spermatogenesis and some effects of colchicine.
Am. J. Anat. 88: 163-76.

Roosen-Runge EC (1961).
Rudimental "genital canals" of the gonad in rat embryos.
Acta Anat. 44: 1-11.

Roosen-Runge EC, Holstein AF (1978).
The human rete testis.
Cell Tissue Res. 189: 409-33.

Roth J (1996).
Protein glycosylation in the endoplasmic reticulum and the Golgi apparatus and cell type-specificity of cell surface glycoconjugate expression: analysis by the protein A-gold and lectin-gold techniques.
Histochem. Cell Biol. 106: 79-92.

Roth J (1983).
Application of lectin-gold complexes for electron microscopic localization of glycoconjugates on thin sections.
J. Histochem. Cytochem. 31: 987-999

Rudolfsson SH, Wikstrom P, Jonsson A, Collin O, Bergh A (2004).
Hormonal regulation and functional role of vascular endothelial growth factor a in the rat testis.
Biol. Reprod. 70: 340-7

Rüsse I (1991).
In: Rüsse I, Sinowatz F (Eds). Lehrbuch der Embryologie der Haustiere. Paul Parey Verlag, Berlin und Hamburg.

Rüsse I, Sinowatz F (1991).
Lehrbuch der Embryologie der Haustiere. Verlag Paul Parey. Berlin und Hamburg

Russell LD (1978).
The blood-testis barrier and its formation relative to spermatocyte maturation in the adult rat: a lanthanum tracer study.
Anat. Rec. 190: 99-111.

Russell LD, Peterson RN (1985).
Sertoli cell junctions: morphological and functional correlates.
Int. Rev. Cytol. 94: 177-211.

Sabeur K, Vo AT, Ball BA (2001).
Characterization of angiotensin-converting enzyme in canine testis.
Reproduction 122: 139-46.

Saez JC, Berthoud VM, Branes MC, Martinez AD, Beyer EC (2003).
Plasma membrane channels formed by connexins: their regulation and functions.
Physiol. Rev. 83: 1359-400.

Salomon F, Hedinger CE (1982).
Abnormal basement membrane structures of seminiferous tubules in infertile men.
Lab. Invest. 47: 543-54.

Santamaria L, Martinez-Onsurbe P, Paniagua R, Nistal M (1990).
Laminin, type IV collagen, and fibronectin in normal and cryptorchid human testes. An immunohistochemical study.
Int. J. Androl. 13: 135-46.

Santamarina E, Reece RP (1957).
Normal development of the germinal epithelium and seminiferous tubules in the bull.
Am. J. Vet. Res. 18: 261-78.

Santi CM, Santos T, Hernandez-Cruz A, Darszon A (1998).
Properties of a novel pH-dependent Ca2+ permeation pathway present in male germ cells with possible roles in spermatogenesis and mature sperm function.
J. Gen. Physiol. 112: 33-53.

Satoh M (1991).
Histogenesis and organogenesis of the gonad in human embryos.
J. Anat. 177: 85-107.

Schafer BW, Heizmann CW (1996).
The S100 family of EF-hand calcium-binding proteins: functions and pathology.
Trends Biochem. Sci. 21: 134-40.

Schlatt S, Meinhardt A, Nieschlag E (1997).
Paracrine regulation of cellular interactions in the testis: factors in search of a function.
Eur. J. Endocrinol. 137:107-17

Schlatt S, Weinbauer GF, Arslan M, Nieschlag E (1993).
Appearance of alpha-smooth muscle actin in peritubular cells of monkey testes is induced by androgens, modulated by follicle-stimulating hormone, and maintained after hormonal withdrawal.
J. Androl. 14: 340-50.

Schmahl J, Eicher EM, Washburn LL, Capel B (2000).
Sry induces cell proliferation in the mouse gonad.
Development 127: 65-73.

Schön J, Blottner S (2004).
Testicular FGF-1 protein is involved in Sertoli cell-spermatid interaction in roe deer.
Gen. Comp. Endocrinol. 139: 168-72.

Schrag D (1983).
Licht-und elektronenmikroskopische Untersuchungen zur fetalen Differenzierung der männlichen Keimdrüse des Rindes.
Thesis, Institute of Veterinary Anatomy II, Faculty of Veterinary Medicine, LMU, Munich, Germany.

Schulze C (1984).
Sertoli cells and Leydig cells in man.
Adv. Anat. Embryol. Cell Biol. 88: 1-104.

Scully NF, Shaper JH, Shur BD (1987).
Spatial and temporal expression of cell surface galactosyltransferase during mouse spermatogenesis and epididymal maturation.
Dev. Biol. 124: 111-24.

Segretain D, Falk MM (2004).
Regulation of connexin biosynthesis, assembly, gap junction formation, and removal.
Biochim. Biophys. Acta. 1662: 3-21.

Setchell BP (1970).
The secretion of fluid by the testes of rats, rams and goats with some observations on the effect of age, cryptorchidism, and hypophysectomy.
J. Reprod. Fertil. 23: 79-85.

Setchell BP (1986).
The movement of fluids and substances in the testis.
Aust. J. Biol. Sci. 39: 193-207.

Setchell BP, Maddocks S, Brooks DE (1994).
Anatomy, vasculature, innervation, and fluids of the male reproductive tract. In: Knobil E, Neill JD (eds.), The Physiology of Reproduction, 2nd ed. New York: Raven Press, 1063-1175.

Setijanto H. (1992).
Lichtmikroskopische, ultrastrukturelle, und histochemische Untersuchung am fetalen Hoden des Rindes (*Bos taurus*).
Thesis, Institute of Veterinary Anatomy II, Faculty of Veterinary Medicine, LMU, Munich, Germany.

Shaper NL, Wright WW, Shaper JH (1990).
Murine beta 1, 4-galactosyltransferase: both the amounts and structure of the mRNA are regulated during spermatogenesis.
Proc. Natl. Acad. Sci. U S A. 87: 791-5.

Sharon N (1977).
Lectins.
Scient. Americ. 236: 108-119

Sharpe RM (1983).
Local control of testicular function.
Q. J. Exp. Physiol. 68: 265-87.

Shur BD, Evans S, Lu Q (1998).
Cell surface galactosyltransferase: current issues.
Glycoconj. J. 15: 537-48.

Shur BD, Neely CA (1988).
Plasma membrane association, purification, and partial characterization of mouse sperm beta 1, 4-galactosyltransferase.
J. Biol. Chem. 263: 17706-14.

Sibony M, Gasc JM, Soubrier F, Alhenc-Gelas F, Corvol P (1993).
Gene expression and tissue localization of the two isoforms of angiotensin I converting enzyme.
Hypertension. 21: 827-835.

Sibony M, Segretain D, Gasc JM (1994).
Angiotensin-converting enzyme in murine testis: step-specific expression of the germinal isoform during spermiogenesis.
Biol. Reprod. 50: 1015-26.

Sinclair AH, Berta P, Palmer MS, Hawkins JR, Griffiths BL, Smith MJ, Foster JW, Frischauf AM, Lovell-Badge R, Goodfellow PN (1990).
A gene from the human sex-determining region encodes a protein with homology to a conserved DNA-binding motif.
Nature 346: 240-4.

Sinowatz F, Amselgruber W (1986).
Postnatal development of bovine Sertoli cells.
Anat. Embryol. 174: 413-23.

Sinowatz F, Amselgruber W (1988).
Ultrastructure of sustentacular (Sertoli) cells in the bovine testis.
Acta. Anat. 133: 274-81.

Sinowatz F, Wrobel KH (1981).
Development of the bovine acrosome. An ultrastructural and cytochemical study.
Cell Tissue Res. 219: 511-24.

Sinowatz F, Wrobel KH, Sinowatz S, Kugler P (1979).
Ultrastructural evidence for phagocytosis of spermatozoa in the bovine rete testis and testicular straight tubules.
J. Reprod. Fertil. 57: 1-4.

Sinowatz F, Wrobel KH, Fischerleitner F, Schilling E (1983).
Morphologische Aspekte der postnatalen Hodendifferenzierung.
Wien. tierärztl. Mschr. 70:194-197

Sinowatz F, Amselgruber W, Rüsse I (1987).
Prä-und Postnatal Differenzierung der Leydig Zellen beim Rind.
Fertilität. 3: 191-196

Skalli O, Ropraz P, Trzeciak A, Benzonana G, Gillessen D, Gabbiani G (1986).
A monoclonal antibody against alpha-smooth muscle actin: a new probe for smooth muscle differentiation.
J. Cell Biol. 103: 2787-96.

Skinner MK, Tung PS, Fritz IB (1985).
Cooperativity between Sertoli cells and testicular peritubular cells in the production and deposition of extracellular matrix components.
J. Cell Biol. 100: 1941-7.

Soder O, Sultana T, Jonsson C, Wahlgren A, Petersen C, Holst M (2000).
The interleukin-1 system in the testis.
Andrologia 32: 52-5.

Söderström KO, Malmi R, Karjalainen K (1984).
Binding of fluorescein isothiocyanate conjugated lectins to rat Spermatogenic cells in tissue section. Enhancement of lectin fluorescence obtained by fixation in Bouin's fluid.
Histochemistry 80: 575-579

Sohl G, Willecke K (2004).
Gap junctions and the connexin protein family.

Cardiovasc. Res. 62: 228-32.

Sone H, Deo BK, Kumagai AK (2000).
Enhancement of glucose transport by vascular endothelial growth factor in retinal endothelial cells.
Invest. Ophthalmol. Vis. Sci. 41:1876-84.

Speth RC, Daubert DL, Grove KL (1999).
Angiotensin II: a reproductive hormone too?
Regul. Pept. 79: 25-40.

Spicer SS, Schulte BA (1992).
Diversity of cell glycoconjugates shown histochemically: a perspective.
J. Histochem. Cytochem. 40: 1-38.

Spicer SS, Schulte BA, Thomopoulos GN, Panuley RT, Takagi M (1983).
Cytochemistry of complex carbohydrates by light and electron microscopy. In: Wagner BM,
Fleischmajer R, Kaufman N (Eds). Connective tissue diseases. Baltimore: William and Wilkins,
pp.163-211.

Steger K, Schimmel M, Wrobel KH (1994).
Immunocytochemical demonstration of cytoskeletal proteins in seminiferous tubules of adult rams
and bulls.
Arch. Histol. Cytol. 57: 17-28.

Steger K, Tetens F, Seitz J, Grothe C and Bergmann M. (1998).
Localization of fibroblast growth factor 2 (FGF-2) protein and the receptors FGFR 1-4 in normal
human seminiferous epithelium.
Histochem. Cell Biol. 110: 57-62.

Steger K, Wrobel KH (1994).
Immunohistochemical demonstration of cytoskeletal proteins in the ovine testis during postnatal
development.
Anat. Embryol. 189: 521-30.

Steger K, Tetens F, Bergmann M (1999).
Expression of connexin 43 in human testis.
Histochem. Cell Biol. 112: 215-20.

Suganuma T, Muramatsu H, Muramatsu T, Ihida K, Kawano J, Murata F (1991).
Subcellular localization of N-acetylglucosaminide beta 1, 4 galactosyltransferase revealed by
immunoelectron microscopy.
J. Histochem. Cytochem. 39: 299-309.

Süß F (1998).
Identifizierung, Lokalisation, und Kinetik der Urgeschlechtszellen des Rindes sowie
morphodynamische Aspekte der Gonadogenese.
Thesis, Institute of Veterinary Anatomy, Faculty of Veterinary Medicine, Berlin, Germany.

Swain A, Lovell-Badge R (1999).
Mammalian sex determination: a molecular drama.
Genes Dev. 13: 755-67.

Szebenyi G, Fallon JF (1999).
Fibroblast growth factors as multifunctional signaling factors.
Int. Rev. Cytol. 185: 45-106.

Taketo T, Thau RB, Adeyemo O, Koide SS (1984).
Influence of adenosine 3':5'-cyclic monophosphate analogues on testicular organization of fetal mouse gonads in vitro.
Biol. Reprod. 30: 189-98.

Tang Y (1998).
Galactosyltransferase, pyrophosphatase and phosphatase activities in luminal plasma of the cauda epididymidis and in the rete testis fluid of some mammals.
J. Reprod. Fertil. 114: 277-85.

Tilmann C, Capel B (1999).
Mesonephric cell migration induces testis cord formation and Sertoli cell differentiation in the mammalian gonad.
Development 126: 2883-90.

Tilmann C, Capel B (2002).
Cellular and molecular pathways regulating mammalian sex determination.
Recent Prog. Horm. Res. 57: 1-18.

Tohonen V, Ritzen EM, Nordqvist K, Wedell A (2003).
Male sex determination and prenatal differentiation of the testis.
Endocr. Dev. 5: 1-23.

Töpfer-Petersen E (1999).
Carbohydrate-based interactions on the route of a spermatozoon to fertilization.
Hum. Reprod. Update 5: 314-29.

Tulsiani DR, Skudlarek MD, Holland MK, Orgebin-Crist MC (1993).
Glycosylation of rat sperm plasma membrane during epididymal maturation.
Biol. Reprod. 48: 417-28.

Tung PS, Fritz IB (1993).
Interactions of Sertoli cells with laminin are essential to maintain integrity of the cytoskeleton and barrier functions of cells in culture in the two-chambered assembly.
J. Cell Physiol. 156: 1-11.

Tung PS, Fritz IB (1980).
Interactions of Sertoli cells with myoid cells in vitro.
Biol. Reprod. 23:207-17.

Ueno N, Baird A, Esch F, Ling N, Guillemin R (1987).
Isolation and partial characterization of basic fibroblast growth factor from bovine testis.
Mol. Cell Endocrinol. 49: 189-94.

Vaiman D, Pailhoux E (2000).
Mammalian sex reversal and intersexuality: deciphering the sex-determination cascade.
Trends Genet. 16: 488-94.

Van Dissel-Emiliani FM, De Boer-Brouwer M, De Rooij DG (1996).
Effect of fibroblast growth factor-2 on Sertoli cells and gonocytes in coculture during the perinatal period.
Endocrinology 137: 647-54.

van Vorstenbosch CJ, Colenbrander B, Wensing CJ (1984).
Leydig cell development in the pig testis during the late fetal and early postnatal period: an electron microscopic study with attention to the influence of fetal decapitation.
Am. J. Anat. 169: 121-36.

Varanda WA, de Carvalho AC (1994).
Intercellular communication between mouse Leydig cells.
Am. J. Physiol. 267: C563-9.

Verhoeven G, Hoeben E, De Gendt K (2000).
Peritubular cell-Sertoli cell interactions: factors involved in P-mod-S activity.
Andrologia 32: 42-5.

Verini-Supplizi A, Stradaioli G, Fagioli O, Prillo F (2000).
Localization of the lectin reactive sites in adult and prepubertal horse testes.
Res. Vet. Sci. 69 : 113-118

Virtanen I, Lohi J, Tani T, Korhonen M, Burgeson RE, Lehto VP, Leivo I (1997).
Distinct changes in the laminin composition of basement membranes in human seminiferous tubules during development and degeneration.
Am. J. Pathol. 150: 1421-31.

Vitale R, Fawcett DW, Dym M (1973).
The normal development of the blood-testis barrier and the effects of clomiphene and estrogen treatment.
Anat. Rec. 176: 331-44.

Wagener A, Blottner S, Goritz F, Fickel J (2000).
Detection of growth factors in the testis of roe deer (*Capreolus capreolus*).
Anim. Reprod. Sci. 64: 65-75.

Wagener A, Blottner S, Goritz F, Streich WJ, Fickel J. (2003).
Differential changes in expression of a and b FGF, IGF-1 and -2, and TGF-alpha during seasonal growth and involution of roe deer testis.
Growth Factors 21: 95-102.

Wahlgren A (2003).
Growth factors in spermatogenesis.
Thesis, Department of women and child health, Karolinska Institute, Stockholm, Sweden

Walker RA (1988).
The use of lectins in histology and histopathology. In Bog Hansen TC, Freed DLJ (Eds). Lectins: biology, biochemistry, clinical biochemistry, Vol. 6 .Sigma Chem. Co., St. Louis, Missouri, USA. 591-600

Wang J, Wreford NG, Lan HY, Atkins R, Hedger MP (1994).
Leukocyte populations of the adult rat testis following removal of the Leydig cells by treatment with ethane dimethane sulfonate and subcutaneous testosterone implants.
Biol. Reprod. 51: 551-61.

Wartenberg H (1985).
Origin of gonadal blastemal cells in mammalian gonadogenesis.
Arch. Anat. Microsc. Morphol. Exp. 74: 60-3.

Wartenberg H (1981).
Differentiation and development of the testis. In: Burger H, de Kretser D (Eds). The testis. Raven Press, New York, pp. 39-80.

Wheatley M, Hawtin SR (1999).
Glycosylation of G-protein-coupled receptors for hormones central to normal reproductive functioning: its occurrence and role.
Hum. Reprod. Update 5: 356-64.

Willecke K, Eiberger J, Degen J, Eckardt D, Romualdi A, Guldenagel M, Deutsch U, Sohl G (2002).
Structural and functional diversity of connexin genes in the mouse and human genome.
Biol. Chem. 383: 725-37.

Wollina V, Schireiber G, Zollmann C, Hipler C, Gunther E (1989).
Lectin-binding sites in normal human testis.
Andrologia 21: 127-130

Wrobel KH (2000a).
Morphogenesis of the bovine rete testis: the intratesticular rete and its connection to the seminiferous tubules.
Anat. Embryol. 202: 475-90.

Wrobel KH (2000b).
Prespermatogenesis and spermatogoniogenesis in the bovine testis.
Anat. Embryol. 202: 209-22.

Wrobel KH, Süß F (1998).
Identification and temporospatial distribution of bovine primordial germ cells prior to gonadal sexual differentiation.
Anat. Embryol. 197: 451-67.

Wrobel KH, Süß F (1999).
On the origin and prenatal development of the bovine adrenal gland.
Anat. Embryol. 199: 301-18.

Wrobel KH, Süß F (2000).
The significance of rudimentary nephrostomial tubules for the origin of the vertebrate gonad.
Anat. Embryol. 201: 273-90.

Wrobel KH, Abu-Ghali N (1997).
Autonomic innervation of the bovine testis.
Acta. Anat. 160: 1-14.

Wrobel KH, Bickel D, Kujat R, Schimmel M (1995a).
Configuration and distribution of bovine spermatogonia.
Cell Tissue Res. 279: 277-89.

Wrobel KH, Bickel D, Kujat R, Schimmel M (1995b).
Evolution and ultrastructure of the bovine spermatogonia precursor cell line.
Cell Tissue Res. 281: 249-59.

Wrobel KH, Reichold J, Schimmel M (1995c).
Quantitative morphology of the ovine seminiferous epithelium.
Anat. Anz. 177: 19-32.

Wrobel KH, Dostal S, Schimmel M (1988).
Postnatal development of the tubular lamina propria and the intertubular tissue in the bovine testis.
Cell Tissue Res. 252: 639-53.

Wrobel KH, Hees H (1987).
Heterotopic Leydig cells in the cat.
Anat. Histol. Embryol. 16: 289-92.

Wrobel KH, Hees I, Schimmel M, Stauber E (2002).
The genus Acipenser as a model system for vertebrate urogenital development: nephrostomial tubules

and their significance for the origin of the gonad.
Anat. Embryol. 205: 67-80.

Wrobel KH, Pawar HS (1992).
Quantitative morphology of the testicular tubular epithelium in the water buffalo (*Bubalus bubalis*).
Andrologia 24: 63-8.

Wrobel KH, Schilling E, Zwack M (1986).
Postnatal development of the connexion between tubulus seminiferous and tubulus rectus in the bovine testis.
Cell Tissue Res. 246: 387-400.

Wrobel KH, Schimmel M (1989).
Morphology of the bovine Sertoli cell during the spermatogenetic cycle.
Cell Tissue Res. 257: 93-103.

Wrobel KH, Sinowatz F, Kugler P (1978).
The functional morphology of the rete testis, tubuli recti and terminal segments of the seminiferous tubules in the mature bull.
Anat. Histol. Embryol. 7: 320-35.

Wrobel KH, Sinowatz F, Mademann R (1981).
Intertubular topography in the bovine testis.
Cell Tissue Res. 217: 289-310.

Wrobel KH, Sinowatz F, Mademann R (1982).
The fine structure of the terminal segment of the bovine seminiferous tubule.
Cell Tissue Res. 225: 29-44.

Wrobel KH (1998).
Male reproductive system. In Dellmann HD, Eurell J.A (Eds). Textbook of Veterinary Histology.5th.ed. Williams and Wilkins, Pennsylvania, USA. 226-235

Wrobel KH, Mademann R, Sinowatz F (1979).
The lamina propria of the bovine seminiferous tubule.
Cell Tissue Res. 202: 357-77.

Yazama F, Esaki M, Sawada H (1997).
Immunocytochemistry of extracellular matrix components in the rat seminiferous tubule: electron microscopic localization with improved methodology.
Anat. Rec. 248: 51-62.

Yin JL, Shackel NA, Zekry A, McGuinness PH, Richards C, Putten KV, McCaughan GW, Eris JM, Bishop GA. (2001).
Real-time reverse transcriptase-polymerase chain reaction (RT-PCR) for measurement of cytokine and growth factor mRNA expression with fluorogenic probes or SYBR Green I.
Immunol. Cell Biol. 79: 213-221.

Yono M, Takahashi W, Pouresmail M, Johnson DR, Foster HE Jr, Weiss RM, Latifpour J (2002).
Quantification of endothelins, their receptors, and endothelin-converting enzyme mRNAs in rat genitourinary tract using real-time RT-PCR.
J. Pharmacol. Toxicol. Methods 48: 87-95.

You S, Li W, Lin T (2000).
Expression and regulation of connexin43 in rat Leydig cells.
J. Endocrinol. 166: 447-53.

Young KA, Nelson RJ (2000).
Short photoperiods reduce vascular endothelial growth factor in the testes of Peromyscus leucopus.
Am. J. Physiol. Regul. Integr. Comp. Physiol. 279: R1132-7

Zamboni L, Upadhyay S (1982).
The contribution of the mesonephros to the development of the sheep fetal testis.
Am. J. Anat. 165: 339-56.

Zhang QY, Qiu SD, Ge L (2004).
Studies on expression and location of VEGF protein in rat testis and epididymis.
Shi Yan Sheng Wu Xue Bao. 37:1-8 (Abstract).

Zhu D, Shen A, Sun M, Gu J (2003).
Distinct patterns of expression of the beta-1, 4-galactosyltransferases during testicular development in the mouse.
Mol. Cell Biochem. 247:147-53.

Zibrin M (1972).
Multivesicular nuclear body with nucleolar activity in Sertoli cells of bulls. An ultrastructural study.
Z. Zellforsch. Mikrosk. Anat. 135: 155-64.

Zimmer DB, Cornwall EH, Landar A, Song W (1995).
The S100 protein family: history, function, and expression.
Brain Res. Bull. 37: 417-29.

Zuckermann S, Baker TG (1977).
The development of the ovary and the process of oogenesis. In: Zuckermann S, Weir BJ (Eds), Ovary. Academic press, New York 1:41-67

9. ABBREVIATIONS

AA	Amino acid
ABC	Avidin Biotin complex
ABP	Androgen binding protein
ACE	Angiotensin converting enzyme.
AMH	Anti-Müllerian hormone
ASPC	Aggregated spermatogonia precursor cells
BM	Basement membrane.
BSC	Basal spermatogonia stem cell line
cAMP	cyclic Adenosine monophosphate.
Con A	*Concanavalin* Agglutinin.
CRL	Crown Rump Length.
CSPC	Committed spermatogonia precursor cells
Cx43	Connexin 43
° C	Degree centigrade.
Da	Dalton.
DAX1	Dosage-sensitive sex reversal
DBA	*Dolichos biflorus* Agglutinin.
dpc	Day post conception
dsDNA	Double strand deoxyribonucleic acid
ECA	*Erythrina cristagalli* Agglutinin.
ECM	Extracellular matrix.
EDS	Ethane dimethane sulphonate
EGF	Epidermal growth factor
EM	Electron microscope
ER	Endoplasmic reticulum.
FGF-1	Acidic Fibroblast Growth Factor (aFGF).
FGF-2	Basic Fibroblast Growth Factor (bFGF).
FGFRs	Fibroblast Growth Factor Receptors.
FGFs	Fibroblast Growth Factors.
FITC	Fluoroisothiocyanate.
FSH	Follicular stimulating hormone
GalNAc	N-acetyl-galactosamine.

GalTase	Galactosyltransferase.
GlcNAc	N-acetyl-glucosamine.
GSA I	*Griffonia simplicifolia* Agglutinin I.
H&E	Haematoxylin and Eosin.
hCG	human chorionic gonadotropin
HGF	Hepatocyte growth factor
HPA	*Helix pomatia* Agglutinin
IGF-I	Insulin growth factor-I
IL1	Interleukin-1
IP3	Inositol triphosphate
IRES	Internal ribosome entry site
LCA	*Lens culinaris* Agglutinin.
LIC	Light intercalated cell
LM	Light microscope
LTA.	*Lotus tetragonolobus* Agglutinin
MCSF	Macrophage colony stimulating factor
mER	Mixed endoplasmic reticulum
MHC	Major histocompatability complex.
mRNA	Messenger ribonucleic acid
MIS	Müllerian inhibiting substance
Ndr	Nuclear Dbf2-related (family of protein serine/threonine kinases)
NO	Nitric oxide
p53	Tumor suppressor gene p53
PAS	Periodic acid Schiff.
PCNA	Proliferating cell nuclear antigen
PGC	Primordial germ cell.
PModS	Peritubular factor that modulates Sertoli cell function
PNA	Peanut Agglutinin.
PSA	*Pisum sativum* Agglutinin.
RAGE	Receptor for Advanced Glycation End Product
rER	Rough Endoplasmic Reticulum.
ROS	Reactive oxygen species
RT-PCR	Reverse-transcriptase polymerase chain reaction
RTF	Rete testis fluid

sACE	Somatic Angiotensin Converting Enzyme.
SBA	Soybean (*Glycine maximus)* Agglutinin.
SCF	Stem cell factor
sER	Smooth Endoplasmic Reticulum.
SF-1	Steroidogenic factor-1
SMA	Smooth Muscle Actin.
SOX9	SRY box-related gene 9
SRY	Sex determining region of the Y-chromosome
SSC	Saline sodium citrate
SSL	Scheitel-Steiß Länge (German synonym of CRL).
StAR	Steroidogenic acute regulatory protein
TA	Tunica albuginea
tACE	Testicular Angiotensin Converting Enzyme.
Tag p. c.	Tag post coitum (German synonym of dpc).
TGF-β	Transforming growth factor β
TNFα	Tumor necrosis factor-alpha
UEA I.	*Ulex Europaeus* Agglutinin
μm	Micrometer.
VEGF	Vascular Endothelial Growth Factor.
VVA	*Vicia villosa* Agglutinin.
WGA	Wheat germ Agglutinin.
WT-1	Wilms tumor gene product
ZO-1	Zonula occludens-1
ZP	Zona pellucida

10. APPENDIX

Chemicals

Bouin's solution:

Saturated solution of picric acid	750 ml
Formaldehyde	250 ml
Glacial acetic acid	50 ml

Cacodylate Buffer:

a) Solution A

$Na(CH_3)_2AsO_2$ x $3H_2O$	8.56 g
(Polyscienc Inc.,Warrington/USA)	
Distilled water	200 ml

b) Solution B
HCl 0,2 M
(Merck, Darmstadt)

For Cacodylate buffer 0, 2 M, pH 7.2:

Solution A	50 ml
Solution B	4.2 ml
Distilled water	100 ml

For Cacodylate buffer 0,1 M, pH 7.2:

0.2 M solution	50 ml
Distilled water	50 ml

Contrasting solution for electron microscopy

OsO_4, 4%	2 ml
(Polysciences Inc., Warrington/USA)	
Distilled water	6 ml
Potassiumferrocyanide	0.12 g
(Sigma, Deisenhofen	

DAB preparation

Solution A: 50 ml TBS buffer + 0.15 ml 30% H_2O_2

Solution B: 60 ml PBS + 3 DAB tablets

0.4 ml of solution A are mixed with solution B. Filtration of the mixture

Karnovsky solution (Karnovsky, 1965)

Paraformaldehyde	10 g
Distilled water	100 ml
NaOH, 1M	6 drops

PBS Buffer (phosphate buffered saline)

Sodium chloride	42.5 g
Disodiumhydrogenphosphate-dihydrate	6.35 g
Sodiumdihydrogenphosphate-monohydrate	1.95 g

Add 5 liters distilled water and adjust pH at 7.4 to 7.6

11. CURRICULUM VITAE

Personal Data:

Name:	Ahmed Shawkey Esmaeil Abd-Elmaksoud
Date of Birth :	04-10-1971
Place of birth:	Kafr El sheikh, Egypt
Nationality:	Egyptian
Marital Status:	Married
Profession:	Assistant lecturer in department of Anatomy and Histology, Faculty of Veterinary Medicine, Mansoura University, Mansoura, Egypt.

II. Education:

1977-1983:	Primary school, result: (Excellent).
1983-1986:	Preparatory School, result: (Excellent)
1986-1989:	Secondary school, result: (Very Good).
1989-1994:	Student in Faculty of Veterinary Medicine - Alexandria University - Egypt, Grade: (Very Good with honours degree).

III. Degrees:

1994:	Bachelor of Veterinary Medical Sciences, Faculty of Veterinary Medicine, Alexandria University, Alexandria, Egypt. General Grade: Very Good with honours degree
1999:	Master Degree in Veterinary Histology from Tanta University Egypt. Title of Master Thesis: Some histological and histochemical studies on the spleen of Quail during pre-and post-hatching period.

IV. Positions Held:

Current:

3.9.2001 - 3.9.2005:   Scholarship from Egyptian government for a Ph.D. study at Institute of Anatomy II, Ludwig-Maximilians-Universität, Munich, Germany

Previous:

1995-1999:   Demonstrator in Department of Anatomy and Histology, Faculty Veterinary Medicine, Mansoura University, Mansoura, Egypt.

1999 (September):   Assistant lecturer in Department of Anatomy and Histology, Faculty of Veterinary Medicine, Mansoura University, Mansoura, Egypt.

V. Scientific Activities & Researches:

Teaching: Teaching the practical histological courses in department of Cytology and Histology, Faculty of Veterinary Medicine, Mansoura University, Mansoura, Egypt.

Researches and publications: -The research project of the Master degree. "Some histological and histochemical studies on the spleen of Quail during pre-and post-hatching period"

-"Immunohistochemical Localization of Acidic (FGF-1) and Basic (FGF-2) Fibroblast Growth Factor in the Bovine Testis"
Presented at the 37th Annual Meeting of Physiology and Pathology of Reproduction, Munich, Germany, 2004

- Abd-Elmaksoud, A., M. Vermehren, F. Nützel, F. Habermann, and F. Sinowatz, 2005: "Analysis of fibroblast growth factor 2 (FGF2) gene transcription and protein distribution in the bovine testis" *Growth Factors*, Accepted for publication.

- Abd-Elmaksoud, A. and Sinowatz, F. (2005): "Expression and localization of growth factors and their Receptors in the mammalian testis" Review/part I. *Anat. Histol. Embryol.* Accepted for publication.

228

12. ACKNOWLEDGEMENT

Abd-Elmaksoud Ahmed